ACTIONS OF NOVEL HYBRID PEPTIDES ON HYPERGLYCAEMIA AND IMMUNOMODULATION IN EXPERIMENTAL DIABETES

W. A. OFOSU

Ph.D.

2020

ACTIONS OF NOVEL HYBRID PEPTIDES ON HYPERGLYCAEMIA AND IMMUNOMODULATION IN EXPERIMENTAL DIABETES

WENDY AMY OFOSU

A thesis submitted in partial fulfilment of the requirements of the University of East London for the degree of Doctor of Philosophy

January 2020

ABSTRACT

Type 2 diabetes (T2D) represents one of the major disease challenges worldwide, with epidemic proportions of more than 400 million affected across the globe. Therapeutic agents for disease management are often met by challenges such as the inability to restore long-term glucose homeostasis; highlighting the need for novel agents with increased potency or better therapeutic efficacy. The discovery of exendin-4, a compound isolated from venom of the Gila monster lizard (*Heloderma suspectum)* and developed into a potent anti-diabetic drug, further motivated interests in the search animal sources for novel therapeutic agents.

Over the last decade, much attention has been drawn towards amphibian skin peptides, which have uncovered their previously unexplored anti-diabetic actions. Among many other peptides, tigerinin-1R (isolated from *Hoplobatracus rugulosus*) and magainin-AM$_2$ (isolated from *Xenopus amieti*) have been extensively characterised for their anti-diabetic actions both *in vitro* and *in vivo*, showing promise for further investigations. In the context of T2D, a recently explored approach yielding pre-clinical success is based on the creation of hybrid peptides with established anti-diabetic components into a single molecular entity. The rationale for this concept is the generation of hybrids presenting features of their individual components, while introducing additional beneficial effects.

This study characterised the *in vitro* potential of novel hybrid peptides, designed by combining established anti-diabetic agents, exendin-4 and d-Ala^2-GIP, with the amphibian peptides tigerinin-1R and magainin-AM$_2$. After assessing their insulinotropic actions in the clonal pancreatic cells, BRIN-BD11, and in isolated primary islets, specific modulators of insulin secretion were employed to elucidate the mechanism of action of the peptides. This screening revealed that combining magainin-AM2 with exendin-4 produced the best augmented and non-toxic actions on insulin secretion from BRIN-BD11 cells and isolated islets through the activation of the ATP-dependent pathway of insulin secretion. Metabolomic analysis under hyperglycaemic conditions, using ^{1}H-NMR and GC-MS, along with gene expression studies further highlighted the anti-diabetic actions of these peptides. A reduction in lipid abundance as well as an increase in glucose metabolism were observed. Gene

expression studies revealed increase in the genes encoding for insulin and beta-cell proliferation, further expanding on the anti-diabetic potential of these compounds.

Finally, by considering the inflammatory component associated with T2D, characterisation of the peptides' actions on bone-marrow derived dendritic cells (BM-DCs) revealed, for the first time in this model, reduction of perpetuating inflammatory signals, in favour of an anti-inflammatory environment.

Taken together, these studies revealed that combining the selected amphibian skin peptides with exendin-4 significantly enhanced the therapeutic promise of these peptides and encourage further analysis of their in vivo actions as well as further development into a clinically available therapy for type 2 diabetes.

Declaration

I declare that the work reported in this thesis was carried out in accordance with the regulations of the University of East London.

Wendy Amy Ofosu

<u>LIST OF TABLES</u>

List of accompanying material

Accepted publication during the PhD period prior to thesis submission:

- **Ofosu W.A.**, Mohamed D., Corcoran O., Ojo O.O. (2019) The Role of Oestrogen Receptor Beta (ERβ) in the Aetiology and Treatment of Type 2 Diabetes Mellitus. *Curr Diabetes Rev.*, 15(2):100-104. https://doi: 10.2174/1573399814666180119141836.

Abbreviations

¹H-NMR – proton nuclear magnetic resonance

AA – Aminoacid

AAT – Aminoacid transporter

ABCC8 – ATP-binding cassette, subfamily C, member 8

ACK – Ammonium-chloride-potassium

ADP – Adenosine Diphosphate

AMDIS – Automated Mass spectral Deconvolution and Identification System

AMP – Adenosine Monophosphate

ANOVA – Analysis of Variance

APC – Allophycocyanin

ATP – Adenosine Triphosphate

BCAA – Branched-Chain Amminoacid

BM-DC – Bone-Marrow Derived Dendritic Cells

BMRB – Biological Magnetic Resonance Bank

BSA – Bovine Serum Albumin

cAMP – Cyclic Adenosine Monophosphate

CCK – Cholecystokinin

CD – Cluster differentiation

CDF – Computable document format

D_2O – deuterium oxide

DC – Dendritic Cell

DMSO – Dimethylsulphoxide

DPP-4 – Dipeptidyl Peptidase 4

ECM – Extracellular Matrix

EGTA – Egtazic Acid

Epac – Exchange Protein Activated By cAMP

FA – Fatty acid

FACS – Flow activated cell sorting

FBS – Fœtal Bovine serum

FDA – Food And Drug Administration

FITC – Fluorescein isothiocyanate

GAVIN – GC-MS Assignment Validator and Integrator

GC – Gas chromatography

GC-MS – Gas chromatography-mass spectrometry

GIP – Glucose-Dependent Insulinotropic Peptide

GIPR – Glucose-Dependent Insulinotropic Peptide Receptor

GK - Glucokinase

GLP-1 – Glucagon-Like Peptide 1

GLP-1R – Glucagon-Like Peptide 1 Receptor

GLP-1RA – Glucagon-Like Peptide 1 Receptor Agonist

GLUT2 - Glucose Transporter 2

GM-CSF – Granulocyte-Macrophage Colony-Stimulating Factor

GPCR – G-Protein Coupled Receptor

GPR40 – G-Protein Coupled Receptor 40

HBSS – Hank's Balanced Salt Solution

HPLC – High Performance Liquid Chromatography

HRP – Horseradish peroxidase

HMDB – Human Metabolome Database

IBMX – (3-isobutyl-1-methylxanthine)

INS1 – Insulin 1

IP$_3$ – Inositol Triphosphate

K$_{ATP}$ – ATP-Dependent Potassium Channel

KIR6.2 – Potassium Inward Rectifier Subunit 6.2

KRB – Krebs Ringer buffer

LC-MS – Liquid Chromatography – Mass Spectrometry

LDH – Lactate Dehydrogenase

LPS – Lipopolysaccharide

MALDI-TOF – Matrix-Assisted Laser Desorption/Ionization Time-Of-Flight

MAM$_2$ – Magainin-AM$_2$

MHC – Major Histocompatibility Complex

MOX – Methoxamine

MTBSTFA – N-tert-Butyldimethylsilyl-N-methyltrifluoroacetamide

MTT – 3-(4,5-dimethylthiazol-2-yl)-2,5-diphenyltetrazolium bromide

NADH – Reduced Nicotinamide Adenine Dinucleotide

NEDH – New England Deaconess Hospital

NFkB – Nuclear factor kB

NMR – Nuclear magnetic resonance

NO – Nitric Oxide

PBM – Probability based match

PBMC – Peripheral Blood Mononuclear Cell

PDX-1 – Pancreatic duodenal homeobox 1

PEG – Polyethylene Glycol

PKA – Protein Kinase A

RPMI-1640 – Roswell Park Memorial Institute 1640

SEM – Standard Error Mean

SUR1 – Sulfonylurea Receptor -1

T2D - Type 2 Diabetes

TCA – Tricarboxylic Acid

TEA – Triethanolammine

TFA – Trifluroacetic acid

TGN – Tigerinin-1R

Th1 – Type 1 T-Helper

Th2 – Type 2 T-Helper

TIC – Total ion chromatogram

TLR – Toll-Like Receptor

TMB – 3,3′,5,5′-Tetramethylbenzidine

TNF-A – Tumor Necrosis Factor Alpha

TSP – Trimethylsilylpropanoic acid

VDCC – Voltage-Dependent Calcium Channel

ZDF – Zucker Diabetic Fatty

Acknowledgments

"For the things we have to learn before we can do them, we learn by doing them."

- Aristotle

CHAPTER 1

<u>INTRODUCTION</u>

1. BACKGROUND

1.1 Type 2 Diabetes (T2D): the challenge of a metabolic disorder

Diabetes is a metabolic disease mainly characterized by hyperglycaemia and glucose intolerance, due to disorders ranging from insufficient insulin production by pancreatic beta-cells, ineffective use of the hormone and their combination with several environmental factors (Stumvoll et al., 2005; Kahn et al., 2014).

Despite having similar outcomes, two main types of diabetes have been classified based on their pathogenesis: type 1, caused by insufficient production of insulin, and type 2 which results from a combination of insulin-resistance, sedentary lifestyle and genetic predisposition, among others (Kahn et al., 2014). Type 2 Diabetes (T2D) represents the focus of this work as the disease represents a global issue, with socio-economical implications (Hu, 2011), and underlying causes yet to be fully established.

T2D accounts for the majority (around 90-95%) of diabetes cases globally (Stumvoll et al., 2005; Vetere et al., 2014), with the prevalence of 415 million people predicted for 2030 already being reached at present (Chatterjee et al., 2017). Associated complications, such as microvascular complications leading to amputations, and increased risk of macrovascular events associated with the disease (Sicree et al., 2011) add to its complexity. From a biochemical perspective, persistent high glucose levels react with extracellular proteins generating advance glycation end-products (AGEs), which modify collagen in the extracellular matrix, altering blood vessel function (Brownlee, 2001). This causes release of a number of stress-associated mediators, ultimately leading to beta-cell failure (Boland et al., 2017) and a chronic inflammatory state (Donath & Shoelson, 2011).

Given the pandemic nature of the disease, the complexity of both its diagnosis and treatment, T2D and its associated complications are at the fore-front of biomedical research and translational medicine, with a view to improving global health and alleviating the socio-economical burdens it carries.

1.2 Insulin synthesis and mechanism of secretion

Insulin is a peptide hormone synthesized by pancreatic beta-cells, where it is stored in cytoplasmic vesicles in its most densely packed form and released upon interaction with intracellular calcium ions (MacDonald and Rorsman, 2006). Both its transcription and translation are regulated by glucose. In the short term (8 hours), glucose stimulates proinsulin to be processed to its mature form, replenishing the depleted stores following insulin secretion. On the long term (24 hours), transcriptional regulation occurs, and the mRNA levels of insulin can be affected by circulating levels of glucose (Boland et al., 2017).

The mechanism of insulin secretion is a continuous process occurring due to an oscillatory electrical activity of depolarization and repolarization within beta cells. This is associated with variations in the concentration of calcium ions mainly caused by glucose metabolism (Kanno et al., 2002; MacDonald and Rorsman, 2006). In healthy humans, pancreatic beta-cells are sophisticated glucose sensors with the ability to regulate insulin secretion, according to circulating blood glucose levels, owing to the action of the GLUT1 and GLUT3 transporters. The importance of GLUT1 in the secretory process has been confirmed by using a selective inhibitor for this isoform, which caused a 50% decrease in glucose-stimulated insulin secretion in human islets (Pingitore et al., 2017). In the cytoplasm, glucose is phosphorylated by the glucokinase enzyme (GK) to yield glucose-6-phosphate. This critical step for glycolysis ultimately leads to the production of pyruvate, NADH and ATP, which all contribute to insulin release (Kalwat and Cobb, 2017).

The main pathway for insulin secretion, known as the triggering pathway, is activated by an increase in ATP concentration, mostly deriving from the TCA cycle. It has in fact been reported that pancreatic beta-cells possess lower levels of lactate dehydrogenase in their cytoplasm to favour the entry of pyruvate into the TCA cycle, for an aerobic generation of ATP (Macdonald et al., 2005). The increase in the ATP/ADP ratio causes the closure of the ATP-dependent potassium channels (K_{ATP}), resulting in cell depolarization. The voltage-dependent calcium channels open, increasing the intracellular levels of the ion and the process culminates in the release of insulin from its pre-formed granules (Figure 1.1). Potassium and calcium channels play important roles in balancing electrical activity in beta cells. Following insulin release, the intracellular calcium ions have a net action of repolarizing the cell

membrane by both depleting ATP (Kanno et al., 2002) and directly favouring the opening of the potassium channels after a firing potential (Zhang et al., 2005).

The activity of alpha and beta cells within the pancreatic islets are also controlled by sympathetic and parasympathetic neuronal innervations, which contribute to the amplification pathway. Pioneering studies linking stimulation of sympathetic innervation via the splanchnic nerve to glucose homeostasis were performed in dogs, where stimulation at low (2.0 c/s) and high (10 c/s) frequency showed a positive correlation with increases in plasma glucose concentrations and a near-total inhibition of insulin secretion over a 30-minute period (Bloom and Edwards, 1975). Suggesting sympathetic stimulation inhibits insulin release, this mechanism was later attributed to a calcium-independent action performed at distal sites of insulin secretion in rat pancreatic beta-cells, which showed a reversible suppression of insulin secretion in the absence of extracellular calcium (Yajima et al., 2001). Given autonomic control in beta-cells between humans and other mammals are very similar (Rosario et al., 2016), these networks and pathways highlight the complexity of the regulation of insulin secretion and prompt research towards agents directed towards multiple targets.

Besides glucose, insulin is also released in response to other stimuli such as amino acids and fatty acids. Beta cells possess transport systems for amino acids, and these stimulate insulin secretion either by direct metabolism, resulting in an increase of ATP, due to their cationic nature or through co-transportation with sodium ions that directly depolarize the cell membrane (McClenaghan et al., 1996b). Free fatty acids promote acute insulin secretion by binding and activating the Gq subunit of a G-coupled receptor protein, GPR40, expressed in beta cells (Itoh et al., 2003). Considering they also promote an increase in the glycolytic flux in the mitochondria (Cen et al., 2016), these findings might come across as striking, as the presence of free fatty acids is naturally associated with obesity, an established risk factor for T2D. In Zucker fatty (ZF) rats, which represent a non-diabetic model of hyperlipidaemia and insulin resistance, lipid signalling has been reported to work synergistically with GLP-1 in glucose-stimulated insulin secretion, however, prolonged exposure might be responsible for beta cell failure (Nolan et al., 2006).

With regards to the dynamics of insulin granule exocytosis, linking insulin to a yellow fluorescent protein also revealed the importance of cyclic AMP (cAMP) in the process. In fact, this secondary messenger can directly activate Epac, a protein

involved in processes of exocytosis (Cheng et al., 2008), and promote both docking of the granules in proximity of the plasma membrane and exocytosis (Shibasaki et al., 2007). These aspects emphasize the complexity of the mechanism of insulin secretion (Figure 1.1) and the contribution of different factors to the maintenance of glucose homeostasis. Notably, compounds which can serve as insulin secreting agents also have extra-pancreatic actions (Kastin and Akerstrom, 2003; Ojo et al., 2013). With this project, we also aim to take these effects into consideration, with a view of evaluating how they could potentially aid in preventing and tackling the consequences of T2D.
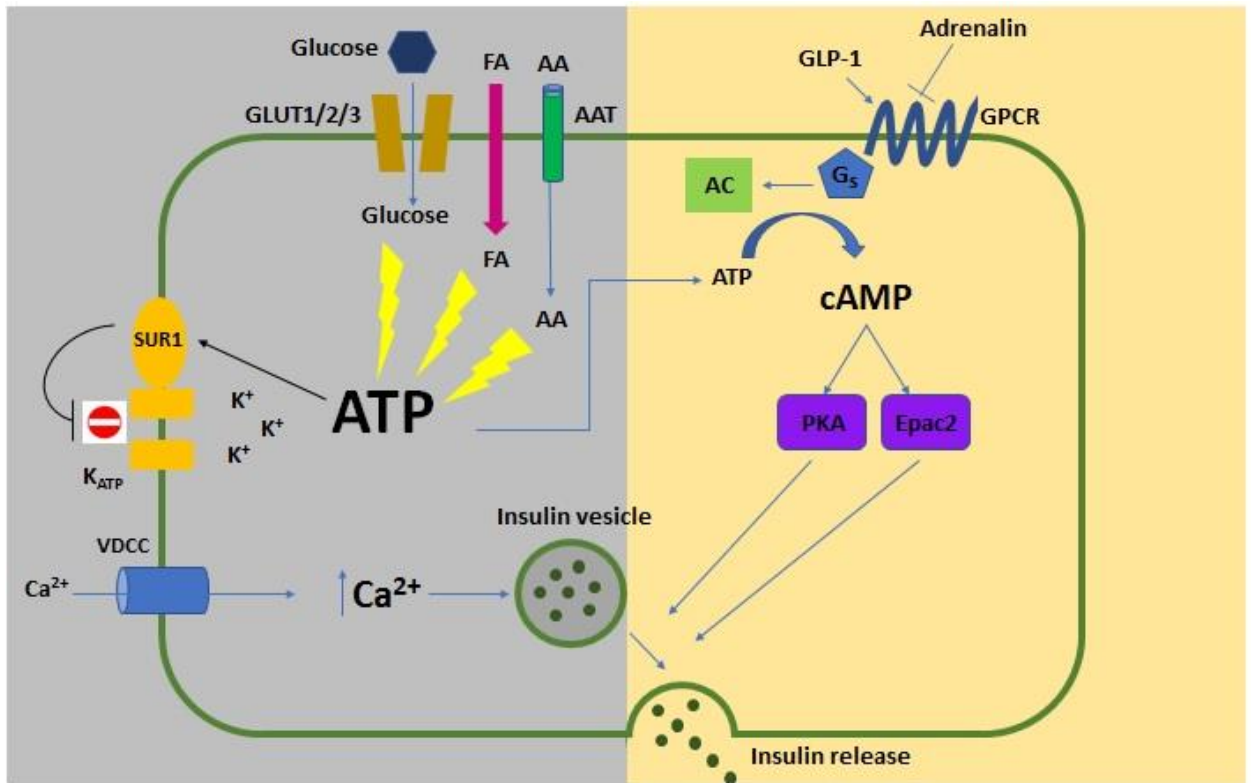
Figure 1.1. Mechanism of insulin secretion.
Glucose, fatty acids and aminoacids belong to the triggering pathway of insulin secretion
(highlighted in grey). Mechanisms responding to the activation of the G-protein coupled
receptors (GPCRs) and activation of intracellular messengers such as cyclic AMP (cAMP)
belong to the amplification pathway of insulin secretion (highlighted in yellow).

1.3 Metabolomics: unravelling biological complexity

Metabolomics analysis, defined as a characterisation of small metabolites resulting from chemical reactions within a system (Tzoulaki et al., 2014), represents a recent approach for assessing and understanding the underlying features of biological complexity. Both quantitative and qualitative information obtainable from metabolomic analysis carry diagnostic potential for complex diseases such as coronary heart disease, cancer and diabetes (Gowda et al., 2008). For T2D, the importance of detecting early changes in metabolites lies in the notion that these take place before overt diabetes is established (Zeng et al., 2009; Sas et al., 2015). Interest in establishing the power of metabolomics in both the prediction and the prognosis of T2D (Klein and Shearer, 2016) led to several studies in this field.

With regards to establishing predictive metabolites, correlating the concentration of branched-chain amino acids (BCAA), such as leucine, valine, tyrosine and phenylalanine with the onset and progression of T2D has positive association (Langenberg and Savage, 2011). A study found that manipulation of the foregut, defined as stomach and duodenum in rats, determined a reduction of tyrosine conversion to levodopa (L-DOPA) and dopamine (DA), neurotransmitters that inhibit insulin secretion as a mechanism for protection from hypoglycaemia (Korner et al., 2019), suggesting measurements of metabolites could potentially be exploited for therapeutic interventions. This is further supported by the possibility to detect changes in levels of these compounds about a decade before the onset of T2D via liquid chromatography-mass spectroscopy (LC-MS) (Wang et al., 2011).

Metabolites have also been studied in further understanding the outcome of the disease. This task is even more challenging, considering the association of T2D with co-morbodities such as retinopathy, renal and cardiac dysfunction that might contribute to altered metabolism (Klein and Shearer, 2016). The limited number of prospective studies in this area show that metabolites, such as BCAA and α-hydroxybutyric acid increased (Klein and Shearer, 2016), which seems to contradict what was observed in predictive studies. This highlights the need to optimize the analysis of metabolites, highlighting differences preceding and following anti-diabetic treatments.

1.4 Therapeutic agents for T2D management

The discovery of insulin in 1921 (Best and Scott, 1923) represents the foundation of diabetes medicine, embodying the first, necessary step towards life-compatible management therapies for the disease. Several anti-diabetic drugs currently on the market for T2D management are aimed at lowering circulating glucose levels to a physiological range (Kahn et al., 2014). Despite being historically classified as "non-insulin dependent", in many cases T2D patients rely on insulin administration where glycaemic control is not achieved by lifestyle interventions alone (Wu et al., 2014).

Among the eight classes of current drugs used, the most common are biguanides (e.g. metformin), α-Glucosidase inhibitors, insulin secretagogues, thiazolidinediones and incretin mimetics. Biguanides and α-glucosidase inhibitors, often administered in combination, have positive effects on glycaemic reduction. The biguanide metformin (traded under the name of Glucophage®, Bristol-Myers Squibb, Princeton, NJ) preserves sensitivity to glucose and reduces gluconeogenesis whereas the α-glucosidase inhibitor, Acarbose (Precose, Bayer Health-Care Pharmaceuticals Inc, Wayne, NJ) slows gastric emptying, giving the pancreas more time to fulfil the increasing demand for insulin (Nyenwe et al., 2011). The class of thiazolidinediones act by regulating storage of free fatty acids via the peroxisome proliferator-activated receptors (PPAR), favouring glucose metabolism over storage of excess fat in the form of adipose tissue (Nanjan et al., 2018).

Ideally, an effective anti-diabetic therapy would target beta-cell function directly, by enhancing its residual ability to secrete insulin (Vetere et al., 2014), while also preventing development of associated complications. Although large clinical trials evaluating the effects of antidiabetic drugs on cardiovascular risk have shown some benefit, as for metformin (Lamanna et al., 2011; Boussageon et al., 2012), or have yielded controversial results, as in the case of thiazolidinediones (Lago et al., 2007; Koska et al., 2013), substantial evidence is presented for GLP-1 receptor agonists. A randomized trial with administration of Semaglutide for 104 weeks showed treatment decreased macrovascular complications by 26% (Marso et al., 2016).

The extra-pancreatic actions of these drugs are relevant to the management of diabetes, and some of these actions will be taken into consideration in this study, with a view to improving the pathophysiology of the disease.

1.5 Incretins and incretin-based anti-diabetic agents

The discovery and characterisation of incretins occurred followed the finding that oral glucose administration stimulated insulin secretion to a greater extent, compared to an intravenous challenge (Drucker, 2006). Incretins are accountable for half of the insulin produced following oral glucose load (Kim & Egan 2008; Hansen et al., 2010).

There are two known incretins conserved among mammals, both acting mainly through G-protein coupled receptors, the glucose-dependent insulinotropic polypeptide (GIP) and glucagon-like peptide 1 (GLP-1), which are released from the K and L-type cells of the intestine, respectively. However, both incretins are subject to early degradation by dipeptidyl peptidase-4 (DPP-4), an enzyme naturally occurring in the bloodstream which keeps their half-life between 1 and 1.6 minutes (Hansen et al., 2010). Different modifications of both GIP and GLP-1 have been studied with a view to overcoming DPP-4 degradation while retaining the anti-diabetic potential of the native forms (Irwin and Flatt, 2013). This approach has shown promising results for both GIP and GLP-1, which we are going to discuss separately below.

1.5.1 Glucose-dependent insulinotropic polypeptide (GIP)

Initially isolated from a porcine model as an inhibitor of gastric acid secretion (Seino et al., 2010), levels of released GIP have been reported to remain unaltered in T2D (Aaboe et al., 2009), even though earlier studies supported the inability of GIP to retain insulinotropic activities in T2D (Nauck et al., 1993).

More recent evidence has pointed to an improvement in glucose tolerance and adipose tissue metabolism following disruption of the GIP receptor in high-fat fed mice (Irwin and Flatt, 2009), further opposing any antidiabetic effect related with the peptide. However, the truncated form of GIP (GIP(1-30)) was later found to stimulate insulin secretion, without promoting GIP signalling in 3T3-L1 adipocytes, and restored glucose metabolism for up to 48 hours in obese, diabetic rats in which the native GIP had little effect (Widenmaier et al., 2010). This strongly suggests that the GIP(1-30) form could have anti-diabetic effects while preventing lipid metabolism impairment.

Alongside this, chemical modifications allowed for enhanced activity or resistance to degradation, providing further evidence for pre-clinical success of GIP. N-terminus modifications (N-acetyl-GIP and N-pyroglutamil-GIP) have contributed to increasing the half-life of the peptide above 24 hours and confer improved glucose tolerance to diabetic mice, compared to the native form of GIP (O'Harte et al., 2002).

Receptor binding studies in Chinese Hamster Ovary (CHO) cells transfected with the GIP receptor (GIPR) enabled the characterisation of amino-acid substitutions yielding DPP-4 resistant peptides and retaining binding affinity to GIPR (Hinke et al., 2002). One of the analogues, termed d-Ala^2-GIP(1-30) in its truncated form retaining insulinotropic activity *in vitro*, enhanced glycaemic control in diabetic mice, further highlighting the effectiveness of this analogue (Gault et al., 2011).

The ability of incretins to stimulate insulin release in a glucose-dependent fashion, together with the discovery of new, more potent analogues of GIP, could have potential to be exploited for therapeutic purposes in diabetes. To this end, we selected the stable analogue d-Ala^2-GIP(1-30) as a component of the hybrid peptides selected for this study, in order to extend its potential to different aspects of the pathogenesis of T2D.

1.5.2 Glucagon-like peptide 1 (GLP-1)

The role of GLP-1 in regulating beta-cell function and metabolism has been extensively characterised. It is known to decrease the production of glucagon from alpha-cells, to promote beta-cell proliferation and preservation while controlling ER stress (Yusta et al., 2006). The main downstream signalling pathway from the activation of its receptor (GLP-1R) involves the activation of cyclic AMP (cAMP), PKA and the increase of intracellular Ca^{2+} via channels found on the cell surface membrane and those gating intracellular stores (IP_3 receptors) on the endoplasmic reticulum (Jones et al., 2018) (Figure 1.2).

The presence of GLP-1R in several different tissues, including the central nervous system and the duodenum, allows for the actions of GLP-1 to relate to the gut-brain axis, with regulation of some behaviour such as food intake and sense of satiety as evidenced by the response of vagal neurons to different degrees of proximal intestine distention (Drucker 2018). Moreover, the production of the gut hormone gherlin, which is involved in stimulating appetite and food intake, undergoes a significant reduction following GLP-1 administration. Although this appears to be an indirect effect, correlating with the levels of insulin rather than GLP-1 itself (Hageman et al., 2007), GLP-1 and gherlin levels have been found to be good predictors of lipid reduction as a measure of cardiovascular risk control, as well as good predictors of the outcome of GLP-1R agonists therapy (Babenko et al., 2019).

The identification of another pathway downstream of the GLP-1 receptor involving the activation of β-arrestins via the G_S-subunit of the receptor, which are also critical in the insulin-secretion process (Zhang et al., 2015) hints to the possibility of creating "biased agonists" with functional selectivity towards one of the signals downstream of the receptor, with a view to controlling existing therapeutic side effects. However, the success of GLP-1R agonists as therapeutic option for T2D is met with the limitation of not being effective for about 30-50% of patients, who are not able to restore normoglycaemia and insulin sensitivity (Babenko et al., 2019).
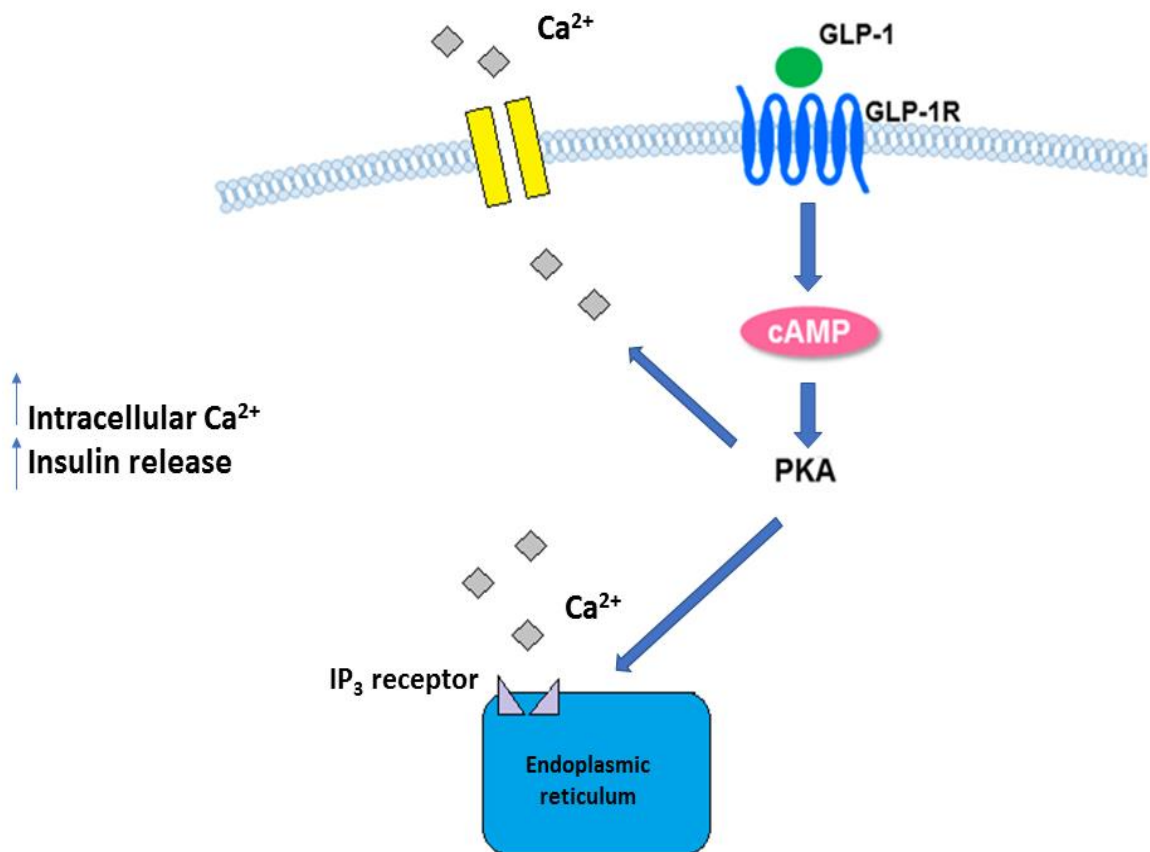
Figure 1.2. Main pathway for GLP-1 receptor signalling.
GLP-1 binds to its G-protein coupled receptor (GPCR) causing the activation of protein kinase A (PKA). This messenger activates both intracellular (IP3) and cell membrane Ca^{2+} receptors, causing an increase of Ca^{2+} within the cells and consequently increased insulin release.

1.6.Naturally occurring peptides as therapeutic agents for Type 2 Diabetes

1.6.1 The importance of exendin-4

In the early 90s, chemical assays identified exendin-4, which caused pancreas enlargement and triggered insulin release from beta-cells ("National Institute of Health", 2017). Originally isolated from the saliva of the Gila monster lizard (*H. suspectum*) (Eng et al., 1992), exendin-4 is a biologically active compound harbouring 53% of homology with GLP-1 (Drucker 2006; Hansen et al., 2010) and is an FDA approved anti-diabetic drug since 2005 (Byetta ®, AstraZeneca).

Following the identification of exendin-4, early studies focused on comparing its action to that of native GLP-1 using *in vitro* and *in vivo* models to also take into consideration pharmacokinetics differences between the two peptides. With regards to insulin secretion, exendin-4 was more efficient in stimulating insulin secretion *in vitro* (both static and perfusion incubations with rat islets), and *in vivo*, with the biggest differences being observed for exendin-4 as opposed to GLP-1 (Parkes et al., 2001). Another important difference between the two compounds is that exendin-4 is considered a poor substrate for DPP-4 and other endopeptidases. In pigs, it has been shown that exendin-4 is mainly cleared by glomerular filtration, as opposed to GLP-1 that is enzymatically cleaved (Simonsen et al., 2006).

The generation of this drug came as a result of two apparently unrelated events: the development of the incretin concept and the ongoing research on compounds in the Gila monster venom (Furman, 2012). This discovery caused two important shifts, in terms of diabetes therapy. One is the study and design of GLP-1 receptor agonists to mimick the effects of exendin-4, and the other is the screen of animal-derived compounds, in search for potent and targeted biological activities. Studies conducted on human subjects evaluating the effects of synthetic exendin-4 (Exenatide) on vascular function and metabolism showed that acute postprandial vascular dysfunction in diabetes can be rescued by GLP-1 receptor agonists via an increased production of NO (Torimoto et al., 2015). Exendin-4 also promotes extra-cellular matrix (ECM) remodelling by modulating the Akt/GSK-3β signalling in ventricular and atrial cardiomyocytes (Robinson et al., 2015).

Again, a synthetic form of exendin-4, AC2993, was reported to reduce plasma fasting and postprandial levels of glucose in T2D patients, through its multiple effects on reducing glucagon secretion and slowing gastric emptying (Kolterman et al., 2003). Reduction of glucagon secretion is independent of the insulinotropic

action of the peptides (Ahrén 2005), further highlighting the multiple actions of this important GLP-1RA.

These reports and the documented use of Exenatide in the clinic (Advani et al., 2013; Kim and Egan 2008) with minor adverse effects (Hansen et al., 2010) demonstrate the power of incretin-based therapies in T2D and highlights the potential therapeutic benefits of naturally occurring compounds.

1.6.2 Amphibian skin peptides with anti-diabetic potential

Research focusing on the pharmacological potential of amphibian skin peptides was initiated in the 1980s, when Erspamer and Melchiorri (1980) chemically assayed skin extracts and found a vast array of bioactive compounds belonging to different families, including bradykinins, caerulins and bombesins. These drew much attention due to the presence, in most cases, of mammalian counterparts belonging to the gut-brain axis (Erspamer and Melchiorri, 1980; Marenah et al., 2006). Biological actions of amphibian skin peptides have been extensively studied and exhibit anti-inflammatory and antimicrobial effects (Pukala et al., 2006). An important example of this was the discovery of xenopsin-like peptide in mammals. Naturally present in the amphibian skin secretion, similar compounds have been found in rats and avian models and immunohistochemical studies show the presence of a similar peptide in the human gut, specifically with the six C-terminal amino acids identical to xenopsin. More importantly, this peptide, denoted xenin-25, is secreted into the bloodstream in response to a glucose-load and has a stimulatory effect on the exocrine pancreas (Feurle et al., 1992).

Given the involvement of the gut in the regulation of insulin secretion and energy regulation (Marenah et al., 2004; Irwin and Flatt 2013), amphibian skin peptides have also been considered for potential anti-diabetic actions. Preliminary studies on skin secretions of the toad *Bombina variegata* were conducted with a focus on establishing the role of bombesin-like peptides in stimulating insulin release *in vitro*. Results from this analysis showed that the mammalian counterpart retained homology with the C-teminus, which contains the biological activity of bombesin, and stimulated insulin release to an extent comparable to those of other gut-associated secretagogues such as GIP, GLP-1 and cholecystokinin (CCK) (Marenah et al., 2004).

However, not all peptides with insulinotropic actions are antimicrobial peptides. In fact, a member of the phylloseptin family, phylloseptin-L2, was found to stimulate insulin secretion to levels comparable of tolbutamide and GLP-1, despite not having any gut mammalian counterpart or a strong antimicrobial activity (Abdel-Wahab et al., 2008), suggesting different peptides could be potential candidates for insulinotropic studies. Fractions from the skin of the *Rana saharica* frog were chromatographed twice to reveal 4 peptides belonging to the brevinin (brevinin-1E and -2EC) and esculentin (esculentin-1 and -1B) families with insulinotropic actions.

The results from studies of these peptides, which are known for antimicrobial activities, led to further characterization of other species of frogs and toads, in order to exploit the variety of pharmacologically active peptides in the quest for new therapeutic options for diabetes (Marenah et al., 2006).

Brevinin-2-related peptide, for example, isolated from *Lithobathes septentrionalis* was reported for its insulinotropic actions, and its analogue with increased cationicity generated by Asp→Lys substitution was associated with increased antimicrobial and insulinotropic activity (Abdel-Wahab et al., 2010). This suggests that the action of amphibian peptides might be potentiated by increasing their cationicity, possibly due to a better interaction with the phospholipid bilayer of cell membranes.

1.6.2.1 Tigerinin-1R (TGN)

In light of the successful isolation and characterization of different frog skin secretions with insulin-releasing potential, such as brevinin-1 (Marenah et al., 2004) and phylloseptin-L2 (Abdel-Wahab et al., 2008), the same rationale was applied to other species of frogs producing dermal secretions with biological activities. Skin extracts of the Asian common lowland frog (*Hoplobatrachus rugulosus*) were purified and screened for insulinotropic peptides. Purification by HPLC revealed a peptide displaying insulinotropic activities which were not associated with increased cytotoxicity. The identified peptide presented structural similarities to the tigerinin family and was termed tigerinin-1R (Ojo et al., 2011). Tigerinin-1R stimulated insulin secretion in the clonal BRIN-BD11 cell line, at concentrations as low as 0.1 nM at both physiological (5.6 mM) and high (16.7 mM) glucose concentrations (Ojo et al., 2011), an essential feature for a valid candidate for T2D therapy.

The acute anti-diabetic actions of tigerinin-1R, were further supported by enzymatic stability assays and long-term *in vivo* studies. Tigerinin-1R remained intact up to 8 hours when incubated with plasma enzymes and despite not having effects on food intake behaviour, as with GLP-1 receptor agonists, tigerinin-1R improved glucose tolerance. This was achieved by reducing plasma glucose and increasing insulin over 60 min following treatment, and long-term studies also showed no association to toxicity (Ojo et al., 2015c), highlighting its role in maintaining safe glucose homeostasis.

Structure-activity studies also determined the importance of structural properties within tigerinin-1R in exerting its biological activities. With regards to insulin release, increase in cationicity by aminoacid substitution to generate [S4R] and [H12K] analogues of tigerinin resulted in a greater maximum response in both BRIN-BD11 cell line and primary pancreatic islets (Srinivasan et al., 2014). Increased hydrophobicity of tigerinin-1R was also shown to favour the anti-diabetic actions of the peptides. The effectiveness and potency of the *in vitro* actions of the [I10W] substitution were extended *in vivo*. In high-fat fed NIH Swiss mice, [I10W]tigerinin-1R had the additional benefit of determining weight loss as part of its anti-diabetic action following twice daily administration (Srinivasan et al., 2016).

Taken together, these results show the potential of tigerinin-1R and its modified analogues for further studies in the field of T2D therapy, exploiting the properties and findings described above as a strong rationale for these investigations.

1.6.2.2 Magainin-AM$_2$

Within the family of Xenopus, the African claw frog, a class of glycine-leucine-amide peptides (PGLa) orthologs, termed magainins, were isolated. Specifically, in *X. amieti*, the peptides had been initially characterised for their antimicrobial activity (Matsuzaki, 1998), with magainin-AM$_1$ being the most potent, and magainin-AM$_2$ being the most abundant (Conlon et al., 2010). With regards to insulin secretion, magainin-AM$_1$ and magainin-AM$_2$ exhibited insulinotropic actions *in vitro*, with magainin-AM$_2$ yielding a superior result (Ojo et al., 2015a).

Magainin-AM$_2$ (MAM$_2$) stimulated insulin release in BRIN-BD11 cells in a concentration-dependent manner, in range from 3 nM to 3 μM, with no associated cytotoxicity (Ojo et al., 2015a). The stability of the peptide in murine plasma for at

least 8 hours, also corresponded to potent *in vivo* actions. Glucose tolerance was improved through a 20% reduction in plasma glucose following peptide administration, and as a 1.8-fold increase in insulin secretion in high-fat fed mice. (Ojo et al., 2015a).

Further to this, the ability of amphibian skin peptides such as TGN and MAM$_2$ to induce secretion of GLP-1 was also investigated. Both peptides were found to increase the secretion of GLP-1 from a proglucagon precursor in the GLUTag cell line (Ojo et al., 2013). This strengthens the anti-diabetic potential of these peptides and opens the possibility of both TGN and MAM$_2$ causing the long-term actions on beta-cell function that could be further investigated and exploited *in vivo* (Ojo et al., 2013).

1.7 The therapeutic potential of peptides

After its decline in the late 90s, due to a general preference in using biologics such as antibodies, the use of peptide leads in drug discovery is currently gaining momentum and peptide hormones, including oxytocin, desmopressin and modified versions of GLP-1 are currently on the market (Henninot et al., 2017). Large and small pharmaceutical companies are investing in peptide drug discovery, especially venom peptides, due to both their potent and targeted activities but also their cyclic structure that confers stability (Henninot et al., 2017, Table 1.1).

Though peptides can elicit acute biological function and rapid cell responses, an important limitation identified in the field of peptide drug discovery is their short half-life (Wang et al., 2019). Numerous efforts have been made to increase peptides half-life, by conjugation with larger molecules serving as protection against enzymatic cleavage. An example of efforts in prolonging half-life in antidiabetic peptides was presented with xenin-25(Lys^{13}PAL). This analogue of the anti-diabetic agent naturally occurring in human duodenum (Craig et al., 2018) possesses a derivatised fatty acid chain strategically positioned as to not mask the regions crucial for peptide activity. Xenin-25(Lys^{13}PAL), maintained the anti-diabetic actions of its native peptide xenin-25 whilst being resistant to plasma degradation *in vitro* (Gault et al., 2015), providing strong support to the therapeutic potential of this modified peptide. Moreover, an additional stimulatory effect towards (d-Ala^2)-GIP actions

both *in vitro* and in diabetic mice models *in vivo* was reported for the modified peptide (Martin et al., 2012).

Another promising option for higher peptide efficacy is the conjugation of polyethylene glycol (PEG), a biologically inert and hydrophilic molecule, to a known bioactive compound. By taking into consideration the ability of PEG-conjugates to remain intact in circulation and be released only *in situ* by activating mechanisms such as pH and enzymatic activity, the potential of these modified polymers could have enormous fields of application (Banerjee et al., 2012). The increased half-life *in vivo*, together with reduced immunogenicity, makes PEGylation an interesting option for T2D therapies, especially given that these are the limitations often known to cause treatment failure (Harris and Chess, 2003). GIP was selected for PEGylation due to its early degradation by the DPP-4 enzyme, but especially for the rapid renal clearance of its metabolites, which had not been fully addressed (Gault et al., 2008). As a strategy to avoid possible immunogenicity of conjugates, a mini-PEGylated form of GIP was tested for its anti-diabetic potential in comparison to its native counterpart. GIP[mPEG] maintained the glucose-lowering potential of GIP alone, with the added advantage of increased bioactivity, measured as a lower EC_{50} for cAMP production (Gault et al., 2008).

The enzymatically stable cholecystokinin (pGlu-Gln)-CCK-8 conjugated with a mini-PEG molecule, did not display a reduction in appetite control compared to the native, unPEGylated form. Further to this, the modified (pGlu-Gln)-CCK-8[mPEG] conferred prolonged metabolic control, and a twice-daily administration did not induce tolerance that could diminish its efficacy *in vivo* (Irwin et al., 2013). In light of these properties, PEGylation was also explored in the creating hybrid peptides.

One of the first promising examples in this context was the idea of creating a potent GLP-1 receptor agonist that could also antagonise the actions of glucagon, known to increase gluconeogenesis and glycogenolysis and increase glycaemic levels. After detailed structure-activity studies, a GLP-1 agonist and a glucagon antagonist were joined without significantly affecting their receptor binding activity. C-terminal PEGylation of the novel hybrid peptide allowed for an increased half-life, by masking the enzymatic cleavage site, and preventing renal filtration (Pan et al., 2006).

A GLP-1:CCK fusion protein, designed with a mini-PEG linker interconnecting the two peptides was studied following previous knowledge of safe and synergistic anti-diabetic effects of a similar hybrid (Irwin et al., 2015).

The synergistic effect was confirmed and by keeping the functional C-terminus of CCK untouched, a greater action on food intake reduction was observed in GLP-1R KO mice (Hornigold et al., 2018), suggesting that the available portion for CCK might bind to its receptor and contribute to the additive effect.

Taken together, these findings represent a promising route in peptide drug discovery for type 2 diabetes, encouraging studies that lead into the rationale for our peptide design for this project.

1.8 T2D and inflammation

Inflammation represents an important aspect of T2D (Wellen and Hotamisligil, 2005; Nunemaker, 2016; O'Neill et al., 2013), through which the disease can also be viewed as an exacerbation of a metabolic syndrome characterised by a chronic inflammatory state (Eguchi and Nagai, 2017). Overall, this feature is hypothesised to be either the cause or the consequence of the observed cellular stress (Donath and Shoelson, 2011) reflected in the increasingly sedentary lifestyle (Kolb and Mandrup-Poulsen, 2010) of people living with the disease. At the molecular level, in altered lipid metabolism, cytokines released by the adipose tissue serve as ligands for Toll-like receptors (TLR) in the activation of an immune response (Nicolajczyk et al., 2011). Moreover, cardiovascular complications arising from diabetes have inflammatory nature, as components found in the atheroma of plaques are involved in the process (Yao et al., 2011), further supporting the role of lipogenic factors in perpetuating diabetes associated complications.

However, it is important to take into consideration the consequences of abnormal glucose tolerance and hyperglycaemia on the immune system. In fact, the inflammatory milieu deriving from the increase in adipose tissue mass in obese individuals represents a risk factor for T2D, but not a direct causality. Inflammation in T2D can have different causes, including hypoxia where the shortage of oxygen promotes angiogenesis (Donath and Shoelson, 2011), and beta-cell dysfunction itself. *In vitro*, the creation of a type 2 diabetic environment by treating pancreatic clonal cell lines MIN-6 and INS-1 with 33 mM glucose concentrations or palmitate (0.5 mM) resulted in about 2-fold increase of inflammatory cytokines, including IL-6

and IL-8 (Ehses et al., 2007). This same result was also observed in islets directly isolated from type 2 diabetic patients highlighting the role of islets in mediating the inflammatory response in diabetes and increasing the number of circulating macrophages (Ehses et al., 2007).

A human prospective study evaluating the effects of cytokines on the risk of developing type 2 diabetes highlighted the importance of IL-1β and IL-6 as contributors to reduced glucose-stimulated insulin secretion and to beta-cell failure (Spranger et al., 2003). Actions of cytokines in normo-glycaemic conditions are not directly linked to the pathogenesis of the disease (O'Neill et al., 2013). This indicates the importance of studying inflammation as an environment where changes in both antigen-presenting ability of immune cells and cytokines play significant roles in the development of type 2 diabetes.

The decline in beta-cell function associated with macrophage infiltration has been extensively related to obesity (Ying et al., 2019), however another inflammatory mechanism is activated in response to chronic hyperglycaemia as well. Evaluating its contribution to gene expression patterns and cytokine release, hyperglycaemia was in fact shown to directly induce inflammation after a 6-week culture of macrophages in the presence of 25 mM glucose (Morey et al., 2019). These findings indicate that T2D and inflammation are linked by both obesity and free fatty acids, and chronic high blood glucose concentrations.

The role of inflammation in the pathophysiology of T2D was first described as a link to obesity. Evaluating the role of cytokines in metabolic disease, specifically starting from the adipose tissue, was prompted by the role of adipocytes in energy storage and metabolism (Hotamisligil et al., 1993). Increased mRNA levels of TNF-α from the adipose tissue of obese, diabetic (db/db) mice were detected, and antagonizing the TNF-α receptor resulted in improved insulin sensitivity *in vivo*. Though this model links obesity to insulin resistance, subsequent studies extended the inflammatory component of diabetes beyond the adipose tissue. The activation of the inflammatory pathway of NFkB following exposure of rodent islets to the inflammatory cytokine IL-1β was attributed to high glucose concentrations (33 mM) in human islets of T2D patients (Maedler et al., 2002). The induction of IL-1β was also shown to accompany development of T2D in *Psammomys obesus*, when switched to the high energy diet for the generation of the disease (Maedler et al., 2002). Overall, the increased metabolic activity of beta-cells generated by high

glucose concentrations disrupts their secretory function, ultimately leading to their distruction in conjunction with an exacerbated inflammatory state (Donath et al., 2019).

For these reasons, anti-inflammatory agents have been considered as therapeutic options for T2D and have already been studied in clinical trials. The anti-inflammatory compound, salicylate, was shown to stimulate insulin secretion in obese, non-diabetic patients (Koska et al., 2009). Similarly, following treatment with anakinra, a drug used to treat rheumatoid arthritis, glycaemic control and beta-cell secretory function improved in T2D subjects by the drug's antagonist action on IL-1 receptor (Larsen et al., 2009).

Given their function in protecting amphibians from environmental pathogens (Mangoni, 2011), the recently uncovered anti-diabetic effects of frog skin peptides have been investigated for similar potential in modulating inflammatory responses. Amphibian skin peptides present chemoattractant properties towards phagocytes in human peripheral blood cells, and they are known to also participate in skin repair and to activate macrophages and cellular mediators of the immune response in mammals (Pantic et al., 2017).

1.8.1 Anti-diabetic peptides and inflammation

The main features observed under the chronic inflammatory state that characterizes T2D include the infiltration of immune cells, and more specifically islet macrophages. Evidence was provided by studies considering the number of infiltrating macrophages within pancreatic cells from db/db, Goto-Kakizaki and high fat fed mice, and by the role of the cellular environment created by T2D in releasing pro-inflammatory cytokines such as IL-6 and IL-1β (Ehses et al., 2007).

As inflammation is also defined by an environment where changes in both antigen-presenting ability of immune cells and cytokines play significant roles (Banchereau and Steinman, 1998), anti-diabetic agents have also been studied for their ability to modulate immune responses.

By considering the feature of wound healing, often compromised and leading to ulcers in T2D (Wu et al., 2014), it was found that exendin-4 promotes wound healing in Zucker diabetic fatty mice (ZDF) fibroblasts (Wolak et al., 2019). The same peptide displays anti-inflammatory actions in both the nervous (Teramoto et

al., 2011) and the cardiovascular system (Advani et al., 2013), highlighting its systemic anti-inflammatory actions.

Given their function in protecting amphibians from environmental pathogens (Mangoni, 2011), the recently uncovered anti-diabetic effects of frog skin peptides have been investigated for similar potential in modulating inflammatory responses. Amphibian skin peptides present chemoattractant properties, they are known to participate in skin repair also in mammals and to activate macrophages and cellular mediators of the immune response (Pantic et al., 2017). Among the amphibian peptides with anti-diabetic properties characterized also for their ability to modulate inflammation, esculentin-2CHa increased the production of the pro-inflammatory cytokine, TNF-α, from murine macrophages only where these were not activated by lipopolysaccharide (LPS) and with no effect on IL-1β or IL-6. In the same study, the production of anti-inflammatory cytokine IL-10 was increased in both the absence or presence of the activating stimulus for the release of this cytokine, concanavalin A (Attoub et al., 2013). This suggests esculentin-2CHa could potentially reduce inflammatory markers during infection, while potentiating the innate immune response (Attoub et al., 2013).

Similarly, TGN increased the production of IL-10 both in murine peritoneal macrophages and human PBMCs, suggesting the anti-inflammatory actions of the peptides are not organism or specific to one cellular model (Pantic et al., 2014). This prompted us to focus on the anti-inflammatory cytokine IL-10 in a cellular model that is different from macrophages, in order to understand whether the actions observed for the aforementioned peptides were applicable to our novel hybrids and could be extended to yet another cellular model of antigen-presenting cell, as discussed in the sections that follow.

1.9 Cellular models used for the study

1.9.1 BRIN-BD11 cell line

The BRIN-BD11 cell line was created by cellular electrofusion between RINm5f cells (rat insulinoma) and New England Deaconess Hospital (NEDH) pancreatic islets. This reflected the need to explore features of a tumorigenic cell line, such as immortality and rapid expansion, together with an uncompromised insulin biosynthesis machinery (McClenaghan et al., 1996a; McClenaghan, 2007).

In fact, this cell line is reported to overcome the long-term variation in insulinotropic potential observed in primary cells due to progressive degradation of insulin stores in these models (McClenaghan and Flatt, 1999).

With an intact glucose-sensing mechanism, confirmed by the presence of GLUT2 and glucokinase (McClenaghan et al., 1996b), BRIN-BD11 also responds to depolarising agents such as KCl (McClenaghan et al., 1996a) and amino acids (McClenaghan et al., 1996b). Charged amino acids such as L-lysine and L-arginine directly induce cell depolarisation (McClenaghan et al., 1996b), while the neutral L-Alanine displays insulinotropic activity by co-transport with Na^+, resulting in an overall more efficient cell depolarisation (McClenaghan et al., 1998; Cunningham et al., 2005). Early studies using the amphibian peptide brevinin-1 in this cellular model allowed a bioassay-led purification of insulinotropic fractions from crude extract of *R. Palustris* frogs (Marenah et al., 2004), paving the way to numerous studies using similar experimental conditions as part of an initial peptide screen (Ojo et al., 2011; Moore et al., 2015; Ojo et al., 2015a; Conlon et al., 2018; Tapadia et al., 2019; Mechkarska et al., 2019).

Studies regarding broader metabolic reprogramming, by investigating changes in parameters such as lactate production and ATP content in the presence of exendin-4 were also successfully performed in BRIN-BD11 cells (Carlessi et al., 2017). The extensive characterisation of this cell line and the efficient glucose and peptide responsiveness of this cell line justifies our choice in selecting it for the majority of the studies here reported, starting from the initial screen for insulinotropic actions of the novel peptides.

1.9.2 Primary mouse pancreatic islets

Though the properties of isolated primary cell cultures have a limited life span *in vitro* as opposed to immortalised cell lines, they represent a more sophisticated model for extending observations performed on a tumorigenic cell line. We aimed to take into consideration how the peptides function in isolated islets, which are made up of a more heterogenous population of cells including alfa, beta, delta and epsilon cells. A commonly used protocol for pancreatic islet isolation was initially defined by Lernmark (1974) and details of its adaptation to our study are described in in section 2.1.5.With this technique, islets were dispersed from their connective tissue

and they can be individually picked and assayed for insulin release under different conditions.

1.9.3 Bone marrow-derived dendritic cells (BM-DCs)

Dendritic cells (DCs) are potent antigen-presenting cells produced by the haemopoietic bone marrow in an immature state. Extensive characterisation is reported for type 1 diabetes, where a small proportion of dendritic cells, together with macrophages are shown to uptake beta-cell antigens deriving from secretory granules and present them to CD4^{+} T-cells (Calderon et al., 2014). DCs are generally responsible for maintaining immune system homeostasis, directing innate and immune responses (Mbongue et al., 2017). The mechanism by which DCs present antigens exploits their ability to internalise, process and present antigens upon maturation. The activation of DCs is accompanied by the upregulation of their surface markers major histocompatibility complex II (MHC II), CD80 and CD86 and determines their maturation and migration towards spleen and lymph nodes to present antigens to naïve T-cells. This process involves the secretion of cytokines, mainly IL-10 and IL-12, that determine polarisation of T-cells towards and anti-inflammatory or pro-inflammatory type (Mbongue et al.,2017) (Figure 1.3).

One of the shortcomings of using dendritic cells to study antigen-presenting ability, as well as the cytokine environment they generate, is their small number and expense associated with their isolation (Roney, 2013).

Alternative methods have been generated, which are based on the induction of bone-marrow derived monocytes into a population of cells bearing phenotypical features of dendritic cells using the granulocyte/macrophage colony stimulating factor (GM-CSF) (Inaba et al., 1992). Details of the protocol used for the study are described in section 2.5.1.

The possibility to generate millions of cells from one mouse makes this technique particularly advantageous for studying the response of this class of antigen-presenting cells to different stimuli (Inaba et al., 1992). In our study this model was particularly relevant for the establishing the effects of the hybrid peptides on the phenotype and cytokine release associated with DCs activation.
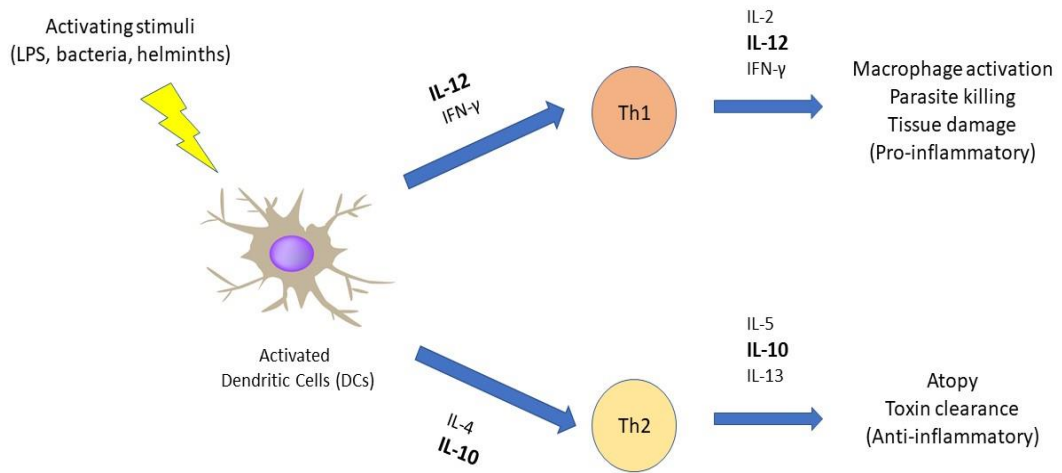
Figure 1.3. Schematic representation of DC activation.
Upon activation, DCs release cytokines associated with the stimulation of a Th1 or Th2 polarization of T-helper cells. These are associated with a pro-inflammatory and anti-inflammatory response, respectively.

AIM & OBJECTIVES OF THE STUDY

The aim of the study is to characterize the anti-diabetic potential of novel hybrid peptides, created by joining exendin-4 or d-Ala^2-GIP with the selected amphibian skin peptides TGN and MAM$_2$. The rationale behind this study is the possibility of enhancing the anti-diabetic actions of previously established incretin analogues. Specific objectives include:

1)   Assessment of the insulinotropic actions of the peptides and how they compare to their native incretins (exendin-4 or d-Ala^2-GIP), in both BRIN-BD11 cells and primary islets. Loss of cell viability and cytotoxicity were also be considered

2)   Evaluation of the mechanism of action of the peptides. This will consist in establishing the insulinotropic activities of the peptides in the presence of modulators of insulin secretion, or in the absence of extracellular calcium to gain insight on their mechanism of action.

3)   Studying the action of exendin-4 on metabolites in both intracellular and extracellular spaces. Metabolomics analysis in BRIN-BD11 using gas chromatography-mass spectrometry (GC-MS) for intracellular metabolites and proton nuclear magnetic resonance (^{1}H-NMR) for metabolites in the supernatant.

4)   Gene expression analysis using real-time PCR (RT-PCR) on genes related to the main pathway of insulin secretion, and comparison to the actions of exendin-4.

5)   Immunomodulatory studies to assess the effects of the peptides on the activation of the antigen-presenting model of bone marrow derived dendritic cells (BM-DCs). The actions were assessed according to the phenotype of BM-DCs, as well as their cytokine release profile.

CHAPTER 2

<u>MATERIALS AND METHODS</u>

2.1 PEPTIDE SCREENING

2.1.1 Peptide structural design and synthesis

The peptides used in this study contain different combinations of known incretin analogues (exendin-4 (E) and d-Ala-GIP (G)), and selected amphibian skin peptides with reported insulinotropic activities (tigerinin (TGN) and magainin-AM$_2$ (MAM$_2$). Peptide design was conducted with a view to maintaining basic structural properties of the native peptides while potentiating their activity by combination. The inert polyethylene glycol (PEG) molecule was chosen as a linker between peptides. Following the design, amino acid sequences for each peptide were commercially synthesised (Synpeptide Co. Ltd., Shanghai, China). Details about the peptides sequence are presented in Table 2.1.

Table 2.1 List of peptides synthesised for the study by Synpeptide Co. Ltd.

Peptide name	Peptides joined	Sequence	Mass (Da)
exendin-4	exendin-4 only	HGEGTFTSDLSKQMEEEAVRLFIEWLKNGGPSSGAPPPS-NH2	4186.63
E-TGN	exendin-4 + tigerinin-1R	HGEGTFTSDLSKQMEEEAVRLFIEWLKN-(PEG)3-RVCSAIPLPWCH-NH2	4847.84
E-MAM₂	exendin-4 + magainin-AM₂	HGEGTFTSDLSKQMEEEAVRLFIEWLKN-(PEG)3-GVSKILHSAGKFGKAFLGEIMKS	5873.02
GIP	d-Ala-GIP(1-30) only	YAEGTFISDYSIAMDKIHQQDFVNWLLAQK-NH2	3531.99
G-TGN	d-Ala-GIP(1-30) + tigerinin-1R	YAEGTFISDYSIAMDKIHQQDFVN-(PEG)3-RVCSAIPLPWCH-NH2	4345.22
G-MAM₂	d-Ala-GIP(1-30) + magainin-AM₂	YAEGTFISDYSIAMDKIHQQDFVN-(PEG)3-GVSKILHSAGKFGKAFLGEIMKS	5370.41
TGN	tigerinin-1R only	RVCSAIPLPWCH	1380.70
MAM₂	magainin-AM₂ only	GVSKILHSAGKFGKAFLGEIMKS	2405.89

2.1.2 Peptide purity check

The purity of commercially synthesised peptides was checked by reverse-phase high performance liquid chromatography (HPLC), using an Agilent Technologies® 1200 system. Peptides were chromatographed on a C18 column (ZORBAX® Eclipse XDB-C18) equilibrated with 0.12% TFA/water (solvent A). The solvent for peptide separation was 0.1%/29.9/%70% TFA/water/acetonitrile solvent (B). The column's temperature was kept at 20°C. Peptides were reconstituted in 0.001N HCl, at a concentration of 1 mM or 100 µM. For each peptide, a 50-minutes run was performed in triplicates with the concentration of acetonitrile increasing from 0% to 21% over 10 minutes and from 21% to 56% over the following 25 minutes at a flow rate of 1 mL/min. The concentration was increased to 70% over 5 minutes and maintained constant for the same amount of time. Absorbance was monitored by UV detection at wavelengths of 254 and 280 nm. Peaks were analysed using Agilent Technologies® 1200 offline software.

2.1.3 BRIN-BD11 cell culture

Clonal pancreatic beta cell line, BRIN-BD11 (p18) was kindly donated by Professor Peter R. Flatt (Ulster University, Coleraine, Northern Ireland). Cells were preserved in liquid nitrogen and revived by rapid thaw at 37°C, resuspended in about 10 mL of complete RPMI-1640 media supplemented with 11mM glucose, 10% (v/v) foetal bovine serum (FBS – Gibco®) and 50 U/mL penicillin and 50 µg/mL streptomycin (Pen Strep – ThermoFisher®). Following a 5 min centrifugation (1800 rpm), the cell pellet was resuspended in 5 mL, added to 10mL of pre-warmed media and cultured overnight in a T25 flask (Jet Biofil®) at a density of 10^6 cells.

Sub-culturing took place every 3 days, by removing media and washing cells with 5 ml of Hanks' Balanced Salt Solution (HBSS). The addition of 1 mL of 1X Trypsin-EDTA (Gibco) for 10 minutes at 37°C allows cell detachment from flask surface. Following resuspension of detached cells in about 10 mL of media to dilute the enzyme, cells were pelleted by centrifugation (1800 rpm, 5 minutes), resuspended in 10 mL of media and counted by Trypan Blue® exclusion. Cells from each flask were then split into three new T75 flask, each containing a 10:1 ratio between fresh media and cell suspension. Maintenance of the cells occurred in an RSBiotech® incubator with 5% CO_2, 95% air at 37°C.

2.1.4 *In vitro* insulin release studies

In this study, concentrations of insulin secreted by BRIN-BD11 cells following incubation with peptides or other agents were measured by acute insulin tests, following a previously described protocol (McClenaghan et al., 1999; Ojo et al., 2013). Cells (P20-35) were seeded at a density of 1.5×10^5 cells/well in a 24-well plate and left to adhere overnight in complete RPMI-1640 media. After 18 hours, the medium was removed from each well and replaced with 1 mL of Krebs Ringer Bicarbonate (KRB) buffer (115 mM NaCl, 4.7 mM KCl, 1.28 mM $CaCl_2$, 1.2 mM $MgSO_4$, 1.2 mM KH_2PO_4, 25 mM HEPES, 8.4% (w/v) $NaHCO_3$ and 1% bovine serum albumin) (pH 7.4) supplemented with 1.1mM glucose for 40 min. Following the pre-incubation step, the buffer in each well was replaced with KRB buffer containing 5.6mM glucose and supplemented with graded concentrations of peptides (1 and 3 µM) or known insulin secretion modulators.

After a 20-minute incubation with the test solutions at 37°C, aliquots from each well were collected and stored at -20°C until insulin release was measured by ELISA (Ultrasensitive Rat Inuslin ELISA – Mercodia AB, Uppsala, Sweden), according to the manufacturer's protocol. For ELISA, samples and standards (25 µL) were added to the antibody pre-coated plates in the presence of the enzyme conjugate for 2 hours at room temperature. Following 6 washes, 200 µL of substrate were added to the wells for 15 minutes and the reaction was stopped with 0.5M H_2SO_4. Absorbance was recorded at 450 nm.

2.1.5 Mouse pancreatic islet isolation

Islets were isolated from whole mice pancreata (aged 6-8 weeks) by the method of Lernmark (1974). Excised pancreata were re-suspended in Krebs-Ringer-HEPES solution (115 mM NaCl, 4.7 mM KCl, 1.28 mM $CaCl_2$, 1.2 mM $MgSO_4$ X $7H_2O$, 1.2 mM KH_2PO_4, 25 mM HEPES, 8.4% (w/v) $NaHCO_3$ and 1% bovine serum albumin) and cut into small pieces in a petri dish. The suspension was transferred into a vial containing Collagenase P from *Clostridium histolyticum* (1mg/mL/pancreas, Cat. No. 11 213 857 001 – Roche©) and placed to digest in a water bath at 37°C for 8 minutes or until the solution appeared homogenous. The activity of the enzyme was interrupted by adding 10mL of ice-cold Hank's Balanced Salt Solution (HBSS)-HEPES solution containing 0.4 g/l KCl, 0.06 g/l KH_2PO_4, 8 g/l NaCl, 0.09 g/l Na_2HPO_4 X $7H_2O$, 1 g/l glucose, 10 mM HEPES, 1% BSA. Two

washes with this solution were performed by spinning cell suspension at 900 rpm for 5 minutes and discarding the supernatant. Pellet was resuspended in 10 mL of complete RPMI-1640 media and cultured overnight.

2.1.6 Acute test on isolated mouse islets

Within 24 hours from isolation, intact pancreatic islets (3 to 5 per tube) were manually picked and placed into 1.5 mL Eppendorf tubes for acute insulin release studies. Islets were subjected to a 40-minutes pre-incubation with KRB buffer supplemented with 1.1mM glucose. Test solutions were made up in KRB buffer containing either 5.6 or 11.1mM glucose and graded peptide concentrations (either 1 or 3 μM). Following incubation with test agents for 1 h, supernatant was retrieved and stored at -20°C for insulin ELISA.

2.1.7 Lactate dehydrogenase (LDH) assay

The level of LDH, an enzyme exclusively present in the cytoplasm in normal conditions, is a reliable indicator of cellular membrane integrity (Chan et al., 2013). The effect of peptides and other test agents on cell membrane integrity was assessed by measuring the levels of lactate dehydrogenase (LDH) released by BRIN-BD11 cells following incubation with peptides. This was carried out using a commercially available CytoTox 96® Non-radioactive assay kit (Promega), according to the manufacturer's protocol. Supernatants (50 μL) retrieved from acute insulin tests (described in Section 2.4) were added to a 96-well plate, together with an equal volume of substrate mix (reconstituted in 12 mL of buffer). Following incubation in the dark for 30 min, the reaction was stopped by the addition of 50 μL of stop solution and absorbance was measured at 490 nm.

2.1.8 Thiazolyl Blue Tetrazolium Bromide (MTT) assay

The ability of living cells to convert a dye, Thiazolyl Blue Tetrazolium Bromide (MTT – Merck Cat. No. M2128), into a formazan product was used as an index of cell viability, following a procedure described by Asalla et al (2016). Optimal cell density was confirmed by performing the assay using a range of cell densities (10^3-$2X10^5$) and verifying that with the suggested seeding density ($2.5x10^4$ cells/well), the relationship between the cell count and the absorbance measured was

linear (Figure 2.2). Cells (2.5×10^4 cells/well) were seeded in a 96-well plate and left to adhere overnight. The following day, the media was discarded and replaced with fresh media supplemented with 1 or 3 μM of each peptide for 24 hours. After treatment, the supernatant was discarded and replaced with MTT solution. A stock of MTT was prepared in HBSS buffer at a concentration of 1 mg/mL and diluted with media in each well to a final concentration of 0.2 mg/mL. Cells were then placed at 37°C for 4 hours, following which MTT solution was removed, leaving the insoluble crystals on the plate. These were dissolved in slightly acidified isopropanol (in 0.001 N HCl) and absorbance was read at 570 nm.

Recent reports using the MTT assay in BRIN-BD11 cells as an index of cell viability upon pharmacological treatment justifies the choice of this assay for our screen (Asalla et al., 2016). Despite the existence of newer technologies (Carlessi et al., 2015), the MTT assay still represents a valid high throughput screening method for *in vitro* peptide cytotoxicity (Kiely et al., 2007; Asalla et al., 2016).
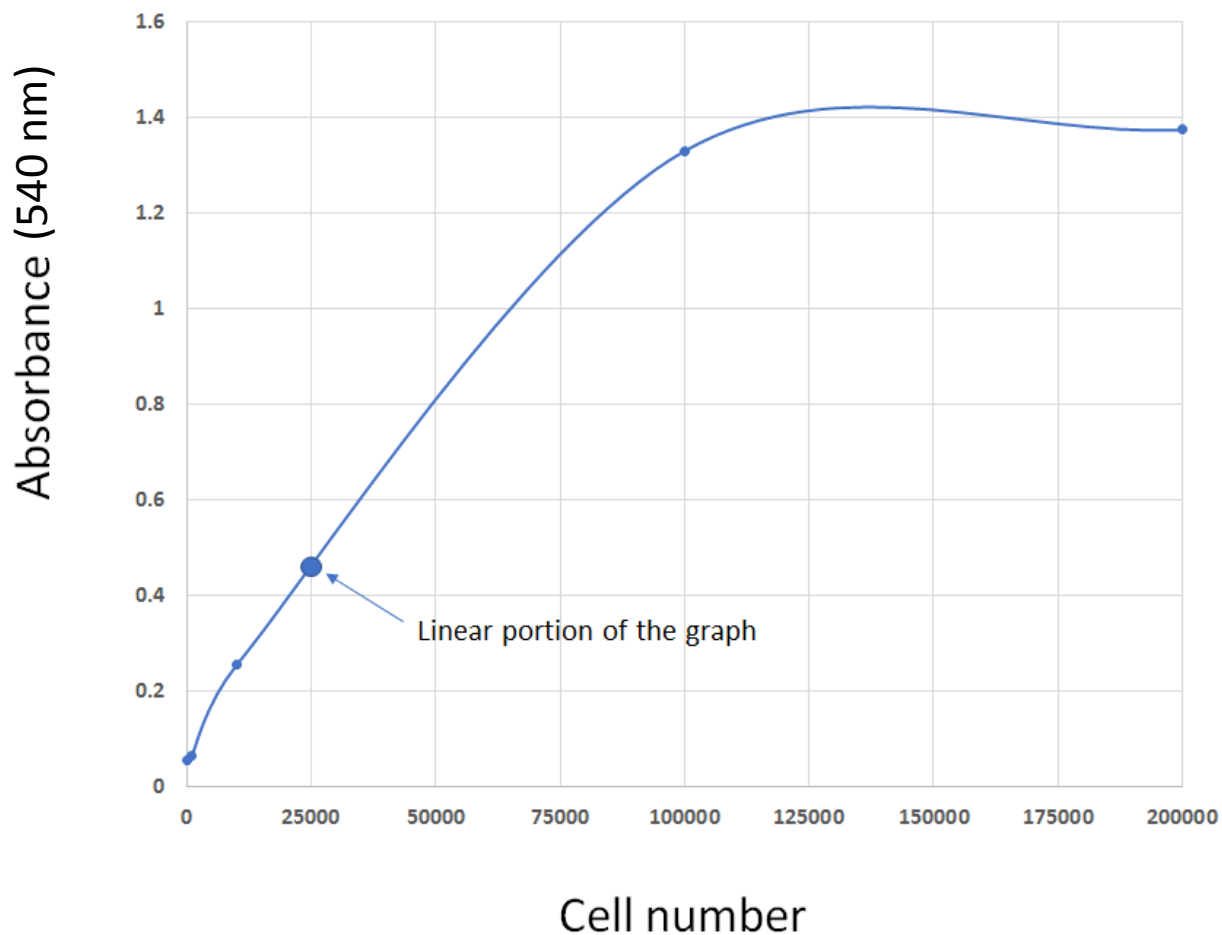
Figure 2.1. Optimal cell count for MTT assay in BRIN-BD11 cells.
Cell titration was performed in cells to verify the seeding density corresponded to the linear portion of the graph, where absorbance, measured at 540 nm, is directly proportional to the number of cells.

2.2 MECHANISM OF ACTION STUDIES

To elucidate underlying mechanisms through which selected peptides stimulate insulin secretion, established modulators of insulin secretion were used alongside novel hybrid peptide, as previously described (Vasu et al., 2017). Cells were seeded at a density of 1.5×10^5 cells/well in a 24-well plate and left to adhere overnight. Prior to the experiment, cells were pre-incubated with KRB buffer (115 mM NaCl, 4.7 mM KCl, 1.28 mM CaCl$_2$, 1.2 mM MgSO$_4$, 1.2 mM KH$_2$PO$_4$, 25 mM HEPES, 8.4% (w/v) NaHCO$_3$ and 1% bovine serum albumin) (pH 7.4) supplemented with 1.1 mM glucose. Supernatants were discarded and cells were incubated with KRB buffer supplemented with 300 µM diazoxide, 200 µM tolbutamide, 200 µM IBMX or 50 µM in the absence or presence of the sub-optimal, stimulatory peptide concentration. Other incubations were performed using KRB buffer containing 30 mM KCl and 16.7 mM glucose.

In another set of experiments, the effect of calcium on insulin secretion was evaluated by incubating cells in the absence of extracellular calcium (by using a calcium free KRB buffer containing 115 mM NaCl, 4.7 mM KCl, 10 mM EGTA, 1.2 mM MgSO$_4$. 7H$_2$O, 1.2 mM KH$_2$PO$_4$, 25 mM HEPES, 8.4% (w/v) NaHCO$_3$ and 1% bovine serum albumin) (pH 7.4). All the other test solutions were made up in KRB buffer (115 mM NaCl, 4.7 mM KCl, 1.28 mM CaCl$_2$, 1.2 mM MgSO$_4$ X 7H$_2$O, 1.2 mM KH$_2$PO$_4$, 25 mM HEPES, 8.4% (w/v) NaHCO$_3$ and 1% bovine serum albumin) (pH 7.4). Insulin test was performed as detailed in section 2.1.4.

2.3 METABOLOMICS STUDIES

2.3.1 Sample preparation for metabolomics analysis

The analysis of metabolite extracts was performed using the BRIN-BD11 cells. These were cultured in RPMI-1640 medium containing 11.1 mM glucose, 10% (v/v) foetal bovine serum (FBS – Gibco®) and 50 U/mL penicillin and 50 μg/mL streptomycin (Pen Strep – ThermoFisher®), at 37°C in a 5% CO_2, 95% air sterile environment. Cells ($5x10^5$/well) were seeded in a 6-well plate and pre-treated with 5.6 or 25 mM glucose, in the absence or presence of exendin-4 (3 μM). After 20 hrs, media was discarded and replaced with KRB buffer (2 ml) supplemented with ^{13}C-labelled glucose (14 mM) for 1 hour. Following glucose challenge, the supernatant was harvested and 25 μl were used for insulin ELISA and the remaining stored at -80°C for analysis nuclear magnetic resonance (NMR). The cells were also processed for metabolite extraction and GC-MS analysis. Metabolomic experiments were performed at Imperial College London, Hammersmith Campus.

2.3.2 Nuclear Magnetic Resonance (NMR)

A popular technique employed for studies on metabolites deriving from an array of samples including cell supernatants (Behrends et al., 2019) is nuclear magnetic resonance (NMR) spectroscopy. For NMR metabolite extraction, 420 μL of supernatant were added to 120 μl of deuterium oxide (D_2O) containing 1 mM trimethylsilylpropanoic acid (TSP), 25 mM sodium azide (NaN_3) and 60 μL of phosphate buffer (500 mM). Samples were mixed and transferred to 5mm glass NMR tubes. Using the Brucker Biospin® NMR flow-injection system (located at Imperial College London, Hammersmith Campus), 1H-NMR spectra were acquired over 5 minutes (16 scans) and measured at a frequency of 600 MHz, at a temperature of 300 K. TSP was used as in internal reference (0.0 δ) for signal intensity.

2.3.3 Gas Chromatography – Mass Spectrometry (GC-MS)

Gas-Chromatography Mass Spectrometry (GC-MS) allows separation and characterization of molecular entities within a sample. Based on the ability of volatile compounds to be separated and the possibility to derivatise samples to enable them to do so, GC-MS is highly reproducible across different platforms (Huang and Joseph, 2012), with patterns and retention times usually being consistent across experiments (Sas et al., 2015). By using labelled isotopomers, a comparison between the natural abundance of sugars and amino acids, combined with the amount of the labelled species incorporated at a given metabolic step, can also provide information around metabolite fluxes within a pathway (Koubaa et al., 2012).

For this analysis, BRIN-BD11 cells in the 6-well plates were washed with ice-cold KRB buffer before undergoing methanol quenching, which consisted in the addition of 2 ml of methanol to each well and scraping cells from the wells, on ice. Samples were dried using a speedvac for 1.5 hrs. A chloroform-methanol extraction was performed by adding a $CHCl_3$/MeOH 2:1 solution to the dried pellet, on ice, followed by centrifugation to separate the two phases (16,000 g, 10 minutes). The aqueous phase was dried to pellet and derivatised by methoximation. MOX reagent (20 μL, 2% methoxyamine·HCl in pyridine, ThermoFisher®) was added to the samples, before placing them on a heat block at 30°C for 90 minutes (900 rpm). This was followed by methyl-sylylation with *N*-methyl-*N*-(*tert*-butyldimethylsilyl)trifluoroacetamide (MTBSTFA). MTBSTFA (80 μl) were added to the samples, which were placed on a heat block at 70°C for 60 minutes. Samples were spun in a speedvac with no vacuum to separate insoluble material. Supernatants were transferred to GC-MS glass vials for analysis (aqueous extract).

The organic phase was dried to pellet and lipids were transmethylated for 1 hr at room temperature by addition of 300 μL of a toluene/methanol 1:1 solution and 200 μL of sodium methoxide. After stopping the reaction (500 μL of NaCl (1 M) and 20 μL of conc. HCl), hexane extraction was performed. After the addition of 500 μL of hexane, layers were separated by centrifugation and the top organic layer was added to 10 μg of $MgSO_4$ in a glass vial. Samples were dried under N_2 before derivatization by addition of 40 μl of both acetonitrile and MTBSTFA, and place on a heat block at 70°C for 1 hr. Insoluble material was excluded by centrifugation and the top layer was transferred to a clean glass vial (organic extract).

Samples were run in triplicates on the Agilent Technologies 7890A GC System, with the Agilent 5975 mass selective detector (MSD) system (located at Imperial College London, Hammersmith Campus), using a time-of-flight GC-MS with electon impact ionization. Separation took place in a polysiloxane column (0.32 mm ID, 30 m) and metabolites were carried by a mobile phase gas (Helium) at a flow of 1ml/min and a temperature of 250°C for a total of 40 mins.

Peaks resulting from the total ion chromatograms (TICs) were identified using the PBM library on the instrument. For the labelling experiment, the raw data was acquired from the ChemStation software, and deconvoluted using the Automated Mass spectral Deconvolution and Identification System (AMDIS) software. The resulting data was imported as computable document format (CDF) file in the GC-MS Assignment Validator and Integrator (GAVIN) script for Matlab. This matrix allows for metabolite integration and discrimination of co-eluting peaks differing only by the number of ions (Behrends et al., 2011). Correction for natural abundance of ^{13}C is also integrated within the matrix (Behrends et al., 2019).

2.4 GENE EXPRESSION STUDIES

2.4.1 Treatment of BRIN-BD11 cells and RNA isolation

We studied alterations in gene expression following treatment of BRIN-BD11 cells with hybrid peptides. Cells were seeded at a density of 2.5×10^5 cells/well in a 12-well plate and upon adhesion, media was replaced with RPMI-1640 supplemented with exendin-4, E-TGN, E-MAM$_2$ or MAM$_2$ (3 µM) for 24 h. Following the incubation, cells were pelleted and air-dried for total RNA isolation using Isolate II RNA Mini Kit (Bioline©, London, UK) following the manufacturer's recommended protocol. Cells were lysed with lysis buffer (350 µL) and ß-mercaptoethanol (3.5 µL) and lysate was filtered by centrifugation at 11,000 g for 1 minute. RNA was precipitated with the addition of 70% ethanol and bound to a silica membrane by a 30-second centrifugation (11,000 g). Residual DNA was digested with DNAse solution, the silica membrane was de-salted, washed and dried by successive 30-seconds centrifugation steps (at 11,000 g). RNA was finally eluted in a volume of 40 µL RNAse-free water and quantified using Nanodrop™ 1000 (ThermoScientific). The instrument measured the concentration of each sample (ng/µL), the 280/260 and 260/230nm absorbance ratios.

2.4.2 cDNA synthesis

cDNA synthesis was achieved using Sensifast™ cDNA Synthesis kit (Bioline©, London, UK) according to manufacturer's protocol. For each reaction, 1µg of RNA, 4µL of TransAmp buffer, 1 µL of Reverse-Trascriptase (RT) and RNase-free water were added to RNAse-free PCR tubes, to a final volume of 20 µL. The thermal cycles for the reaction were a 10-minute primer annealing at 25°C, 15-minute reverse transcription at 42°C, followed by a 5-minute inactivation at 85°C. Samples were stored at -20°C until qPCR reaction.

2.4.3 Primer quality check and Real time quantitative PCR (RT-qPCR)

Changes in the expression of genes involved in insulin secretion, beta-cell proliferation and inflammation were quantified using real time quantitative PCR (RT-qPCR). Optimal primer concentration supplied by manufacturer (Eurofins©, Luxemburg) (Table 2.2) was validated with a conventional PCR (MyFi™ DNA polymerase – Bioline©, London, UK) by running untreated samples (100 ng) with each primer set on a 2% agarose gel (Figure 2.2 and 2.3). PCR cycles are as follows: a 1-minute cycle of initial denaturation at 95°C, followed by 30 cycles of 15 sec denaturation, 15 sec annealing at the same temperature, and an extension step at 72°C for another 15 sec. PCR products on the gel were visualised using ChemiDoc™ Gel Imaging System (BioRad).

For each gene, a standard curve of cDNA was performed in the range of 0.1-100ng. A reaction contained 1X Sensifast™ SYBR® NO-ROX (Bioline©, London, UK), 400-500 nM of forward and reverse primers for the given gene, 100 ng of cDNA and deionized water to a final volume of 20µL. A "no-RT" control with the primers for the housekeeping gene (ß-actin) and a "no template control" was included for each gene of the differentially treated cDNA samples.

The qPCR reaction was performed using the AriaMx Real-time PCR System (Agilent© Technologies, Santa Clara, CA, USA) with the following cycles: a hot start at 95°C for 3 minutes, 40 amplification cycles of 5 and 10 seconds, at 95°C and 60°C respectively. A melt-curve cycle was also added to detect any other amplification products in the reaction, with steps of 30 seconds each at 95°C, 63°C and back to 95°C.

Table 2.2 List of primers for gene expression studies

Gene	Common name	Sequence	Prod. Size	Tm (°C)
B-actin	Beta actin	F – TACAACCTTCTTGCAGCTCCTC R - CATACCCACCATCACACCCTG	195	60
Ins1	Insulin 1	F- AGCACCTTTGTGGTCCTCAC R- CCAAGGTCTGAAGATCCCCG	159	60
Abcc8	ATP-binding cassette, subfamily C, member 8	F – CTCATCTACTGGACCCTGGC R - GCTTTACTTCCCTTGGTGTCTTG	199	60
Glp1r	GLP-1 receptor	F – CGAGCACTGTCCGTCTTCAT R - TCCTGATACGAGAGGAGCCC	98	60
Pdx-1	Pancreatic and duodenal homeobox 1	F – AAGAGGACCCGTACAGCCTA R – TCCACTTCATGCGACGGTTT	166	60
NFkB1	Nuclear factor kappa B 1	F – TGGACGATCTGTTTCCCCTC R - CCCTCGCACTTGTAACGGAA	118	60

Primer concentration (nM, each)

A)
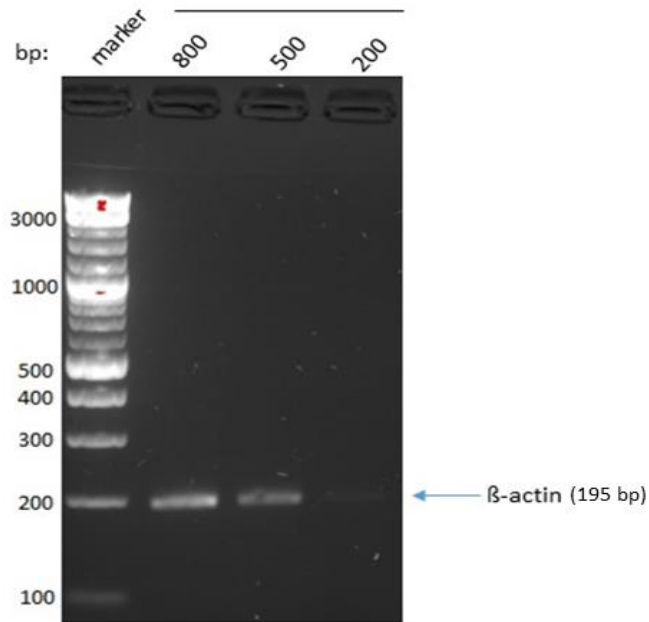
Primer concentration (nM, each)

B)
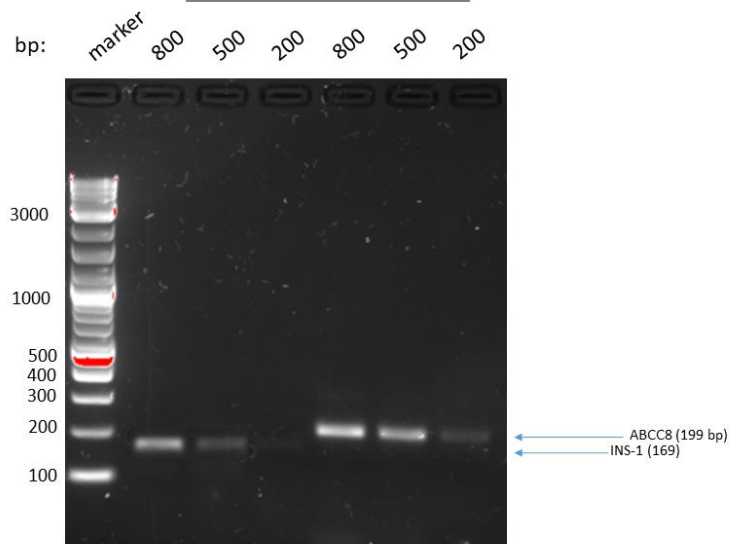
Figure 2.2. Determination of optimal primer concentration for (A) beta-actin and (B) ABCC8 (bands on the right) and INS-1 (bands on the left) and using PCR. Untreated cDNA samples (100 ng), obtained from cells incubated in 5.6 mM glucose, were run on a 2% agarose gel, using the above stated concentrations of primers. Concentrations corresponding to visible bands were chosen for the experiment (400-500 nM).
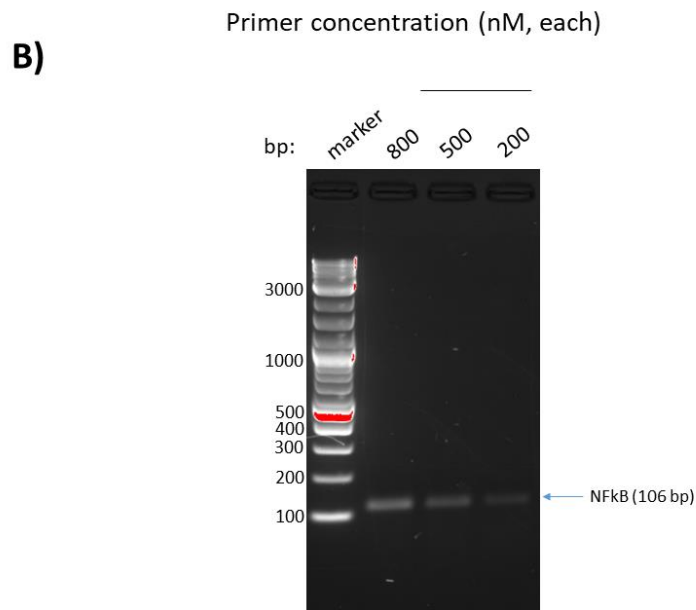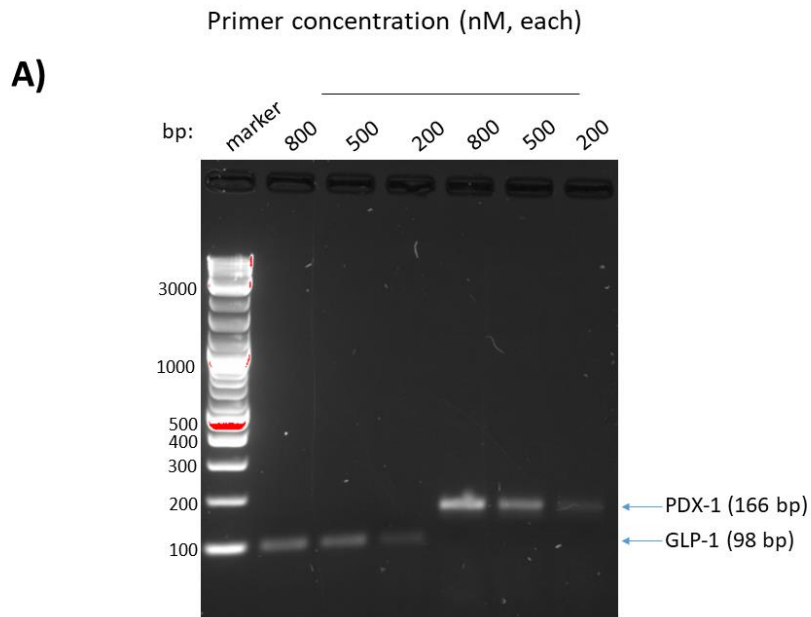
Figure 2.3. Titration for optimal primer concentration for (A) PDX and GLP-1 and (B) NFkB using PCR.
Untreated cDNA samples (100 ng), obtained from cells incubated in 5.6 mM glucose, were run on a 2% agarose gel, using the above stated concentrations of primers. Concentrations corresponding to visible bands were chosen for the experiment (400-500 nM).

2.5 NITRIC OXIDE METABOLITE PRODUCTION

Production of the nitric oxide metabolie NO_2- was used as in index of nitric oxide release from BRIN-BD11 following cell treatment. This represented a link between the gene expression studies on NFkB and studies regarding immunomodulatory effects of the peptides on the dendritic cell antigen-presenting model.

NO_2- release in the extracellular space was determined using the Griess reagent, as reported previously (Kiss et al., 2010) (Figure 11.1), according to the manufacturer's protocol (Sigma). BRIN-BD11 cells grown in KRB buffer, supplemented with 11.1 mM glucose and 10% FBS. Cells were seeded in a 96-well plate ($2.5x10^4$ cells/well) and treated with peptides (3 μM) for 24 hours. Following treatment, 50 μl of cell supernatants were collected and added to another 96-well plate, complemented by 50 μl of assay buffer for the detection of NO_2-.

Additional 10 μl of both nitrate reductase and enzyme co-factors were added, yielding a final volume of 100 μl. Griess reagents A and B were added to all wells (50 μl) for 5 and 10 minutes, respectively, before absorbance was read at 540 nm.

2.6 IMMUNOMODULATION STUDIES

2.6.1 Isolation of bone marrow dendritic cells and treatment

Bone marrow-derived dendritic cells (BM-DCs) were generated from tibias and femurs of C57/BL6 mice. The ends of each bone were cut to expose the medullary cavity. Using a 27G, ½" needle (BD Microlance™ 3), the bones were flushed with plain RPMI-1640 media and the flow-through was filtered with a 70 μm cell-strainer (Falcon™). Cells were pelleted by centrifugation (1800 rpm, 5 minutes), the supernatant was discarded and cells were treated with 500 μL/pair of legs of Ammonium-Chloride-Potassium (ACK) buffer (1X) for red blood cells lysis for 30 seconds. The reaction was terminated by addition of 10 mL of plain media and centrifugation (1800 rpm, 5 minutes). A negative selection in the presence of the following antibodies (300 μL/pair of legs) was performed: M5-114 (anti-MHC II, American Type Culture Collection (ATCC), RA3-3A1 (anti-B220, ATCC), YTS 191 (anti-CD4, ATCC) and YTS 169 (anti-CD8, ATCC). Cell suspension was incubated in the presence of the antibodies for 30 min at 4°C, with shaking. Mouse depletion Dynabeads™ CD4 (Invitrogen) were placed on a magnet (300 μL/pair of

legs) and washed twice with plain media prior to incubation with cell suspension (30 min at 4°C). The bone-marrow derived cells resulting from the negative selection were centrifuged, resuspended in dendritic cell (DC) media (AIM V® + AlbuMAX® (BSA) 1X, 50 μM ß-ME, 1 mM HEPES) and seeded in a 24-well plate, at a density of 1×10^6 cells/well.

Cell feeding with fresh DC media took place on day 3 and 5 from plating and on day 7 precursor cells would have matured into DCs, for pre-treatment with peptides for 24-hours. Following pre-treatment, supernatants were collected for cytokine analysis and cells were harvested for surface markers staining and flow cytometry analysis. To study the effect of the peptides in the presence of activated DCs, commercially sourced Lipopolysaccharide (LPS from E. coli 0111:B4, Lot. No. 095M4165V, Sigma) was added to the cells (200 ng/mL) following pre-treatment, for another 18 hours. The supernatant was then collected for cytokine analysis and cells were stained for surface markers expression.

2.6.2 DCs staining for surface markers

DCs were harvested with a syringe plunge and washed with FACS buffer, before being counted on a haemocytometer by Trypan blue exclusion. An equal number of cells ($0.9\text{-}1 \times 10^5$) were seeded in a U-bottom 96-well plate and pelleted by centrifugation (1800 rpm, 5 minutes). Prior to cell staining, the Fc portion of the cell surface antibodies was blocked for 30 minutes at 4°C. This was performed by addition of a CD16/CD32 antibody (clone 93, eBioscience™), diluted 1:100 in FACS buffer (2% Foetal Calf Serum (FCS), 2Mm EDTA in PBS).

Following the 30-minute incubation period, cells were pelleted (1800 rpm, 5 minutes) and supernatant was discarded. The antibodies used for this study were raised against the surface markers involved in the antigen-presenting process (Table 2.3). They were prepared in FACS buffer, in a 0.5:100 dilution and added to the cells for 30 minutes at 4°C. After a couple of wash steps with FACS buffer, cells were fixed with 1X CellFIX™ (BD Bioscience) and ran on the flow cytometer the next day.

Table 2.3 Antibodies used for DCs staining.

Antibody name	Target	Working concentration	Fluorochrome	Company
CD16/CD32 Monoclonal Antibody (clone 93)	Fc receptors	1:100	None	eBioscience™
APC anti-mouse CD11c antibody	CD11c	0.5:100	APC	eBioscience™
MHC Class II (I-Ab, FITC, clone: AF6-120.1)	MHC II	0.5:100	FITC	eBioscience™
CD80 (B7-1), clone: 10-10A1	CD80	0.5:100	FITC	eBioscience™
CD86 (B7-2) clone: GL1	CD86	0.5:100	FITC	eBioscience™

2.6.3 Flow cytometry

Flow cytometry was employed to evaluate the expression of DCs surface makers under the different test conditions. The instrument (BD Accuri™ C6) excites the APC and FITC fluorochromes conjugated to the antibodies by using FL-4 and FL-1 lasers, respectively.

The distinct emission wavelengths of the excited fluorochromes (660 nm for APC and 520 nm for FITC) allowed simultaneous use when staining for the surface markers (conjugated with FITC) within the CD11c positive population (conjugated with the APC dye). Results were analysed using the CFlow® Plus Analysis software.

2.6.4 Cytokine measurement

The supernatant collected from DCs pre-treated with the peptides in the presence or absence of LPS were assayed for the measurement of pro- and anti-inflammatory cytokine levels (IL-12 and IL-10, respectively), according to the manufacturer's protocol. For IL-12 (Mouse IL-12 (p70) ELISA MAX™ Deluxe), plates were coated with a capture antibody overnight before being blocked with the assay diluent for 1 hour the following day. Prior to addition of samples and standards (100 μL), plate was washed 4 times (with PBS + 0.05% Tween-20). After a 2-hour incubation with shaking, samples unbound samples were washed off and a 100 μL of Avidin-HRP solution were added to each well, for a 30-minute incubation. This was followed by another round of washes, before adding 100 μL of substrate solution and stopping the reaction after 15 minutes with 2N H_2PO_4.

Similarly, IL-10 (IL-10 Mouse Uncoated ELISA Kit – Invitrogen) plates were coated with capture antibody overnight before blocking with 1X ELISPOT diluent (100 μL for 1 hour). Following 4 washes (with PBS + 0.05% Tween-20), samples and standards were added (100 μL), together with an equal volume of 1X ELISPOT and incubated overnight at 4°C for maximum sensitivity. The following day, 4 washes were performed prior to the addition of 100 μL of detection antibody for 1 hour at room temperature. Preceded and followed by another series of 4 washes, streptavidin-HRP (100 μL) was added to each well. After the final was step, the plate was coated with 1X substrate TMB for 15 minutes, in the dark, and the reaction was terminated by adding 2N H2PO4. The plates were read at a wavelength of 450 nm.

2.7 STATISTICAL ANALYSIS

Statistical analysis was performed using GraphPad Prism® 3. For MTT, LDH, acute insulin assays and metabolite labelling abundance, a one-way analysis of variance (ANOVA) followed by the Newman-Keuls post-hoc test was employed to compare test samples with controls. For mechanism of action assays, multiple unpaired t-tests were performed comparing each sample with control (treated with 5.6 Mm glucose) and with respective incubation in the absence of the peptide. For gene expression studies, relative gene expression quantification (R) was corrected by the AriaMx Software as detailed in section 5.3.2. For changes in the expression of genes, in DCs surface markers and cytokine measurements, a one-way ANOVA followed by Newman-Keuls post-hoc test were employed to compare all sets of data.

CHAPTER 3

<u>PEPTIDE SCREENING</u>

3.1 BACKGROUND

The confirmation of insulinotropic actions of newly designed hybrid peptides is essential prior to other characterization of their anti-diabetic actions or the investigation of their mechanisms of actions. Therefore, the screening strategy employed in this study involves the incubation of BRIN-BD11 cells, as well as primary mouse islets, with newly synthesized peptides and parent peptides to examine their insulin releasing effects. The efficacy of this approach in selecting active peptides from a library has been proved by previous studies (Marenah et al., 2006; Ojo et al., 2015d; Moore et al., 2015).

Peptides found in crude skin extracts of amphibians were purified by HPLC, screened for acute insulinotropic activity and their ability in preserving cell membrane integrity or any other cytotoxic effect. This approach allowed identification and characterization of an insulinotropic peptide isolated from *Rana palustris* skin secretions (Marenah et al., 2004). An initial skin extract containing 80 fractions was probed for acute insulinotropic actions in BRIN-BD11 cells. Successive rounds of chromatographic purification of the single insulinotropic fractions, along with sequence and mass analysis, allowed identification of Palustrin-1c, carrying 48% homology with Brevinin-1. This finding highlighted the importance of the previously identified class of brevinin/esculentin peptides and motivated successive studies in the field.

Considering cationicity as an important component of the biological activity of amphibian-derived peptides, when comparing esculentin-2CHa, isolated from the *Lithobates ciricahuensis* frog, with its cationic analogues, insulinotropic screening was performed in both the BRIN-BD11 cell line and primary mouse pancreatic islets, in the presence of 5.6 and 16.7 mM glucose, respectively (Ojo et al., 2015d). A lactate dehydrogenase (LDH) assay for cytotoxicity was also performed to rule out the possibility of cell membrane rupture. The combination of these studies revealed the most promising candidates of this class, the [L28K] and [C21S] analogues,

which had a higher potency at 3 μM compared to native esculentin (Ojo et al., 2015d).

The amphibian peptides adopted in our study, tigerinin-1R (TGN) and magainin-AM$_2$ (MAM$_2$) were also selected using a funnel-like screening based on insulinotropic action lacking cytotoxicity (Figure 3.1) as described above. For tigerinin-1R, skin extracts of *H. rugulosus* were purified and separated by HPLC and individual peptides were screened for both insulin releasing actions and LDH release contributions, which allowed cytotoxic peptides to be discarded. With this criterion, the selected peptide was further characterized using Edman degradation and MALDI-TOF and identified as tigerinin-1R, which yielded a maximal insulinotropic activity at 3 μM (Ojo et al., 2011).

Magainin-AM$_2$, which we also selected as a component of our hybrid peptides, is one of two orthologs present in skin secretions of *X. amieti*, along with magainin-AM$_1$. Activities of the peptides were measured at both physiological (5.6 mM) and stimulatory (16.7 mM) concentrations of glucose in BRIN-BD11 cells and mouse islets, respectively. Results showed a maximal response at 3 μM for magainin-AM$_2$ which was double that of magainin-AM$_1$ in BRIN-BD11 cells. Though to a lower extent, a similar trend was observed also in primary pancreatic mouse islets (Ojo et al., 2015a).

Following promising results from plasma degradation studies, both the activities of TGN and MAM$_2$ were also studied *in vivo* in diabetic mouse models, where lack of cytotoxicity was maintained and anti-diabetic actions such as controlled glycaemia following co-administration of the peptides with a glucose load (Ojo et al., 2011; Ojo et al., 2015b) highlighted their potential for further development into anti-diabetic agents.

PEPTIDE SCREENING
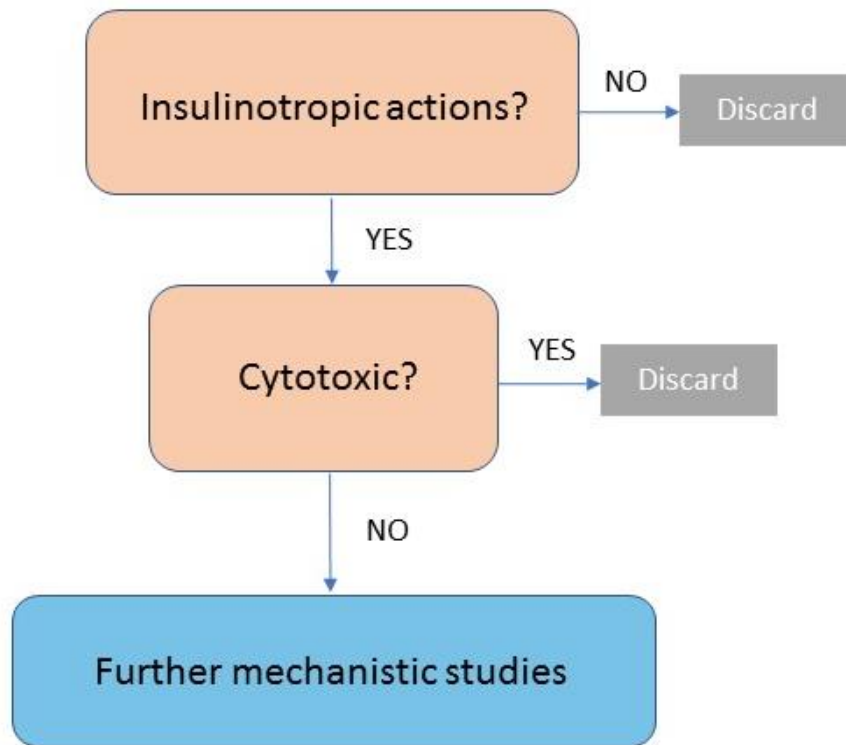
Figure 3.1. Peptide screening rationale for insulinotropic candidates.

3.1.1 Hybrid peptides

Exendin-4 and d-Ala^2-GIP were PEGylated with the amphibian skin peptides TGN and MAM$_2$, as detailed in Chapter 2 (Table 1) with a view to enhancing the action of these incretins while revealing possible novel anti-diabetic potential originating from the conjugation.

In the field of T2D, a similar rationale has been already been proven successful in several studies (Fourmy, 2017). For instance, by searching for a molecule acting as a GLP-1 agonist and a glucagon antagonist, different hybrids were screened for their receptor-binding activity, followed by an optimization that allowed identification of the most potent among these hybrids, peptide A10. The peptide retained insulinotropic activity at 8 mM glucose, equivalent to that of GLP-1 alone, while having an increased stability in mouse plasma, due to amino acid substitution. By eliminating cleavage site for the DPP-4 enzyme, *in vivo* glucose tolerance was improved for up to 17 h post injection (Pan et al., 2006).

In our study, we chose polyethylene glycol (PEG) as a linker for peptide conjugation. Its ability to prolong half-life *in vivo*, together with its reduced immunogenicity make it an attractive option for type 2 diabetes therapies, given these are the limitations often known to cause treatment failure (Harris and Chess, 2003). An important result for synergistic effects of a PEGylated peptides was confirmed in the GLP-1:CCK fusion protein, where by keeping the functional C-terminus of CCK untouched a greater reduction of food intake was observed in GLP-1R-KO mice (Hornigold et al., 2018). This strongly suggests that the available portion for CCK might bind to its receptor and contribute to the additive effect. These findings, along with the idea of hybrid peptides having novel, additional effects compared to their single components, represent a promising route in peptide drug discovery for type 2 diabetes, supporting the rationale of peptide design for this project.

3.2 AIM AND OBJECTIVES

The aim of this chapter was to screen newly synthesized parent and hybrid peptides for their beneficial antidiabetic actions and to select peptides to be used in subsequent studies, based on their insulinotropic potency. Specific objectives of the study conducted in this chapter included:

1. Confirmation of peptide purity by reversed phase HPLC.

2. Assessment of *in vitro* acute insulin releasing effects of newly synthesized peptides, comparing them to the actions of native exendin-4.

3. Assessment of cytotoxic effects of newly synthesized peptides by LDH and MTT assays.

As a means of validating our screen in house, the known insulinotropic agents TGN and MAM$_2$ were tested alongside exendin-4 and d-Ala-GIP hybrids.

3.3 RESEARCH DESIGN

3.3.1 Reverse-phase HPLC

Reverse-phase HPLC was performed as detailed in Section 2.1.2. Each peptide (exendin-4, E-TGN, E-MAM$_2$, GIP, G-TGN, G-MAM$_2$, TGN and MAM$_2$) was resuspended in 0.001N HCl to a final concentration of 1 μM and 5μL were used for HPLC analysis. Separation was achieved using a ZORBAX® Eclipse XDB-C18 column kept at 20°C and at a flow rate of 1 ml/min over a period of 50 mins. Analysis were performed in triplicates for each peptide. The concentration of acetonitrile in the elution solution was increased gradually from 0% to 21% over 10 minutes and from 21% to 56% over the following 25 minutes. The gradient was increased to 70% over 5 minutes and maintained constant for the same amount of time. A final decrease to 0% over the following 3 minutes was maintained until the conclusion of the run. Peptide elution was monitored using a UV detector by measuring absorbance at 254 and 280 nm. Peaks were analysed using the Agilent Technologies® 1200 software.

3.3.2 Acute insulin secretion test on BRIN-BD11 cells

BRIN-BD11 cells were grown and maintained in sterile T75 flasks, as described in section 2.1.3, and all solutions were prepared in KRBB as detailed in section 2.1.4. Prior to the experiment, cells were seeded into a 24-well plate at a density of 1.5×10^5 cells/well for overnight attachment. Following a 40-minute pre-incubation with 1.1 mM glucose, cells were incubated with KRB buffer supplemented with 5.6 mM glucose in the presence or absence of alanine (10 mM) or peptides (1 μM and 3μM) for 20 minutes.

3.3.3 Mouse pancreatic islet isolation

Mouse pancreatic islets were isolated as described in section 2.1.5. Briefly, whole pancreata were cut in pieces and resuspended in Krebs-Ringer-HEPES solution. Following an 8-minute digestion in the presence of Collagenase P at 37°C until homogeneous appearance, the activity of the enzyme was interrupted by adding 10mL of ice-cold Hank's Balanced Salt-HEPES solution. Two washes with this solution were performed and pellet was resuspended in 10 mL of complete RPMI-1640 media for overnight culture.

3.3.4 Insulin release assay in mouse primary islets

Acute insulin test on isolated mouse islet was performed as specified in section 2.1.6. Within 24 hours from isolation, intact pancreatic islets were placed into 1.5 mL Eppendorf tubes and subjected to a 40-minutes pre-incubation with KRB buffer supplemented with 1.1mM glucose. Test solutions were made up in KRB buffer containing 11.1mM glucose and peptide concentrations of either 1 or 3 μM. Following pre-incubation, 1 h test incubation was performed and supernatant was retrieved for insulin ELISA and LDH assays. To assess total insulin content in primary islets, islet cells were lysed with 100μL of lysis buffer (1.5% HCl in 70% EtOH) and placed in the fridge for insulin ELISA assay.

3.3.5 Determination of insulin concentration by ELISA

Insulin ELISA was performed using an Ultrasensitive Insulin ELISA kit (Mercodia AB, Uppsala, Sweden) according to manufacturer's protocol. Briefly, following the addition of samples or calibrators (25μL), 100μL of enzyme conjugate buffer containing the insulin antibody were added to each well for a 2-hour incubation at room temperature. Plates were washed 6 times and completely dried before a 30-minute incubation in the presence of Substrate TMB. The reaction was terminated by addition of H_2SO_4 (0.5 M) and absorbance was measured 450 nm. Samples were prepared in triplicates, for each experiment (n=3).

For pancreatic islets, the assay was performed following a 10-fold dilution of original samples. Insulin assayed in the supernatants of these samples was expressed as percentage of insulin content, which was also assayed using the same technique. Experiment was performed twice (n=2), in quadruplicates for each experiment.

3.3.6 Cell viability assay (MTT)

Details on the MTT assay were described in section 2.1.8. BRIN-BD11 cells were seeded in a 96-well flat-bottomed plate at a density of $2.5x10^4$ cells/well and left overnight to adhere. The culture media was discarded the following day and replaced with 200μL of media containing either DMSO (50% v/v), vehicle (0.001N HCl), or peptides (1 and 3 μM) followed by incubation for further 24 hrs. Cell supernatants were discarded and replaced with MTT solution (0.2 mg/mL) followed by incubation at 37°C for 4 hours. The insoluble formazan crystals left on the plate

after MTT solution removal were solubilised using 40 mM HCl isopropanol and absorbance was measured at 570 nm. Samples were prepared in triplicates, for each experiment (n=3).

3.3.7 Lactate dehydrogenase assay

LDH assay was performed using the CytoTox 96® non-radioactive assay kit (Promega, Madison, Wisconsin USA), according to the manufacturer's protocol, as detailed in section 2.1.7. Briefly, 50µL of both cell supernatants from the insulin acute test and substrate mix were added to a 96-well plate. Following a 30 min incubation in the dark, the reaction was stopped with 50µL of stop solution and absorbance read at 490 nm. Samples were prepared in triplicates, for each experiment (n=3).

3.3.8 Statistical analysis

Values were presented as mean ± SEM with n=3, unless otherwise specified. Data obtained for peptide treatment groups were compared to data obtained for untreated control (5.6 mM glucose) using one-way analysis of variance (ANOVA) with a Newman-Keuls post-hoc test. Results were considered significant if $P<0.05$.

3.4 RESULTS

3.4.1 Confirmation of the purity of commercially synthesised peptides

The chromatogram obtained following the HPLC analysis of commercially synthesized exendin-4 and its related hybrids are shown in Figure 3.2. Compared to the chromatogram obtained for reagent blank (Figure 3.2A), results obtained for native exendin-4 (Figure 3.2B), E-TGN (Figure 3.2C), and E-MAM$_2$ (Figure 3.2D) revealed a single peak for each of the peptides. This is indicative of the absence of other peptide impurities. The retention time observed for native exendin-4, E-TGN and E-MAM$_2$ were 22.598 min, 25.654 min and 27.648 min respectively.

Similarly, analysis of purity conducted for GIP-related peptides (Figures 3.3) indicated single peaks for GIP (Figure 3.3B) and G-MAM$_2$ (Figure 3.3D). Retention times obtained for GIP and G-MAM$_2$ were 21.280 min, and 22.906 min, respectively. For G-TGN (Figure 3.3C), a major peak at a retention time of 20.964 min and a minor peak at 21.847 min were observed. Purity of commercially synthesized native tigerinin-1R (Figure 3.4A) and magainin-AM$_2$ (Figure 3.4B) were also assessed. Results revealed prominent single peaks for tigerinin-1R (retention time = 17.111min) and magainin-AM$_2$ (retention time = 19.297 min).

The early eluting peaks detected a few minutes after the start of each run were considered as background, given their presence in the vehicle only (0.001N HCl) chromatogram (top panel). With this study, we assessed the presence of unique chromatographic peaks in each sample as a qualitative measure of peptide purity and confirmed their suitability for the studies that follow, starting from the acute insulin test screen.
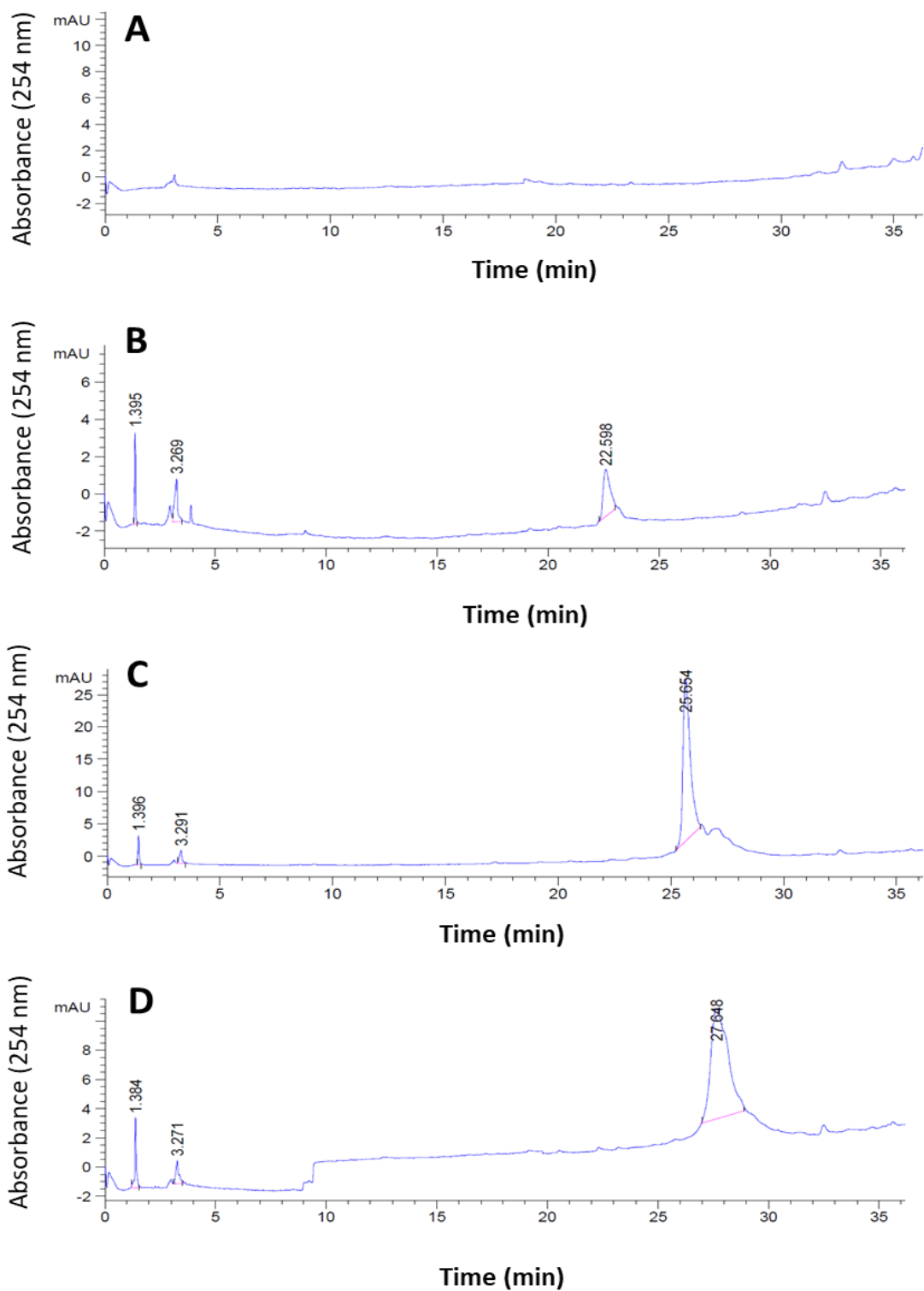
Figure 3.2. HPLC profile for samples with no peptide (A), exendin-4 (B), E-TGN (C) and E-MAM$_2$ (D).

Elution profiles were obtained using an Eclipse XDB-C18 (4.6 x 150mm, 5µm) column. Absorbance was read at 254 nm.
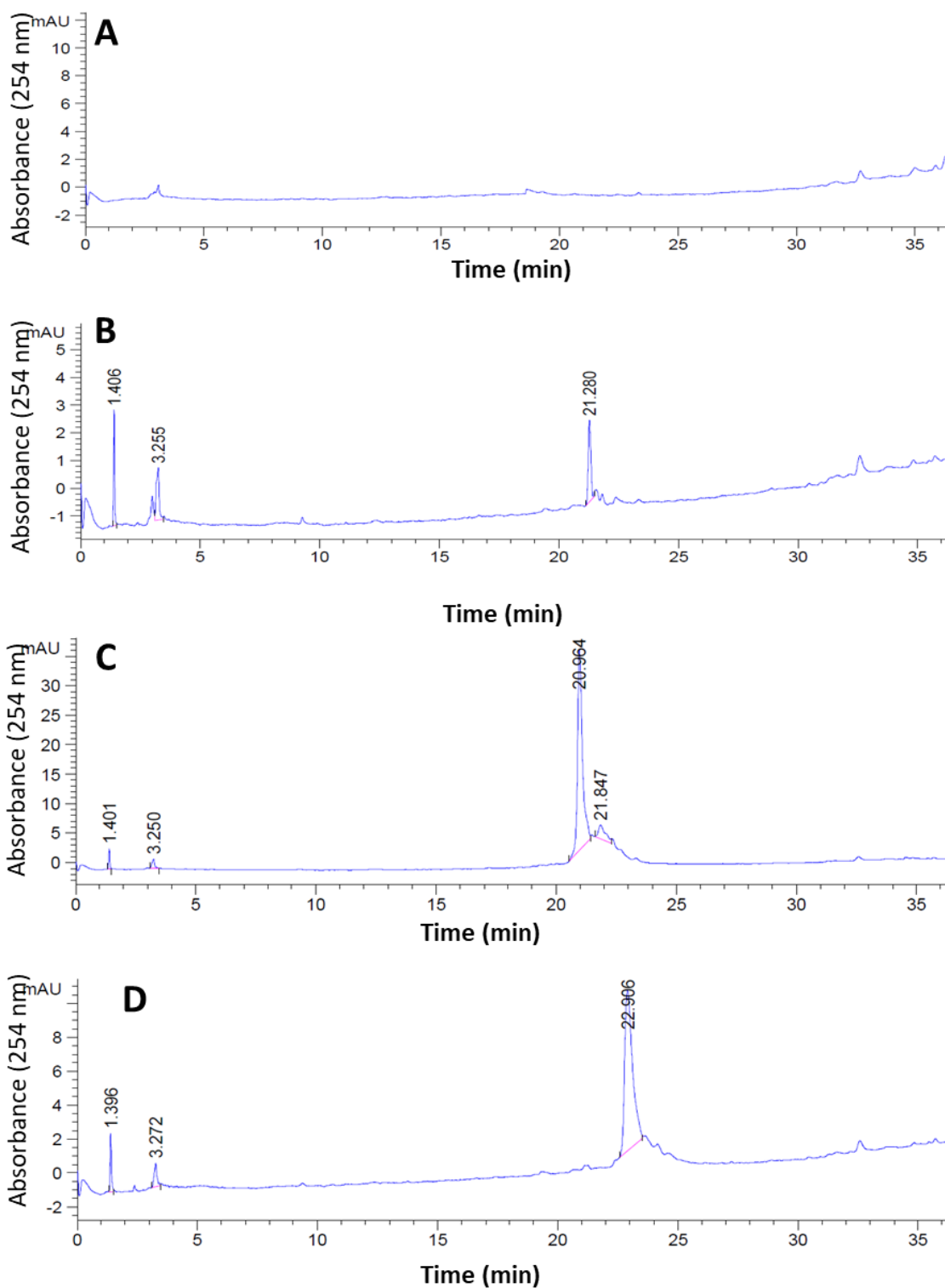
Figure 3.3. HPLC profiles for samples with no peptide (A), GIP (B), G-TGN (C) and G-MAM$_2$ (D).
Elution profiles were obtained using an Eclipse XDB-C18 (4.6 x 150mm, 5µm) column.
Absorbance was read at 254 nm.
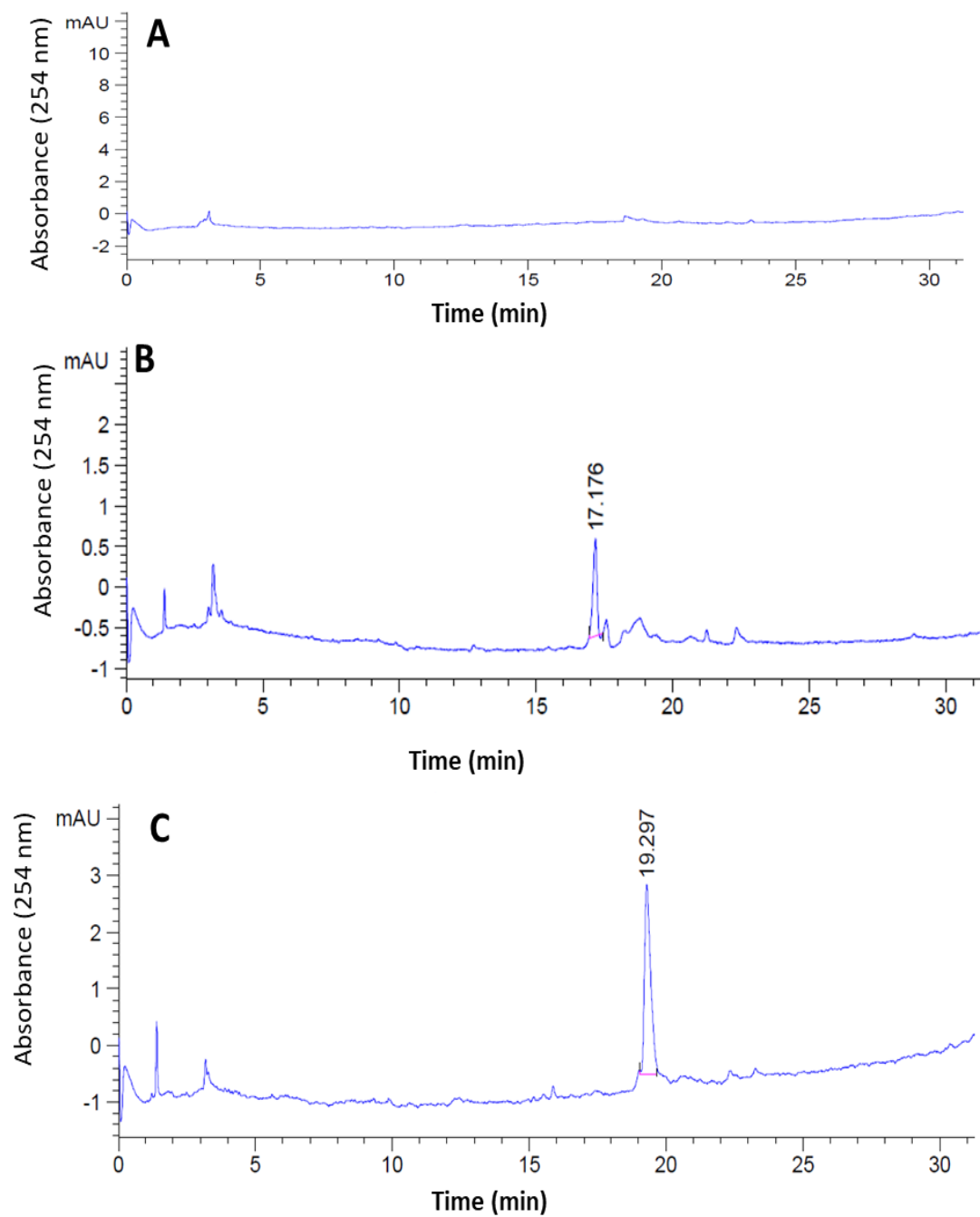
Figure 3.4. HPLC profile for samples with no peptide (A), TGN (B) and MAM$_2$ (C).
Elution profiles were obtained using an Eclipse XDB-C18 (4.6 x 150mm, 5μm) column.
Absorbance was read at 254 nm.

3.4.4 *In vitro* insulinotropic activities of the peptides

3.4.4.1 Actions at physiological glucose concentrations

Basal insulin release from BRIN-BD11 cells in the presence of 5.6 mM glucose was 0.44 ± 0.09 ng/L. As expected, the addition of the established secretagogue alanine increased insulin output to 1.1 ± 0.06 (P<0.05). The insulinotropic effects of peptides were assessed at concentrations of 1 and 3 μM.

With regards to the exendin-4 related peptides, the parent peptide exendin-4 stimulated insulin release at 1 μM by 1.7-fold (P<0.05), compared to glucose alone. This was increased to 3.9-fold (P<0.001) at a concentration of 3 μM (Figure 3.5A). The hybrid E-TGN generated a 1.88-fold increase at a concentration of 1 μM (P<0.05). At 3 μM, the peptide stimulated insulin secretion by 4.87-fold (P<0.001) of basal rate of insulin release. This increase in insulin release was the highest found among this class of peptides (Figure 3.5B). Insulin secretion in the presence of E-MAM$_2$ increased by 2.89- (P<0.01) and 4.59-fold (P<0.001) at 1 and 3 μM, respectively (Figure 3.5C).

The same assessment was performed for GIP and its related hybrids (Figure 3.6). Incubation of cells with GIP, G-TGN and G-MAM$_2$ (1 μM) increased insulin output from 0.44 ± 0.09 to 1.15 ± 0.29 ng/L (P<0.05), 0.95 ± 0.16 ng/L (P<0.05) and 0.65 ± 0.01 ng/L respectively (Figure 3.6A-C). At 3μM peptide concentration, insulin secretion increased to 2.08 ± 0.45 ng/L (P<0.001, GIP, Figure 3.6A), 1.80 ± 0.22ng/L (P<0.001, G-TGN, Figure 3.6B) and 1.34 ± 0.25 ng/L (P<0.001, G-MAM$_2$, Figure 3.6C).

Native TGN stimulated insulin secretion by 0.82 ± 0.19 and 1.6 ± 0.5 ng/L (P<0.001) at 1 and 3 μM respectively (Figure 3.7A and B). For MAM$_2$, insulin release observed was 2.54 ± 0.38 (P<0.001) and 2.7 ± 0.35ng/L (P<0.001) at 1μM and 3μM respectively (Figure 3.7A and B).

This experiment represents the initial screen on which we based the choice of peptides to further investigate in our study. By comparing the insulinotropic activities of the incretins exendin-4 and GIP to their respective hybrids (Figure 3.8), we found that E-MAM$_2$ stimulated a 1.7-fold higher insulin secretion at 1 μM (**P<0.01, Figure 3.8A), compared to exendin-4 alone. E-TGN was 1.4-fold more potent at 3 at μM (*P<0.05, Figure 3.8B) compared to exendin-4.

For GIP hybrids, the actions of the hybrids were comparable to those of the incretin alone, therefore we decided to carry on further studies by focusing on the exendin-4 related hybrids (Figure 3.8A and B).

A)
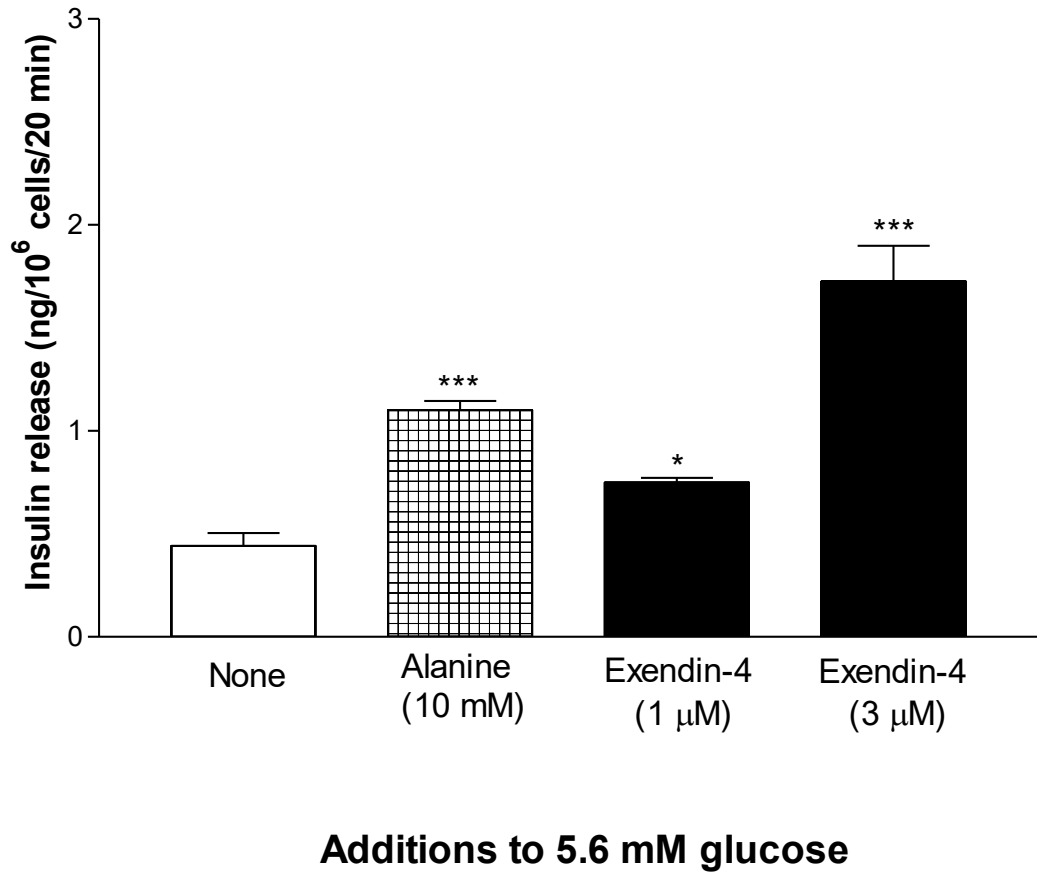
Figure 3.5.A. Exendin-4 (A) induced insulin secretion in BRIN-BD11 cells.
BRIN-BD11 cells were challenged with 5.6 mM glucose alone, or in the presence of Alanine
(10 mM), or 1 and 3 μM of exendin-4, as shown above, for 20 minutes. Following the
incubation, cell supernatant was assayed for insulin release using ELISA. Values are mean ±
SEM (n=3). *P<0.05, ***P<0.01 compared to 5.6mM glucose.

B)

Additions to 5.6 mM glucose
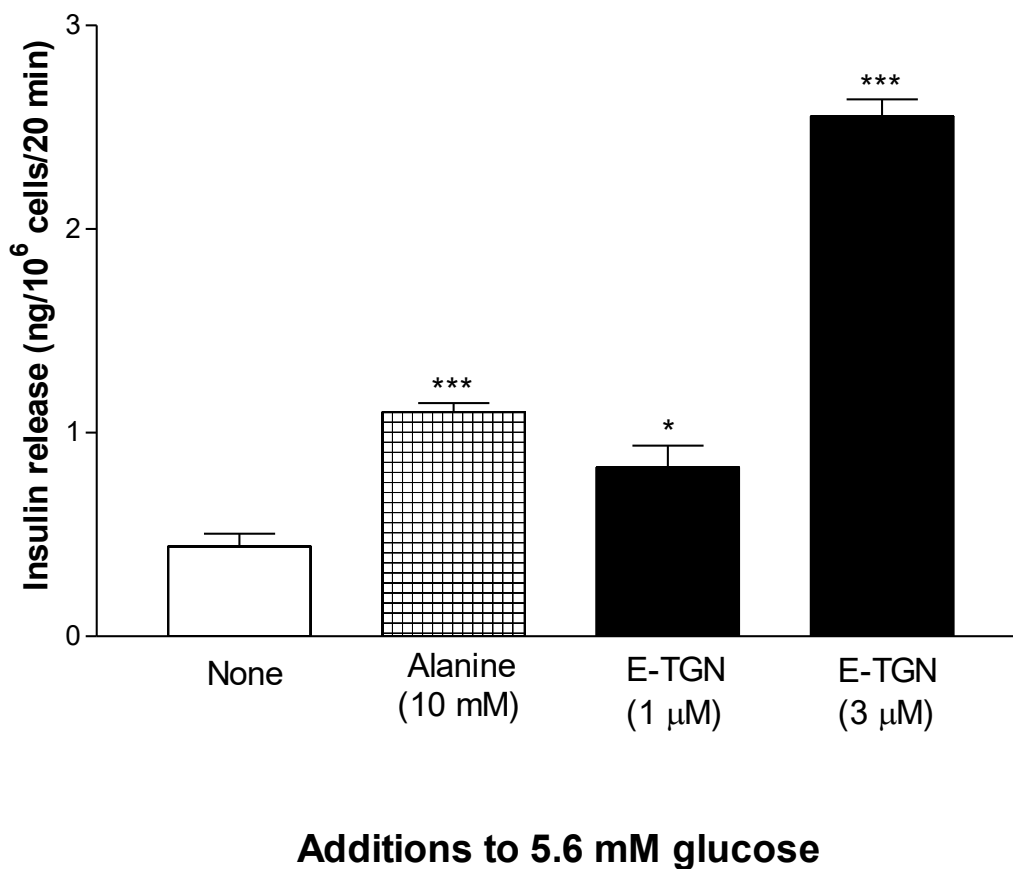
Figure 3.5.B. E-TGN (B) stimulated insulin secretion from BRIN-BD11 cells.
Cells were challenged with 5.6 mM glucose in the presence of absence of Alanine (10 mM),
or 1 and 3 μM E-TGN, as shown above, for 20 minutes. Following the incubation, cell
supernatant was assayed for insulin release using ELISA. Values are mean ± SEM (n=3).
*P<0.05, ***P<0.01 compared to 5.6mM glucose.

C)
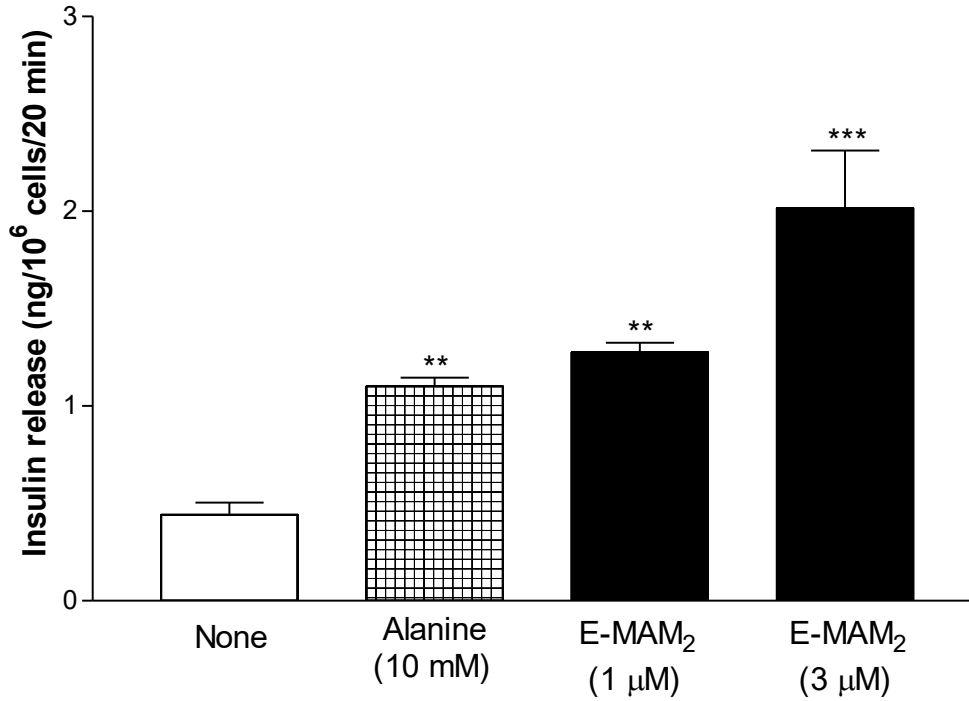
Figure 3.5.C. E-MAM$_2$ (C) has insulinotropic actions on BRIN-BD11 cells.
Cells were challenged with 5.6 mM glucose, in the presence or absence of Alanine (10 mM) for 20 minutes. The same glucose concentration was used to test 1 and 3 μM of E-MAM$_2$, as shown above. Following the incubation, cell supernatant was assayed for insulin release using ELISA. Values are mean ± SEM (n=3). **P<0.01, ***P<0.01 compared to 5.6mM glucose.

A)
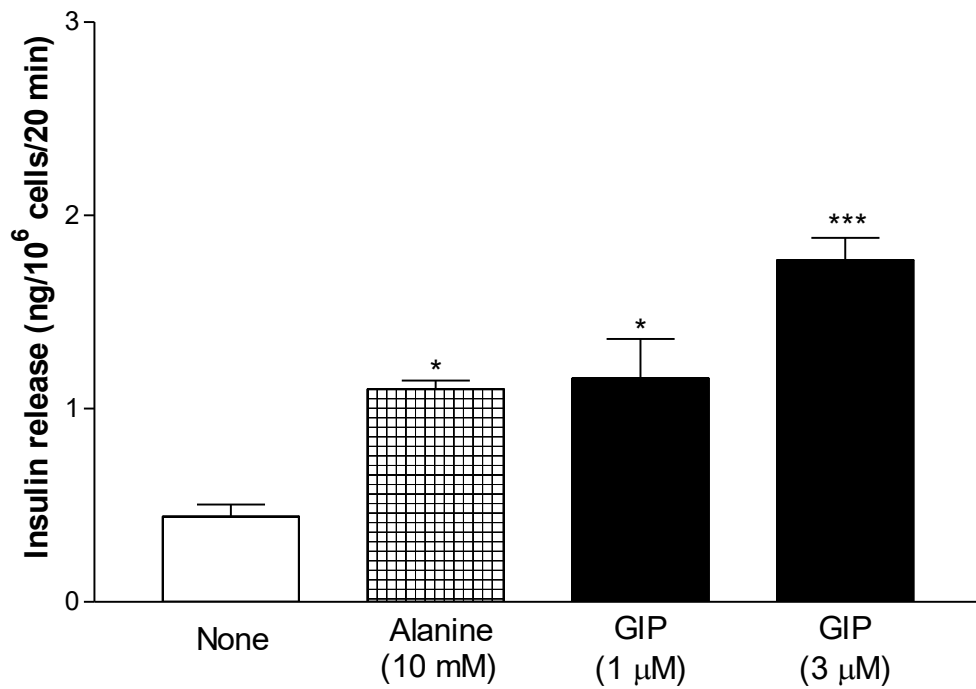
Figure 3.6.A. GIP (d-Ala^2-GIP, A) induced insulin secretion in BRIN-BD11 cells.
In a 20-minute acute test, BRIN-BD11 cells were treated with 5.6 mM glucose in the presence of Alanine (10 mM or 1 μM and 3 μM of GIP, as stated above. Following the incubation, cell supernatant was collected and insulin release was measured by ELISA. Values are mean ± SEM (n=3). *P<0.05, ***P<0.001 compared to 5.6mM glucose.

B)

Additions to 5.6 mM glucose
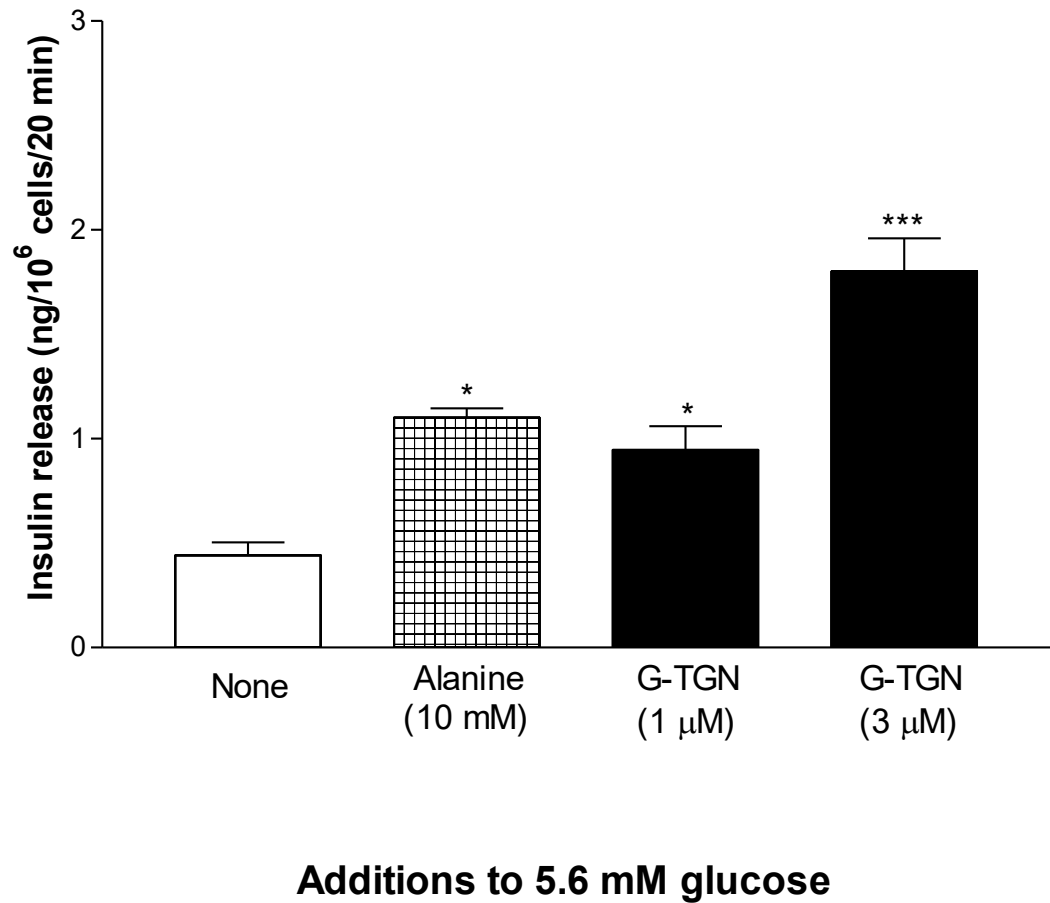
Figure 3.6.B. G-TGN (d-Ala^2-G-TGN, B) stimulates insulin secretion in BRIN-BD11 cells.
Cells were challenged with 5.6 mM glucose in the presence of absence of Alanine (10 mM), or 1 and 3 μM of G-TGN, as shown above, for 20 minutes. Following the incubation, cell supernatant was assayed for insulin release using ELISA. Values are mean ± SEM (n=3). *P<0.05, ***P<0.01 compared to 5.6mM glucose.

C)
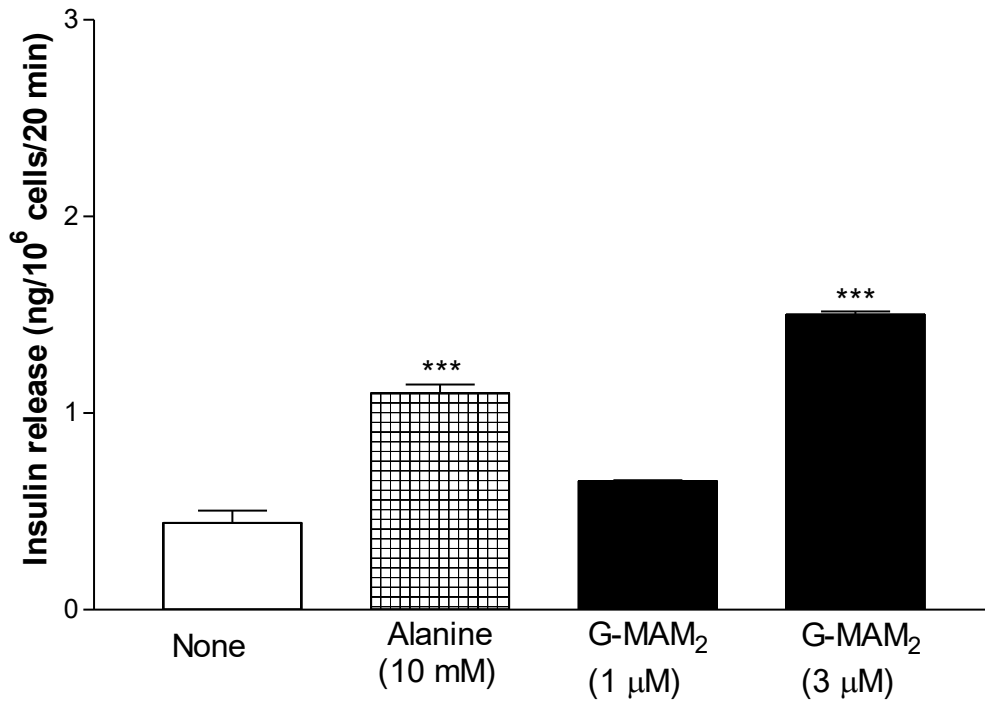
Additions to 5.6 mM glucose

Figure 3.6.C. G-MAM^2 (d-Ala^2-G- MAM^2, C) induced insulin secretion in BRIN-BD11 cells.
Cells were challenged with 5.6 mM glucose alone, or in the presence of Alanine (10 mM), or 1 and 3 μM of exendin-4, as shown above, for 20 minutes. Following the incubation, cell supernatant was assayed for insulin release using ELISA. Values are mean ± SEM (n=3). ***P<0.01 compared to 5.6mM glucose.

A)

Additions to 5.6 mM glucose

B)
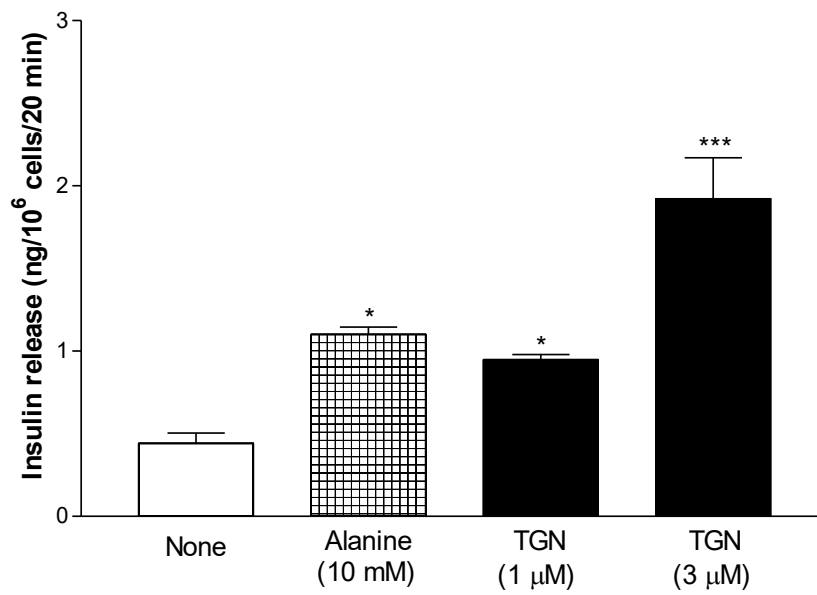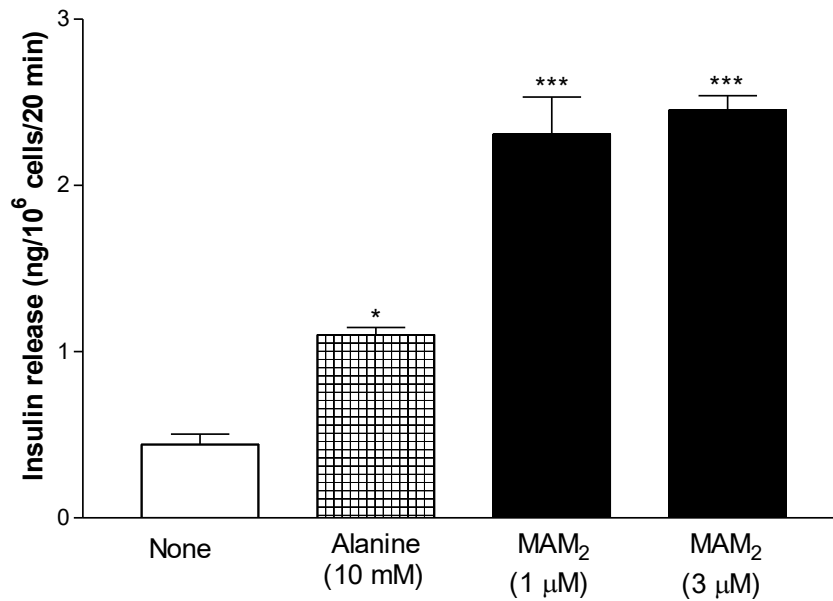
Additions to 5.6 mM glucose

Figure 3.7. TGN (A) and MAM$_2$ (B) induced insulin secretion in BRIN-BD11 cells.
BRIN-BD11 cells were treated with 5.6 mM glucose in the absence (white bar) or presence of Alanine (10 mM, checked bar), or 1 μM and 3 μM of exendin-4, as stated above. Following a 20 minutes incubation, cell supernatants were collected and insulin release was measured by ELISA. Results are shown as mean ± SEM (n=3). ***P<0.001, compared to 5.6mM glucose alone.

66

A)

Additions to 5.6 mM glucose

B)
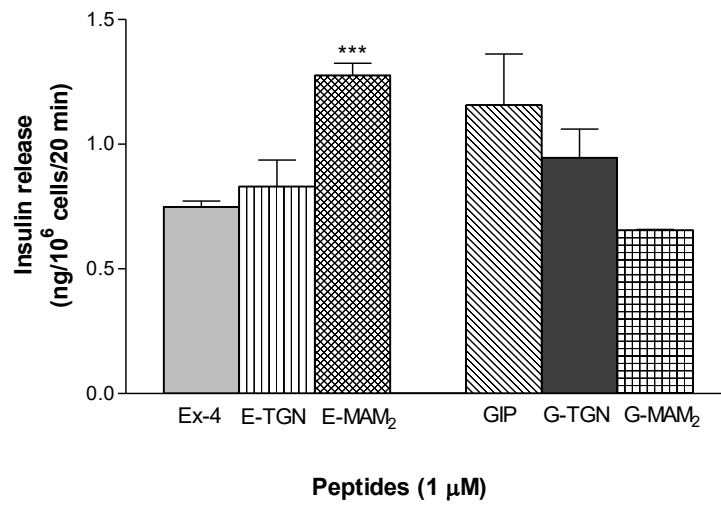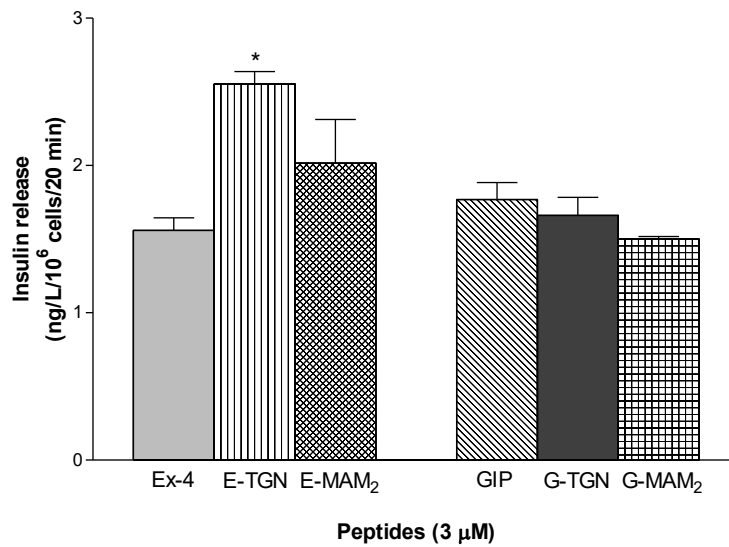
Additions to 5.6 mM glucose

Figure 3.8. Comparative analysis of the insulinotropic effects of hybrid peptides at 1 µM (A) and 3 µM (B) in BRIN-BD11 cells.
Values are mean ± SEM with n=3 . *$P<0.05$, ***$P<0.001$ compared to exendin-4.

3.4.4.2 Insulin secretion at high glucose concentration

Following the establishment of insulinotropic activities in BRIN-BD11 cells at 5.6 mM and the choice of exendin-4 hybrids for subsequent studies, we assessed whether their actions were maintained at a higher glucose concentration, namely 11.1 mM.

Under this condition, insulin output was 0.87 ± 0.14 ng/L. The vehicle treated samples maintained this value in the same range, reaching 1.04 ± 0.08 ng/L but without a statistically significant difference compared to control (Figure 3.9).

In the presence of exendin-4 at the concentrations of 1 and 3 µM, insulin release was measured at 1.41 ± 0.29 and 1.45 ± 0.19 ng/L ($P<0.001$), respectively (Figure 3.9A).

The insulinotropic action of E-TGN was not statistically significant at 1 µM, (1.14 ± 0.23 ng/L) compared to 11.1 mM glucose control, but generated an increase in insulin release up to 1.77 ± 0.44 ng/L ($P<0.001$, Figure 3.9B) at 3 µM. At a concentration of 1 µM, E-MAM$_2$ generated a 1.68-fold increase in insulin secretion (1.46 ± 0.47 ng/L, $P<0.05$) compared to control. This was further increased to 1.78 ± 0.48 ng/L ($P<0.001$) in the presence of 3 µM peptide (Figure 3.9C).

A)
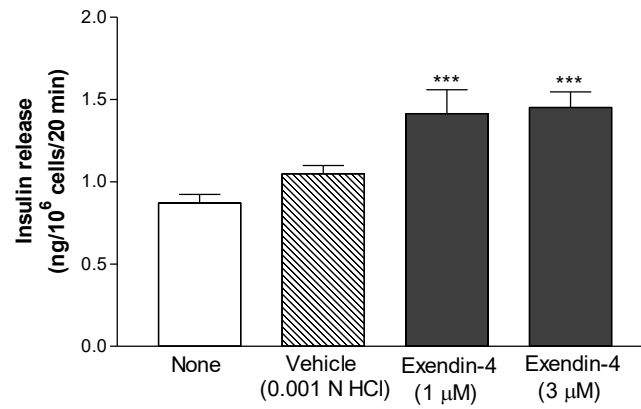
Additions to 11.1 mM glucose

B)

Additions to 11.1 mM glucose

C)
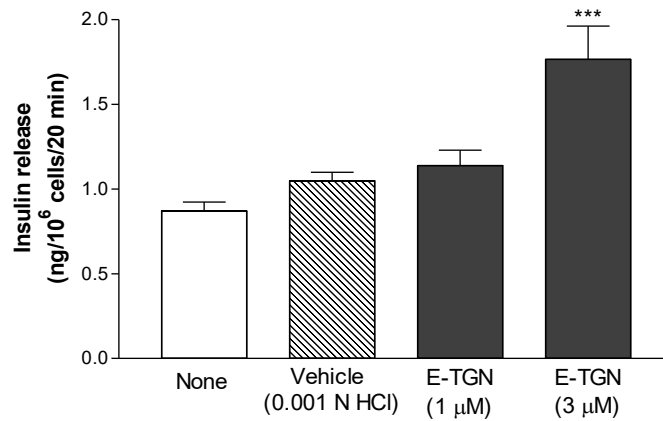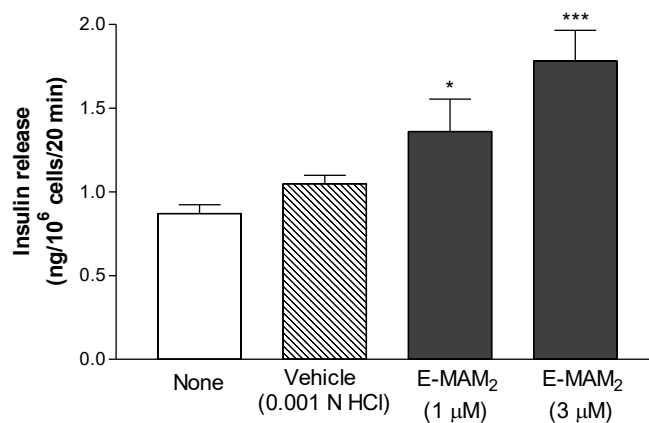
Additions to 11.1 mM glucose

Figure 3.9. Insulinotropic activities of exendin-4 (A), E-TGN (B) and E-MAM$_2$ (C) at high glucose concentrations.
BRIN-BD11 cells were incubated with 5.6 mM glucose, in the presence or absence of the vehicle control (0.001 N HCl). After a 20-minute incubation, insulin release was measured in the supernatant buffer. Values are mean ± SEM (n=3).

3.4.4.3 Actions in mouse pancreatic islets

The effects of the peptides in the presence of high glucose (11.1mM) were also investigated in primary mouse islets (Figure 3.10). In untreated islets, basal insulin release was $5.47 \pm 1.57\%$ of total insulin content. A vehicle control (0.001N HCl) was included in the study, where insulin secretion was recorded at $5.59 \pm 1.05\%$.

Insulin release increased to $5.59 \pm 1.05\%$, $7.72 \pm 3.65\%$ and $10.95 \pm 3.87\%$ ($P<0.05$) in the presence of 1 μM exendin-4 (Figure 10A), E-TGN (Figure 3.10B) and E-MAM$_2$ (Figure 3.10C) respectively. At a peptide concentration of 3 μM, significant increase in insulin secretion was observed, ranging from $10.64 \pm 5.13\%$ ($P<0.05$) for exendin-4 (Figure 3.10A), to $13.9 \pm 5.35\%$ ($P<0.01$) for E-TGN (Figure 10B), and $13.16 \pm 4.08\%$ ($P<0.01$) for E-MAM$_2$ (Figure 3.10C).

A)

Additions to 11.1 mM glucose

B)

Additions to 11.1 mM glucose

C)

Additions to 11.1 mM glucose
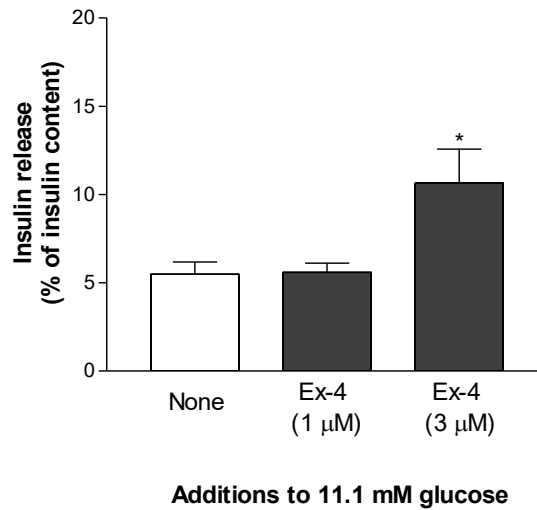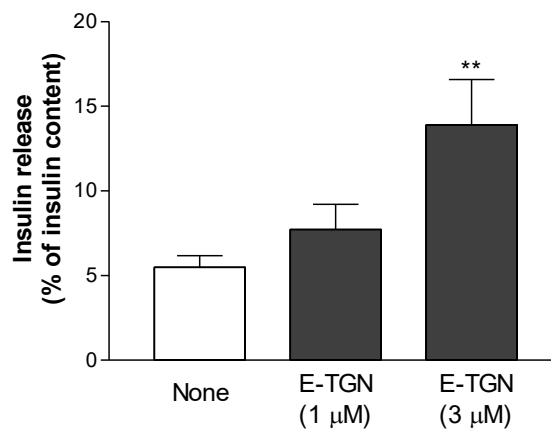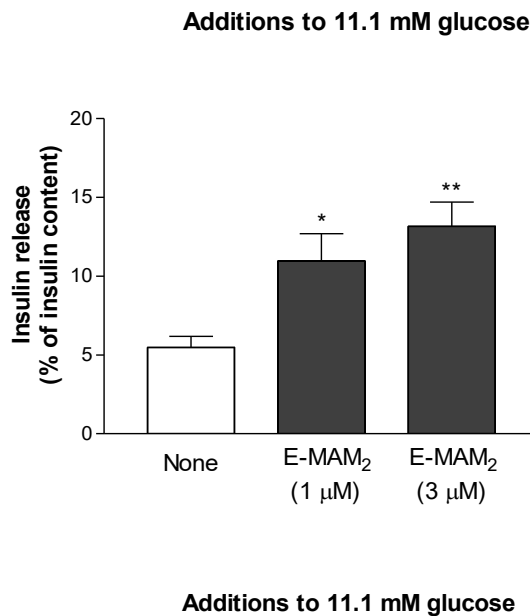
Figure 3.10. Insulinotropic actions of exendin-4-related peptides on isolated islets.
In a 20-minute test, 3-4 islets/well were treated with 11.1 mM glucose in the presence of Alanine (10 mM), 1 or 3 μM of exendin-4 (A), E-TGN (B) or E-MAM$_2$ (C), as stated above. Following the incubation, cell supernatant was collected and insulin release was measured by ELISA. Values are mean ± SEM (3 replicates). *P<0.01, compared to 5.6mM glucose.

3.4.5 Cytotoxicity and cell viability assessment

To assess whether the newly synthesised peptides had cytotoxic effects LDH and MTT assays were performed. The LDH concentrations present in the assay buffers retrieved from BRIN-BD11 cells incubated with glucose alone or in combination with peptides were similar. LDH release from cells incubated with glucose alone was set to $100 \pm 0.01\%$ and the values resulting from the other treatment samples were expressed as a percentage of this value. There was no significant LDH release in all incubations performed for established secretagogues and test agents in this study (Table 3.1).

LDH release measured in treated and untreated pancreatic islets were statistically similar. The maximum value of $110 \pm 38.5\%$ obtained in the presence of E-MAM$_2$ is not statistically different compared with control incubations at 11.1 mM glucose (Table 3.2).

Data obtained for MTT assay with BRIN-BD11 cells is shown in Table 3.3. Cell viability in cells incubated with glucose alone at 5.6mM was set at $100 \pm 9.96\%$. In the presence of DMSO (50% v/v), cell viability decreased to $13 \pm 5.35\%$ (P<0.001). Treatment with the peptides did not significantly affect cell viability. Values obtained ranged between $92 \pm 10.6\%$ for E-TGN and $116 \pm 18.4\%$ for MAM$_2$. These values were not significantly different from those obtained for control cells in the presence of glucose (5.6mM).

Table 3.1. LDH release from BRIN-BD11 cells

Addition to 5.6 mM glucose	Concentration (µM)	LDH release at (% of control)	Significance?
No peptide	-	100 ± 0.01	-
Alanine	10 000	90 ± 15.6	-
KCl	30 000	108 ± 20	-
exendin-4	1	87 ± 8.9	-
	3	111 ± 27.1	-
E-TGN	1	95 ± 14.7	-
	3	100 ± 0.8	-
E-MAM$_2$	1	110 ± 38.5	-
	3	92 ± 14.5	-
GIP	1	114 ± 10.8	-
	3	90 ± 14.5	-
G-TGN	1	88 ± 3.3	-
	3	91 ± 1.3	-
G-MAM$_2$	1	104 ± 22	-
	3	101 ± 18.5	-
TGN	1	91 ± 11.4	-
	3	101 ± 6	-
MAM$_2$	1	90 ± 16.4	-
	3	90 ± 16.3	-

Following the 20-minute acute test at 5.6 mM glucose under the different conditions (stated above), supernatant was assayed for LDH release. Values are ± SEM, n=3.

Table 3.2. LDH release from isolated mouse islets

Addition to 11.1 mM glucose	Concentration (µM)	LDH release at (% of control)	Significance?
No peptide	-	100 ± 1.8	-
exendin-4	1	87 ± 8.9	-
	3	111 ± 27.1	-
E-TGN	1	95 ± 14.7	-
	3	100 ± 0.8	-
E-MAM$_2$	1	110 ± 38.5	-
	3	92 ± 14.5	-

Effects of peptides on lactate dehydrogenase (LDH) release from isolated mouse islets treated with either 1 or 3 µM of exendin-4 related hybrids, in the presence of 11.1mM glucose. Values are ± SEM, n=3.

Table 3.3. MTT assay for cell viability in BRIN-BD11 cells.

Addition to 5.6 mM glucose	Concentration (µM)	MTT (% of control)	Significance?
No peptide	-	100 ± 9.96	-
DMSO (50%)	-	13 ± 5.35	***p<0.001
Vehicle (0.001 N HCl)	-	99 ± 13	-
exendin-4	1	100 ± 16.82	-
	3	107 ± 17.8	-
E-TGN	1	92 ± 10.6	-
	3	96 ± 17.8	-
E-MAM$_2$	1	93 ± 18.1	-
	3	102 ± 11	-
GIP	1	100 ± 13.7	-
	3	108 ± 26	-
G-TGN	1	97 ± 12.8	-
	3	112 ± 20.4	-
G-MAM$_2$	1	107 ± 18.4	-
	3	98 ± 19.2	-
TGN	1	99 ± 13.6	-
	3	94 ± 13.4	-
MAM	1	116 ± 25	-
	3	116 ± 18.4	-

The ability to reduce 3-(4,5-dimethylthiazol-2-yl)-2,5-diphenyltetrazolium bromide (MTT) to insoluble formazan was considered an index of cell viability. Cells were pre-treated under the different conditions (stated above) for 24 hours before undergoing MTT analysis. Viability is expressed as percentage of control (5.6 mM glucose). Values are ± SEM, n=3.***P<0.001.

3.5 DISCUSSION

Novel hybrid peptides (Table 2.1) were designed and created by PEGylation of the known insulinotropic agents exendin-4 and d-Ala^2-GIP (here termed GIP) with selected amphibian skin peptides (TGN and MAM$_2$). The rationale behind the creation of such hybrids lies firstly in the extensive characterisation of incretins and their pre-clinical/clinical values (Irwin and Flatt, 2015) and secondly, in the good knowledge regarding the receptor signalling actions of such peptides (Martin et al., 2013). By combining these activities with previously characterised amphibian skin peptides, namely TGN and MAM$_2$, this study aimed to establish whether hybrid peptides possessed additional and more potent insulinotropic actions compared to the respective incretins alone.

The purity confirmation of synthesized peptides conducted in this study ruled out the presence of possible additional components in the compounds generated during chemical synthesis. According to profiles obtained from our HPLC experiment, samples with exendin-4, E-TGN, E-MAM$_2$, GIP, G-MAM$_2$ and MAM$_2$ suggest peptide purity. For G-TGN, an additional, lower peak was detected (21.847 min), and for TGN an additional peak was detected right after the one eluting at 17.176, opening the possibility that these peptides could have been degraded during the HPLC run. However, previous reports detailed the presence of disulphide bonds, between cysteine residues at the carboxyterminal of TGN, leading to the formation of a cyclic version of TGN (Sai et al., 2001; Ojo et al., 2011). According to Ojo et al (2011), the presence of both cyclic and non-cyclic versions of TGN may lead to the observation of double peaks, similar to the chromatograms observed in this study. This could also explain the shoulder-peak observed also within the E-TGN run, bringing us to the conclusion that additional peaks in these samples could represent disulphide bonds within the TGN peptide as opposed to degraded products. However, to validate this hypothesis further studies using mass-spectrometry are needed. Determining the mass corresponding to the individual peaks and comparing it to the calculated theoretical masses of the peptides (listed in Table 1, Chapter 2) would expand on this supposition.

With regards to insulin secretion, increased insulin output generated by alanine is consistent with previous studies using similar experimental conditions (McClenaghan et al., 1996a; Abdel-Wahab et al., 2008; Owolabi et al., 2017).

Though exendin-4 and GIP have been shown to be insulinotropic in BRIN-BD11 cells at concentrations as low as 1 pM (Irwin et al., 2015) and 1 µM (Martin et

al., 2013), respectively, we chose 1 and 3 μM for our studies based on previous reports on the insulinotropic effects of TGN and MAM$_2$. In fact, the maximum stimulatory effect on insulin secretion, in the absence of cytotoxicity was previously observed at 3 μM for both TGN (Ojo et al., 2011) and MAM$_2$ (Ojo et al., 2015a). Therefore, we aimed to obtain the most potent effects of the hybrids under these conditions. Consistent with this hypothesis, all peptides stimulated insulin release in a concentration-dependent fashion. As the concentration of the peptides increased from 1 to 3 μM, insulin secretion increased accordingly, with E-TGN producing the highest stimulatory effects at a physiological glucose concentration.

Comparing the activities of GIP with those of its hybrids, this study showed that at both concentrations, insulinotropic actions of GIP decreased, although not significantly, in conjugation with TGN or MAM$_2$. This indicates that PEGylation with the amphibian skin peptides might have modified the insulinotropic actions of GIP, despite not abolishing them, as it has been reported that PEG molecules may cause a reduction of the biological activity of the compound they are attached to (Hadadian et al., 2015).

For exendin-4 and its hybrids, this study showed that at 1 μM, exendin-4 and E-TGN displayed similar insulinotropic activities. PEGylation of Exendin-4 with the amphibian peptide MAM$_2$ nearly doubled the effects of the known GLP-1 receptor agonist and validated the hypothesis that conjugating exendin-4 with MAM$_2$ will improve the original insulinotropic actions of the peptide. At 3 μM, the differences between the insulinotropic activities of exendin-4 and its related peptides were further amplified. The additional effect of TGN and MAM$_2$ on exendin-4 showed promise for compounds that might enhance the anti-diabetic actions of a validated and approved therapeutic agent, such as exendin-4, for type 2 diabetes.

To further support this, the additive effects observed in BRIN-BD11 cells were found detected under hyperglycaemic conditions in isolated primary islets, which represent a more comprehensive pancreatic cell model for the assessment of anti-diabetic activities *in vitro* (Owolabi et al., 2017; Vasu et al., 2017).

This study also investigated cytotoxic effects that may be associated with the novel peptides, given the insulin-release peptides previously identified in amphibians have anti-microbial and anti-fungal properties (Conlon et al., 2017). Lactate Dehydrogenase (LDH) and Thiazolyl Blue Tetrazolium Bromide (MTT) assays served as high throughput cytotoxicity tests. Measuring levels of LDH, an enzyme confined to the cytoplasm under normal conditions, has been reported as a reliable

indicator of cellular membrane integrity (Chan et al., 2013). Within our screen, this parameter was exceptionally relevant for two reasons. The first resides in the evidence that cationic peptides of natural origin, such as those of the TGN family, are known to exert their main cytotoxic effects towards bacteria by permeabilizing the cell membrane (Sai et al., 2001). The lack of LDH release in cells incubated with the peptides in this study therefore strongly suggest that cell membrane integrity was not affected by peptide treatment. This result is consistent with findings of several previous studies involving animal-derived peptides with anti-diabetic potential (Moore et al., 2015; Ojo et al., 2011; Ojo et al., 2015b).

The second reason that justifies the use of LDH assay relates to the presence of insulin in pre-formed granules within the cytoplasm. Cell membrane rupture would lead to an increase in insulin levels measured in the assay buffer even in the absence of insulinotropic stimulus. In that case, insulin release would not be informative of the peptides' activity or of existing cellular mechanisms. The lack of cytotoxicity and the preserved cell viability following all treatments were consistent. The MTT assay provided additional confirmation of the *in vitro* safety of the peptides, as no differences between peptide-treated samples and our control was detected, indicating the insulinotropic actions observed are a result of an active cell mechanism.

A limitation of this study is the lack of data regarding the use of combination of both peptides, as a cocktail, on BRIN-BD11 cells under these conditions. This experiment would validate and prove the concept of the hybrid peptides having a validated advantage over the use of the single, individual hybrids. In this study, we only compared the action of the peptides to their native incretins. Though the actions of TGN and MAM_2 alone are more potent than those of the hybrids, we focused on the increased potency they confer to the native incretin Exendin-4 which is, among the peptides tested, the only peptide approved for anti-diabetic therapy.

Given the potential of E-TGN and E-MAM_2, showing higher insulinotropic activity compared to exendin-4 *in vitro*, these peptides were selected for further mechanistic studies. Subsequent studies will investigate how the actions of these peptides are modulated by higher glucose concentrations, and by the presence of insulin secretion modulators. In addition, exendin-4 was also selected for further studies, in comparison with the hybrids, and details on its role in modulating metabolism are presented in Chapter 5.

Chapter 4

MECHANISM OF ACTION STUDIES

4.1 BACKGROUND

4.1.1 Glucose and insulin secretion

In healthy organisms, pancreatic beta-cells are sophisticated glucose sensors with the ability to regulate insulin secretion, according to circulating blood glucose levels. Glucose-stimulated insulin secretion (GSIS) is considered the central feature for metabolic homeostasis, as it also indirectly regulates the actions of other secretagogues such as fatty acids, amino acids and incretins (Newsholme and Krause, 2012).

In pancreatic beta-cells, the GLUT2 transporter allows glucose flow by facilitated diffusion in a physiologically relevant range (2-20 mmol/L) (Newsholme and Krause, 2012). Once in the cytoplasm, glucose is phosphorylated, by the glucokinase enzyme to yield glucose-6-phosphate. This critical step for glycolysis ultimately leads to the production of pyruvate, NADH, ATP and other metabolic coupling factors, which all contribute to insulin release. Insulin release is biphasic, with the first phase using a pool of readily available granules in the cell membrane proximity (Straub and Sharp, 2004). The second phase, involving recruitment of deeper intracellular pools, is responsible for the majority of insulin released, which is abrogated in type 2 diabetes (Kalwat et al., 2017).

The main pathway leading to insulin secretion is triggered by an increase in ATP concentration, mostly deriving from the TCA cycle. Pancreatic beta-cells possess low levels of lactate dehydrogenase in their cytoplasm to favour the entry of pyruvate into the TCA cycle, as opposed to being reduced to lactate (Macdonald et al., 2005; Newsholme and Krause, 2012), highlighting the pivotal role of mitochondrial glucose oxidation in the production of ATP. The increase in the ATP/ADP ratio causes the closure of the ATP-dependent potassium channels (K_{ATP}), resulting in cell depolarization by reduction of K^+ ion efflux. Subsequently, the voltage-dependent calcium channels (VDCC) open, increasing Ca^{2+} influx and triggering granule exocytosis (MacDonald and Rorsman, 2006).

The pathway of insulin secretion involves secondary products of glucose metabolism. Incretins are known to exploit the cAMP pathway in perpetuating GSIS, both via protein kinase A (PKA) dependent and independent mechanisms (Fu et al., 2013).

Potassium and calcium play important roles in balancing electrical activity in beta cells. Following insulin release, the intracellular calcium ions also have a net action of repolarizing the cell membrane by both depleting ATP (Kanno et al., 2002) and directly favouring the opening of the potassium channels after a firing potential (Zhang et al., 2005). For these reasons, we focused on understanding how targeting the K_{ATP} and Ca^{2+} channels could modulate the insulinotropic activities of the novel hybrid peptides.

4.1.2 The role of K_{ATP} channel in insulin secretion

The ability to couple metabolic states to membrane excitability is a unique feature of K_{ATP} channels (Jonkers et al., 2011; Han et al., 2018; Silkimic et al., 2019). In pancreatic beta-cells, K_{ATP} channels play an important role in regulating membrane potential, which is associated with insulin release. In the absence of glucose stimulation, the K_{ATP} channels only allow a slight inward rectifier current to maintain the resting membrane potential at -70 mV (Tarasov et al., 2004). In the presence of stimulatory glucose concentrations, ATP deriving from metabolism binds to the Kir6.2/SUR1 subunit of the channel causing displacement of ADP and leading to channel closure (Macdonald et al., 2005). The closure of K_{ATP} channels is associated with insulin secretion, even in the absence of a stimulatory glucose concentration (Han et al., 2018), indicating a glucose-independent effect of these channels on insulin release. To further understand the relevance of K_{ATP} channels in pancreatic beta-cells *in vivo*, studies involving animal models or naturally occurring polymorphisms have been performed. Inhibition of the Kir6.2/SUR1 subunit of the channel in mice generates hyperinsulinemia, which is associated with a diabetic phenotype later in life (Seino and Miki, 2003). Reports of gain-of-function or loss-of-function mutations in K_{ATP} channels are correlated with severe metabolic diseases such as congenital hyperinsulinism and neonatal diabetes, respectively (Gloyn et al., 2004; Sikimic et al., 2019).

With regards to newly identified insulinotropic peptides, much attention has also been directed to understanding their mechanistic properties, by modulating the activity of K_{ATP} channels with different pharmacological agents (Ojo et al., 2015c). Secretagogues such KCl and sulphonylureas are known to induce a robust beta-cell depolarisation, representing an established model for first phase insulin secretion (Straub and Sharp 2004). On the other hand, allowing ion efflux with potassium channel openers dampens the electrical activity of pancreatic beta-cells, thus reducing insulin secretion (Seino and Miki, 2003). Two main agents have been reported to have clear actions in modulating the insulin secreting process.

Diazoxide is a potassium channel opener responsible for inhibiting insulin secretion by preventing cell depolarisation induced by the closure of the K_{ATP} channels (Gembal et al., 1992). Conversely, tolbutamide determines a sustained cell depolarization responsible for the closure of the K_{ATP} channels and the activation of the voltage-dependent L-type calcium channels (VDCC), triggering insulin release (Gilon and Henquin,1992). Under these conditions, exposing cells to these K_{ATP} channel modulators allowed us to evaluate the contribution of K_{ATP} channels to the actions of the hybrid peptides.

4.1.3 Calcium ions and insulin secretion

The concentration of intracellular Ca^{2+} ions is critical to numerous biological functions, including maintenance of glucose homeostasis (Carvalho et al., 2018). Increasing concentrations of Ca^{2+} stimulate insulin secretion in a glucose-free medium, as reported in early studies pancreatic islets from fasted diabetic ob/ob mice (Andersson et al., 1981), highlighting the critical role of this ion in insulin release. As part of the triggering pathway, calcium enters pancreatic beta-cells via voltage-dependent calcium channels (VDCC), to interact with pre-formed insulin granules.

Beta-cells are also known to possess extracellular calcium-sensing receptors that identify fluctuations in local Ca^{2+} concentrations (Rácz et al., 2002; Jones et al., 2007). By integrating these signals with neighbouring cells, beta cells within an islet coordinate and potentiate the secretory response to insulin secretagogues, exploiting cell-to-cell communication (Hodgkin et al., 2008). In the field of T2D, pharmacological inhibition of VDCCs using verapamil represents a tool for

investigating dependency of the insulinotropic peptide actions on extracellular sources of Ca^{2+} (Srinivasan et al., 2014; Ojo et al., 2015a).

In addition to Ca^{2+}, cAMP plays an important role in insulin secretion. By directly promoting Ca^{2+} signalling, increasing the activity of VDCCs (Seino and Tadeo, 2005) or indirectly participating in exocytosis (Tengholm 2012; Carvalho et al., 2018), hormones such as incretins and neurotransmitters favour insulin secretion by increasing the levels of cAMP (Seino and Tadeo, 2005). This intracellular secondary messenger has been shown to be involved in intracellular movement of insulin granules towards a localisation that promotes insulin exocytosis (Hisatomi et al., 1996), supporting the role of cAMP in regulating insulin granule dynamics. Under sub-optimal concentrations of glucose, 3-isobutyl-1-methylxanthine (IBMX) inhibits phosphodiesterases, preventing degradation of cAMP and therefore favouring the activation of PKA involved in maintaining cytoplasmic Ca^{2+} levels (Tengholm, 2012).

There is long standing evidence of this phosphodiesterase inhibitor triggering insulin release even in the absence of a stimulatory glucose concentration, with effects detected in the presence of 2.8 mM glucose (Siegel et al., 1980). Given the existence of these different pathways, modulating key targets of these processes in the presence of the hybrid peptides could shed light on their preferred mechanism of action in the acute phase of insulin release.

4.2 AIM AND OBJECTIVES

The aim is to understand the mechanism of insulinotropic actions of hybrid peptides E-TGN and E-MAM$_2$, using BRIN-BD11 cells. As discussed in Chapter 3, these compounds were selected for further studies as they showed the most potent insulinotropic activities, when compared to the established GLP-1 receptor agonist exendin-4.

Specific objectives include:

1. Evaluating the effects of an increase in glucose concentrations on the insulinotropic activities of the hybrid peptides E-TGN and E-MAM$_2$.

2. Assessing the involvement of the K_{ATP} channel in the actions of E-TGN and E-MAM$_2$.

3. Evaluation of the role of the voltage-dependent calcium channels (VDCC) and extracellular calcium in the actions of the aforementioned hybrid peptides.

4.3 RESEARCH DESIGN

4.3.1 Cell culture

For mechanism of action studies, BRIN-BD11 cells were grown and maintained in sterile T75 flasks, and all solutions were prepared in KRB buffer as detailed in section 2.1.3. One day prior to treatment, cells were seeded into a 24-well plate, at a density of $1.5X10^5$ cells/well and allowed to adhere overnight as previously described (see section 2.2). Prior to incubation with hybrid peptides and/or channel inhibitors, cells were washed for 40 mins with KRB buffer supplemented with 1.1 mM glucose.

4.3.2 Determination of the action of glucose on the activity of the hybrid peptides

An acute insulin test was performed as detailed in section 3.3.2. In this set of experiments, following 40 min pre-incubation in KRBB in the presence of 1.1 mM glucose, BRIN-BD11 cells were treated with 1.1, 5.6 or 11.1 mM glucose, in the presence or absence of the peptides (1μM of E-TGN or E-MAM$_2$). Following the acute test, supernatants were retrieved from each well and stored at -20°C before insulin ELISA and LDH assays.

4.3.3 Assessment of the involvement of K$_{ATP}$-channel in insulinotropic actions

Cells were incubated with KRB buffer supplemented with glucose (5.6 mM) and modulators of th K$_{ATP}$-channel (300 μM diazoxide or 200 μM tolbutamide), in the absence or presence of the peptide (1 μM). Test solutions with KCl (30 mM) were prepared in KRBB supplemented with 16.7 mM glucose. Following the 40 min pre-incubation with 1.1 mM glucose, cells were exposed to the test solutions, in a 20-minute acute test, as described in section 3.3.2. Supernatants were collected from each well and stored at -20°C for insulin measurements.

4.3.4 Acute insulin test in the presence of calcium modulators

In a separate set of experiment, BRIN-BD11 cells were incubated with 5.6 mM glucose in the presence of Verapamil (50 nM) or IBMX (200 µM). Solutions were prepared in KRBB, as detailed previously in section 2.2. Cells were also incubated with or without peptides (1 µM) in the absence of extracellular calcium using a modified KRB buffer, free from Ca^{2+} (115 mM NaCl, 4.7 mM KCl, 10 mM EGTA, 1.2 mM $MgSO_4 \cdot 7H_2O$, 1.2 mM KH_2PO_4, 25 mM HEPES, 8.4% (w/v) $NaHCO_3$ and 1% bovine serum albumin) (pH 7.4), supplemented with 5.6mM glucose and in the absence or presence of each peptide (1 µM). Following the 40-minute pre-incubation in the presence of 1.1 mM glucose, a 20-minute acute test with the different treatments was performed. Supernatants were stored at -20°C for insulin ELISA measurements.

4.3.5 Insulin concentration measurement by ELISA

An insulin specific ELISA was performed using the Ultrasensitive Insulin ELISA kit (Mercodia AB, Uppsala, Sweden) according to the manufacturer's protocol (See Section 3.3.5). Briefly, 25 µL of samples and standards, and 100 µL of enzyme conjugate buffer were added to each well for a 2-hour incubation. At the end of the incubation wells were washed (x6), and 50 µl of the substrate TMB was added. After 30 minutes H_2SO_4 (0.5 M) was added and the absorbance was measured by a spectrophotometer at a wavelength of 450 nm.

4.4 RESULTS

4.4.1 Effects of E-TGN and E-MAM$_2$ on GSIS

Insulin release in the presence of 1.1 and 5.6 mM glucose was 0.63 ± 0.14 ng/L and 0.69 ± 0.06, respectively. At 11.1 mM glucose the concentration of insulin measured increased to 0.98 ± 0.02 ng/L (P<0.01). The addition of E-TGN (1 μM) generated a significant increase in insulin secretion (2.2-fold, P<0.05) reaching 1.52 ± 0.32 ng/L in the presence of 1.1 mM glucose. At 5.6 mM glucose, E-TGN also increased insulin secretion by 2.8-fold (P<0.05), compared to control incubation in the absence of the peptide. At 11.1 mM glucose, E-TGN stimulated insulin release by 1.9-fold (P<0.01) compared to its respective control incubation in the absence of the peptide (Figure. 4.1A).

Like E-TGN, the addition of E-MAM$_2$ (1 μM) to BRIN-BD11 cells in the presence of 1.1 mM glucose generated a 2.2-fold increase (P<0.01) in insulin secretion, which increased slightly in the presence of 5.6 mM glucose (2.54-fold, P<0.01). In the presence of 11.1 mM glucose, E-MAM$_2$ exhibited the highest stimulatory effects, increasing the amount of insulin secreted by 2.49-fold, compared to 11.1 mM glucose alone. and a 3.88-fold increase (P<0.05) compared to the actions of the peptide at a non-stimulatory glucose concentration (5.6 mM) (Figure. 4.1B).

A)
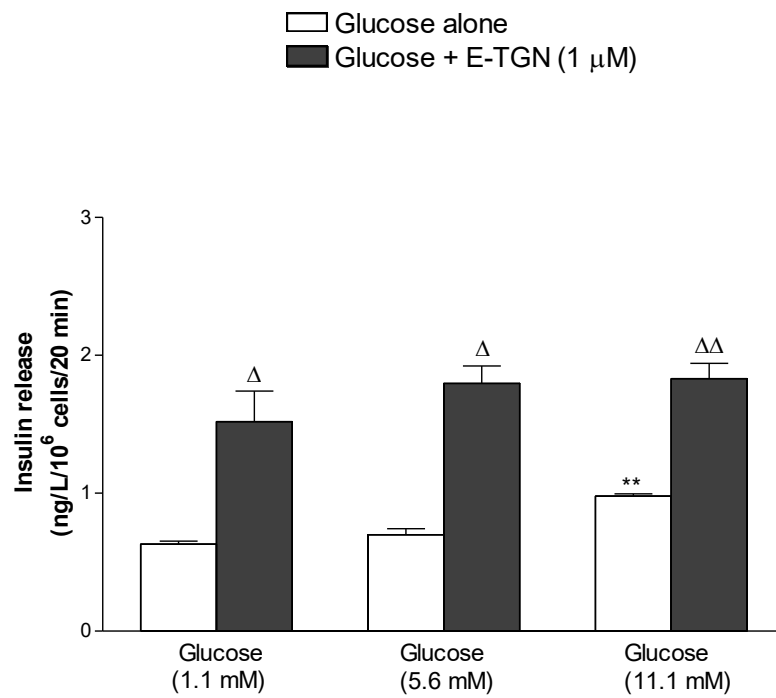
B)
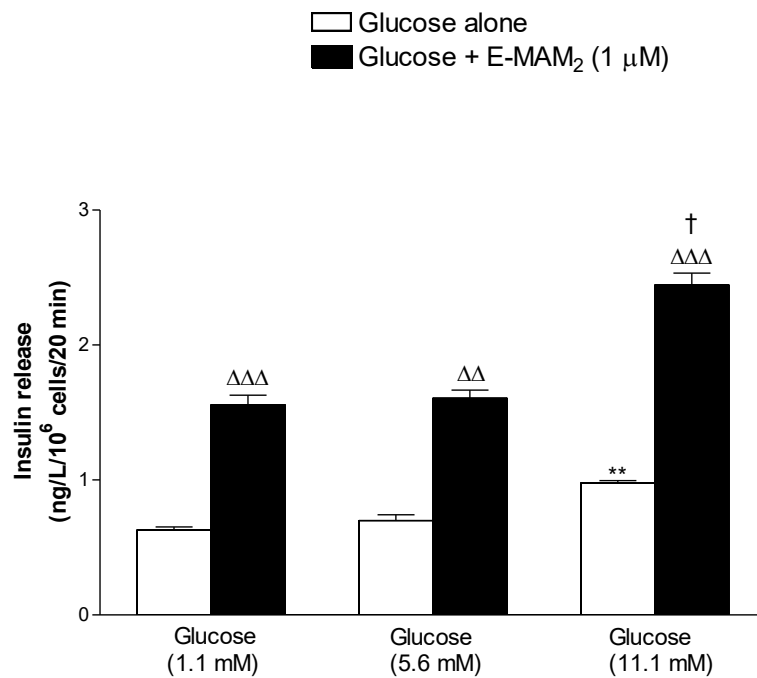
Figure 4.1. GSIS in the presence of (A) E-TGN or (B) E-MAM$_2$.
Values are mean ± SEM (n=3). **P<0.01 compared to 5.6 mM glucose. $^{\Delta\Delta\Delta}$P<0.001, $^{\Delta\Delta}$P<0.01, $^{\Delta}$P<0.05 compared to respective incubation without peptide. $^{+}$P<0.05 compared to 5.6 mM glucose + peptide (1 μM).

4.4.2 The role of K_{ATP}-channel in the insulinotropic actions of E-TGN and E-MAM$_2$

To evaluate the contribution of the K_{ATP}-channel, a major component of the main pathway of insulin secretion as described in the background section of this chapter, cells were incubated with different modulators of K_{ATP}-channel activity. Basal insulin secretion at 5.6mM glucose (0.96 ± 0.1 ng/L) was increased by 1.5- (P<0.01) and 1.7-fold (P<0.001) in the presence of E-TGN and E-MAM$_2$ respectively (1 µM) (Figure 4.2). The addition of diazoxide (300 µM) reduced basal insulin secretion from 0.96 ± 0.1 ng/L to 0.55 ± 0.1 ng/L (P<0.001). In the presence of this potassium channel opener, diazoxide, both E-TGN and E- MAM$_2$ triggered a significant increase in insulin levels in the buffer (P<0.001), comparable to those in the absence of the modulator (1.29 ± 0.4 ng/L and 1.29 ± 0.3 ng/L).

The depolarizing action of KCl (30 mM) in the presence of 16.7 mM glucose generated the highest increase in insulin secretion compared to control, by 4.8-fold (4.59 ± 0.5 ng/L, P<0.001). The addition of E-MAM$_2$ (1 µM) further expanded the insulinotropic potential of the cell, by increasing the amount of insulin present in the buffer to 6.51 ± 0.2 ng/L (1.4-fold, P<0.001) (Figure 4.2B), while in the presence of E-TGN insulin secretion remained in the same range compared to its respective control incubation (5.36 ± 0.1 ng/L) (Figure 4.2A). Insulin output in the presence of tolbutamide was increased by 1.3-fold (P<0.05). The actions of E-TGN and E-MAM$_2$ were further enhanced in the presence of tolbutamide, with insulin secretion rising by a further 1.5- and 2-fold (P<0.01), respectively (Figure 4.2A and B).
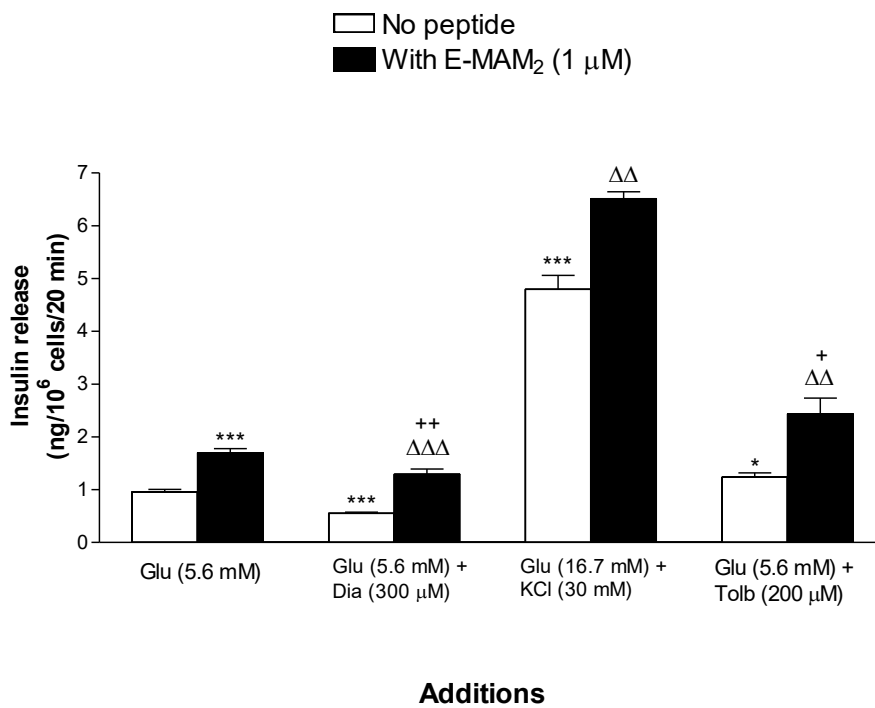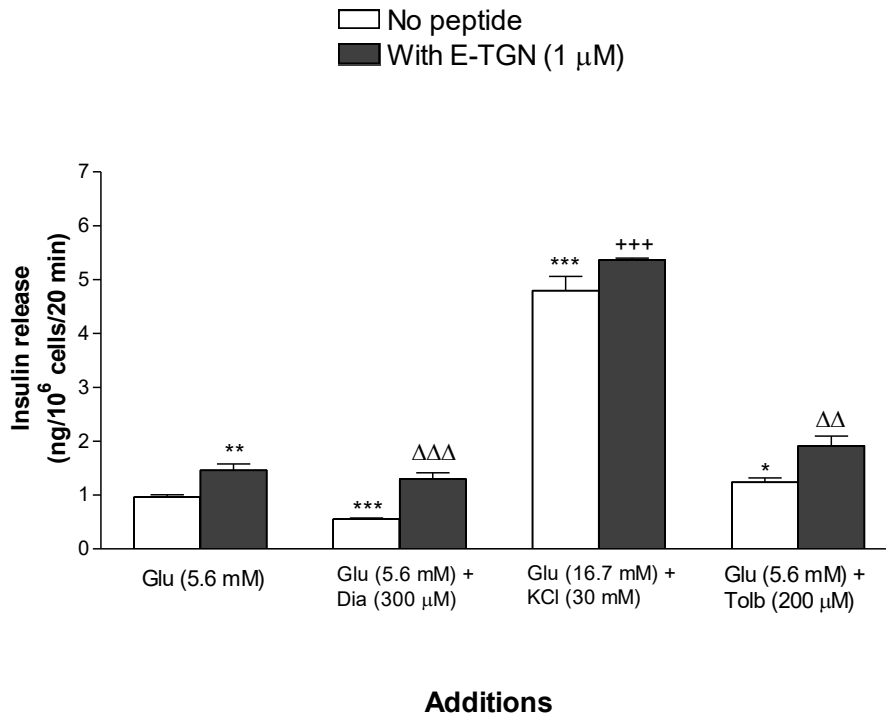
Figure 4.2. Effects of KATP channel modulators on the insulinotropic actions of (A) E-TGN or (B) E-MAM₂.

Values are mean ± SEM (n=3). **$P<0.01$, *$P<0.05$ compared to 5.6 mM glucose. $^{\Delta\Delta}P<0.01$, $^{\Delta}P<0.05$ compared to respective incubation without peptide. $^{+++}P<0.001$, $^{++}P<0.01$, $^{+}P<0.05$ compared to 5.6 mM glucose + peptide (1 μM).

4.4.3 The role of calcium in the insulin-releasing effects of E-TGN and E-MAM₂

As expected, insulin secretion in control incubations (5.6 mM glucose only) was 0.36 ± 0.04 ng/L which increased to 0.80 ± 0.24 ng/L (P<0.01) and 0.91 ± 0.26 ng/L (P<0.01) with the addition of E-TGN and E-MAM₂ (1 μM), respectively (Figure 4.3). In the absence of extracellular calcium, basal insulin secretion decreased from 0.36 ± 0.04 ng/L to 0.21 ± 0.04 ng/L (P<0.01). Under Ca^{2+} free conditions, the insulin inducing properties of E-TGN were decreased to 0.29 ± 0.07 ng/L (P<0.01) (Figure 4.3A) and those of E-MAM₂ to 0.45 ± 0.12 ng/L (P<0.01) (Figure 4.3B) which represent a 2.8- and 2-fold reduction, compared to their activities in the presence of Ca^{2+}.

In this study, the presence of IBMX alone generated an increase in insulin secretion to 2.63 ± 1.5 ng/L (P<0.01). The addition of E-TGN did not increase the amount of insulin secreted, which remained approximately the same (2.51 ± 1.4 ng/L) (Figure. 4.3A). Conversely, the insulinotropic action of E-MAM₂ in the presence of IBMX was increased by 1.6-fold (P<0.01) (Figure 4.3B) to levels comparable to those observed in the presence of 16.7 mM glucose and KCl.

In order to assess the cells' response to blockage of the VDCCs, the insulinotropic actions of the peptides were evaluated in the presence of verapamil (50 μM). In this experiment, basal insulin secretion at 5.6 mM glucose was 0.87 ± 0.07 ng/L, which was reduced to 0.56 ± 0.07 ng/L in the presence of verapamil (P<0.01). The addition of E-TGN resulted in an increase of basal insulin secretion to 1.24 ± 0.04 ng/L (P<0.01). In the presence of verapamil, these actions were reduced, and insulin secretion was recorded at 0.73 ± 0.1 ng/L (P<0.001) (Figure 4.4A). This value was still significantly higher that the respective incubation in the absence of the peptide, suggesting the presence of an alternative pathway exploited by E-TGN to exert its actions.

The actions of E-MAM₂ were tested under the same conditions. At 5.6 mM glucose, the peptide increased insulin secretion to 1.7 ± 0.11 ng/L (P<0.001). Compared to this condition, the addition of verapamil caused the actions of E-MAM₂ to reduce to 1.1 ± 0.09 ng/L, which was still significantly higher than the respective incubation in the absence of the peptide (P<0.001). As opposed to E-TGN, insulin release in the presence of E-MAM₂ and verapamil was 1.27 ± 0.09-fold higher compared to basal levels at 5.6 mM glucose (Figure 4.4B). These results suggest that

the importance of the VDCC in the mechanism of action of E-MAM$_2$ are less pronounced that those of E-TGN, given the latter seems to be affected to a greater extent by inhibition of the channel.

A)
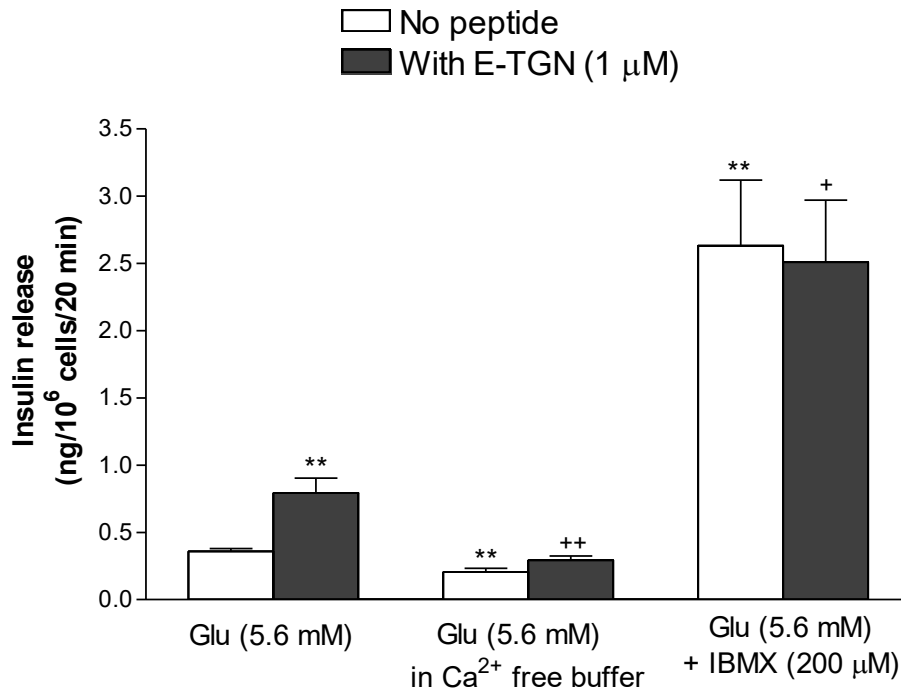
B)
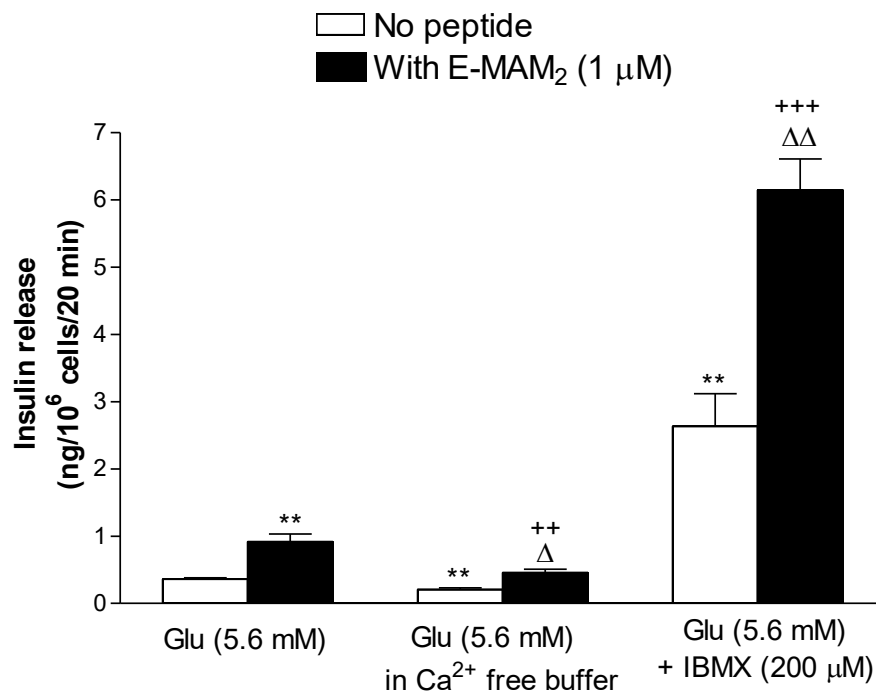
Figure 4.3. Effect of Ca2+ on the insulinotropic actions of (A) E-TGN or (B) E-MAM2.
Values are mean ± SEM (n=3). **$P<0.01$, *$P<0.05$ compared to 5.6 mM glucose. $^{\Delta\Delta}P<0.01$, $^{\Delta}P<0.05$ compared to respective incubation without peptide. $^{+++}P<0.001$, $^{++}P<0.01$, $^{+}P<0.05$ compared to 5.6 mM glucose + peptide (1 μM).

A)
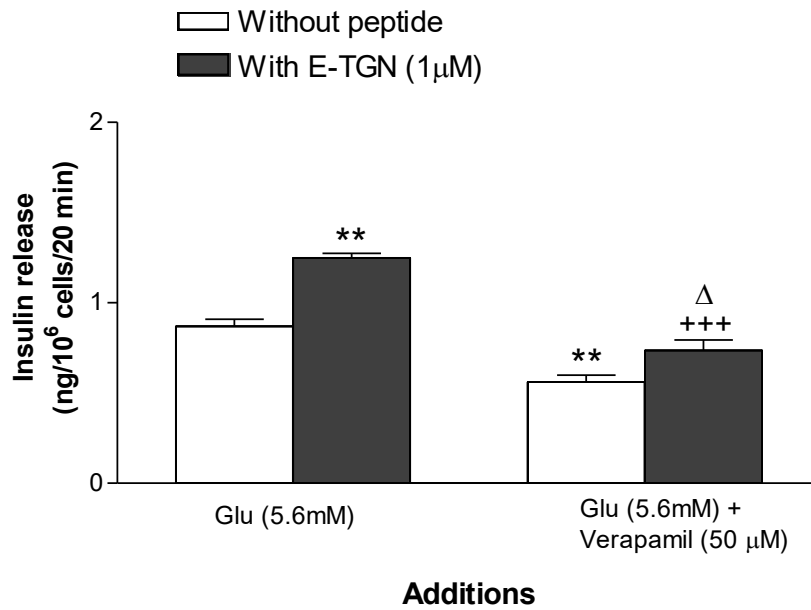
B)
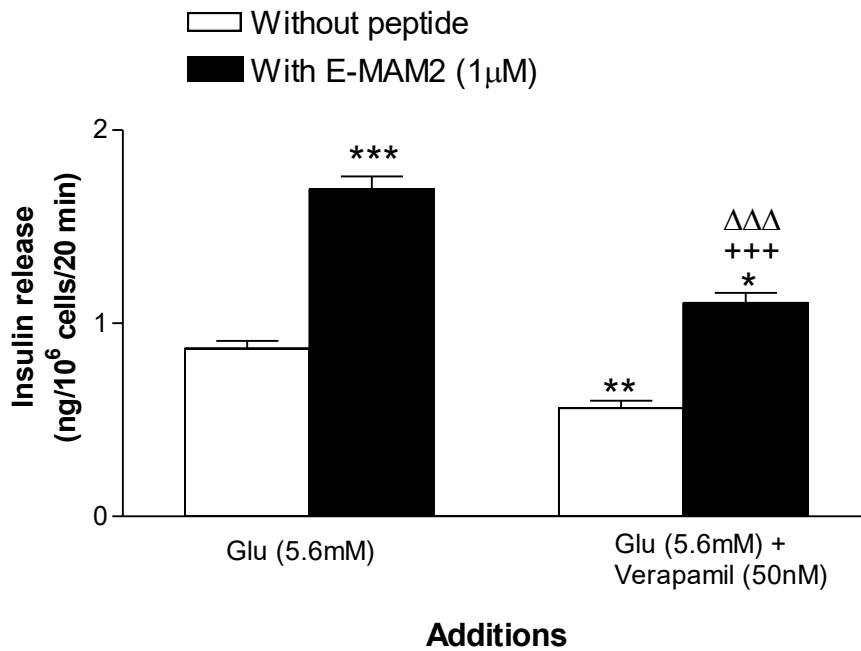
Figure 4.4. Effect of VDCC inhibition on the insulinotropic actions of (A) E-TGN or (B) E-MAM₂.
Values are mean ± SEM (n=3). ***P<0.001, **P<0.01, *P<0.05 compared to 5.6 mM glucose. ᐃᐃᐃP<0.001, ᐃP<0.05 compared to respective incubation without peptide. +++P<0.001 compared to 5.6 mM glucose + peptide (1 μM).

4.5 DISCUSSION

The inability of cells to respond to glucose and endogenous incretins, and the contribution of hyperglycaemia to insulin secretion defects in T2D has been examined (Solomon et al., 2012; Meier and Nauck, 2010). A randomized clinical trial, comparing diabetic patients to healthy subjects under experimental hyperglycaemia, revealed that even though hyperglycaemia is not solely responsible for pancreatic endocrine dysfunction, it contributes to the reduction of beta cell responses to non-glucose stimuli such as GLP-1 (Solomon et al., 2012). This could partially explain failure of anti-diabetic treatment in subjects where beta-cell responsiveness is lost.

To understand if beta-cells were responsive in experimental hyperglycaemia, this study tested the actions of the peptides on the clonal pancreatic beta-cell line at three different concentrations. At concentrations lower or equal to the physiological fasting glucose level (5.6 mM), insulin release in the absence of the peptide was not significantly different. By addition of E-TGN, the level of insulin release doubled, reaching similar levels at all glucose concentrations. The insulinotropic actions detected in the presence of the peptide at the glucose concentrations of 1.1 mM and 5.6 mM suggest glucose-independent actions under these conditions. For the low glucose concentration, this mirrors the actions of exendin-4 in static incubations with rat islets *in vitro*, where at a non-stimulatory concentrations of 3 mM glucose, the peptide still retained its insulinotropic actions (Parkes et al., 2001). Nonetheless, the absence of further enhancement of the peptide's actions at 11.1 mM glucose might suggest the activity of the peptide is already maximal at physiological glucose concentrations and the glucose-dependent feature of exendin-4 is not here retained.

Similarly to E-TGN, E-MAM$_2$ maintains its insulinotropic actions at non-stimulatory glucose concentrations. With regards to the higher glucose concentration, mimicking fasting diabetic blood glucose levels, E-MAM$_2$ further increased insulin secretion, compared to the incubation with non-stimulatory glucose concentration. This result corroborates previous reports in mouse islets challenged with MAM$_2$ in the presence of high glucose concentrations (Ojo et al., 2015a), suggesting this property is maintained following the creation of the hybrid peptide E-MAM$_2$.

For both peptides, insulinotropic activities are present at 1.1mM glucose, a concentration 5-fold lower than physiological levels. Notably, there is evidence of loss of glucose-dependent effects of incretins in the presence of other antidiabetic drugs such as sulfonylureas. Episodes of hypoglycaemia in patients on combination therapy with GLP-1 mimetics and sulfonylureas led to the assessment of insulin secretion *in vitro* under these conditions. At 3 mM glucose, the actions of GLP-1 on insulin release were absent, but the addition of tolbutamide to this condition caused insulinotropic actions 2-fold higher than those of tolbutamide alone, suggesting the glucose dependency of GLP-1 was lost under these conditions (De Heer and Holst, 2007). E-TGN and E-MAM$_2$ might have lost their glucose-dependent actions by a similar mechanism, and the amphibian peptides might contribute to the loss by generation of insulinotropic actions independent from glucose concentrations. To test this hypothesis, further mechanistic studies including those on receptor activity might shed light on the role of glucose in the action of the peptides.

The process of insulin secretion is regulated by extracellular signals, that interact with cell membrane channels, and intracellular messengers responsible for perpetuating the response and couple the metabolic state of the cell with its electrical activity (Yang and Berggren, 2006; Sikimic et al., 2019).

The potassium channel opener, diazoxide, allows intracellular potassium ions to exit beta-cells via the K_{ATP} channels, causing a reduction in depolarisation. As the insulinotropic activity of both peptides was not significantly affected by the presence of diazoxide this may reflect their ability to use another K_{ATP}-independent pathway to cause cell depolarisation. For example, for incretins such as GLP-1 receptor agonists, the mechanism for insulin secretion involves binding to GPCRs, leading to activation of adenylyl cyclase and an increase in cAMP production (Meloni et al., 2013).

KCl is known to stimulate insulin secretion by depolarising the cell and inducing Ca^{2+} entry in the beta-cell as reported in previous studies on this cell line (Hamid et al., 2002). Therefore it represents a valid tool used for studying the role of K_{ATP} channels in pancreatic cells (Ojo et al., 2015a). Insulinotropic actions of E-MAM$_2$ were further potentiated by KCl in the presence of 16.7 mM glucose, indicating that beta cells responses to E-MAM$_2$ are not masked by KCl-induced depolarisation, as opposed to what was observed for E-TGN.

Tolbutamide, a drug binding to the SUR1 subunit of the K_{ATP} channel, stimulates insulin secretion by closing these channels and depolarising the cell membrane (Seino and Miki, 2003). By inducing beta-cell clustering, it generates homogeneous Ca^{2+} oscillations for insulin release (Jonkers et al., 2011). The activities of both E-TGN and E-MAM$_2$ in the presence of tolbutamide were enhanced, suggesting the closure of the K_{ATP} channel, associated with cell depolarization, facilitates the actions of the hybrid peptides. This has also been observed with TGN (Ojo et al., 2011), suggesting the hybrid inherited this property from the parent peptide and that the mechanism could be similar for E-MAM$_2$ as well.

With regards to this pathway of insulin secretion, IBMX (3-isobutyl-1-methylxanthine) is well known to maintain levels of cAMP by inhibiting the degradation of intracellular secondary messengers which in turn results in an increase of intracellular calcium and insulin mobilisation (Siegel et al., 1980). Consistent with the possibility of utilizing this pathway, the insulinotropic actions of E-MAM$_2$ were greatly enhanced in the presence of IBMX, indicating the reduced degradation of cAMP favours insulin secretion in the presence of this peptide. The significant increase observed in insulin secretion under this condition could also reflect the ability of cAMP to enhance cell sensitivity to Ca^{2+} permeabilization, which allows insulin secretion at a lower concentration of Ca^{2+} (Skelin et al., 2011). Conversely, E-TGN did not increase insulin output compared to its respective control incubation in the presence of IBMX. A possible explanation for this observation could be that if the actions of E-TGN cannot be further enhanced by this phosphodiesterase inhibitor and the actions of this peptides might be masked by those of IBMX. In support of this, there is evidence of phosphodiesterase inhibitors masking or causing oscillations in cAMP levels (Tian et al., 2012). Therefore, the result might reflect a time where cAMP production was increased but stable.

Calcium plays a fundamental role in beta cells physiology and insulin secretion. It participates in cell growth and proliferation as well as contributing to the exocytotic process by interacting with pre-formed insulin granules (Yang and Berggren, 2006). In our experiments, we studied the effects of E-TGN and E-MAM$_2$ in the absence of extracellular calcium to evaluate the direct contribution of this pathway to the insulinotropic activities of the peptides. For both peptides, chelating extracellular calcium resulted in decreased insulin secretion, suggesting that

extracellular calcium is required for the insulinotropic activities of the hybrid peptides. In support of this, the use of the VDCC blocker verapamil also provided further insight on the action of the peptides under these conditions. The presence of verapamil caused a decrease of E-TGN's insulinotropic activity, strongly suggesting the peptide stimulates insulin secretion relying on the activation of the VDCC. Previous reports using cationic forms of TGN ([S4R]tigerinin-1R and [H12K]tigerinin-1R) revealed that inhibition of the VDCC did not completely abolish the activity of the peptides, which we observed here. However, a study investigating the involvement of incretins in the ATP dynamics of beta-cells revealed that verapamil could reversibly inhibit the increase in the ATP/ADP ratio (Hodson et al., 2014), required for insulin release. Our study could reflect the action of the incretin component of the the E-TGN hybrid, suggesting it predominates in determining the overall mechanism of action of the peptide.

The insulinotropic actions of E-MAM$_2$ in the presence of verapamil were not completely abolished but only attenuated, similarly to what has been reported for MAM$_2$ alone in the presence of this inhibitor (Ojo et al., 2015a), indicating this feature might be conserved in the hybrid, predominating on that of exendin-4. However, relying on potentiated intracellular resources of calcium has a great contribution to the actions of both E-TGN and E-MAM$_2$. This concept aligns with the mechanism of action of incretins, coupled to G-proteins, where an increased influx of calcium in beta-cells for insulin exocytosis relies on the activation of the intracellular protein kinase A and Epac2 (Dzhura et al., 2010).

As diazoxide did not inhibit the insulinotropic action of E-TGN and KCl failed to significantly increase the activities of the peptide on insulin secretion, we hypothesise that E-TGN might not rely K_{ATP} channels for cell depolarisation and there might be an additional stimulus causing activation of VDCC. E-MAM$_2$ seems to rely on both the classical pathway on insulin secretion, involving the K_{ATP} channel, and on the increase of Ca^{2+} from intracellular stores, due to the amplifying pathway.

Despite needing further studies to identify binding sites for the peptides, and further characterisation of VDCC activation under these conditions, the results obtained in this Chapter support the idea that the hybrid peptides might have inherited and maintained mechanistic properties of their native incretin counterpart. Furthermore, novelty associated with the presence of amphibian skin peptides

motivated investigation into the contribution of these peptides in modulating gene expression in the clonal pancreatic cell line of choice, with a view of comparing any changes to the commercially available exendin-4.

Before analysing the transcriptome, given the insulinotropic mechanism of action of exendin-4 has been previously described (Kang et al., 2005), we chose a different approach to investigate the molecular actions of this GLP-1 receptor agonist. We in fact considered how exendin-4 modulates glucose metabolism and its channelling through downstream pathways using metabolomics analysis.

CHAPTER 5

METABOLOMIC ANALYSIS

5.1 BACKGROUND

5.1.1 Further mechanistic aspects underlying T2D: the metabolomics field

Part of the regulation of insulin secretion in beta-cells relies on channelling glucose metabolism towards the oxidative, aerobic pathway (Alcazar et al., 2000). As detailed in the previous chapter, the use of inhibitors and secretagogues suggests the preferred mechanism of insulin secretion for the different hybrid peptides. However, this study only partially explains insulin secretion regulation, as the pathways involved in the process still retain residual activities despite the presence of pharmacological inhibitors (Bain et al., 2009).

We briefly mentioned in Section 1.4.3 that exendin-4 promotes insulin-secretion by binding to the GLP-1 receptor and activating a signalling cascade leading to increased levels of cAMP. Mechanistically, exendin-4 (1 nM) sensitises intracellular Ca^{2+} channels by an increased influx of extracellular Ca^{2+}, following glucose metabolism and thus inducing membrane depolarisation in the insulinoma cell line INS-1 (Kang et al., 2005). As shown in Figure 1.2, this further supports the importance of glucose metabolism in the action of GLP-1 receptor agonists such as exendin-4.

Other recent studies explain how pre-treatment of BRIN-BD11 cells with exendin-4 (50 nM) modulates the metabolic response to glucose, with a 25% increase in glucose uptake which is also accompanied by increased ATP content and insulin secretion, compared to pre-treated sample with glucose only (Carlessi et al., 2017). These results shed light on the anti-diabetic effect of chronic treatment with exendin-4 and highlight the role of a metabolic reprogramming of cells in the process.

For the first time, Mora-Ortiz et al. (2019) reported a comprehensive, organ-specific metabolomic analysis of the diabetic db/db mouse lacking the leptin receptor. What emerged from the studies are the differences between changes in metabolites across tissues, reflecting differential needs in the context of diabetes and

obesity. Metabolomics has also recently been explored to study the effect of anti-diabetic agents. Many of the currently available therapeutic agents for T2D fail in correcting the underlying metabolic impairment of the disease and, as such, this aspect has been taking into consideration in compounds with newly identified anti-diabetic potential (Al-Zuaidy et al., 2017).

Among these, the recently uncovered anti-diabetic actions of the *Melicope lunu-ankenda* (ML) leaf extract were further characterised using metabolomics analysis from animal samples. Following administration of 200 or 400 mg/kg of ML extract to T2D-induced rats, plasma and serum samples were analysed using proton NMR (^{1}H-NMR) spectroscopy, in search of potential biomarkers or metabolic changes. Offering a comprehensive snap-shot of metabolic pathways at the time of the analysis, this study revealed the anti-diabetic actions *in vivo* observed in the diabetic rats resulted in a restored functionality of glucose oxidation via the TCA cycle, essential for homeostasis (Al-Zuaidy et al., 2017) (Figure 5.1). Even though at present it might not directly translate to a clinical outcome, metabolomics analysis could be exploited for further insight on the metabolic profile in T2D and eventually help characterisation of comprehensive and unequivocal biomarkers with predictive and prognostic power.

The results generated so far prompted us to perform a flux analysis using uniformly labelled ^{13}C-glucose ([U-^{13}C glucose]) as a tracer to study how its metabolism is funnelled through its downstream pathways. The pre-treatment conditions we used reflect different cellular states, namely physiological concentration of glucose, where cells are expected to be responsive to a glucose load by performing glycolytic metabolism at a basal, control rate; a hyperglycaemic condition where the previous basal glucose metabolism may be altered and finally, both the conditions mentioned pre-treated with exendin-4 to test its effect on committing glucose and its metabolites towards different pathways and their significance in T2D.
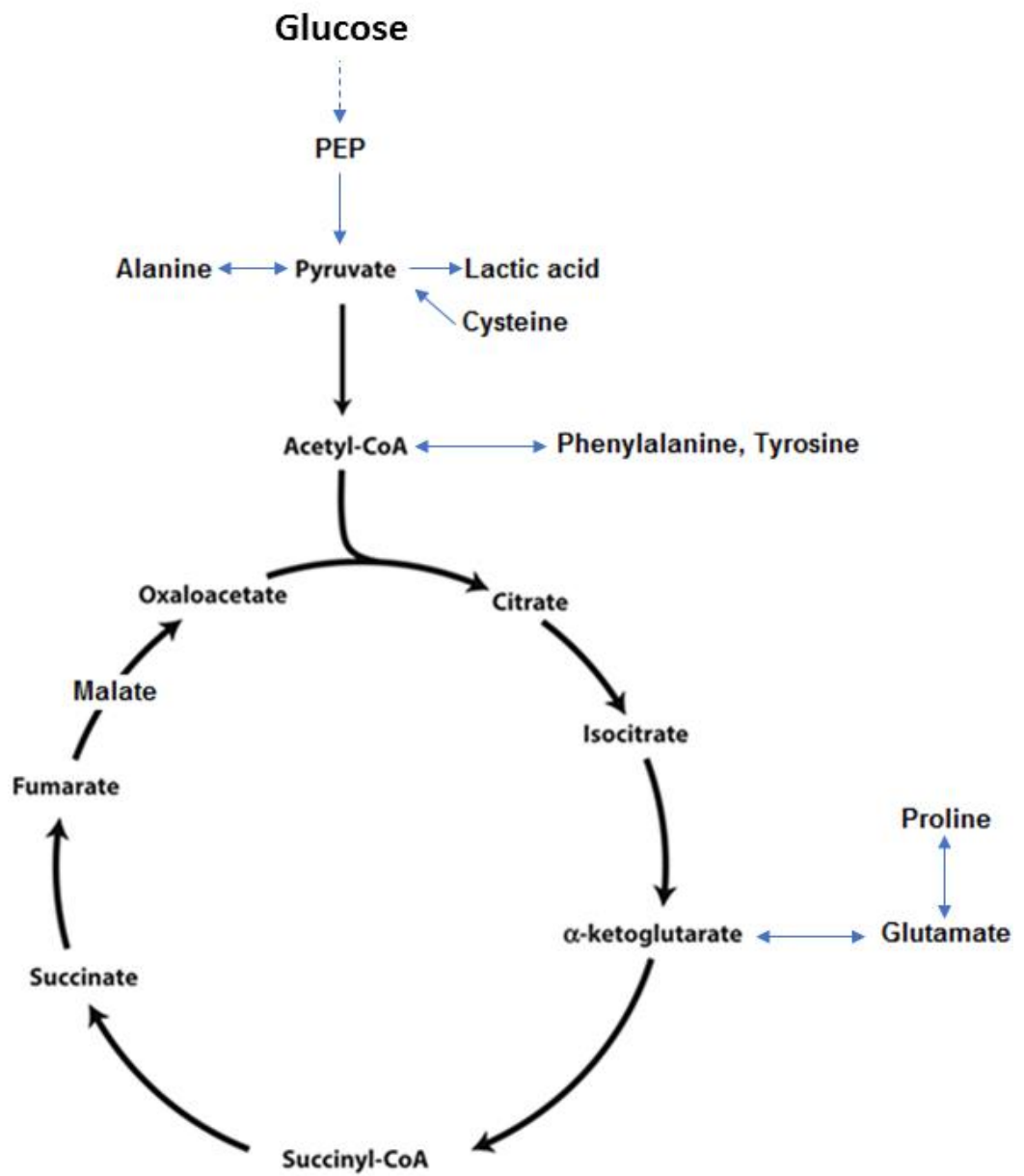
Figure 5.1. Schematic representation of the TCA cycle.

5.2 AIM & OBJECTIVES

The aim of this study is to qualitatively evaluate changes in metabolic fluxes following the treatment of pancreatic beta-cells with exendin-4. The specific objectives are:

1.   Pre-treatment of BRIN-BD11 cells with physiological or high glucose concentrations in the presence of exendin-4.

2.   Feeding pre-treated cells with ^{13}C-labelled glucose and performing metabolite extraction.

3.   Analysing metabolites in the cell supernatant, using NMR, and in order to tracing glucose flux in the intracellular space, using GC-MS.

5.3 RESEARCH DESIGN

5.3.1 Sample preparation for metabolite analysis

Metabolite analysis was performed in BRIN-BD11 cells. Cells were initially seeded at a density of 5×10^5 cells/well in a 6-well plate for overnight attachment as detailed in Section 2.3.1. The following day, they were treated with KRB buffer supplemented with either 5.6 or 25 mM glucose, in the presence or absence of exendin-4 (3 µM) for 20 hrs. After the incubation, media was discarded and replaced with KRB buffer supplemented with 14 mM [U-^{13}C] labelled glucose, for 1 hour. Following the labelled glucose treatment, the supernatant was collected and stored at -80°C for nuclear magnetic resonance (NMR) metabolite extraction. 25 µL of supernatant were also assayed for insulin release, using insulin ELISA as described in section 2.1.4. The adherent BRIN-BD11 cells in the plate were further processed for GC-MS analysis. Experimental flow chart is presented in Figure 5.2.

5.3.2 Nuclear Magnetic Resonance (NMR)

For NMR metabolite extraction, as explained in Section 2.3.2, 120 µl of deuterium oxide (D_2O) containing 1 mM trimethylsilylpropanoic acid (TSP) and 25 mM sodium azide (NaN_3) were added to 60 µl of phosphate buffer (500 mM) and 420 µl of supernatant. Samples were mixed and transferred to 5mm glass NMR tubes. ^{1}H-NMR spectra were acquired over 5 minutes and measured at a frequency of 600 MHz, at a temperature of 300 K. TSP was used as in internal reference (0.0 δ) for peak identification.

5.3.3 Gas Chromatography – Mass Spectrometry (GC-MS)

Treated BRIN-BD11 cells (section 5.3.1) were quenched using methanol and metabolite extraction was performed as per section 2.3.3. The aqueous and organic phases of each sample were methoximated and transmethylated, respectively, before derivatisation with MTBSTFA. Metabolites within the obtained extracts were separated using electron impact ionization as detailed in section 2.3.3.

5.3.4 Statistical analysis

The total ion chromatograms (TICs) were identified by the instrument, through the probability based match (PBM) library database.

For the labelling experiment, the raw data was deconvoluted with the Automated Mass Spectral Deconvolution and Identification System (AMDIS) software and imported into the GC-MS Assignment Validator and Integrator (GAVIN) matrix for Matlab, as detailed in section 2.3.3 of the methodology.

Mass isotopomer distributions (MIDs) resulting from the analysis were used to calculate the percentage of labelling of each compound, as described elsewhere (Buescher et al., 2015), using the following equation:

$$\% \ ^{13}\text{C labelling} = \frac{\sum_{i=0}^{n} i \cdot l_i}{n} \times 100$$

Where i represents a given isotopologue (compound), n the number of its carbon atoms and l is the labelling abundance on each carbon.

Differences between samples were analysed using one-way ANOVA, followed by Newman-Keuls post-hoc test.

BRIN-BD11 seeding
(1.5×10^5 cells/well)

Cell supernatant for insulin ELISA

Cell pre-treated with different conditions (24 hrs)
(5.6 mM glu or 25 mM glu +/- Ex-4)

Cell treated with [U-^{13}C]-glucose (14 mM) (1 h)

Cell supernatant for NMR

Intracellular metabolite extraction

Aqueous
(Glycolysis, TCA cyle, aa)

Organic
(Fatty acid)
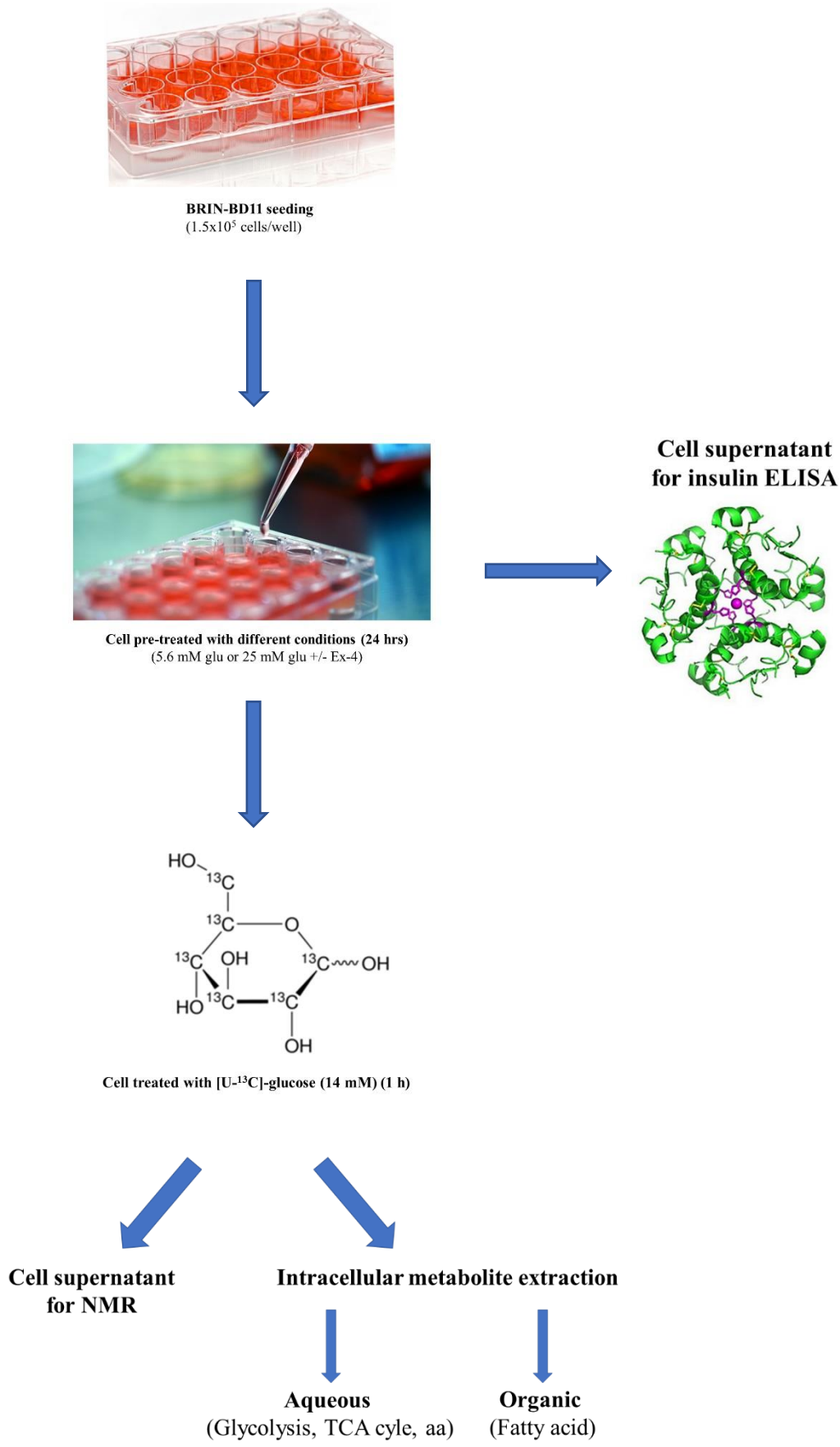
Figure 5.2. Experimental flow chart for metabolomics analysis.

5.4 RESULTS

5.4.1 Functional assay: insulin release

To assess the insulinotropic activities of BRIN-BD11 cells under the different conditions, the cell supernatant was assayed for insulin release, following the 24-hour glucose challenge (Figure 5.3). At 5.6 mM glucose, insulin release was 3.73 ± 0.6 ng/L. At 25 mM glucose, insulin release slightly decreased to 3.29 ± 0.7 ng/L. The addition of exendin-4 to the pre-treatment increased insulin secretion to 9.44 ± 0.6 ng/L and 8.52 ± 0.7 ng/L for low and high glucose, respectively (P<0.001).

5.4.2 NMR spectroscopy on BRIN-BD11 cell supernatants

In order to have a first overview on the differences in metabolites in the extracellular environment in cells pre-treated with either 5.6 or 25 mM glucose, we performed ^{1}H-NMR on BRIN-BD11 cell supernatants. The Biological Magnetic Resonance Data Bank (BMRB), along with previous reports performing ^{1}H-NMR in patient serum samples (Del Coco et al., 2019) allowed a putative identification of some of the peaks detected. Differences between cells treated with 5.6 and 25 mM glucose are presented in Figure 5.4.

We assigned lactate at 1.253 ppm. The intricated pattern found between 2.9 and 4.1 most likely corresponds to sugars in the sample (Del Coco et al., 2019). At 25 mM glucose, we also putatively assigned alanine (1.279 ppm) and leucine (1.488 ppm), which were found in higher abundance in the hyperglycaemic sample. Here, we also assigned beta-glucose, presented in the window between 3 and 3.9 ppm, and displaying a doublet at 4.4 ppm and alpha-glucose at 5.25 ppm. Even though these preliminary results are based on only 16 scans and putative assignments, we can still appreciate differences in the extracellular environment of the pancreatic cell line in the presence of different glucose concentrations and/or exendin-4 treatment (Figure 5.5).

In order to assess differences in metabolites following exendin-4 pre-treatment at physiological glucose concentration, we compared the 5.6 mM sample with the one pre-treated also with exendin-4. The peptide increased the amount of alanine and acetate (1.921 ppm) in the sample, whereas the untreated control maintained higher levels of lactate and acetone (2.235 ppm) (Figure 5.5A).

By comparing exendin-4 treated samples, both at 5.6 and 25 mM we aimed to establish the role of the peptide in changing the levels of these metabolites under the different glucose concentrations. We observed that levels of lactate, alanine and acetone are higher in this sample, compared to the supernatant from cells treated with exendin-4 at 5.6 mM glucose (Figure 5.5B).

We moved on to assess differences in the intracellular metabolites of the samples, using GC-MS and studying the total ion chromatograms (TICs) as well as the flux of U-^{13}C glucose through its downstream pathways.
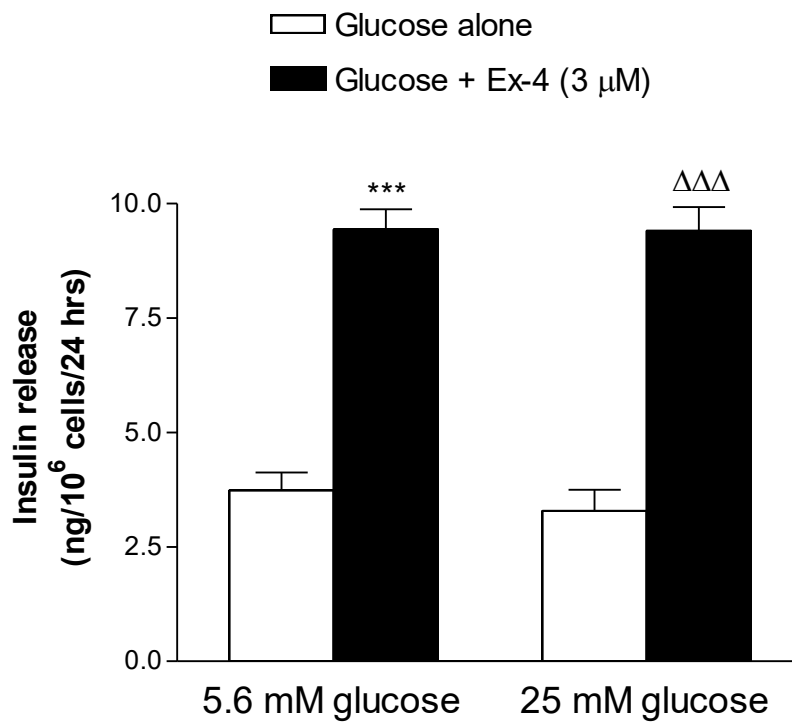
Figure 5.3. Functional assay for insulin release in BRIN-BD11 cells.
Cells were incubated with 5.6 or 25 mM glucose, in the absence or presence of exendin-4 (3 μM) for 24 hours before U-^{13}C glucose challenge (14 mM). Supernatant was collected for insulin release assay. ***P<0.001, compared to 5.6 mM glucose alone. ΔΔΔP<0.001, compared to 25 mM glucose alone.
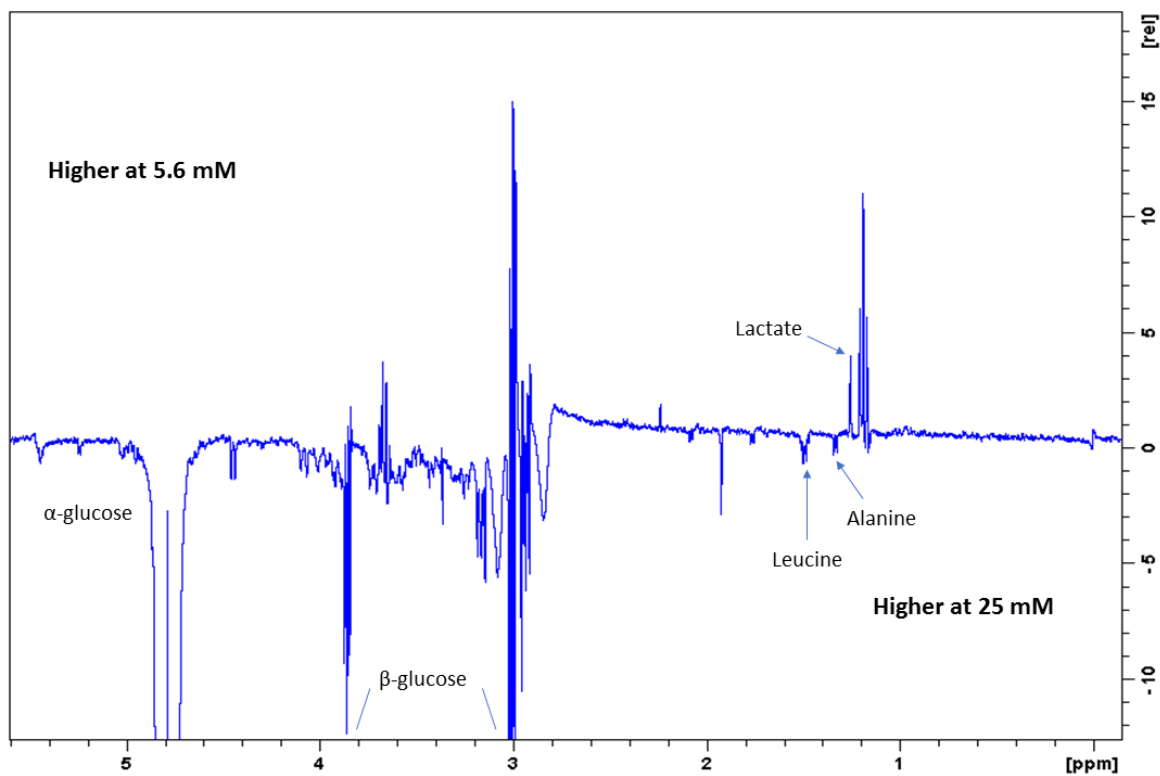
Figure 5.4. ¹H-NMR spectra of BRIN-BD11 cell supernatants displaying differences in metabolites at low and high glucose concentrations.
¹H-NMR analysis was performed on BRIN-BD11 cell supernatants from samples pre-treated with 5.6 or 25 mM glucose, before 14 mM glucose challenge. Spectra at 25 mM were substracted from spectra at 5.6 mM using the Brucker© Topspin software. Metabolites higher in 5.6 mM glucose are displayed at the top, those higher at 25 mM at the bottom.
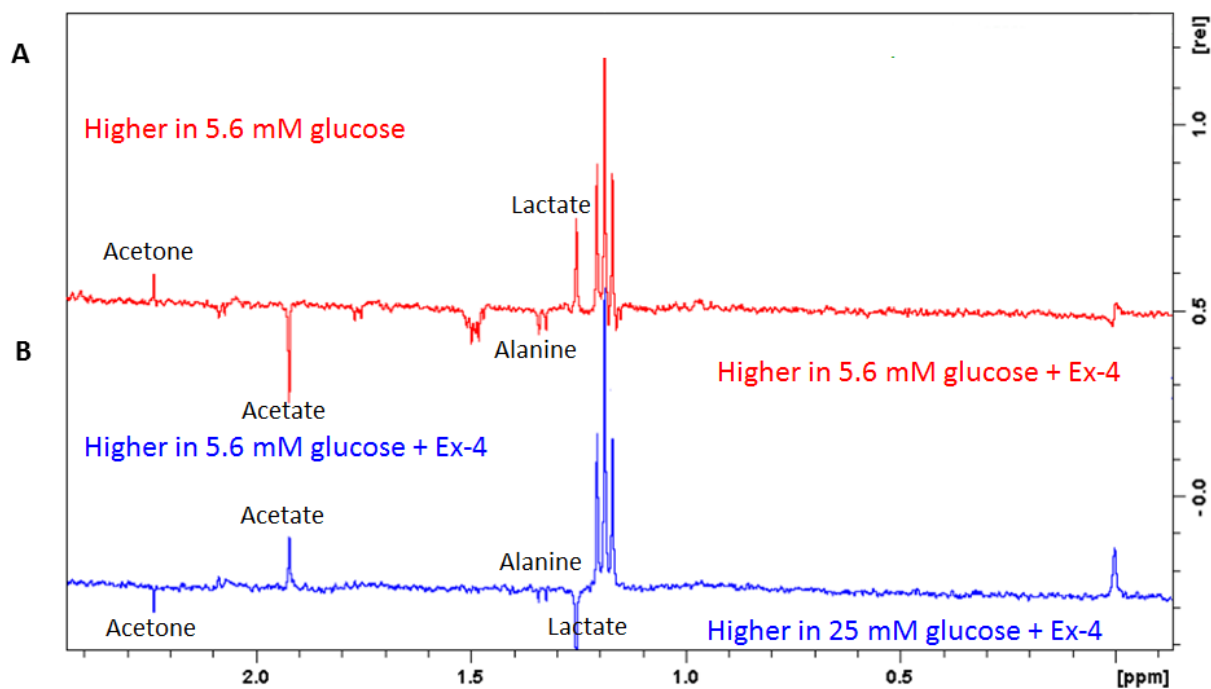
Figure 5.5. ^{1}H-NMR spectra of BRIN-BD11 cell supernatants comparing (A) untreated with exendin-4 treated samples, and treated (B) samples at 5.6 and 25 mM glucose.
^{1}H-NMR analysis from cell supernatants of samples pre-treated with (A) 5.6 mM glucose, in the absence or presence of exendin-4, or (B) 5.6 and 25 mM glucose in the presence of exendin-4, after the 14 mM glucose challenge.

5.4.3 Analysis of BRIN-BD11 intracellular metabolites

5.4.3.1 Total ion chromatograms (TICs)

Total ion chromatograms (TICs) deriving from intracellular metabolites were identified using the PBM library of the instrument. Within the organic phase, this study found differences between samples derived from cells incubated at 5.6 and 25 mM glucose (Figure 5.6A). The most striking differences are observed for saturated fatty acids such as palmitic (RT=16.569), stearic (RT=17.752) and arachidic acid (RT=18.908), which increased by approximately 4-fold, as well as cholesterol (RT=25.378) which increased by nearly 10-fold in the presence of 25 mM glucose. In the aqueous phase, the main difference observed between 5.6 mM and 25 mM glucose was decanoic acid (RT=24.584), which was reduced by about 2-fold at the high glucose concentration. Though the molecular entities eluting at 22.01, 22.07 and 22.16 mins show differences between 5.6 snd 25 mM glucose, they were not detected by the software (Figure 5.6B).

By comparing the TICs from the organic phase 5.6 mM glucose and its respective exendin-4 treatment, this study found a higher abundance of saturated fatty acids in the treated sample, contrary to our expectations, with a similar pattern observed in the 25 mM glucose sample (Figure 5.7A).

In the aqueous phase, treatment with exendin-4 elicited a 3-fold reduction of the abundance of silane (RT=18.8) and a 1.5-fold reduction in docosanoic acid (RT=24.691), a saturated fatty acid (Figure 5.7B).

Certain differences were also observed at 25 mM glucose. The addition of exendin-4 to the samples resulted in a decrease of fatty acid species with overall features resembling the chromatogram at 5.6 mM glucose. This suggests that exendin-4 might reduce the formation of saturated fatty acids to levels comparable to those observed at the physiological concentration of 5.6mM glucose (Figure 5.8A). Under these conditions, the presence of exendin-4 in the aqueous phase caused a 1.5-fold reduction in abundance of silane (RT=18.8), and a slight reduction in d-galactose abundance (1.2-fold, RT=22.572) (Figure 5.8B).

For the labelling experiment, we were not able to determine labelled species originating from [U-^{13}Cglucose] metabolism in the organic phase, therefore it was not possible to perform further analysis on this extract.
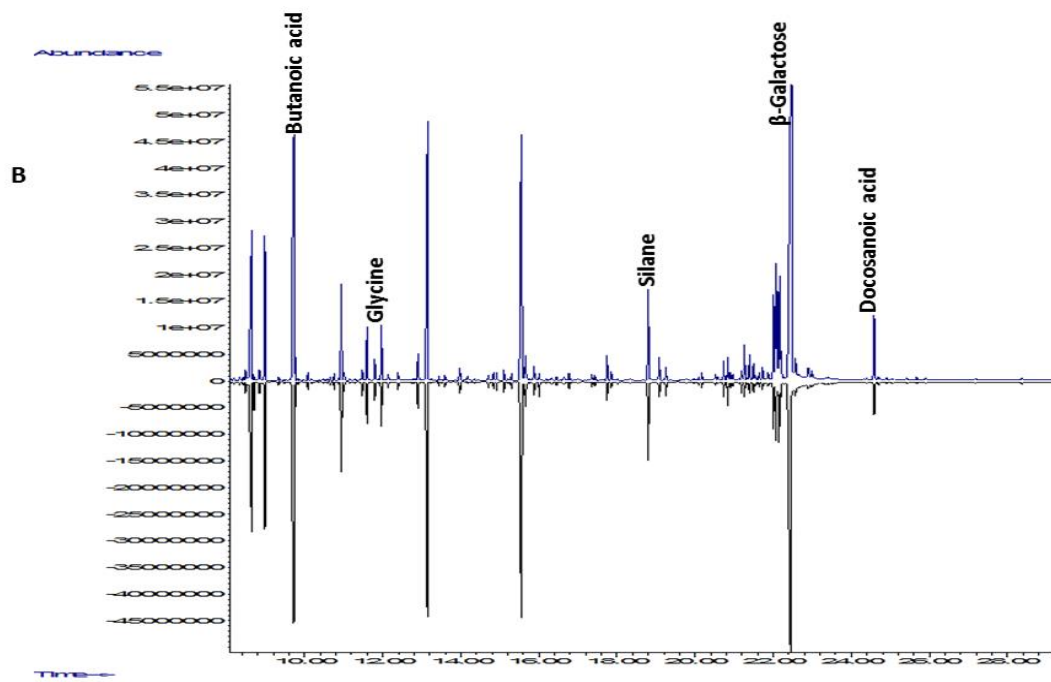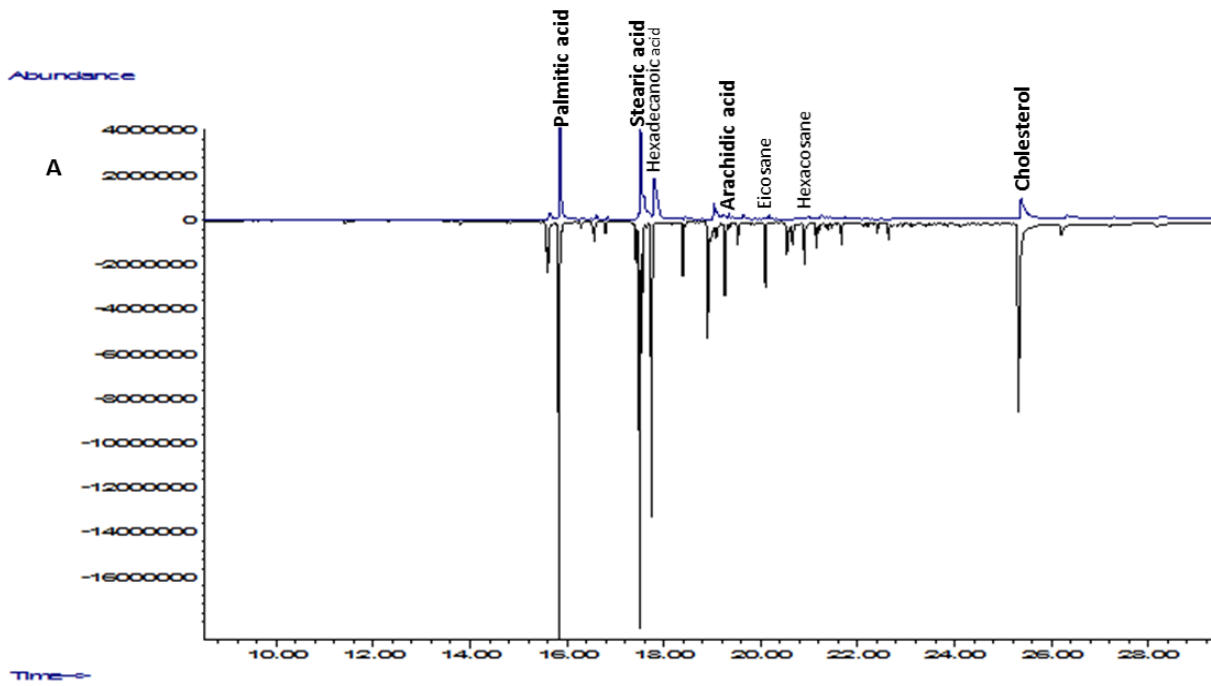
Figure 5.6. TICs displaying intracellular (A) organic and (B) aqueous metabolites at physiological (top, in blue) and high glucose (bottom, in black) concentrations. Following pre-treatment in the presence of 5.6 or 25 mM glucose for 24 hrs, cells were challenged with a glucose load (14 mM) for 20 hrs. The reaction was quenched and metabolites extracted for GC-MS run. TICs were collected by the ChemStation software.
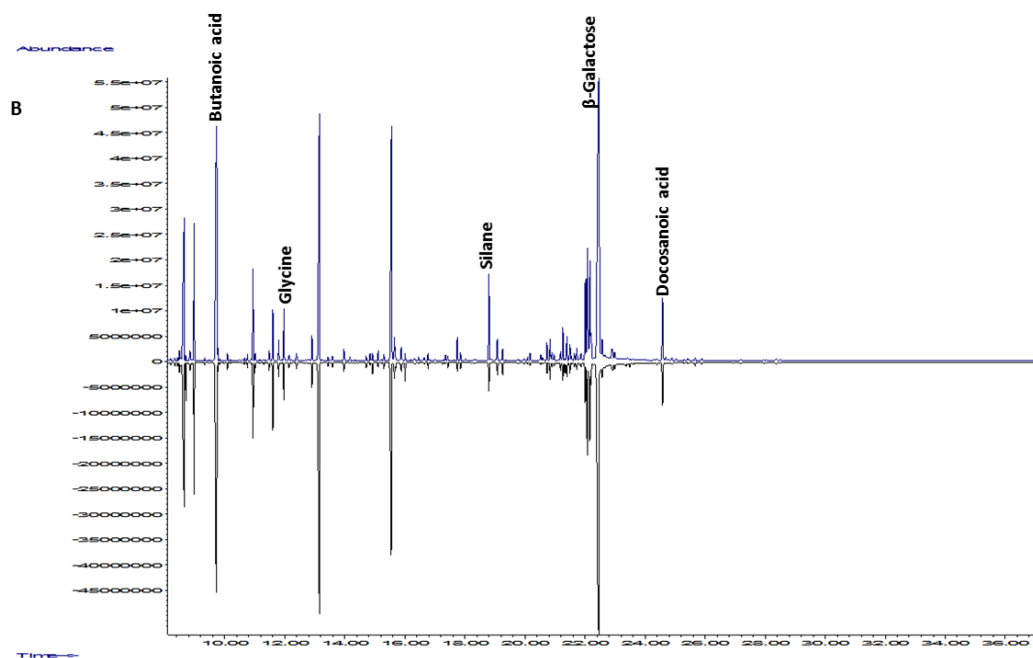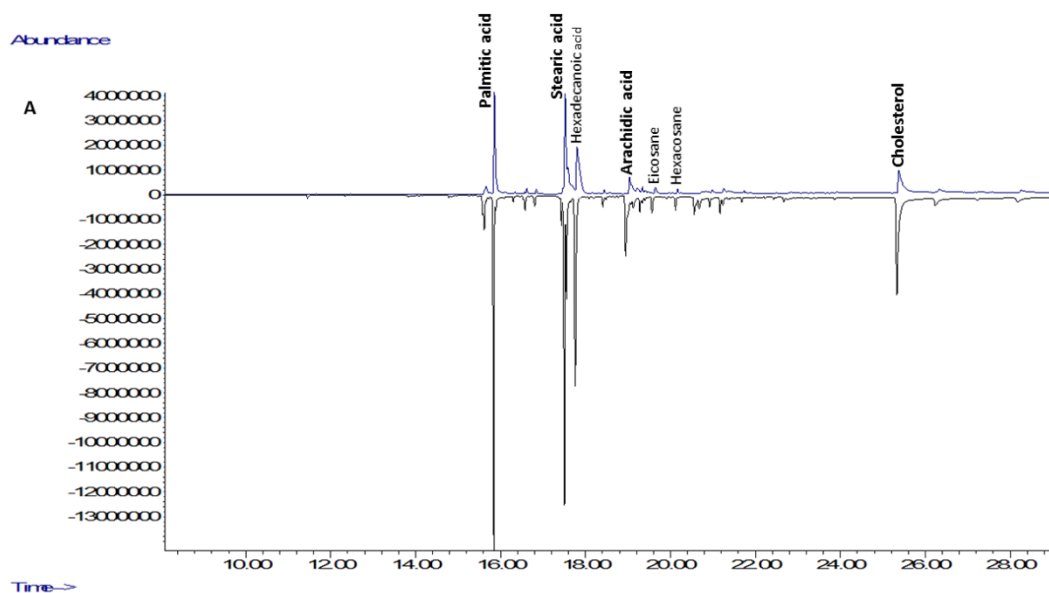
Figure 5.7. TICs for intracellular metabolites in the (A) organic and (B) aqueous phase at physiological glucose in the absence (top) or presence (bottom) of exendin-4.
Metabolites were extracted from BRIN-BD11 cells pre-treated with 5.6 mM glucose, in the absence or presence of exendin-4, for 24 hrs. Cells were treated with glucose (14 mM) and metabolites extracted after 20 hrs. Samples were run on the GC-MS and resulting TICs were collected by the instrument (ChemStation software)
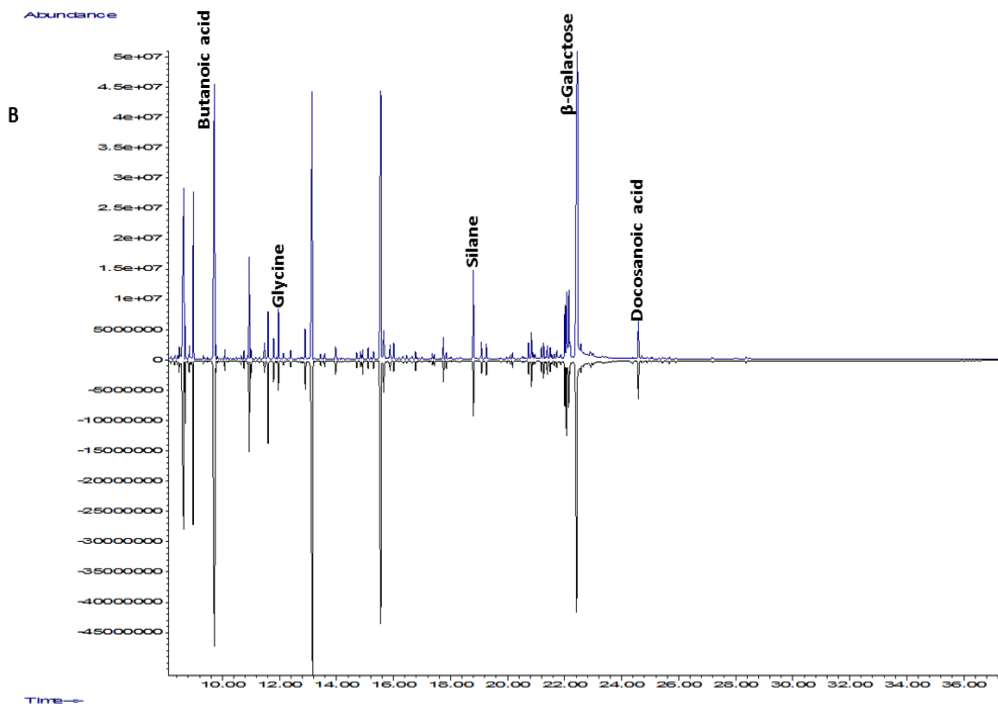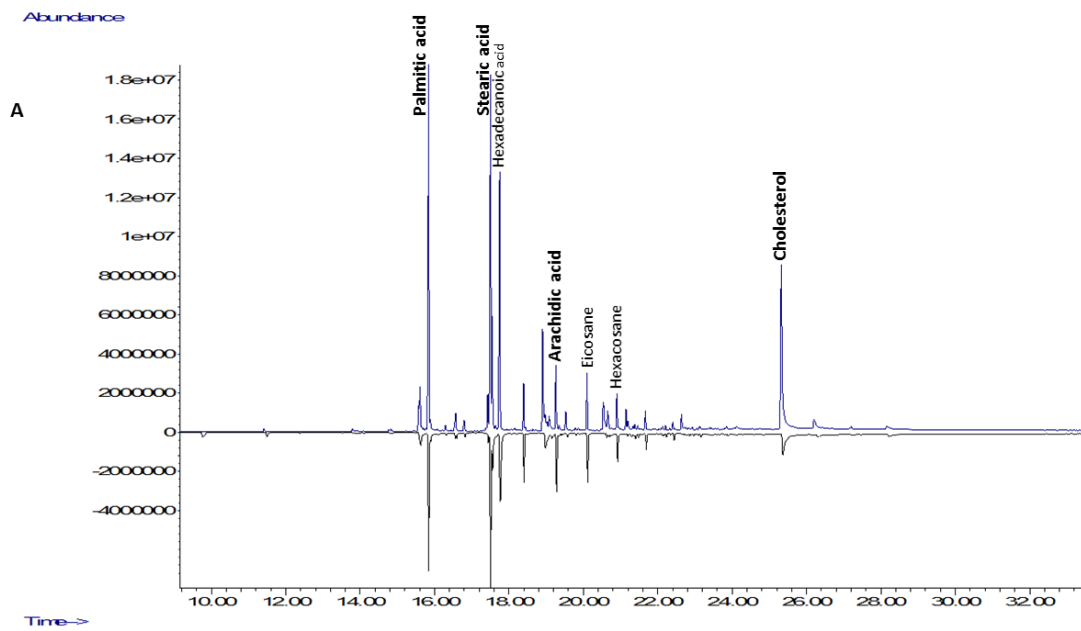
Figure 5.8. TICs displaying high glucose concentrations in the (A) organic and (B) aqueous phase, in the absence (top, in blue) or presence (bottom, in black) of exendin-4. BRIN-BD11 cells were pre-treated with 25 mM glucose in the presence or absence of exendin-4 for 24 hrs before 14 mM glucose challenge. Metabolites of the organic fraction were run on the GC-MS and TICs generated by the Chemstation software on the instrument.

5.4.4.2 TCA cycle intermediates

Enrichment of ^{13}C in metabolites were evaluated after a 20 hr incubation under the differentially treated conditions. With regards to the glycolytic pathway, dihydroxyacetone phosphate (DHAP) (Figure 5.9A), 3-phosphoglycerate (Figure 5.9B) and phosphenolpyruvate (PEP) (Figure 5.9C) were fully labelled under all conditions, before entry into the TCA cycle (represented schematically in Figure 5.1).

^{13}C-labelled pyruvate originating from PEP at the basal concentration of glucose (5.6 mM) was 71 ± 4.75% and did not significantly differ under the other experimental conditions (Figure 5.10). At 5.6 and 25 mM glucose, equilibrium between pyruvate, lactic acid and alanine labelling was maintained in the range from 66.78 ± 2.34% to 74.46 ± 1.73%. Following treatment with exendin-4, ^{13}C-enrichment of lactate at 5.6 mM glucose was reduced by 20.1% (P<0.05), and by 17.1% at 25 mM glucose (Figure 5.11).

The opposite was observed for alanine labelling. After treatment with exendin-4, 10.57% and 10.29% increase at low and high glucose concentrations respectively were observed (Figure 5.12). ^{13}C enrichment for citrate was 36.67 ± 2.2% at 5.6 mM glucose. This was the highest percentage of labelling observed across the different treatments, as the addition of exendin-4 lowered labelling to 26.02 ± 3.3 % (P<0.05). At 25 mM glucose, enrichment of ^{13}C was also lowered to 28.83 ± 2.9 % (P<0.05) and 27.09 ± 0.8 % (P<0.05), in the absence and presence of exendin-4, respectively (Figure 5.13).

2-Ketoglutarate, generated from decarboxylation of isocitrate, was labelled by 63.07 ± 1.6 % at 5.6 mM glucose. The addition of exendin-4 did not significantly impact ^{13}C-enrichment (63.7 ± 0.8 %). Lower levels of 2-ketoglutarate labelling were detected at 25 mM glucose (58.93 ± 0.5 %, P<0.05), which slightly increased to 61.53 ± 0.9 % in the presence of exendin-4 (Figure 5.14). Glutamate, another key component of the TCA cycle, can be generated from 2-Ketoglutarate transamination. Similar to what was observed for 2-Ketoglutarate, this study observed 61.57 ± 0.6 % labelling in glutamate at 5.6 mM glucose,. The addition on exendin-4 did lowered ^{13}C enrichment to 59.20 ± 1 % (P<0.05). A similar reduction was observed at 25 mM glucose, both in the absence (57.78 ± 1.4 %, P<0.05) and the presence (58.17 ± 0.7 %) of exendin-4. (Figure 5.15)

Succinate was labelled at 33.85 ± 0.7 % at 5.6 mM glucose and, at 25mM glucose and in the presence of exendin-4, ^{13}C enrichment was not significantly different among treatment groups (ranging from 32.27 ± 1.4 % to 38.24 ± 4.1 %) (Figure 5.16). Similarly, fumarate ^{13}C enrichment did not vary between the different conditions, and was at 53.3 ± 3.22 % for 5.6 mM glucose, with no increase or decrease with changes in glucose concentration and in the presence of exendin-4 (Figure 5.17). The same applies to malate, with ^{13}C labelling enrichment in the same range as that at 5.6 mM glucose (64.10 ± 1.1 %) (Figure 5.18).

Glucose

Fructose 1,6-Bisphosphate

DHAP → G3P

Triacylglycerols ← **Glycerol-3-phosphate**   1, 3 Biphosphoglycerate

2-phosphoglyceric acid ← **3-phosphoglyceric acid**

PEP

Dihydroxyacetone phosphate

% labelling — 100, 50, 0

5.6 mM glucose   25 mM glucose

☐ Glucose alone
■ Glucose + Ex-4 (3 μM)
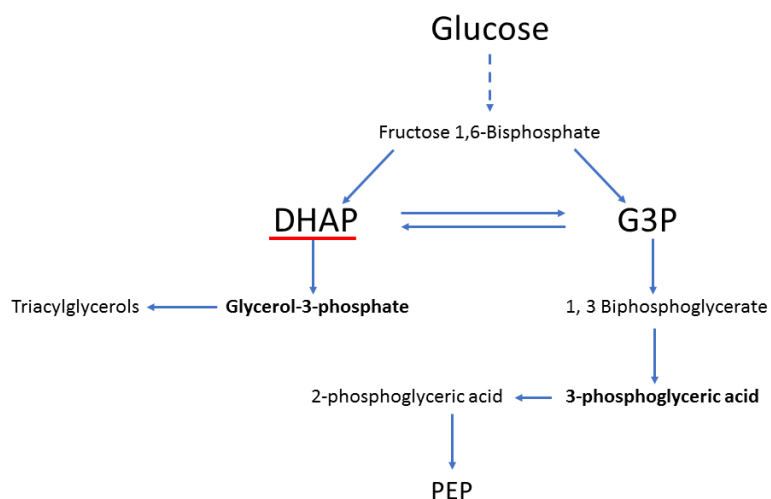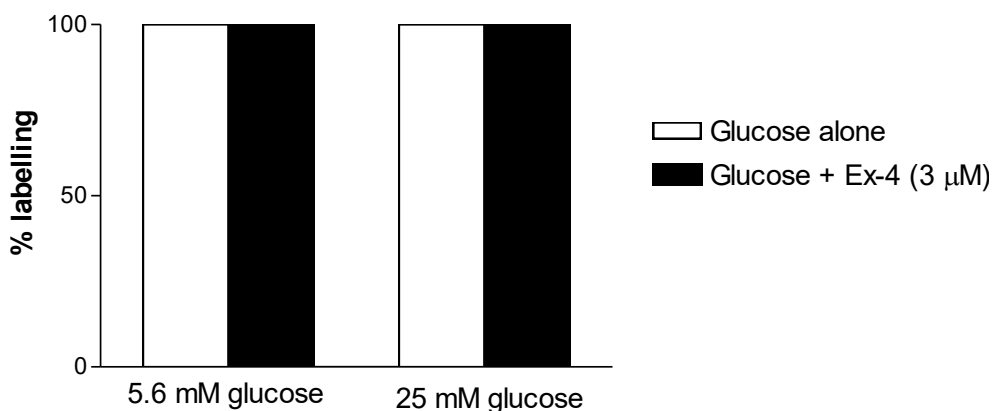
Figure 5.9A. ^{13}C Labelling percentage for dihydroxyacetone phosphate (DHAP).
Cells were pre-treated with 5.6 or 25 mM glucose, in the absence or presence of exendin-4 (3 μM). Following pre-treatment, cells were incubated with [U-^{13}C]-glucose (14 mM) for 1 hour and processed for metabolite extraction. Percentage of labelling was calculated from the mass isotopomer distributions (MIDs) resulting from the GC-MS run. Schematic representation of glycolytic intermediates is shown at the top, with DHAP highlighted.

Glucose

Fructose 1,6-Bisphosphate

DHAP ⟷ G3P

Triacylglycerols ← **Glycerol-3-phosphate**   1, 3 Biphosphoglycerate

2-phosphoglyceric acid ← **3-phosphoglyceric acid**

PEP

3-phosphoglycerate

□ Glucose alone
■ Glucose + Ex-4 (3 μM)
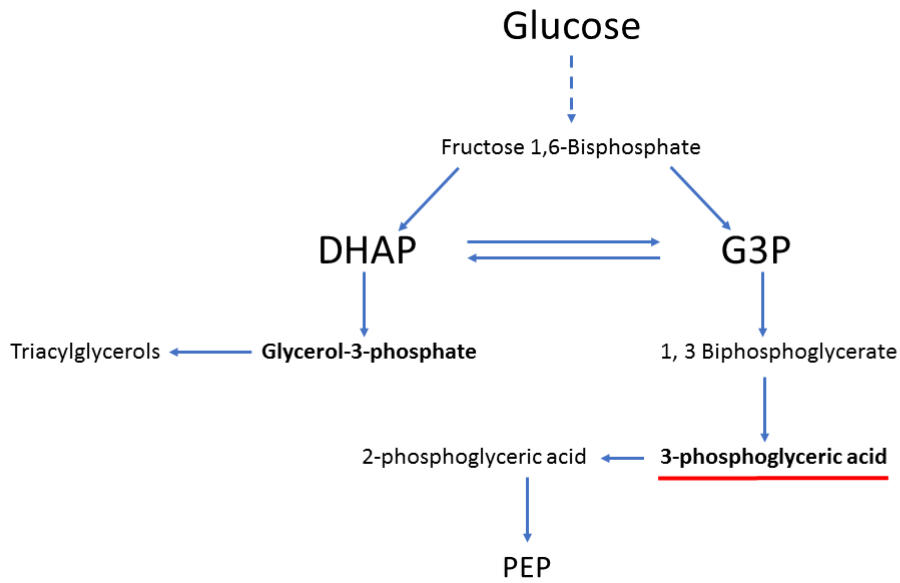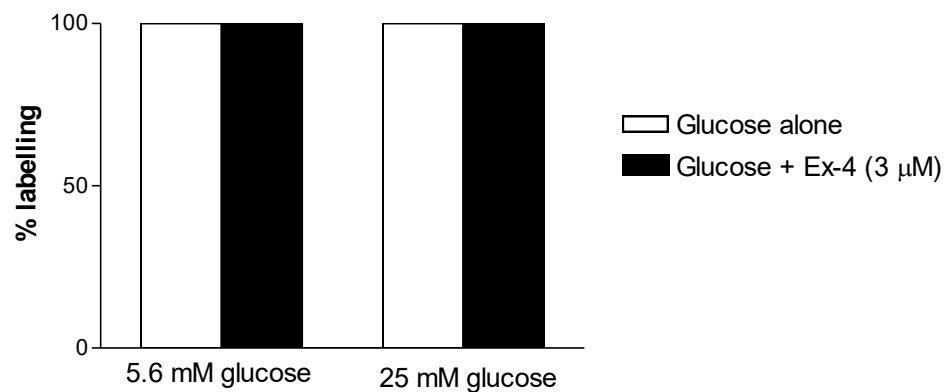
Figure 5.9B. ^{13}C Labelling percentage for 3-phosphoglyceric acid.
Cells were pre-treated with the above conditions were challenged with [U-^{13}C]-glucose (14 mM) for 1 hour. Cells were processed for metabolite extraction and percentage of labelling was calculated from the mass isotopomer distributions (MIDs) resulting from the GC-MS run. Schematic representation of glycolytic intermediates is shown at the top, with glycerol-3-phosphate highlighted. Schematic representation of glycolytic intermediates is shown at the top, with 3-phosphoglycerate highlighted.

Glucose

Fructose 1,6-Bisphosphate

DHAP ⇄ **G3P**

Triacylglycerols ← **Glycerol-3-phosphate**

1, 3 Biphosphoglycerate

2-phosphoglyceric acid ← **3-phosphoglyceric acid**

PEP
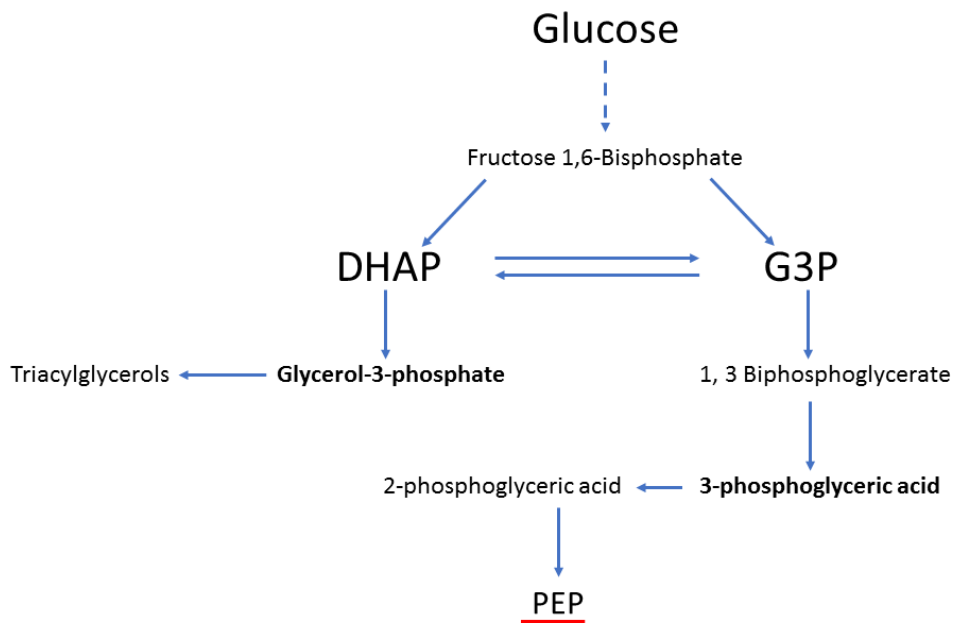
Phosphenolpyruvic acid
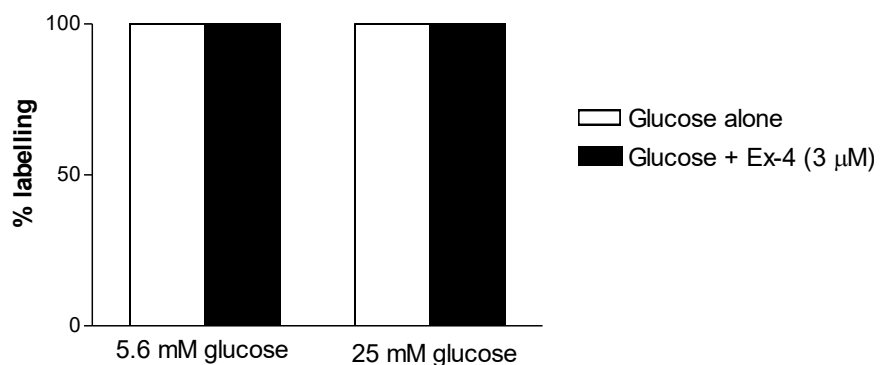
Figure 5.9C. ^{13}C Labelling percentage for phosphenolpyruvate (PEP).
Cells were pre-treated with the above conditions were challenged with [U-^{13}C]-glucose (14 mM) for 1 hour. Cells were processed for metabolite extraction and percentage of labelling was calculated from the mass isotopomer distributions (MIDs) resulting from the GC-MS run. Schematic representation of glycolytic intermediates is shown at the top, with glycerol-3-phosphate highlighted. Schematic representation of glycolytic intermediates is shown at the top, with PEP highlighted.
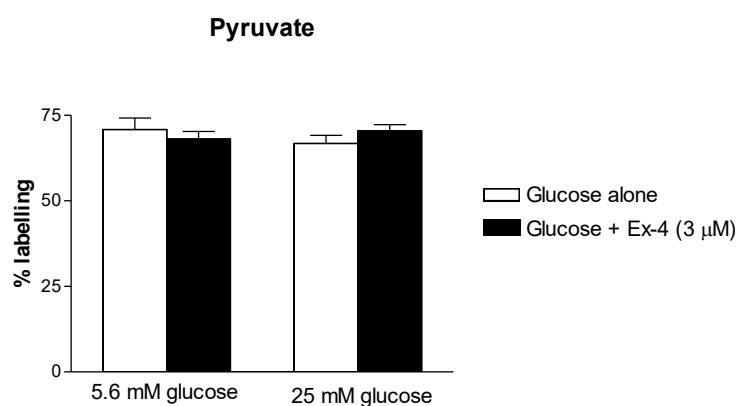
Pyruvate

Figure 5.10. ^{13}C Labelling percentage for pyruvate. [U-^{13}C] glucose (14 mM) was fed to BRIN-BD11 cells following pre-treatment with 5.6 or 25 mM glucose, in the absence or presence of exendin-4. Labelling was calculated from the mass isotopomer distributions (MIDs) detected by the GC-MS.
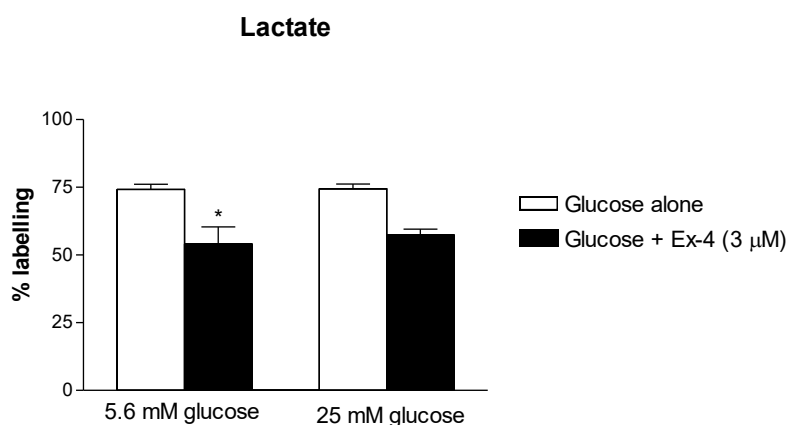
Lactate

Figure 5.11. ^{13}C labelling percentage for lactate. Labelling was calculated from the mass isotopomer distributions (MIDs) detected by the GC-MS. *P<0.05, compared to 5.6 mM glucose alone.
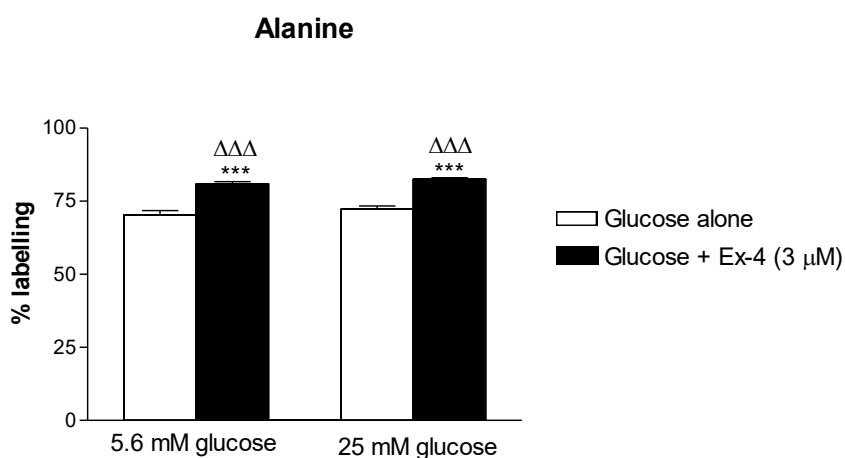
Alanine

Figure 5.12. ^{13}C labelling percentage for alanine. Labelling was calculated from the mass isotopomer distributions (MIDs) detected by the GC-MS. ***P<0.001, compared to 5.6 mM glucose alone, $^{\Delta\Delta\Delta}$P<0.001 compared to 25 mM glucose alone.

Citrate

Figure 5.13. ^{13}C labelling percentage for citrate. [U-^{13}C] glucose (14 mM) labelling percentage for the formation of lactate, following pre-treatment with 5.6 or 25 mM glucose, in the absence or presence of exendin-4. Labelling was calculated from the mass isotopomer distributions (MIDs) detected by the GC-MS. *P<0.05 compared to 5.6 mM glucose alone.

2-Ketoglutaric acid
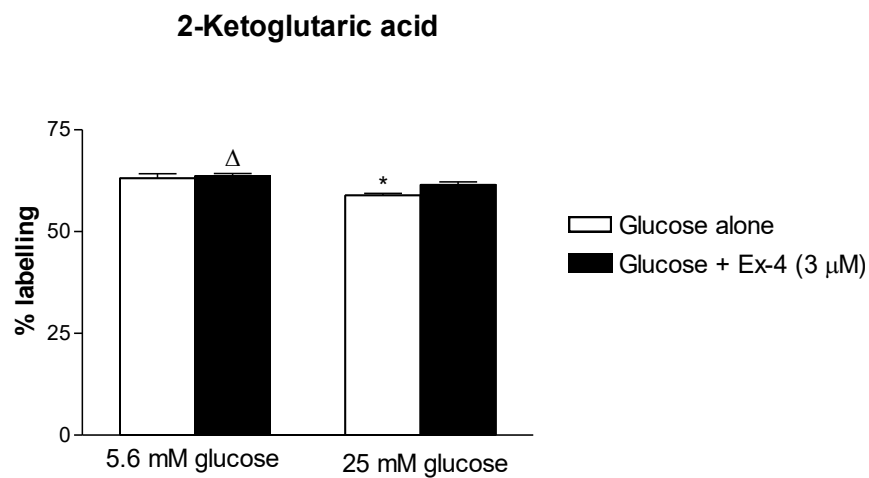
Figure 5.14. ^{13}C labelling for 2-ketoglutarate. Labelling was calculated from the mass isotopomer distributions (MIDs) detected by the GC-MS. *P<0.05 compared to 5.6 mM glucose alone, $^{\Delta}$P<0.05 compared to 25 mM glucose alone.

Glutamate

Figure 5.15. ^{13}C labelling for glutamate. [U-^{13}C] glucose (14 mM) labelling percentage for the formation of lactate, following pre-treatment with 5.6 or 25 mM glucose, in the absence or presence of exendin-4. Labelling was calculated from the mass isotopomer distributions (MIDs) detected by the GC-MS. *P<0.05, compared to 5.6 mM glucose alone.

Succinate

Figure 5.16. ^{13}C labelling for succinate. Labelling was calculated from the mass isotopomer distributions (MIDs) detected by the GC-MS.
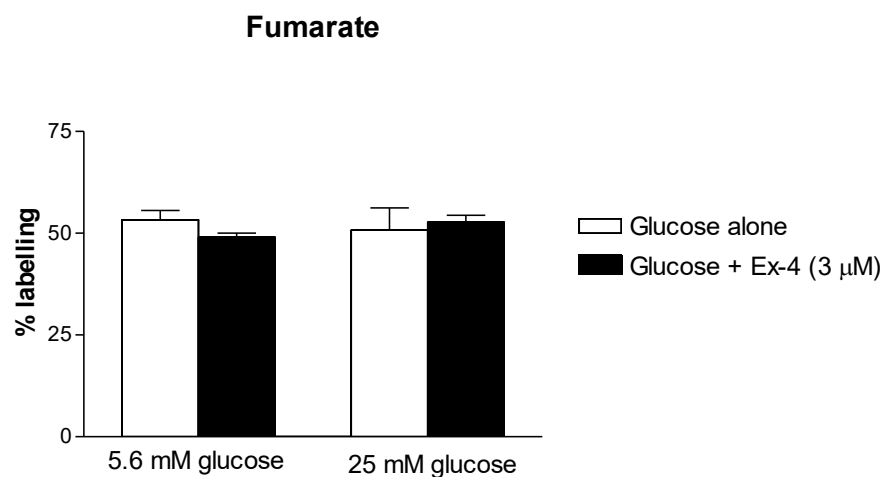
Fumarate

Figure 5.17. ^{13}C labelling for fumarate. Labelling was calculated from the mass isotopomer distributions (MIDs) detected by the GC-MS.

Malate

Figure 5.18. ^{13}C labelling for malate. Labelling was calculated from the mass isotopomer distributions (MIDs) detected by the GC-MS. *P<0.05, compared to 5.6 mM glucose alone.

5.5 DISCUSSION

Though it does not provide quantitative information on the level of metabolites, the importance of this study lies in the possibility to monitor glucose channelling through different pathways and its relative contribution to the formation of key metabolic intermediates. We can consider the model here presented as a pseudo-steady state model, where the number of cells changes over time, whereas the isotopic label was only fed once (Buescher et al., 2015).

What is known regarding metabolism in BRIN-BD11 cells is that an increase in glucose concentration decreases the oxidation of acetyl-derived intermediates in the TCA cycle, as evidenced by a study using the above cellular model to trace different glucose isotopes at low and high concentrations of the hexose sugar. In the study, the conversion D-[3, 4-^{14}C]glucose to $^{14}CO_2$ was used as a means of measuring pyruvate dehydrogenase activity, and conversion of [5-^{3}H]glucose to ^{3}HOH as a means of overall D-glucose metabolism. The ratio between the two processes decreased when increasing glucose concentrations from 1.1 mM to 16.7 mM, indicating a glucose-dependent decrease in its oxidation rate (Rasschaert et al., 1996).

From the insulin assay performed under the established conditions for the metabolite analysis, insulin response to the glucose load (14 mM) was slightly reduced in cells pre-treated with high glucose (25 mM), compared to those under physiological conditions (5.6 mM glucose). This reduction was not significant, in contrast to what was reported by others using this cell model (Wallace et al., 2013). It is possible that the absence of a wash step before glucose stimulation, which we could not perform given possible alteration to metabolite fraction labelling, might have masked the functional impairment previously reported at 25 mM glucose (Wallace et al., 2013). However, underlying metabolic changes might have started taking place, including differences in glucose channelling through its metabolic pathways.

Notably, there is evidence pointing to a link between exendin-4 induced cellular metabolism, via the activation of the hypoxia induced factor α (HIF- α) and the activation of the mTOR pathway (Carlessi et al., 2017). There is pathway conversion between the mTOR pathway and the downstream activation of the insulin receptor signalling loop. However, the ability of exendin-4 to increase cellular

respiratory capacity and glycolytic flux in BRIN-BD11 cells is independent of the presence of insulin growth-like factor receptor (IGFR) or the insulin receptor (IR) (Rowlands et al., 2018). Therefore, though the insulin assay could be informative of the functional state of the cells, it does not directly affect metabolic changes induced by exendin-4.

With regards to other pathways for glucose metabolism, the pentose phosphate pathway does not affect glucose stimulated insulin secretion in the clonal pancreatic cell line INS-1 832/13. Specific inhibition of the enzymes involved in this pathway, namely siG6PDH-1 and 6-AN, both separately and in combination did not alter insulin secretion up to the concentration needed to downregulate the RNA of the enzymes (1000 and 200 μM, respectively) (Huang and Joseph, 2012).

Moreover, pyruvate labelling pattern in our study was either fully labelled or unlabelled under all the experimental conditions tested. This suggests the labelled pyruvate detected originates from glycolysis, given that when labelling occurs, all 3 carbons of the molecule are involved, reinforcing the importance of oxidative metabolism in BRIN-BD11 cells.

For these reasons and given the importance of oxidative glucose metabolism in regulating insulin secretion (Alcazar et al., 2000), we mainly focused our attention on intermediates on glycolysis and the TCA cycle, while considering metabolites we detected also in the organic phase extraction.

5.5.1 Metabolites in the cell supernatants

Our qualitative ^{1}H-NMR revealed differences in metabolites following treatment with exendin-4, at physiological glucose concentrations. Acetate has been attributed a role in type 2 diabetes, in particular that of preventing hypoglycaemia when blood glucose levels are too low (Tang et al., 2015). Consistently, by comparing exendin-4 treatment at low and high glucose, the levels of acetate appear to be higher at 5.6 mM glucose, possibly suggesting a need to prevent hypoglycaemia and reflecting the glucose-dependent actions of the incretin. Conversely, the role of acetone in beta-cells has not yet established and further research in this aspect, starting with the characterisation of this putative metabolite could help establish the potential of this metabolite under these conditions. Alanine

and lactate were also detected in the ^{13}C experiment and their significance will be discussed further below.

5.5.2 Organic phase metabolites

Previous reports measure the total amount of fatty acids present in BRIN-BD11 to be about 120 µg/10^6 cells with palmitate, oleate, stearate and linoleate being the most abundant (Diakogiannaki et al., 2007). The role of fatty acids in T2D can vary according to the type of fatty acid and the length of the stimulation, as they are considered important fuels for beta-cells, but they can impair glucose-stimulated insulin secretion following chronic exposure (McClenaghan, 2007). The action of palmitate suggests association with beta-cell dysfunction, as increases in inflammatory IL-6 has been reported in healthy islets following stimulation with the fatty acid (Eguchi and Nagai, 2017).

Compared to physiological concentrations of glucose, high glucose concentrations increased the abundance of palmitic and arachidic acids, which might impair insulin secretion (Keane et al., 2011). An increase in abundance was also observed for cholesterol, which has been previously associated with an increase in reactive oxygen species (ROS) production at concentrations of 160 µM in BRIN-BD11 cells (Asalla et al., 2016). All these metabolites were reduced by addition of exendin-4 at high glucose concentrations, consistent with the anti-diabetic effects related to such reduction.

In contrast, at 5.6 mM glucose, exendin-4 increased the abundance of fatty acids. Studies have reported saturated fatty acids as mediators of lipotoxicity-induced apoptosis of beta-cells, with concomitant increase in NO (Welters et al., 2004), which we did not observe in the subsequent studies we performed on NO release (described in Chapter 6). In order to assess if the increase in fatty acid species lies within non-toxic levels, further quantification is needed to provide an explanation to the observed result.

Using uniformly labelled glucose was a means of assessing fatty acid synthesis following exendin-4 treatment in physiological and hyperglycaemic conditions. However, the inability to detect labelling in our experiment could be mainly due to two reasons. It could be possible that very low levels of fatty acid concentration might have not allowed calculation of the mass isotopomer distributions (MIDs).

Another reason could be that glucose was not significantly channelled towards fatty acids synthesis under our experimental conditions. Further studies taking into consideration the oxidation of fatty acids could shed light on the preferred mechanism of exendin-4 on this intracellular metabolic pathway and its role in stimulating insulin release.

5.5.3 Aqueous phase metabolites

The total ion chromatograms showing the abundance of aqueous metabolites revealed that increase of glucose concentrations from physiological levels to a hyperglycaemic state determined a reduction of docosanoic acid, a component of the extracellular membrane according to the Human Metabolome Data Base (HMDB). This suggests that chronic hyperglycaemia might direct metabolism towards a reduction of cell membrane synthesis which would be consistent with reduced proliferation under this condition preceding beta-cell failure (Chang-Chen et al., 2008). This finding represents a good example of how, despite the maintenance of insulinotropic activities and responsiveness to exendin-4 under chronic hyperglycaemic state, beta-cells start undergoing changes in their metabolism predicting the features of beta-cell failure. Further studies quantifying these metabolites, as well as measuring them across different time points and alongside functional insulin release assays would help expand on their predictive potential in T2D.

5.5.4 Significance of TCA intermediates

The percentage of labelling for lactate detected in this study was consistent with previous reports considering the effects of metformin on the TCA cycle intermediates in primary rat astrocytes, given the drug's ability to cross the blood-brain barrier (Hohnholt et al., 2017), suggesting the production of this intermediate is consistent across there two cellular models. The high turn-over observed in mice fed with ^{13}C-lactate, which was about 2-fold higher than that of glucose itself, represents an index of increased consumption of this metabolite. This is supported by studies reported in both fed and fasting mice, where about 40-50% of TCA intermediates are generated from lactic acid (Hui et al., 2017). On a broader scale, non-oxidative metabolism, with increased accumulation of lactate has been reported in patients

affected by T2D, compared to healthy controls (Adeva-Andany et al., 2014). An increase in consumption of lactate, for a higher ATP production for insulin release, could reflect the decrease in labelling of this intermediate in samples treated with exendin-4, possibly decreasing accumulation of the metabolite and consistent with an anti-diabetic environment.

With regards to alanine, exendin-4 increased its labelling both under normo- and hyperglycaemic conditions. The suggested insulinotropic mechanism for the amino acid, co-transport with Na^+, has been further characterised as an oxidative metabolism channelling mechanism (Brennan et al., 2002). In fact, by using a ^{13}C-tracer for glucose metabolism in NMR spectroscopy analysis, the same BRIN-BD11 cell line displayed increased release of glutamate and lactate in the supernatant, suggesting the importance of aerobic metabolism for appropriate insulin secretion and glucose homeostasis.

With regards to citrate, labelling of this intermediate was lowered under all experimental conditions, compared to the untreated sample. A decrease in metabolite labelling could be due to either a lower uptake in the labelled species, in our case glucose, or an increase in its consumption. It is possible that treatment with exendin-4 increased the consumption rate of this intermediate, while high glucose alone might have been responsible for channelling towards other pathways. In fact, citrate has another important biological role, as it can be transported to the cytoplasm and broken down to oxaloacetate and acetyl-CoA for free fatty acid (FFA) synthesis. Interestingly, there is evidence supporting the role for FFA in beta-cell signalling for insulin secretion. As the K_{ATP}-channel dependent pathway is involved only in the acute phases of insulin secretion, a model integrating nutrient signalling on a separate yet connected pathway with glycolysis has been proposed. Long-chain acetyl-CoA (LC-acetylCoA) fatty acids deriving from citrate transport and metabolism in the cytoplasm have been shown to enhance glucose-stimulated insulin secretion only in the presence of glucose (Corkey et al., 2000). The reduction of labelling found for citrate for the exendin-4 treated conditions could have led to a FFA-mediated insulin secretion. The sample pre-treated with 25 mM glucose, however, could have simply responded by a decrease in glucose uptake, reflecting an impaired glucose-sensitivity under this condition.

In the reaction from isocitrate to 2-Ketoglutarate, the CO_2 released could be from the unlabelled portion, therefore not directly originating from the glucose we

fed the cells with. The mass distribution vectors (MDVs) of 2-Ketoglutarate and glutamate should match, as the compounds are in complete exchange where correction for natural isotope abundance has been applied (Buescher et al., 2015). We observed a MDV of 63 and 61% for the 2KG and glutamate, respectively, indicating a degree of reliability in the isotope correction in data generated thus far. A slight, yet statistically significant reduction in the labelling pattern of 2-Ketoglutarate was observed in the samples pre-treated with high glucose, both in the presence and absence of exendin-4. A consistent reduction was also observed in the MID for glutamate in these samples. Reports on the function of 2-KG in maintaining homeostasis in the gut, with an increase in the number of immune cells following an infection (Wu et al., 2016), point to an overall anti-inflammatory action related to this metabolite. At 5.6 mM glucose, both in the absence or the presence of exendin-4, there is an increase in channelling glucose towards the formation of 2-Ketoglutarate. Though we can observe a slight increase in labelling also at 25 mM glucose in the presence of exendin-4, this failed to reach statistical significance, suggesting this mechanism is more pronounced at lower glucose concentrations.

Glutamate has been associated to anti-diabetic actions, allowing Goto-Kakizaki rats with insulin defects to respond to GLP-1 due to residual production of glutamate (Yokoi et al., 2016). Conversely, studies using the insulinoma RIN-m5F and MIN6 cell lines showed that following a chronic stimulation (72 hrs) with 16.7mM glucose, there was an increase in glutamate in the cell supernatant. This was associated with impaired GSIS, which was restored by blocking glutamate with glutamate dehydrogenase (GDH) (Huang et al., 2017). Therefore, it seems like a balance between the stimulatory activity of glutamate with regards to insulin secretion needs to exist for cells to maintain a healthy metabolic state. The decrease operated by exendin-4 could work in this direction, whilst chronic stimulation with 25 mM glucose might have reduced production of glutamate from glucose reflecting a metabolic impairment. This hypothesis could be validated by a compartmental analysis of labelled glutamate to determine its localisation, either in the mitochondria to generate 2-Ketoglutarate or in the cytoplasm to contribute to insulin sensitivity.

For succinate, fumarate and malate, we did not detect differences across samples, suggesting the main differences in metabolites under these conditions relate to the initial steps of the TCA cycle or that these metabolites reach a steady state quicker than the upstream intermediates. Given that our experiment is performed in

whole intracellular metabolite extraction, it is not possible to discriminate between metabolite intermediate fractions that are shuttled out of the mitochondria for other roles in the cytoplasm.

Nevertheless, the results observed in this study indicate an overall metabolic state which promotes channelling of glucose towards oxidative metabolism within the TCA cycle, consistent the efficient generation of ATP associated with insulin secretion reflected in the functional assay. We observed similar trends in the actions of exendin-4 between high and low glucose, with the latter being the setting where effects were more pronounced towards a more efficient turn-over in the cycle, suggesting more pronounced enzymatic activities at 5.6 mM glucose. In order to validate this hypothesis, studies measuring labelling abundance as well as enzymatic activity could take this possibility into account. Also using other labelled species for key metabolites such as lactate and pyruvate could isolate the channelling of these compounds and provide further information regarding their cycling in the pathway.

By further understanding metabolic modulation operated by exendin-4, these studies could be extended to the hybrid peptides E-TGN and E-MAM$_2$ for comparison of their actions on glucose metabolism. At present, we instead considered investigating the expression profile of key genes involved in insulin secretion, with a view of understanding how the different treatments, exendin-4, E-TGN and E-MAM$_2$ could also modulate the transcriptome.

Chapter 6

TRANSCRIPTIONAL MODULATION

6.1 BACKGROUND

6.1.1 Regulation of genes involved in insulin secretion

Among the causative and contributing factors to the development of T2D, including glucotoxicity, oxidative and ER stress (Ottosson-Laakso et al., 2017), altered gene expression can potentially lead to altered metabolic homeostasis (Sithara et al., 2017). One of the main pathological traits of diabetes, glucotoxicity, has been referred to as a determinant for altered gene expression in T2D. In fact, glucose concentration has been found to modulate the PKA pathway, through variants associated with *in vivo* insulin secretion (Ottosson-Laakso et al., 2017).

Success in the field of exploiting gene expression fingerprint as a predictive tool has been achieved in outcomes for treatment of breast cancer (van 't Veer et al., 2002), highlighting the power of this tool for complex and multifactorial diseases. In T2D, studies utilising gene expression signatures can harbour information on the state of the disease. By inducing experimental diabetes in adipocytes and comparing their gene expression profile after restoring insulin sensitivity, a characterisation of patients with different levels of insulin sensitivity was possible (Konstantopoulos et al., 2011).

Interestingly, gene expression profile characterisation, performing genome-wide association studies to identify SNPs and patterns which correlate with type 2 diabetes have mainly focused adipocytes (Das and Rao, 2017) or pluripotent stem cells differentiated into islets (Perez-Alcantara et al., 2018). Though less is known regarding patterns in pancreatic beta-cells, some susceptibility genes for T2D have been examined. For example, the expression of KCNJ11, the gene encoding for a subunit of the potassium channel presented a negative association with body mass index levels when comparing healthy and diabetic islet donors, suggesting a link of this gene to obesity (Kirkpatrick et al, 2010). The pancreatic duodenal homeobox (PDX-1), which is responsible for beta-cell differentiation and growth, has also been linked to the upregulation of insulin gene transcription (Iype et al., 2005), suggesting that these genes work together in maintaining healthy and functional beta-cells.

The ability of novel antidiabetic peptides, possessing a native GLP-1 component to modulate gene expression has previously been shown. Skarbaliene and colleagues (2017) presented a novel dual GLP-1-gastrin agonist with antidiabetic action and compared its activity of modulating gene expression with that of exendin-4. Results from this study showed the novel peptide upregulated genes involved in the activation of the MAPK pathway, consistent with the idea of an increased insulin signalling and beta-cell proliferation (Skarbaliene et al., 2017). This highlights how gene expression patterns can be clustered, providing an overview of the beta-cell transcriptome following treatment.

In our experimental setting, we were guided by the rationale of having an overview of any changes in the expression of key genes involved in insulin secretion, using traditional real-time PCR. Though this does not provide a complete overview of the transcriptome, we were aiming to obtain indications on how the peptides could affect gene expression at a time where changes on a transcriptional level were detectable.

6.1.1.1 Pancreatic duodenal homeobox (PDX-1)

The insulin gene promoter, found about 340 bp upstream of the gene, is a known binding site for cis-and trans-acting transcription factors regulated by glucose, calcium and other nutrients (Andrali et al., 2008). Despite differences in regulation of transcription factors between rat and human species, one of the most conserved regulators is PDX-1, whose DNA binding activity is regulated by glucose (Andrali et al., 2008).

The PDX-1 gene is known to regulate insulin production and beta-cell development and is downregulated in type 2 diabetes (Hao et al., 2017; Zhu et al., 2017). An important role in regulating transcription of the insulin gene has also been attributed to PDX-1, as silencing this gene with small-interfering RNA caused a 40% downregulation of pre-insulin mRNA transcripts (Iype et al., 2005). PDX-1 also plays a fundamental part in beta-cell replacement therapy, where the idea of increasing and stimulating the production of insulin-secreting cells could represent a therapeutic option for both type 1 and type 2 diabetes. Pancreatic mesenchymal cells, following transfection with a synthetic form of PDX-1 mRNA, can differentiate in

insulin-producing cells (Guo et al., 2015), highlighting the cellular reprogramming feature of the gene.

Studies aimed at evaluating the contribution of exendin-4 and GLP-1 receptor agonists in carrying out anti-diabetic effects with regards to the growth and maturation of beta-cells have also shown promising results. In islet like cell clusters, exendin-4 stimulates the differentiation of beta-cells, which also corresponds to an *in vivo* increase of PDX-1 positive cells following transplantation of pancreatic precursors in the presence of exendin-4 (Movassat et al., 2002). Another GLP-1 receptor agonist, liraglutide, was tested in insulin resistant mice to assess its relationship to GLP-1 in its anti-diabetic action. Together with preventing beta-cell loss, the GLP-1 receptor agonist increased mRNA levels of PDX-1 and this action was coupled with an improvement of pancreatic function (Hao et al., 2017).

6.1.1.2 GLP-1 receptor (GLP-1R)

The GLP-1 receptor mediates signalling of its agonists in the regulation of glucose concentrations. In T2D, the actions of both GIP and GLP-1 are impaired, with the latter preserving some residual activity (Nauck et al., 1993). In this context, the expression of the GLP-1 receptor has been measured in a diabetic *in vivo* model, the partially pancreatectomized rat. Results from that study show a reduction of GLP-1 receptor expression in the presence of high glucose levels both *in vitro* and *in vivo* over a 48-hour period (Xu et al., 2007). There is also evidence for a 3-fold decrease in the expression of this receptor in diabetic ob/ob mice islets compared to non-diabetic littermates (Kubo et al., 2016), strongly suggesting a correlation between the reduced expression of this receptor and impairment in glucose homeostasis.

Another important link between the expression of GLP-1R and metabolic homeostasis lie in the ability of the receptor to function as a promoter for insulin gene expression, as the beta-cell line INS-1 overexpressing the receptor were able to generate an autocrine stimulation of insulin gene transcription (Chepurny and Holz, 2002). This is in line with the anti-diabetic effects operated by GLP-1 receptor agonists and further supports the importance of this incretin in maintaining glucose homeostasis.

Among the regulators of gene expression within the pancreatic beta-cell, also non-coding microRNAs have been studied for their possible effect on beta-cell specific transcripts in both murine and human islets. In particular, miR-204 downregulates the transcription of both the insulin gene (Xu et al., 2013) and the GLP-1R, as evidenced by gene expression studies in the presence of that specific miRNA (Jo et al., 2018). Interestingly, in the absence of this transcriptional regulator, the beneficial effects on glucose tolerance were observed only following exendin-4 treatment, suggesting the importance of the peptide in mediating transcriptional effects on the GLP-1 receptor (Jo et al., 2018).

For these reasons, we considered measuring mRNA levels of the crucial genes for beta-cell preservation, with a view to evaluating how the peptides modulate their expression.

6.1.1.3 Plasma membrane channels (KCNJ11, ABCC8 and CACNA1C)

K_{ATP} channels couple the electrical activity of beta-cells with the metabolic state of the cells (Ashcroft, 2005). The KCNJ11 gene encodes for the inner core subunit of the channel, Kir6.2. Activating mutations in the gene have been associated with neonatal diabetes, where by a gain of function causes a decrease in sensitivity to ATP, resulting in reduced insulin secretion (Gloyn et al., 2004).

Another key subunit of the potassium channel, SUR1, is encoded by ABCC8. Sulphonylurea drugs bind to this subunit, allowing for an ATP-independent closure of the channel (Gloyn et al., 2004). Mutations in this gene are associated with cases of hyperinsulinism, related to the absence of the functional protein at the plasma membrane or failure of MgADP to activate the channel (Ashcroft, 2005).

The L-type calcium channels located on the membrane of beta-cells are encoded by both CACNA1C and CACNA1D genes. Though the expression of CACNA1D is about 60-fold higher than CACNA1C in human beta-cells (Reinbothe et al., 2013), CACNA1C plays important roles in rodents. The isoform it encodes, $Ca_v1.2$, is vital as a global knockout of the gene is incompatible with life, whereas within the beta-cell the protein is necessary for first phase insulin release (Reinbothe et al., 2013).

Given the results we observed for first phase insulin secretion suggest our novel hybrid peptides have anti-diabetic actions, we considered how that reflects on

the expression of the gene encoding for this channel in pancreatic beta-cells following treatment.

6.1.1.4 Nuclear factor kB (NFkB)

As insulin resistance in T2D arises also as a consequence of chronic inflammation (Kolb and Mandrup-Poulsen, 2010; Pollack et al., 2016), we considered the expression of the NFkB gene in clonal pancreatic beta-cells. With a complex downstream signalling, by which both anti- and pro-inflammatory roles have been attributed to NFkB activation (Lawrence 2009), its function in beta-cells and diabetes has been investigated.

The human beta-cell line 1.1B4, created by electrofusion, was assessed for gene expression following cytokine exposure, which is known to cause inflammation. Even though gene expression does not necessarily translate into an increased protein activity, results from this study indicated NFkB1 gene was upregulated following cytokine treatment and a 50% decrease in cell viability, as well as a decreased insulin content were observed (Vasu et al., 2014). This suggests that the inflammatory cytokines used in the study (IL-β, TNF-α and IFN-γ) acted as regulators of transcription after 18 h incubation within in a cellular model of beta-cells, justifying the use of a similar protocol to understand the actions of our peptides in modulating gene expression.

Information regarding gene expression profiles of beta-cells has also been acquired *in vivo*. Using a zebrafish model, it has been shown that NFkB can be considered a marker for beta-cell ageing. The decline in beta cell proliferation observed with ageing was associated with changes in gene expression, with different components of the NFkB pathway being upregulated (Janjuha et al., 2018), consistent with an increase of inflammatory markers. The activation of NFkB has been also linked to disruption of nitrates in the nitric oxide (NO) pathway (Grumbach et al., 2005), which plays a role in T2D. Beneficial/harmful effects of nitrates have been mostly linked to the source from its biosynthesis. While the endothelial nitrate-nitrite-NO pathway reduces oxidative stress and promotes insulin secretion via mitochondrial depolarization (Ghasemi and Jeddi, 2017), inducible NO contributes to insulin resistance of T2D. This form is enhanced in the presence of free fatty acids, which determine an increased circulation of pro-inflammatory cytokine IL-1β (Ghasemi and Zahediasl, 2013). Assessing the modulatory effects of

the peptides on NFkB, we also considered any changes in nitrate release that could suggest the formation of a pro-inflammatory environment.

With regards to peptide treatment modutating this pathway, there is evidence of exendin-4 improving insulin resistance by modulating NFkB, more specifically by polarising adipose tissue macrophages towards an anti-inflammatory phenotype, inhibiting release of inflammatory cytokines such as IL-β and IL-6 (Guo et al., 2016). For these reasons, NFkB represented a target of interest, as its actions in beta-cells are known to propagate inflammation and exendin-4 can mitigate such effects also by modulating the expression of the gene. Our investigation was pointing to the possibility of the hybrid peptides to affect the number of NFkB transcripts, towards an anti-diabetic profile.

6.2 AIM AND OBJECTIVES

Following up on the mechanism of action studies, which show modulation of the peptides' actions in relation to the activity of calcium and potassium channels, we studied the transcriptome relating to genes associated with T2D. The aim is to assess the expression profiles of key beta cell genes involved in insulin secretion and inflammation following treatment with exendin-4 and its related hybrids (E-TGN and E-MAM$_2$).

Specific objectives include:

1.   Treating BRIN-BD11 cells with insulin inducing concentrations of exendin-4, E-TGN and E-MAM$_2$, according to the previous insulin release experiment.

2.   Extracting RNA and performing real-time quantitative PCR to compare the expression levels of genes involved in cell proliferation (GLP-1 and PDX-1), insulin secretion (INS-1, ABCC8 and CACNA1C) and inflammation (NFkB), using β-actin as the reference housekeeping gene.

3.   Assessment of the production of the nitric oxide metabolite NO$_{2^-}$ as a measure of NO production relating to modulation of NFkB.

6.3 RESEARCH DESIGN

6.3.1 BRIN-BD11 cells treatment and RNA isolation

BRIN-BD11 cells were used for gene expression studies. Cells were seeded and treated as detailed in section 2.4.1 and RNA extraction was performed using the Isolate II RNA Mini Kit (Bioline©, London, UK), as per manufacturer's recommended protocol. Following cell lysis with 350 µL of lysis buffer and 3.5 µL of ß-mercaptoethanol, lysate was filtered by centrifugation at 11,000 g for 1 minute. RNA precipitation was achieved by addition of 70% ethanol followed by a 30-second centrifugation (11,000 g). The silica membrane was de-salted and residual DNA was digested with 95 µl of DNAse I reaction mixture. The membrane was washed and dried by 3 successive 30-second centrifugation steps (at 11,000 g). RNA was eluted in 40 µL RNAse-free water and quantified using Nanodrop™ 1000 (ThermoScientific). The instrument measured the concentration of each sample (ng/µL), the 280/260 and 260/230nm absorbance ratios. For the 280/260 ratio, which indicates purity of the sample from proteins, the acceptable value of a good quality RNA extraction was selected as from 2.0 and above. For the 260/230 ratio, indicating purity from contaminants absorbing at 230 nm such as carbohydrates, an acceptable value was chosen as from 2.0 above.

6.3.2 cDNA synthesis and Real Time quantitative PCR (RT-qPCR)

cDNA strands were transcribed from RNA using Sensifast™ cDNA Synthesis kit (Bioline©, London, UK), as detailed in section 2.4.2. The generated cDNA was stored at -20°C until qPCR reaction. In summary, each reaction contained 1X Sensifast™ SYBR® NO-ROX (Bioline©, London, UK), 400-500 nM of forward and reverse primers for the given gene (Table 2 in Chapter 2), 100 ng of cDNA and deionized water to a final volume of 20µL. The instrument used for the reaction (AriaMx Real-time PCR System (Agilent© Technologies, Santa Clara, CA, USA)) was set up with the qPCR cycles detailed in section 2.4.3.

6.3.3 NO$_2$- measurements

The NO metabolite NO$_2$- was measured according to the protocol detailed in section 2.5. Briefly, BRIN-BD11 cells were seeded at a density of 2.5×10^4 cells/well in a 96-well plate and treated with exendin-4, E-TGN or E-MAM$_2$ (3 µM) for 24 hours. The supernatant (50 µl) was incubated in the presence of assay buffer, as well as nitrate reductase and enzymes co-factors for the detection of NO$_2$-. Griess reagents A and B were added to all wells (50 µl) for 5 and 10 minutes and absorbance was read at 540 nm.

6.3.4 Statistical analysis

Statistical analysis was carried out as detailed in section 2.7. The raw values of relative fluorescence obtained from the AriaMx instrument software were used to quantify gene expression levels. The relative gene expression (R) for each gene was calculated using the following equation:

$$R = \frac{E_{(target)}^{\Delta Ct_{target} \, (control-sample)}}{E_{(ref)}^{\Delta Ct_{ref} \, (control-sample)}}$$

The efficiency of the target gene ($E_{(target)}$) is normalised to the reference gene expression of β-actin ($E_{(ref)}$), according to the cycle threshold difference between the untreated and the sample ($\Delta Ct_{(control-sample)}$) (Pflaffl, 2001).

To compare gene expression levels between each differentially treated sample, an ANOVA followed by Newman-Keuls test were used. Values were normalised by setting the untreated control sample value to 1.

6.4 RESULTS

6.4.1 The peptides increased the expression of GLP-1R and PDX-1

In order to assess the effects of the peptides on cell survival and proliferation, as these aspects are compromised in T2D, the first study was performed on GLP-1R and PDX-1. Consistently with the notion of an agonist increasing the number of receptors on the cell surface, exendin-4 increased the expression of GLP-1R by 7.1 ± 2.08-fold (p<0.05), compared to the untreated control (5.6. mM glucose). Treatment with E-TGN increased the expression of the receptor by 3.5 ± 1.30-fold whilst E-MAM$_2$ increased the level of transcripts for the GLP-1 receptor by 13.3 ± 1.41-fold compared to control (p<0.01) which represented a 1.9 ± 1.41-fold, significantly higher expression (p<0.05) of this gene compared to exendin-4 (Figure 6.1A).

With regards to the expression of the PDX-1 gene, compared to their native peptide exendin-4, both E-TGN and E-MAM$_2$ decreased PDX-1 expression by 3.76 and 10.13-fold, respectively (P<0.001), although treatments with exendin-4 and E-TGN were still significantly higher than glucose alone (607-fold, P<0.001, and 161-fold, P<0.05) (Figure 6.1B).

A) GLP-1R expression
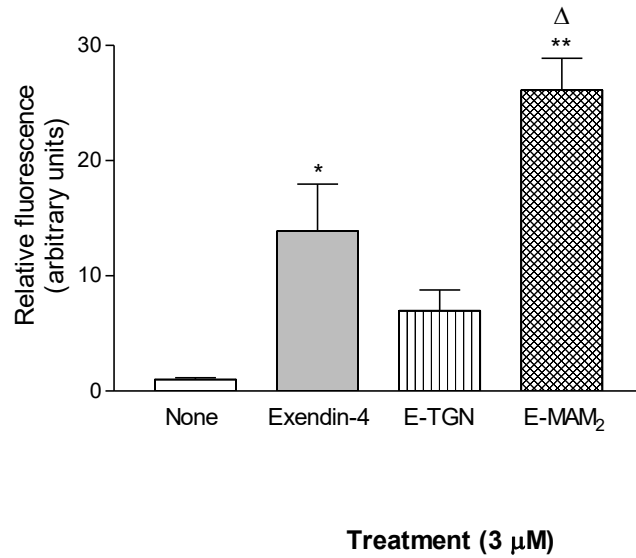
B) PDX-1 gene expression
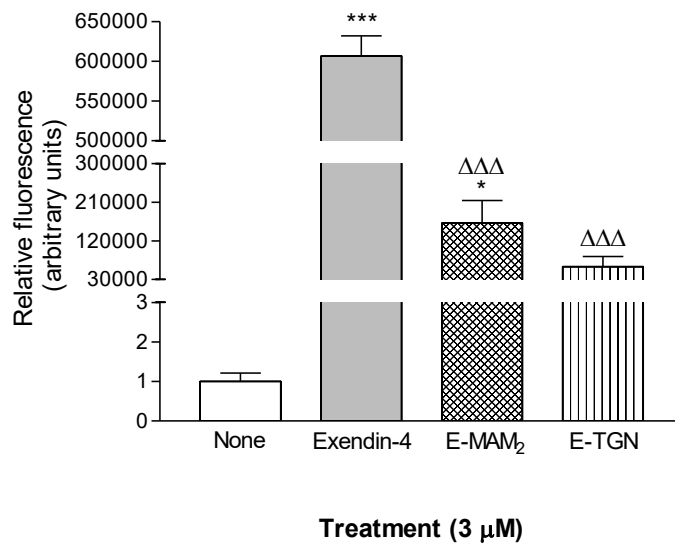
Figure 6.1. Gene expression levels for genes involved in proliferation: GLP-1R (A) and PDX-1 (B).
Following 24-hour treatment with peptides (3 μM), mRNA levels were measured for quantitative gene expression, relative to control. Values are mean ± SEM (3 replicates from one experiment), *p<0.05, **p<0.01, ***p<0.001 compared to control (5.6 mM glucose treated). Δp<0.05, ΔΔΔp<0.001, compared to exendin-4 treatment.

141

6.4.2 The hybrid peptides modulated genes involved in insulin secretion (INS-1, ABCC8, KCNJ11 and CACNA1C)

Treatment with exendin-4 increased INS-1 gene expression by 7.4-fold (P<0.05), compared to control. Similarly, E-TGN also increased INS-1 expression by 6.2-fold (P<0.05). E-MAM$_2$ was the most potent modulator of the expression of this gene, generating a 4.5-fold increase compared to exendin-4 alone (P<0.001) (Figure 6.2A).

With regards to the expression of the ATP-binding cassette on the potassium channel (ABCC8), exendin-4 downregulated the expression of the gene by 1.34-fold, compared to control. E-TGN and E-MAM$_2$ both decreased this level by 2.1-fold (P<0.001) and 1.9-fold (P<0.01), respectively, compared to exendin-4 (Figure 6.2B).

Exendin-4 upregulated the expression of KCNJ11, the gene encoding for the sulphonylurea receptor by 1.45-fold (P<0.05), compared to the untreated control. E-TGN decreased the action of exendin-4 by 4.12-fold (P<0.001), and by 2.84-fold (P<0.01) compared to control. E-MAM$_2$ downregulated KCNJ11 expression by 1.83-fold (P<0.05) compared to control and by 2.65-fold (P<0.001) compared to exendin-4 alone (Figure 6.2C).

The CACNA1C gene, encoding for the Ca$_V$1.2 gene was downregulated following treatment with each peptide. For exendin-4 treated cells, the expression of CACNA1C was reduced by 3.8-fold (P<0.001), compared to untreated control (5.6 mM glucose). A further decrease in the transcription of this gene was observed following treatment with E-TGN and E-MAM$_2$, where a reduction of 3.4- and a 4.26-fold were observed, respectively, compared to exendin-4 (P<0.05) (Figure 6.2D).

A)

INS-1 expression

B)

ABCC8 expression

C)

KCNJ11 expression

D)

CACNA1C gene expression
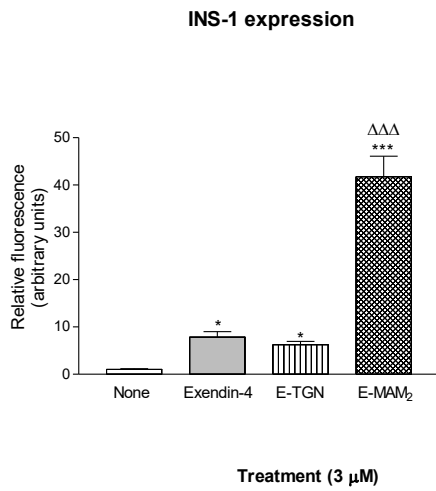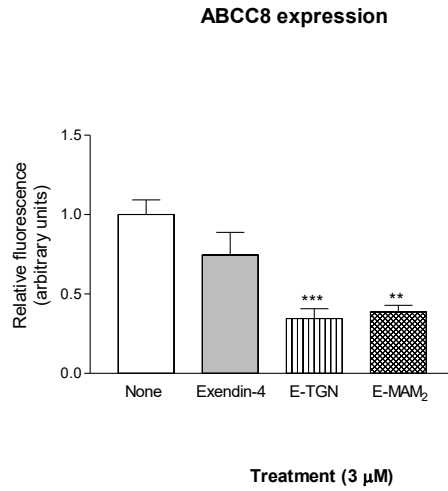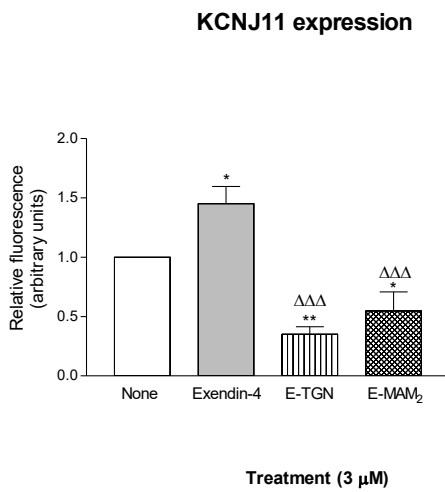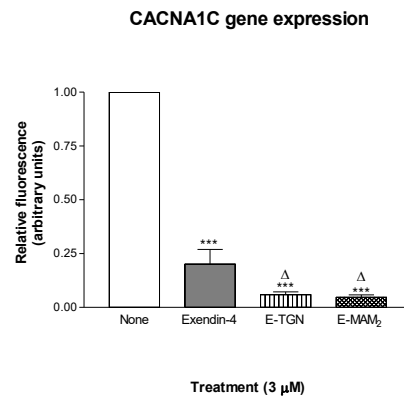
Figure 6.2. Effects on exendin-4 and hybrid peptides on the mRNA expression of INS-1(A), ABCC8 (B), KCNJ11 (C) and CACNA1C (D) in BRIN-BD11 cells
Following 24-hour treatment with peptides (3 μM), mRNA levels were measured for quantitative gene expression, relative to control. Values are mean ± SEM (3 replicates from one experiment for INS-1, n=3 for the other genes), *$p<0.05$, **$p<0.01$, ***$p<0.001$ compared to control (5.6 mM glucose treated). $\Delta p<0.05$, $\Delta\Delta\Delta p<0.001$, compared to exendin-4 treatment.

6.4.3 Exendin-4 related peptides decrease NFkB expression, with no changes is NO$_2$- release

Compared to control, exendin-4 decreased the expression of NFkB by 4.18-fold (P<0.001). E-TGN further decreased this by 7.78-fold (P<0.001), which represents an 11.5-fold reduction compared to control (P<0.001). In the presence of E-MAM$_2$, gene expression of NFkB was 2.37-fold higher than that of exendin-4 alone (P<0.01), but still 1.76-fold lower than control (P<0.001) (Figure 6.3).

With regards to NO$_2$- release, no changes were observed between the control (5.6 mM glucose) or the peptide treated samples (Figure 6.4). This result is relevant both to the inflammatory and metabolic features involved in T2D, as increased release of NO from NO$_2$- can be an index of fatty acid-induced hypoxia (Welters et al., 2014).

NFkB expression
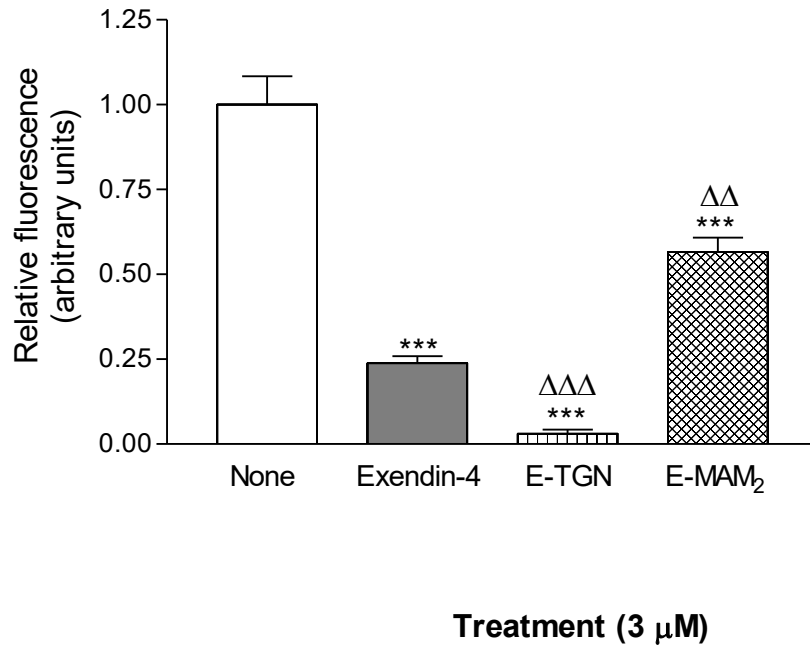
Figure 6.3. Effects of hybrid peptides on the expression of NFkB in BRIN-BD11 cells.
Following 24-hour treatment with peptides (3 µM), mRNA levels were measured for
quantitative gene expression, relative to control. Values are mean ± SEM (3 replicates frpm
one experiment), ***$p < 0.001$ compared to control (5.6 mM glucose treated). ΔΔ$p < 0.01$,
ΔΔΔ$p < 0.001$, compared to exendin-4 treatment.
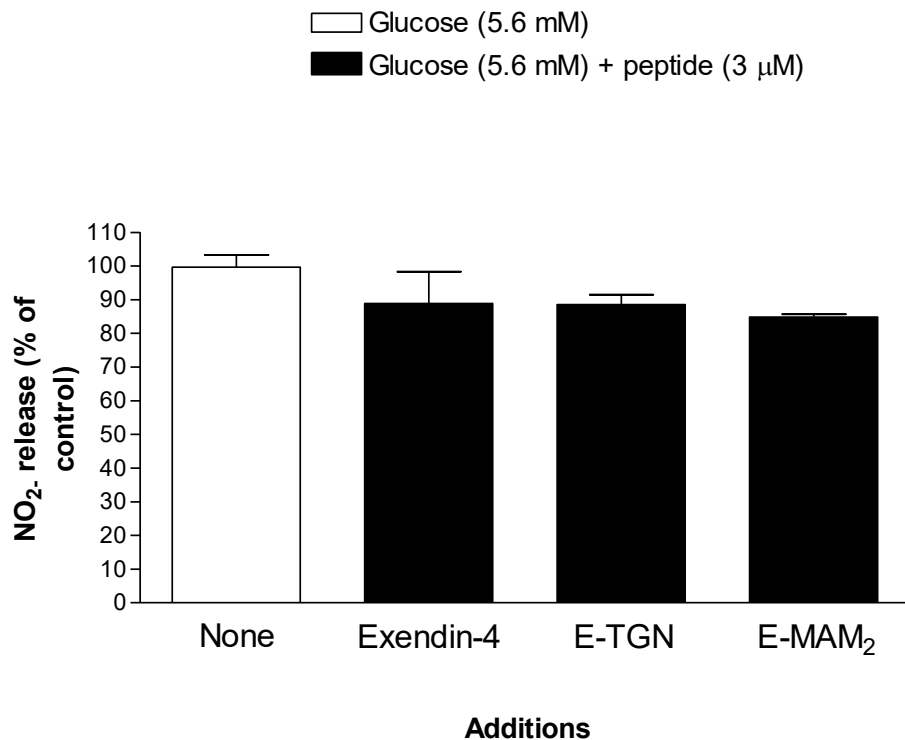
Figure 6.4. Effects of native exendin-4 and hybrid peptides on nitrite (NO$_2$-) release from BRIN-BD11 cells.

NO$_2$- release was measured after chronic treatment (24 hours) of cells with exendin-4. With this colorimetric assay, cells (2.5 X 10^4) were seeded in a 96-well plate for overnight attachment. The following day, BRIN-BD11 cells were treated with exendin-4, E-TGN, or E-MAM$_2$ (3 μM), for 24 hours. The supernatant was assayed for NO$_2$- as described above Values are mean ± SEM (N=2, with 3 replicates per experiment). No changes in NO$_2$- release were observed following treatment with exendin-4 (3 μM).

6.5 DISCUSSION

For the purpose of this study, we focused on assessing changes in expression of genes involved in cell proliferation, insulin secretion and related to the inflammatory pathway of NFkB in order to further understand how exendin-4, E-TGN and E-MAM$_2$ modulate transcription of these genes.

Given previous reports on the action of the FDA approved anti-diabetic drug exendin-4 on modulating gene expression with regards to the insulin-secreting pathway (Li et al., 2005; Fusco et al., 2017), we included the peptide in this study to evaluate how its action compares to those of the hybrid peptides. This allows a better understanding of how the novel peptides modulate insulin secretion compared to baseline.

The expression of the insulin gene, occurring exclusively in pancreatic beta-cells, is regulated both by transcriptional factors and external agents, including glucose, hormones and fatty acids (Melloul et al., 2002). Consistent with the ability of GLP-1 receptor agonists to increase the levels of insulin mRNA transcripts (Drucker et al., 1987; Chepurny et al., 2002; Fusco et al., 2017), exendin-4 increased insulin gene expression. Similarly, E-TGN also increased the expression of insulin. The same applied to E-MAM$_2$, which also conferred increased levels of insulin transcripts to the BRIN-BD11 cell line by about 5-fold, compared to exendin-4. The amount of insulin in the cells can have an additive effect in stimulating gene expression (Le Lay and Stein 2006). Effects of MAM$_2$ alone on gene expression have not yet been reported in the literature. However, peptide screening in Chapter 3 indicated that the amount of insulin secreted by MAM$_2$ was 1.16-fold higher than that of exendin-4. If this is consistent with gene expression levels, the frog peptide might contribute by additive effect to the result obtained here, even though it is understood that several factors may influence insulin gene expression and insulin secretion differentially.

Beta-cell proliferation is impaired in diabetes, as beta-cell failure represents one of the main consequences of the hyperinsulinism defining the first stages of the disease (Shanik et al., 2008). To that end, promoting cell proliferation could be beneficial in reducing metabolic stress that precedes such failure. GLP-1R is the G-protein coupled receptor to which the endogenous incretin, GLP-1, and exendin-4 bind to. A decrease of the expression of this receptor was observed in diabetic

murine islets, where by exogenous overexpression of GLP-1R insulin secretion was restored (Kubo et al., 2016), suggesting the anti-diabetic actions of exendin-4 could relate to this receptor. Consistently with that idea, in our experimental setting, the presence of exendin-4 increased the expression of GLP-1R by 10-fold. Likewise, the hybrid peptides generated a prominent increase in the expression of this receptor, with E-MAM$_2$ having the highest effect. The increase in the expression of GLP-1R following peptide treatment suggests this receptor could contribute to the actions of all the peptides tested. Measurements of the final protein encoded by the gene would be needed to confirm this hypothesis.

To further investigate aspects involved in proliferation, we looked at the expression of PDX-1. This gene is involved in pancreas development and beta-cell maturation and is also known to directly form a complex with insulin, favouring its transcription (Chakrabarti et al., 2002; Melloul et al., 2002). In this study and in corroboration of the reports by Wang et al. (2001), which used a GLP-1 receptor agonist (10 and 50 nM) in RIN cells, exendin-4 upregulated the expression of PDX-1. The hybrids also had a significant effect although to a lower extent. This difference could be explained by understanding the individual contribution of amphibian peptides TGN and MAM$_2$ to the mRNA levels of PDX-1, if any.

By comparing the actions of E-TGN and E-MAM$_2$ with regards to the expression of both GLP-1 receptor and PDX-1 gene, we noticed the effects on PDX-1 transcription are greater in treatment with E-TGN compared to the hybrid E-MAM$_2$. Given the downstream pathway of GLP-1 receptor activation is responsible for transcription of PDX-1 by increasing its DNA binding activity in the insulinoma cell line INS-1 (Buteau et al., 1999), the results obtained for E-MAM$_2$ could suggest that the action of its GLP-1 receptor signalling activation is less potent than that of E-TGN. However, further studies also taking into consideration protein levels of intermediates involved in the process would shed light on the importance of this pathway in the mechanism of action of the hybrids.

For further insight on the involvement of the K$_{ATP}$-dependent pathway in the actions of exendin-4 and its related hybrids, gene expression studies were performed on genes encoding for the K$_{ATP}$ channel. In our experiments, *in vitro* treatment of BRIN-BD11 cells with exendin-4 did not significantly alter the levels of KCJN11 mRNA transcripts. Previous studies, comparing the effects of exendin-4, d-Ala^2-GIP and DPP-4 inhibitors on expression of beta-cell genes following *in vivo* treatment in

high-fat fed mice, also showed that exendin-4 did not change the expression levels of the KCNJ11 gene (Lamont and Drucker, 2008). Our data is consistent with this report that the actions of exendin-4 are not directly associated with changes in gene expression.

On the other hand, treating BRIN-BD11 cells with the newly designed hybrid peptides resulted in KCNJ11 downregulation, with E-TGN leading to a reduction of over 50%. Loss of function in this gene, leading to hyperinsulinism is rare (Flanagan et al., 2009), however KCNJ11 downregulation in pancreatic mice islets can occur as a consequence of hypoxia following accelerated oxygen consumption in cells undergoing hyperglycaemic stress (Sato et al., 2014). In our experimental setting, we did not detect changes in nitrite (NO_{2-}) levels that could point to cellular stress, making it unlikely cells are undergoing hypoxia. Moreover, hypoxia is also associated with NFkB activation (D'Ignazio and Rocha), which we did not observe in our experiment. Therefore, the physiological relevance of this downregulation is unknown as consistencies with an increased cellular stress or transcriptional activation of inflammatory markers such as NFkB were absent.

With regards to the ABCC8 gene, encoding the SUR1 subunit of the channel, a downregulation of transcripts was observed following peptide treatment. This pattern has also been observed in NZO mice islets, where a T2D phenotype of hyperglycaemia, hyperinsulinemia and glucose resistance was established *in vivo* (Andrikopoulos et al., 2016) and a downregulation of the ABCC8 gene was associated with this phenotype. However, the reduced levels of ABCC8 might not necessarily reflect impaired ability of the cells to respond to sulphonylureas following peptide treatment as transcriptional downregulation might not be associated with reduced protein levels. Also, given exendin-4 binds to a G-protein coupled receptor, an unchanged expression of the ATP-binding cassette is consistent with the possibility that the peptide might not utilise that portion of the receptor to exert its actions. It is to note that the binding site for the novel peptides E-TGN and E-MAM$_2$ has not yet been studied or identified.

However, the down-regulation of ABCC8 could indicate that the actions of these peptides may not directly involve the activation of the SUR1 subunit of the KATP channel. This is consistent with our hypothesis when designing the hybrid peptide that the new peptide may activate the GLP-1R to exert its actions. Immunoblotting studies would be able to corroborate this hypothesis.

The expression of CACNA1C, the gene encoding for the L-type Ca^{2+} dependent channel $Ca_V1.2$, was also investigated. It is known to regulate insulin secretion in rodents, as knock-out mice for $Ca_V1.2$ lose first-phase (first 5 minutes) of insulin secretion, due to a 55% reduction in the inward Ca^{2+} current (Schulla et al., 2003). We observed a downregulation in the expression of the CACNA1C gene in the presence of all peptides, following a 24-hour treatment. Schulla et al. (2003) had reported that the diminished insulin secretion observed *in vivo* for $Ca_V1.2$ knock-outs was restored to normal following the first 5 minutes of stimulation and basal insulin secretion was not affected. This result, along with ours, could indicate the disruption in insulin release might not be applicable to our experimental setting, given the peptides were insulinotropic in the 20-minute acute insulin tests described in Chapter 3. The role and physiological relevance of this downregulation are unknown and whether the actions of the peptides are affected on the long term could be determined by further, long-term insulin studies.

The effects of GLP-1 receptor agonists not only lie in their anti-diabetic actions, but the presence of the receptor on different tissues, including kidney, heart, muscle and nervous tissues reflects the pleiotropic actions of these compounds (Lee and Jun, 2016). An increasing body of evidence points to anti-inflammatory actions of GLP-1R agonists, which also mediate the anti-diabetic actions of these drugs. Within a chronic low-grade inflammation state, as that of obesity and type 2 diabetes, the actions of GLP-1 receptor agonists have an overall effect in lowering chronic inflammation, and in isolated human islets exendin-4 (50 nM) mediated some of these actions by reducing the activation of the nuclear factor NFkB (Velmurugan et al., 2012).

All peptides tested for effect on gene expression reduced the expression of the NFkB gene, compared to the untreated cells, but the differences between the peptides could represent differences in the mechanisms used to control this inflammatory pathway. The function attributed to NFkB as an inflammatory signal also relates to beta-cell ageing. By analysing the trascriptome of beta-cells from young and old zebrafish, it was found that the beta-cells with reduced proliferating activities, deriving from the older models, also had a higher activation of the NFkB pathway, according to GFP reporter studies (Janjuha et al., 2018), highlighting the role of this pathway in limiting proliferative capacities in beta-cells.

In our study, we recorded a 75% downregulation of NFkB transcripts in the pancreatic cell line in the presence of exendin-4. This indicates the anti-inflammatory action observed in other cell types such as adipocytes and breast cancer cells (Iwaya et al., 2017). A further, significant reduction of NFkB expression levels is observed in the presence of E-TGN, compared to exendin-4. We found this result of interest as drawing the cellular environment toward a milder inflammatory activation in T2D could have clinical relevance, considering inflammation is one of the causes of insulin resistance (Wu et al., 2014). Moreover, transgenic mice expressing an inactivated form of NFkB revealed a nearly complete protection from the diabetogenic agent streptozotocin (Eldor et al., 2006), indicating the involvement of the gene in the actions of diabetogenic agents. Even though the study focused on type 1 diabetes, streptozotocin is extensively used in the generation of T2D mouse models (Premilovac et al., 2017), justifying our interest in further characterising the inflammatory aspect related to T2D.

Anti-inflammatory properties of TGN have been previously reported (Pantic et al., 2014). The aforementioned authors found that different synthetic forms of the peptide, including the one used for this study stimulated the production of the anti-inflammatory IL-10 from peritoneal macrophages in both C57BL6 and BALB/c mice. This could explain the ability of E-TGN to downregulate the expression of NFkB to a higher degree compared to exendin-4 alone. With regards to E-MAM$_2$, we reported a 50% decrease in the transcription of NFkB, compared to the untreated control, and this value was higher than that of exendin-4. We hypothesised that such a significant reduction in the expression of an inflammatory-related gene such as NFkB could have further implications. Beta-cells are not responsible for perpetuating inflammatory responses in T2D, therefore we carried on investigating this aspect in an antigen-presenting cell model, in the search for novel actions of the peptides in this context, beyond transcriptional regulation. Resident macrophages in insulin-sensitive tissues have been attributed an important role in the inflammatory process (Xia et al., 2017), however further studies have also presented T-cell responses mediated by dendritic cells (DCs) in the adipose tissue as an important component of inflammatory-mediated insulin resistance (Bertola et al., 2012). This study was based on a previous finding linking depletion of CD11c positive cells from the adipose tissue to a beneficial and improved insulin sensitivity (Patsouris et al., 2009). Given CD11c is one of the distinctive surface markers of DCs, we carried

out further studies investigating the role of exendin-4 and its related hybrids in modulating the function of an *in vitro* model of DCs (Chapter 7).

Chapter 7

IMMUNOMODULATION STUDIES

7.1 BACKGROUND

From the previous chapters we found that exendin-4, E-TGN and E-MAM$_2$ lowered the expression of the NFkB gene. Inflammatory stimuli are known to facilitate dissociation of NFkB from its inhibitory subunit IkB, causing activation on the inflammatory pathway, and the downstream elements of this pathway are upregulated in T2D patients (Andreasen et al., 2011). Thus, obtaining a downregulation at the gene transcription level of NFkB in our previous experiment prompted further investigation on the actions of the peptides in the context of inflammation.

7.1.1 The role of dendritic cells (DCs) in T2D

Dendritic cells (DCs) are potent antigen-presenting cells produced by the haemopoietic bone marrow in an immature state (Rajan and Longhi, 2016). Activation or suppression of the immune response depends on the state of activation of DCs, as they are responsible for presenting self-antigens, allowing a tolerogenic environment when immature (Sundara and Longhi, 2016), as well as for activating T-cells and adaptive immune response when triggered by the appropriate stimuli (Collin and Bigley, 2018).

Increasing interest in the role of these cells in the context of diabetes was initiated by the finding that the resident macrophages within the adipose tissue belonged to heterogeneous populations, but the ones expressing the CD11c surface marker were responsible for obesity-related insulin resistance. In fact, selectively ablating the subset of CD11c positive cells from the adipose and muscle tissues *in vivo* restored insulin sensitivity back to the control levels of lean, non-obese mice (Patsouris et al., 2008). This finding was further expanded by Bertola et al. (2012), who presented the possibility that within the CD11c population ablated in the previous study, DCs might have been present, given that this surface marker is one of their distinctive features. This hypothesis was confirmed by the characterization of

a DC subset within the adipose tissue, expressing high levels of CD11c, capable of activating Th17 T-cell responses, further recruiting macrophages and promoting inflammation in both obese and T2D mouse models (Bertola et al., 2012).

Within the pancreatic islet, DCs are found in non-diabetic mouse models in an immature state (Calderon et al., 2008). Treatment with the diabetogenic agent streptozotocin caused an increase in the number of intra-islet DCs, up to 2-fold increase after 8 days stimulation, due to migration of circulatory DCs from the blood (Calderon et al., 2008). In the context of T2D, the number and function of DCs has mostly been associated to an established risk factor for the disease, obesity, and one of its main complications, cardiovascular disease (Parenti et al, 2017). In mouse models of obesity, an increased activation of DCs with consequent T-cell activation has been linked to the inflammatory state causing metabolic disorders such as insulin resistance seen in these mice (Stefanovic-Racic et al., 2012).

Other aspects relating T2D and DCs activation in a human setting have also been investigated. The cytokine responsible for DCs maturation, the granulocyte-macrophage-colony stimulating factor (GM-CSF), is found at higher levels in T2D patients compared to normoglycaemic individuals (Surendar et al., 2012). Surface markers associated with the maturation of human DCs derived from peripheral blood mononuclear cells, such as CD83 and CD86 were upregulated in a glucose-dependent fashion (Lu et al., 2013), suggesting a role for hyperglycaemia as an activating signal for perpetuating inflammation in diabetes. Human DCs were also found to secrete cytokines associated with the progression of atherosclerotic plaques in the presence of high glucose concentrations (30 mM), such as IL-6 and IL-12, whereas the anti-inflammatory chemokine IL-10 was decreased by nearly 40% (Lu et al., 2013). Taken together, these results highlight the role of DCs in contributing to T2D related inflammation and have sparked interest in investigating the anti-inflammatory actions that could be found in anti-diabetic agents, and how they translate in the activation of adaptive cellular immunity.

The residency of DCs within both the pancreas and the adipose tissue suggest an important role of these cells in mediating the inflammatory component associated to T2D, and given about 85% of patients affected by T2D are obese (Parenti et al., 2017), we aimed to understand whether DCs could be modulated towards an anti-inflammatory and anti-diabetic setting in the presence of our novel peptides.

154

7.2 AIM & OBJECTIVES

The aim of this chapter is to examine the effects of exendin-4, E-TGN and E-MAM$_2$ on maturation of DCs and to assess their cytokine profile following peptide treatment.

Specific objectives include:

1)   The generation of bone marrow derived dendritic cells (BM-DCs) from mice using granulocyte-macrophage colony stimulating factor (GM-CSF), and their phenotypic characterisation (expression of surface markers MHC II, CD80 and CD86).

2)   Assessment of BM-DC phenotype following peptide treatment, in the absence or presence of an activation stimulus, lipopolysaccharide (LPS).

3)   Measurement of the pro-inflammatory cytokine IL-12 and anti-inflammatory cytokine IL-10 released by DCs following exposure to exendin-4, E-TGN or E-MAM$_2$, in the absence or presence of LPS.

7.3 RESEARCH DESIGN

7.3.1 Generation of bone-marrow derived dendritic cells (BM-DCs)

Bone marrow progenitor cells were isolated from the bones of C57BL6 mice as detailed in section 2.6.1. During the isolation procedure, the bone marrow was flushed and red blood cells were lysed with Ammonium-Potassium-Chloride solution (1X, 500 μL/pair of legs). A negative bead selection was performed in the presence of M5-114 (anti-MHC II), RA3-3A1 (anti-B220), YTS 191 (anti-CD4) and YTS 169 (anti-CD8), where the antibodies were incubated with the cell suspension for 30 minutes before incubation with isolation beads coated with anti-goat antibodies. The mixture of cells and magnetic beads was placed on a DynaMag™-15 magnet (ThermoFisher) and non-bead associated cells were isolated. Following isolation using this negative bead selection protocol, progenitor cells were plated at a density of 10^6 cells/well of a 24 well plate in the presence of 4ng/ml granulocyte-macrophage colony stimulating factor (GM-CSF). Cells were fed with fresh DC media (AIM V® + AlbuMAX® (BSA) 1X, 50 μM ß-ME, 1 mM HEPES) on days 3 and 5 of culture, as described in section 2.6.1 of Chapter 2.

To study the effect of exendin-4, E-TGN and E-MAM$_2$ peptides, DCs (day 6 from culture) were incubated with 1μM of each of these peptides or 1μl of the vehicle control (0.001N HCL). In some experiments commercially sourced LPS was added to the cells (200 ng/mL) following peptide pre-treatment, for 18 hours. The supernatant (500 μL) was then collected for cytokine analysis. Cells were harvested and stained for surface marker analysis by flow cytometry.

7.3.2 Phenotypic analysis of BM-DCs by Flow cytometry

Following treatment, BM-DCs were harvested and stained for surface markers expression as detailed in section 2.6.2. The antibodies used were against the surface markers involved in the antigen-presenting process (MHC II, CD80 and CD86) are shown in Table 2.3. Flow cytometry analysis was performed as detailed in section 2.6.3 and data analysed using the CFlow® Plus software. The mean fluorescence intensities (MFIs) of MHC II, CD80 and CD86 expression on CD11c$^+$ cells were compared.

7.3.3 Cytokine measurement using IL-12 and IL-10 specific sandwich ELISAs

The culture supernatants collected from control DCs and DCs pre-treated with 0.001N HCL, exendin-4, E-TGN or E-MAM$_2$ peptides in the presence or absence of LPS were assayed for the presence of pro- and anti-inflammatory cytokines IL-12 and IL-10, respectively, according to the manufacturer's protocol and as detailed in section 2.6.4. The plates were read at a wavelength of 450 nm.

7.3.4 Statistical analysis

Data from the phenotype and cytokine ELISA measurements were compared using a one-way analysis of variance (ANOVA) followed by Newman-Keuls post-hoc test (GraphPad Prism® 3).

7.4 RESULTS

7.4.1 BM-DCs were generated and validated by surface marker expression

Many challenges regarding the isolation, due to their low numbers, and characterization of *ex vivo* DCs has limited their *in vitro* use (Syme and Glück, 2001). However, over the last decades, isolation and growth of monocyte derived DCs from murine bone marrow or human blood using GM-CSF, has become a particularly useful tool to study these cells and their ability to control immune responses (Syme and Glück, 2001). The bone marrow in particular contains numerous hematopoietic precursors that can be differentiated into DCs (Wang et al., 2016), justifying our choice of this protocol to obtain these cells *in vitro.* Under the microscope, the progenitor cells undergo morphological changes during maturation in the presence of GM-CSF, starting off as single cells on day 1 (Figure 7.1A), developing the characteristic dendrites on day 3 and 5 (Figure 7.1B and C) and on day 7, BM-DCs formed multiple clusters of large cells, as displayed in Figure 7.1D, and as described by others (Inaba et al., 1992).

On day 7, we performed a phenotypic characterisation of these clustered cells. Within our experiment, we used an unstained population to establish the gating strategy for our experiments. Out of the 59.3% of live cells, within the DC population size, we gated on the unstained population (Figure 7.1E, left) for the fluorescent marker associated to CD11c (APC) (Figure 7.1E, middle plot), in order to assess the presence of a $CD11c^+$ population in the stained samples, by difference. Indeed, 95.1% of cells stained with the APC dye resulted to be positive, indicating this fraction of cells were $CD11c^+$ (Figure 7.1E, middle plot).

This single stained population was also used to gate for the expression of the other surface markers and the mean fluorescence intensity (MFI) for each fluorescent conjugated marker (FITC), namely MHC II, CD80 and CD86, was measured by difference. The presence of these markers (Figure 7.1F) confirmed the generation of mature DCs as reported in previous studies (Wang et al., 2016, Smyth et al., 2013).
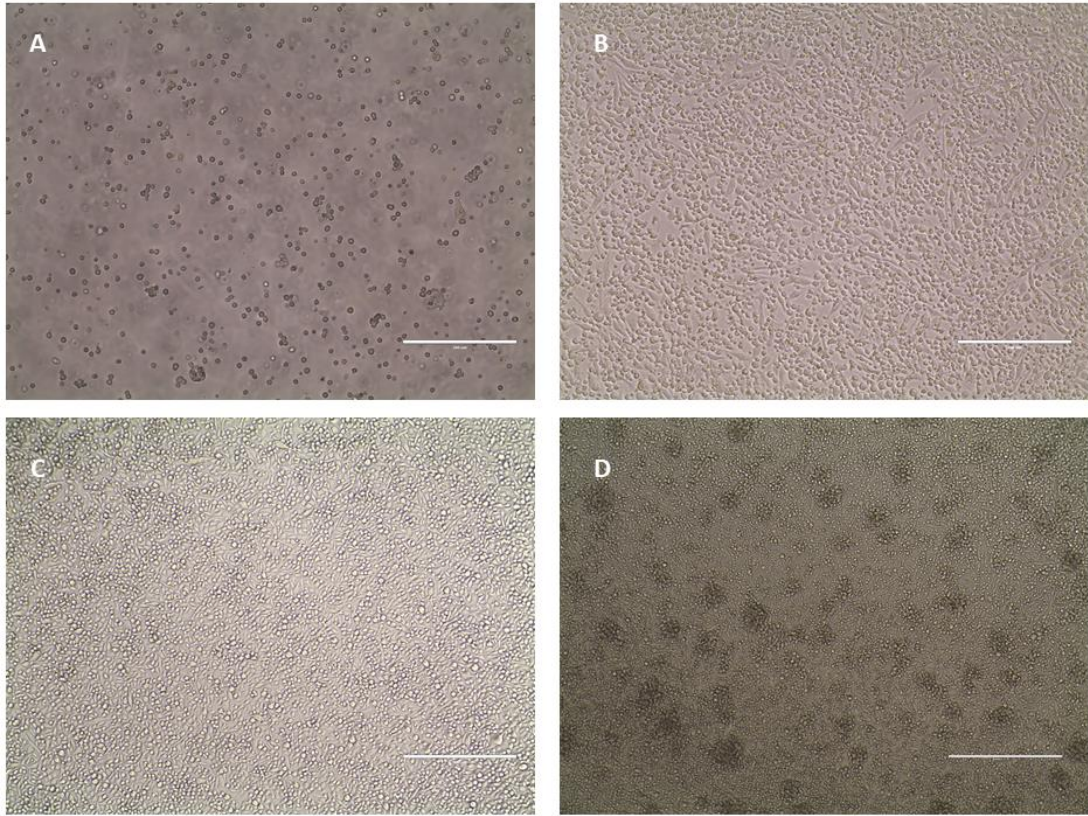
Figure 7.1. Morphological features of BM-DCs
at (A) day 1 (x20), (B) day 3 (x20), (C) day 5 (x40) and (D) day 7 (x40). On day 7 DCs were assessed by flow cytometry, the live cell population (P1) was defined by plotting FSC vs SSC (E, left).

E

F

— Single stain (CD11c$^+$)
— Surface marker (MHC II, CD80, CD86)
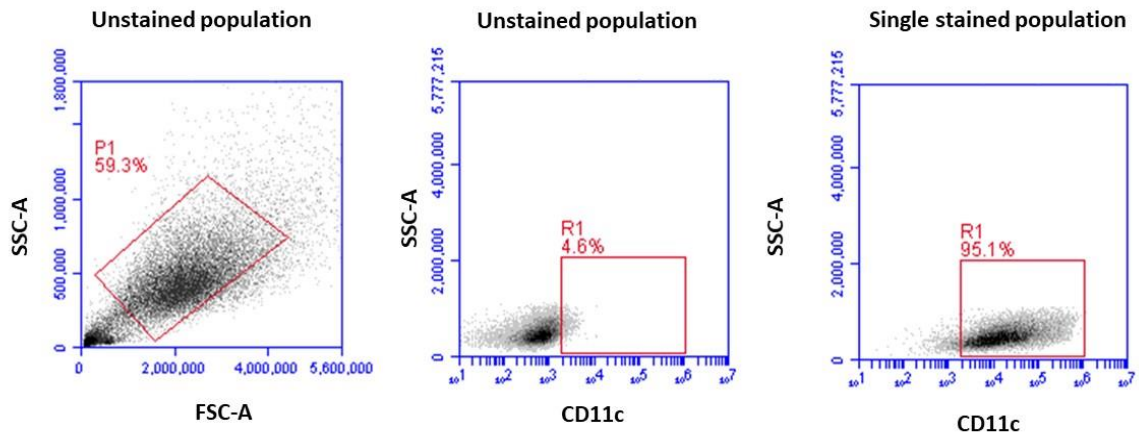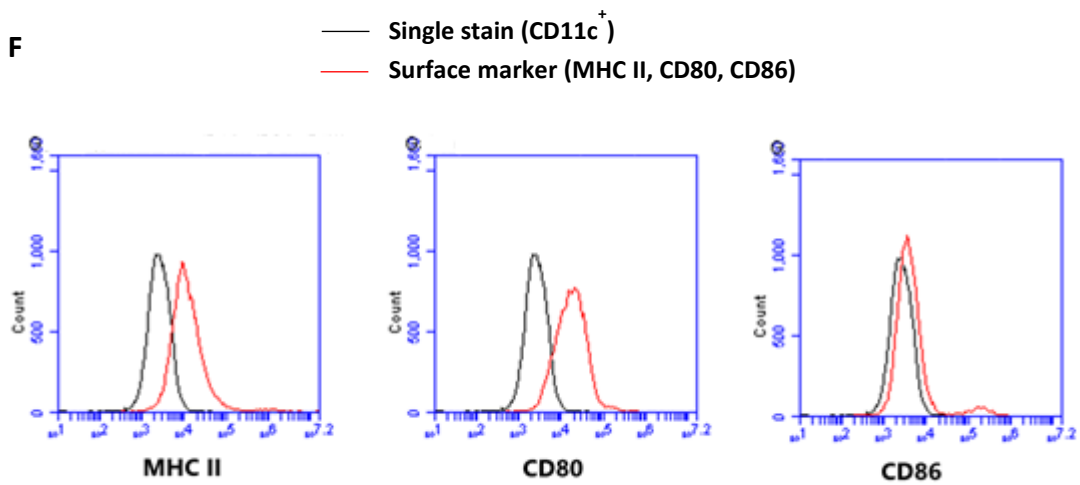
Figure 7.2. BM-DCs express high levels of CD11c as well as MHC II and CD80.
Following staining with anti-CD11c antibodies the CD11c$^+$ cells were gated using unstained cells (E, middle dot blot), within the live population of cells (E, left dot blot). The precentage of the CD11c$^+$ population is shown (E, right dot blot). BM-DCs were stained with one of the following: anti- MHC II, CD80 and CD86- FITC conjugated antibodies. Expression of these surface markers, on CD11c$^+$ DCs were assessed by flow cytometry and are shown as histograms (F).

7.4.2 Exendin-4 and the hybrid peptides do not alter the expression of BM-DCs surface markers

In order to test the effects of exendin-4, E-TGN and E-MAM$_2$ on the generated BM-DCs, the phenotype of these cells was characterised by flow cytometry following peptide treatment. To ensure any changes in the phenotype of DCs were peptide-related, we included a vehicle control (0.001 NHCl) in our analysis. Cells were treated with the peptides or vehicle on day 6 from isolation, and were harvested between 18 and 24-hour following treatment and stained with antibodies to CD11c as well as one of the following antibodies, anti- MHC Class II, CD80 or CD86. We found that like the untreated controls, the CD11c surface marker was expressed on all viable cells regardless of pre-treatment (Figure 7.2A-D).

In order to assess changes in the expression of the surface markers MHC II, CD80 and CD86, and to allow comparison across independent experiments, we set the MFI of the untreated control sample to 100, calculating increases/decreases as a relative percentage of this. For MHC II and CD80, the vehicle control did not significantly alter the expression levels of these markers in comparison to untreated cells (average % MFI 98.7 ± 2.41 and 102.8 ± 8, respectively). In the presence of exendin-4, E-TGN and E-MAM$_2$ both the expression of MHC II (93.7 ± 7.82, 97.9 ± 24.90 and 95.3 ± 17.6 MFI, respectively) and CD80 (97.3 ± 8.59, 98.8 ± 4.79 and 91.7 ± 9.74 MFI, respectively) was not significantly changed as compared to either vehicle or untreated controls (Figure 7.3A and B). In comparison to untreated BM-DCs, there was a slight but not significant increase in the expression of CD86 on DCs following treatment with the vehicle (108.8 ± 6.8 MFI), E-TGN (MFI 107.4 ± 3.31), and E-MAM$_2$ (107.5 ±5.74 MFI) (Figure 7.3C), which was not observed in the presence of exendin-4 (96.8 ± 3.75 MFI). However no statistical difference in the expression of this marker between the treatment groups was observed.

Taken together, these results show that pre-treatment of BM-DCs with exendin-4, E-TGN and E-MAM$_2$ does not lead to either and increase or decrease of MHC II, CD80 or CD86 surface markers. Given these results were obtained in immature DCs, we proceeded to further consider the actions of exendin and the hybrid peptides on LPS-matured BM-DCs, aiming to answer questions regarding their ability to modulate the perpetuation of an inflammatory response associated with DC activation.
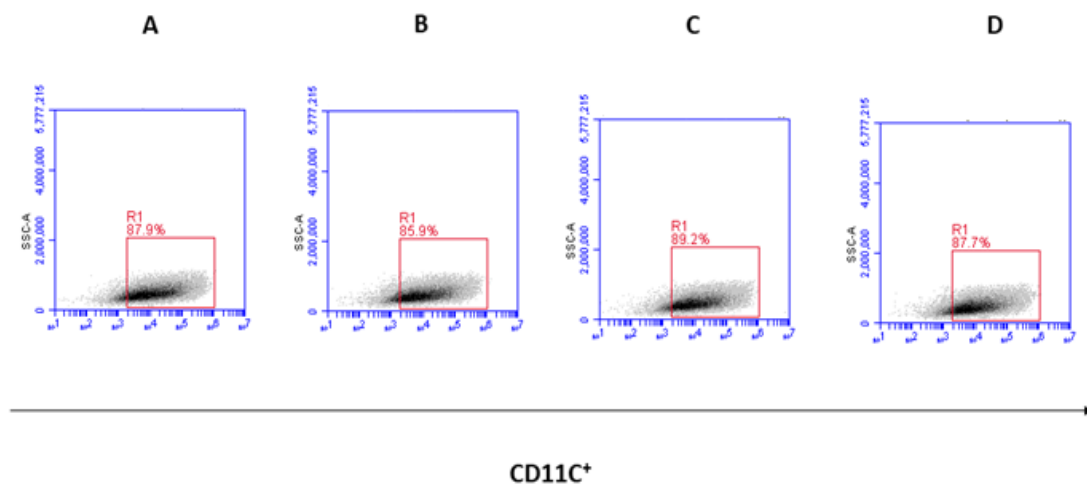
Figure 7.3. BM-DCs pre-treated with vehicle (0.001 N HCl) or peptides retained expression of CD11c.
The gating strategy for the untreated sample, used to determine the CD11c$^+$ populations, was applied to cells pre-treated under the different conditions. This is represented by dot blots for BM-DCs treated with either the vehicle (A), exendin-4 (B), E-TGN (C) or E-MAM$_2$ (D).

A)
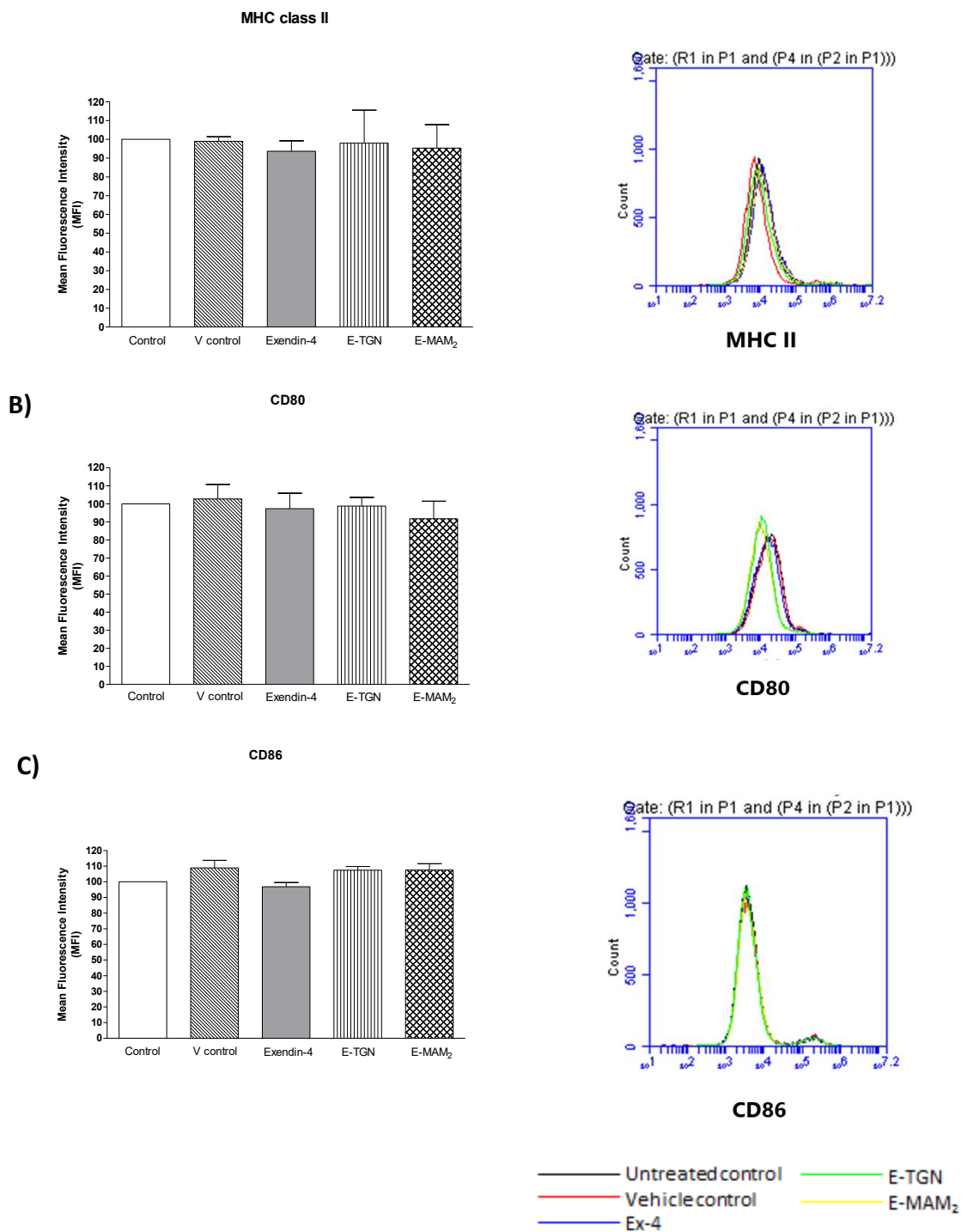
Figure 7.4. Pre-treatment of BM-DCs with the vehicle control, exendin-4, E-TGN or E-MAM2 does not alter the expression of BM-DCs surface markers.
The expression of surface markers (A) MHC II, (B) CD80 and (C) CD86 was assessed by flow cytometry using antibodies, following 24-hour treatment under the different conditions, as indicated in the x axis. Representative histograms from one experiment are shown. Bar charts showing the mean fluorescence intensity (MFI) of expression of these markers from 3 independent experiments are shown. The untreated control was set to 100%. Values are mean ± SEM.

7.4.3 BM-DCs present an activated phenotype after LPS treatment

In order to determine the activation of DCs following an appropriate inflammatory stimulus, we treated BM-DCs with lipopolysaccharide (LPS), known to induce DCs maturation by increasing the expression of MHC II, CD80 and CD86 on the cell surface (Smyth et al., 2013).

As expected, BM-DCs treated with LPS (1 µg/ml) displayed increased expression of MHC II on their surface compared to untreated cells, with a 27 ± 0.02 MFI increase was observed (P<0.05), suggesting DCs respond to LPS as a maturating signal for the increase in expression of this marker. Following pre-treatment with the vehicle control, this increase in expression of MHC II was observed but was not further affected (27.1 ± 0.06 MFI). Similarly, the expression of MHC II increased in all the peptide pre-treated DCs to the same extent as the LPS treated controls (Figure 7.4A).

With regards to CD80, following LPS treatment no increase in the expression of this co-stimulatory molecule was observed (Figure 7.4B). In contrast, CD86 expression was increased by 1.85 ± 0.21-fold in the presence of LPS (P<0.05). This increase was maintained in the peptide as well as vehicle treated DCs (1.72 ± 0.18 MFI for the vehicle to 1.82 ± 0.22 MFI for exendin-4 (Figure 7.4C). No significant difference in CD86 expression was observed between any of the LPS activated DCs regardless of peptide treatment.

Taken together, these results indicate that the maturation of BM-DCs in response to LPS as measured by increasing the expression of MHC II and CD86, is not altered by the action of the exendin-4 or its related peptides E-TGN and E-MAM$_2$. The absence of activation of CD80 in this setting was equally maintained across all treatment samples, suggesting the peptides did not have any additive effect on this marker.

A)
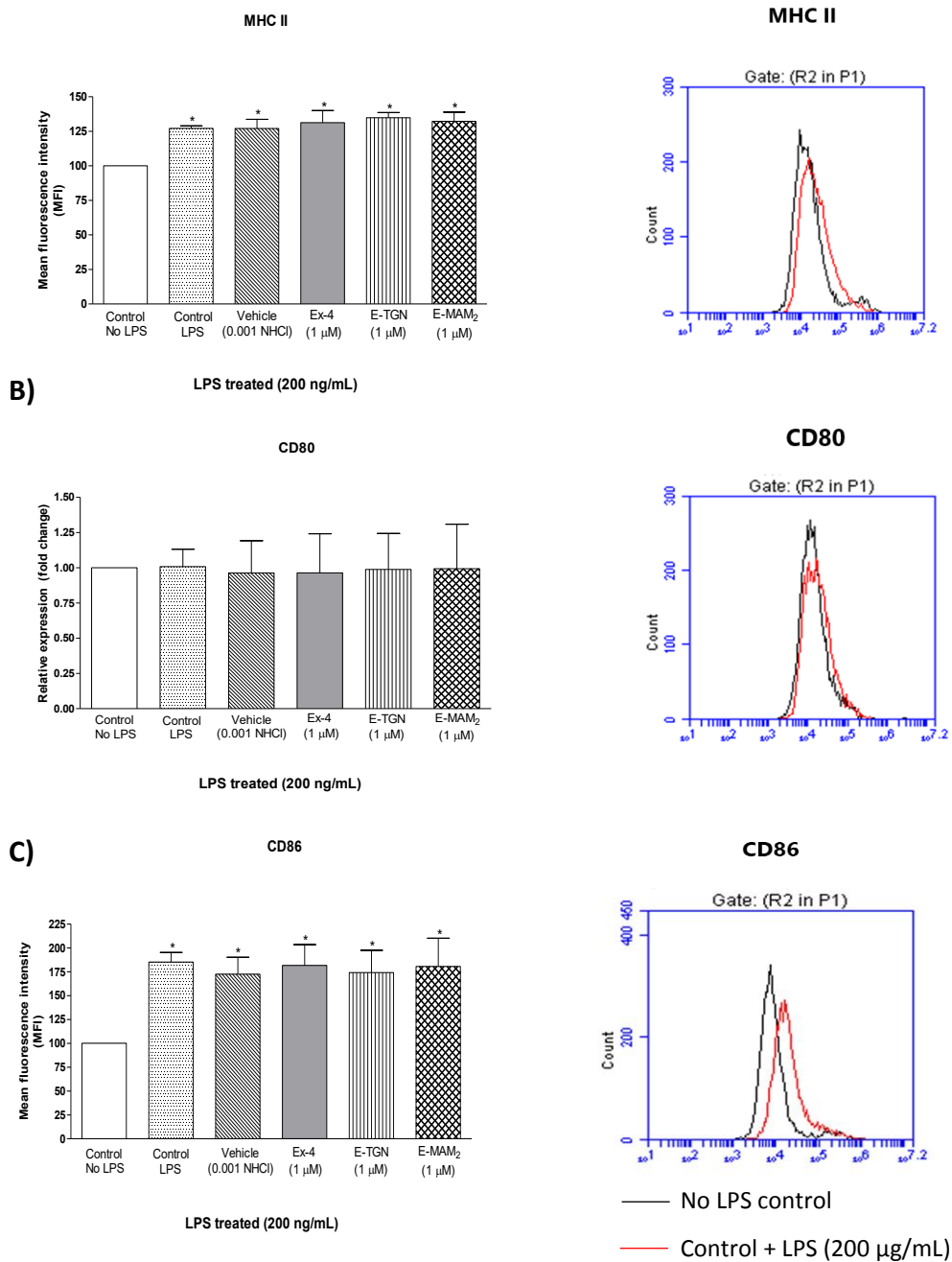
Figure 7.5. Pre-treatment of BM-DCs with vehicle control, exendin-4, E-TGN or E-MAM2 did not alter the ability of cells to respond to LPS stimulation.
Following pre-treatment with the vehicle control, exendin-4, E-TGN or E-MAM$_2$ for 24 hrs, BM-DCs were pulsed with LPS (200 ng/mL) for 18 hrs. The bar charts on the left display the mean fluorescence intensity (MFI) for (A) MHC II, (B) CD80 and (C) CD86. On the right, histograms represent the shift between untreated control (black line) and LPS-treated (red line) cells. Untreated control was set to 100%. Values are mean ± SEM (n=2, with values of each experiment pooled from an average of 3 technical replicates).

7.4.4 LPS stimulates release of IL-10 and IL-12 in BM-DCs

After characterising changes in the DCs phenotype, in order to determine whether the LPS activation of the cells was accompanied by cytokine release, we assayed the cell culture supernatant for IL-10 and IL-12, as the levels of these cytokines are known to be modified upon LPS stimulation (Corinti et al., 2001).

In the presence of LPS, the amount of IL-10 released by BM-DCs increased from 272.63 ± 28.9 pg/ml to 337.9 ± 33.2 pg/ml (P<0.05). However, the vehicle decreased release of IL-10 (P<0.05), compared to the untreated control (204.9 ± 34.2 pg/ml vs 272.63 ± 28.9 pg/ml). Despite this, the addition of LPS to vehicle treated BM-DCs, lead to an increase in IL-10 production, 377.6 ± 50.7 pg/ml. Finally, no difference in IL-10 release was detected comparing the LPS treated samples, suggesting the vehicle does not contribute to changes in IL-10 release following LPS activation of the cells (Figure 7.5A).

The levels of the pro-inflammatory cytokine IL-12 were also measured following LPS stimulation. In untreated cells, the levels of IL-12 averaged as 572.6 ± 38.2 pg/ml, which increased by 1.61-fold to 925.1 ± 78.3 pg/ml (P<0.001) in the presence of LPS. Addition of the vehicle to the culture media did not significantly change the levels of IL-12 released compared to the untreated control (572.6 ± 38.2 pg/ml vs 602.3 ± 32.6 pg/ml, respectively), but the addition of LPS to vehicle treated DCs caused a 1.88-fold increase (P<0.001) of IL-12, compared to the aforementioned. This was also 1.22-fold higher than the amount of IL-12 secreted in the presence of LPS only treated DC (P<0.01) (Figure 7.5B).

These results indicate that the vehicle modifies DCs leading to cells with an increased ability to release IL-12 following LPs exposure. This effect on the DCs should be taken into consideration when assessing the effects of the peptides, which are dissolved in this solution, on cytokine production.
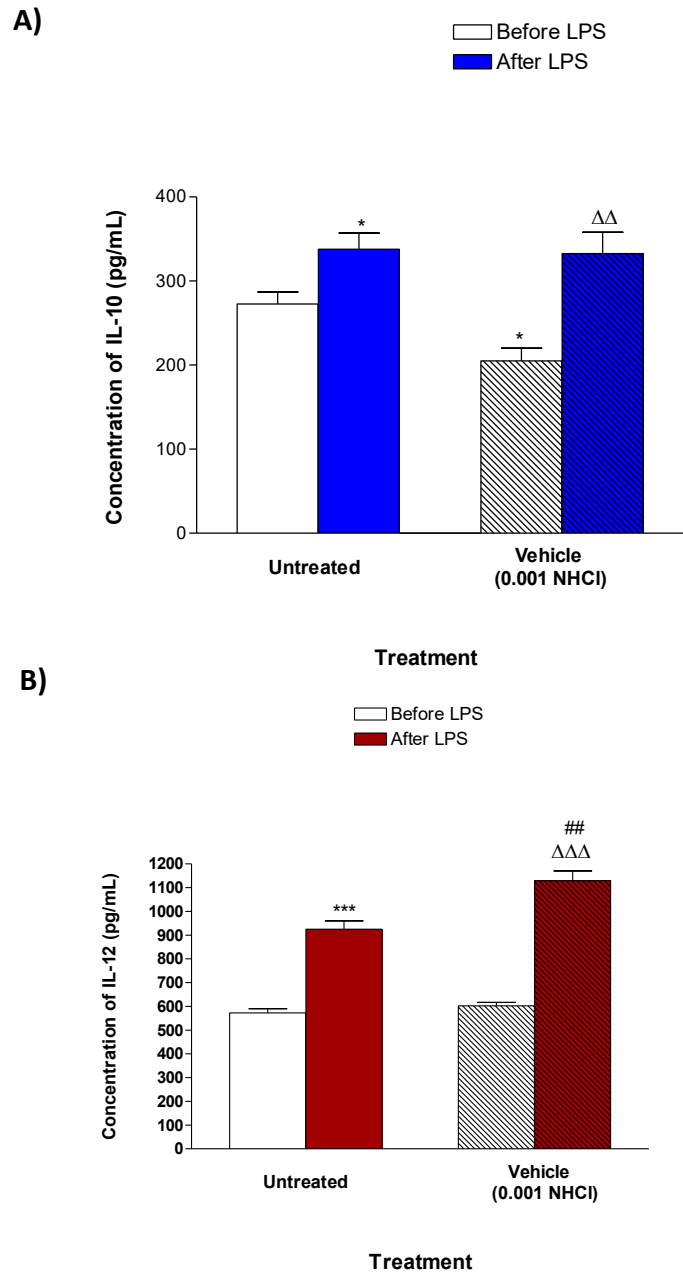
Figure 7.6. LPS increases release of IL-10 (A) and IL-12 from untreated and vehicle-treated BM-DCs.

BM-DCs were pulsed with the vehicle control (0.001 NHCl) before being activated by LPS (200 ng/mL) for 18 hours.Cell supernatants were collected and assayed for cytokine release using ELISA. Values are mean ± SEM (n=3 independent experiments, with each experiment having 3 technical replicates). *P<0.05, ***P<0.001 compared to untreated sample. ΔΔΔP<0.001, ΔΔP<0.01 compared to respective treatment in the absence of LPS. ##P<0.01, compared to untreated sample in the presence of LPS.

7.4.5 Peptide modulation of IL-10 and IL-12 release in BM-DCs in the presence of LPS

As mentioned in the introduction to this chapter Lu et al., (2013) observed that secretion, by human DCs, of the anti-inflammatory cytokine IL-10 was decreased whilst pro-inflammatory cytokines, such as IL-6 and IL-12, were increased in the presence of high glucose concentrations. In order to evaluate the effect of exendin-4, E-TGN and E-MAM$_2$ on the release of IL-10 and IL-12 in the presence of a maturation stimulation, we pre-treated cells with the exendin-4 related peptides before pulsing them with LPS.

As the vehicle alone (0.001 N HCl) had an effect on the expression of IL-10, we considered that sample as the baseline against which we compared the peptide treated samples in the cytokine release study. In the absence of LPS, we found no significant difference in the IL-10 production by BM-DCs following peptide-treatment as compared to the vehicle control (vehicle=204.96 ± 34.2 pg/ml; exendin-4=202.19 ± 49.3 pg/ml; E-TGN=183.55 ± 43.8 pg/ml; E-MAM$_2$=163.52 ± 47.34 pg/ml). Next, we assessed IL-10 production following LPS stimulation. The addition of LPS to DCs following exendin-4, E-TGN or E-MAM$_2$ peptide treatment increased IL-10 release by 2.67-fold (P<0.01), 1.99-fold (P<0.001) and 3.01-fold (P<0.001) respectively, compared to cells treated with the aforementioned peptides in the absence of LPS. Excitingly, exendin-4 as well as E-MAM$_2$ pre-treated BM-DCs generated significantly more IL-10, 1.62-fold (P<0.05) and a 1.48-fold (P<0.05) respectively, in the presence of LPS compared to LPS stimulated cells pre-treated with the vehicle (Figure 7.6A). For E-TGN, although an increase was seen this was not a significant compared to the vehicle only treatment, suggesting the Il-10 measured was due to the vehicle effect.

Next, the release of IL-12 under the same conditions, in both the absence and presence of LPS stimulation was measured. Treatment of immature DCs with the vehicle control only was recorded at 602.3 ± 32.6 pg/ml. Addition of E-TGN and E-MAM$_2$ decreased this value to 547.5 ± 8.83 (P<0.01) and 528.1 ± 35.2 (P<0.01) pg/ml respectively, whereas exendin-4 showed no difference to the vehicle control (576 ± 55.23 pg/ml). As mentioned above, the addition of LPS to the vehicle treated BM-DCs resulted in a significant increase in IL-12 production (1129.3 ± 92.16 (P<0.001)), compared to untreated cells. IL-12 production was decreased following pre-treatment with peptides in the presence of LPS. exendin-4 reduced the levels of

IL-12 by 0.82-fold (P<0.05), E-TGN by 0.74-fold (P<0.01) and E-MAM$_2$ by 0.87-fold (P<0.05) (Figure 7.6B).

Taken together the data suggests that peptide treatment modified the response of BM-DCs to LPS activation, with exendin-4 and E-MAM$_2$ increasing release of IL-10 and all peptides decreasing IL-12 release, suggesting the promotion of an anti-inflammatory environment in this model.

A)
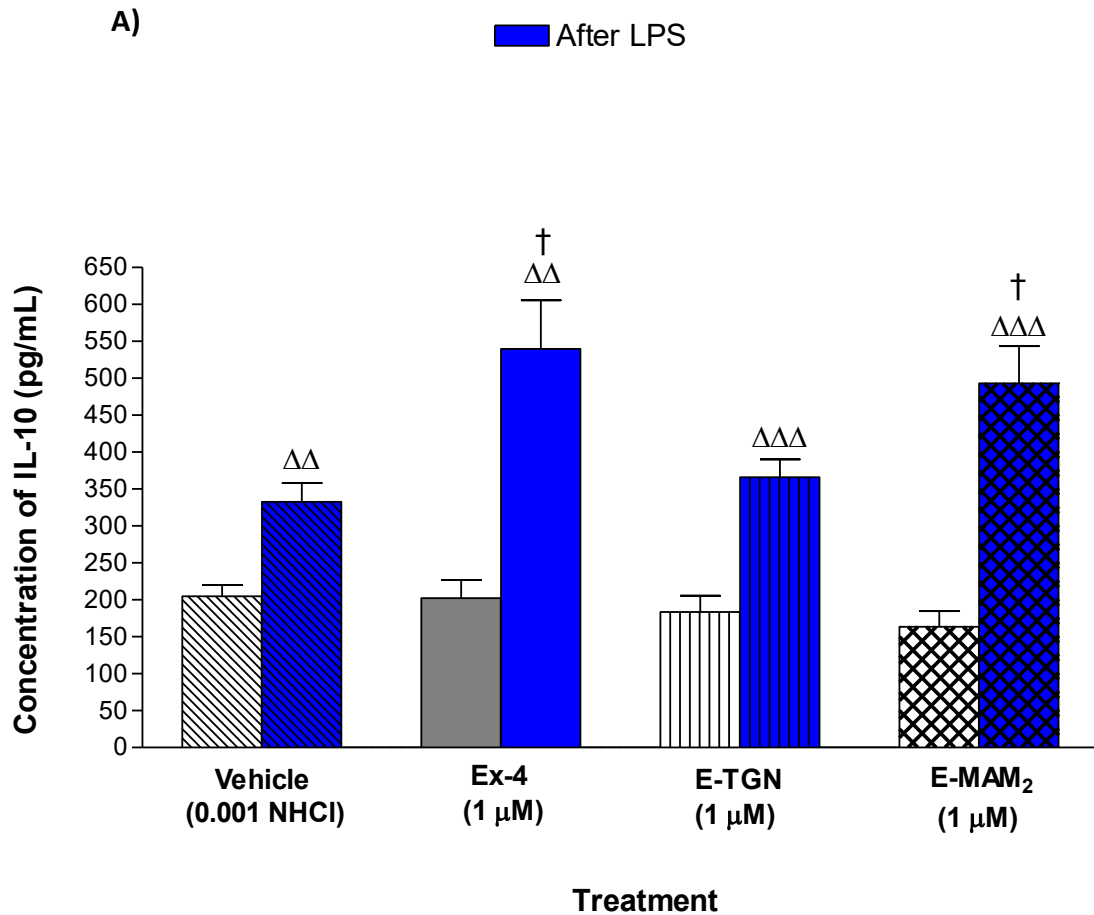
Figure 7.7. (A) Exendin-4 and E-MAM2 treatment of BM-DCs increased the release of IL-10 in the presence of LPS.
Bone marrow-derived dendritic cells (BM-DCs) were pulsed with exendin-4, E-TGN or E-MAM$_2$ for 24 hrs, before being activated by LPS for 18 hrs. IL-10 levels were assessed using an IL-10 specific ELISA. The concentration of IL-10 (pg/ml) are represented in the bar charts with values representing the mean ± SEM of three independent experiments, with each experiment being tested in 3 technical replicates. $^{\Delta\Delta\Delta}P<0.001$, $^{\Delta\Delta}P<0.01$ compared to respective treatment in the absence of LPS; $^{\dagger}P<0.05$ compared to vehicle (0.001 NHCl) in the presence of LPS.
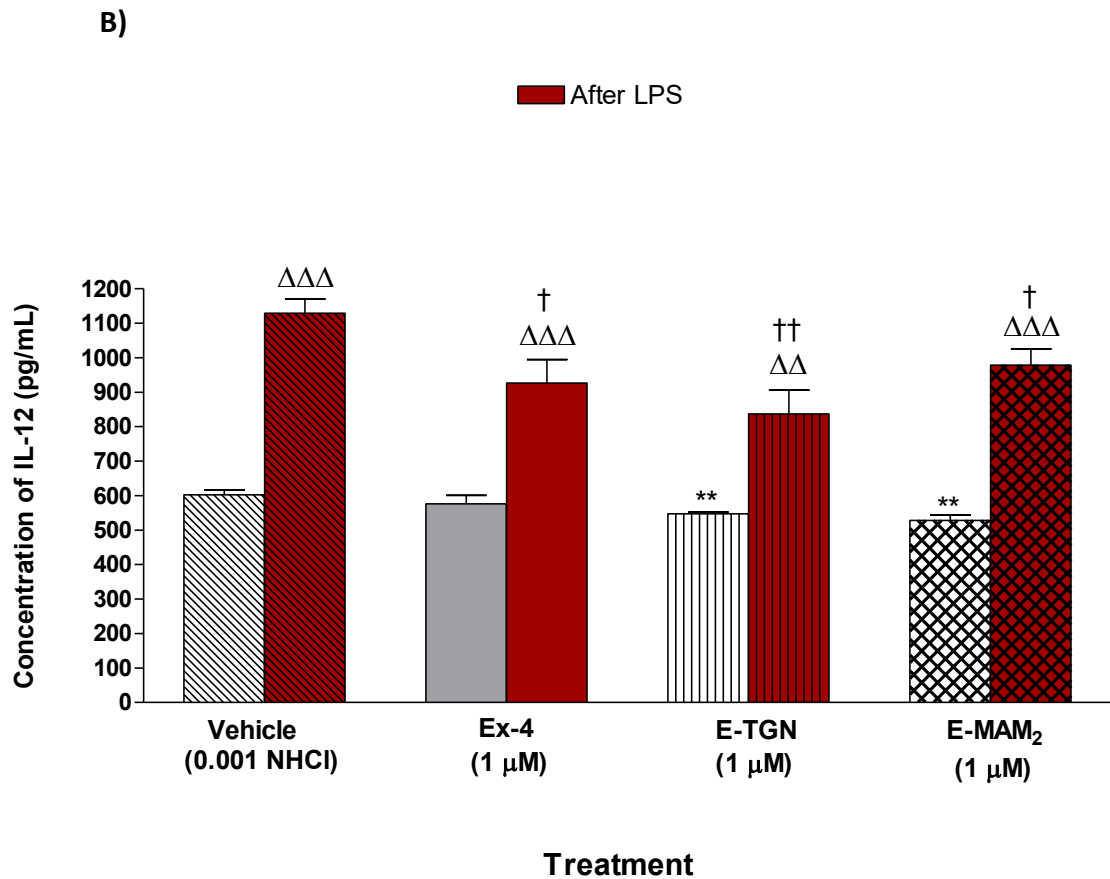
Figure 7.7. (B) Peptide treatment decreases the release of IL-12 following peptide and LPS treatment.

Bone marrow-derived dendritic cells (BM-DCs) were pulsed with exendin-4, E-TGN and E-MAM$_2$, before being activated by LPS for 24 hours. Values are mean ± SEM (n=3). **P<0.01 compared to vehicle only (0.001 NHCl); $^{\Delta\Delta\Delta}$P<0.001, $^{\Delta\Delta}$P<0.01 compared to respective treatment without LPS.

7.5 DISCUSSION

Given the role of inflammation in T2D, as both a cause and a consequence of insulin resistance, we examined whether our hybrid peptides, alongside exendin-4, could modulate this feature by inhibiting the antigen presentation capacity and pro-inflammatory cytokine production of DCs. Firstly, we addressed whether exendin and the hybrid peptides were recognised as a pathogen associated molecular patterns (PAMP) or damage associated molecular patterns (DAMP) by DCs. In BM-DCs pre-treated with exendin-4, E-TGN or E-MAM$_2$, no change in the expression of the cell surface markers examined was observed, suggesting that these peptides, if engaging with receptors expressed on DCs, do not lead to DC maturation. This finding aligns with the low immunogenicity associated with PEGylated compounds (Banerjee et al., 2012), such as our hybrid peptides.

The acidic vehicle (0.001N HCL) slightly upregulated the expression of CD86. Though the increase was not significant, it supports the possibility of changes in pH affecting the activation of DCs, as described by others (Martínez et al., 2007). More specifically, the acidic environment created by inflammation in human DCs could also be responsible for their activation, as it has been reported that a slight decrease in pH to 6.5 could increase the expression of CD80 and CD86 following a short exposure as that of 30-minutes to slightly acidic conditions (Martínez et al., 2007). Similarly, given our vehicle was slightly acidified water (0.001N HCl), this extracellular environment could have favoured a slight increase in the CD86 surface marker, which was then maintained in range by the presence of the peptides. Notably, vehicle treated DCs produced more IL-12 following LPS activation, suggesting that acid environments trigger partial DC maturation also in our experimental setting.

LPS plays a role in the development of T2D, as it has been shown to cause insulin resistance by migrating from bacteria in the gut, following high-fat diets, into systemic circulation leading to inflammation (Cani et al., 2007). LPS is a PAMP associated with the activation of DCs by interaction with Toll-like receptors (TLR 4) found on the cell surface. Other studies have identified the *in vitro* ability of this toxin to upregulate the expression of surface cell markers such as CD80, CD86 and MHC II in DCs (Alexis et al., 2005; Smyth et al., 2013), which is consistent with what we observed here. LPS also activates the release of the pro-inflammatory IL-12 cytokine from DCs (Corinti et al., 2001). Consistently, BM-DCs matured in the

presence of LPS in our study produced IL-12. Interestingly, pre-treatment of BM-DCs with exendin-4, E-TGN and E-MAM$_2$ significantly reduced IL-12 levels suggesting that these peptides might modulate TLR-4 activation and reduce the inflammatory response directed by DCs towards an anti-inflammatory setting.

This hypothesis was further supported by the increased release of IL-10 following exposure to exendin and the hybrid peptides. This cytokine, responsible for limiting the ability of DCs to trigger Th1 response (Corinti et al., 2001), was significantly increased in the presence of exendin-4 and E-MAM$_2$. Previous reports detail the action of TGN in stimulating release of IL-10 from peritoneal macrophages (Pantic et al., 2014). Although we did not assess TGN alone in our assays, we did not observe an increase in IL-10 in its related hybrid E-TGN. This could indicate that by creation of the hybrid, the activity observed by the aforementioned study was not conserved or is not applicable to the cellular model of our choice. To corroborate this hypothesis, studies in BM-DCs and macrophages with both TGN and the E-TGN hybrid could provide further insight on how the actions of the peptides compare in these two cellular models.

This study highlights the modulatory action of exendin-4 and E-MAM$_2$ on BM-DCs, recalling the importance of the balance between inflammatory and anti-inflammatory signals for homeostasis (Khondkaryan et al., 2018). An imbalance in these two components is known to play a role in the development of metabolic impairments, in particular with an increased number of CD11c$^+$ cells producing pro-inflammatory cytokines in the adipose tissue linked to obesity-induced insulin resistance (Chen et al., 2014). A proposed mechanism of the adipose-tissue mediated insulin resistance was published by Zhong et al. (2013) who reported an increased expression of the DPP-4 enzyme, responsible for GLP-1 degradation, in human adipose tissue DCs. Moreover, in T2D patients circulating levels of the growth-factor for development of DCs from myeloid progenitors, GM-CSF, have been reported to increase as a consequence of hyperglycaemia (Surendar et al., 2012). These findings highlight the need to consider tipping the balance of the systemic environment in T2D towards an anti-inflammatory setting.

As exendin-4 and the hybrid peptides did not alter the expression of both MHC and co-stimulation molecules it is feasible that antigen presentation by DCs has not been impaired. Given the increase in IL-10, T-cell polarisation may be affected following activation by these DCs as compared to untreated DCs (Mbongue et al.,

2017). As a subset of DCs in the adipose tissue has been characterised, as outlined in section 7.1.1, comparing the expression of surface markers in DCs originating from lean mice to those of their obese littermates following peptide treatment could be a tool for assessing changes in the resident population of DCs in this tissue. These changes could reflect different polarisation of T-cell responses, specifically Th1 and Th17 responses which have been previously characterised in the context of T2D and insulin resistance (Bertola et al., 2012).

Further analysis, involving co-culture of antigen pulsed peptide treated BM-DCs in the presence of T-cells could provide an even more comprehensive picture of the cell activation state and whether this translates to a perpetuation of the inflammatory state, or in the release of anti-inflammatory cellular mediators. Once these properties are assessed in BM-DCs, studies on how these results translate to a human subset of DCs could further elucidate the actions of exendin-4 related peptides in this model and replicate the inflammatory events that take places during T2D.

Chapter 8

<u>GENERAL DISCUSSION</u>

As the foundation of our work, hybrid peptides were created by joining incretins, which have been extensively characterised, with selected amphibian skin peptides, previously reported to be anti-diabetic, both *in vitro* and *in vivo*. The approach of using hybrid peptides has been recently explored in the context of T2D and obesity, where the rationale was to create an agent efficiently stimulating insulin secretion while targeting multiple aspects of the disease (Finan et al., 2013). The goal of this approach is to merge the well characterised anti-diabetic effects of incretins, while increasing efficiency by having a single administration as opposed to using different agents simultaneously (Hasib et al., 2017).

Our study showed that the actions of exendin-4 were potentiated within its related hybrids, indicating an additional anti-diabetic effect with the generation of these novel peptides. Non-toxic, insulinotropic actions superior to those of exendin-4 have also been reported for other hybrid peptides yielding anti-diabetic actions *in vivo*. Dual agonists for both GLP-1 and GIP receptors, revealed potent, anti-diabetic outcomes in rodents (Finan et al., 2013). Also the actions of the d-Ala^2-GIP-oxyntomodulin hybrid described by Bhat et al., (2013) conferred improved glycaemic control *in vivo*, compared to its individual counterparts, suggesting the actions we observed could be extended further. Mechanistic investigations revealed glucose-independency in the insulinotropic actions. These actions partially relied on K_{ATP}-independent mechanisms, but ultimately depended on intracellular and extracellular sources of calcium. This mechanism recalls that of GLP-1R agonists, where the activation of adenylyl cyclase for release of Ca^{2+} from intracellular stores relies on the availability of ATP generated from glucose (Meloni et al., 2013). These properties also suggest the peptides could bind to the GLP-1 receptor or work through G-protein coupled receptors as exendin-4. Conserving this mechanism could be central to unravelling potential anti-diabetic actions in other cell types and tissue, given the extra-pancreatic localisation of those receptors (Lee and Jun, 2016).

Relating to the diagnosis of diabetes, underlying metabolic changes within the pancreatic beta-cells, as well as other insulin target tissues, take place before hyperglycaemic and glucotoxic features clearly manifest (Zeng et al., 2009; Wang et al., 2011). Though previous studies had highlighted changes in metabolites following

chronic glucotoxic conditions in BRIN-BD11 cells (Wallace et al., 2013), investigations regarding the metabolomic profile of these cells following treatment with exendin-4 was a novel, unexplored approach to understand the metabolic actions of this incretin in the BRIN-BD11 cell line.

An overall promotion of oxidative metabolism, consistent with the appropriate maintenance of glucose homeostasis (Brennan et al., 2002), favours increased generation of ATP and might underlie the anti-diabetic actions of exendin-4. A study considering the oxidative capacity of exendin-4 (50 nM) in BRIN-BD11 cells reported enhanced glycolytic rates (Wallace et al., 2013), however metabolic flux analysis for the individual metabolites of the TCA cycle had not been previously reported.

Future studies performing metabolomics analysis on the hybrids, as we did for exendin-4 here, could deepen understanding of the underlying mechanisms used by the peptides for their activity and contextualise the findings of the gene expression studies. We found results that suggested different molecular actions by the hybrids compared to exendin-4 alone. For example, the downregulation of the ATP-binding cassette on the potassium channel, as well as lowered expression of the voltage-dependent calcium channel seem in apparent contrast with the importance of these channels in the mechanism of insulin release. These channels are crucial for insulin secretion, and though looking at individual genes can provide suggestions for further investigation, gene expression analysis of given pathways, using more advanced technologies such as microarray offer a more comprehensive overview of transcriptomics in the context of the disease (Taneera et al., 2014) and how therapeutic agents modulate these processes.

As part of the assessment of the peptides' effects on associated complications, we investigated the inflammatory component of T2D (Donath and Shoelson, 2011; Eguchi and Nagai, 2017; Gonzalez et al., 2018) in an *ex vivo* dendritic cell lineage. What we learned about the peptides is that neither exendin-4 or its related hybrids E-TGN or E-MAM$_2$ compromised or affected the phenotype of this model of antigen-presenting cells, which suggests the peptides do not alter the cellular environment that could potentially activate these cells. Moreover, in the presence of an inflammatory stimulus, the peptides promote an anti-inflammatory environment which could prompt research interest in fields beyond diabetes, such as that of tolerogenic aspects of transplantation.

What is known of exendin-4 (50 nM) in the context of the inflammation related to T2D is the downregulation of NFkB, which we also observed for its related hybrids, as well as its protective action on beta-cells from experimentally induced diabetes in the presence of streptozotocin *in vivo* (Lee and Jun, 2016). In the same diabetic model, bone marrow derived dendritic cells showed reduced response to a previously established bacterial activator of these cells (Williams et al., 2011). The aforementioned study reported differences after chronic high fat diet (70 days), and no difference was observed in acute diabetes (9 days of high fat diet). In our study, anti-inflammatory modulation of exendin-4 and its related hybrids was observed after only 24 hr of pre-treatment, which might suggest that the actions of the peptides precede the impairments generated by diabetes. This further expands on the novelty associated with these hybrid peptides and their initial *in vitro* characterisation here presented represents an original contribution to knowledge.

Based on the results from this study, E-TGN and E-MAM$_2$ have improved insulinotropic activity *in vitro*, compared to exendin-4, while promoting an anti-inflammatory environment in the presence of an activating stimulus to a greater extent than that created by the incretin alone.

The potential for exploration of these peptides for further studies exploring different aspects of the disease is broad, but data generated so far and representing an orginial contribution to knowledge includes:

1)   The characterization of insulinotropic actions of novel, exendin-4 related hybrids, resulting in greater activity compared to that of exendin-4 alone.

2)   Insight into the mechanism of action of E-TGN and E-MAM$_2$ using insulin secretion modulators. This allowed determination of the importance of calcium in the actions of the peptides.

3)   The finding that exendin-4 channels glucose towards the formation of alanine, linked to increased insulinotropic actions, while preventing formation of lactic acid and increasing citrate consumptions. These actions are consistent with the anti-diabetic properties of oxidative glucose metabolism, obtained for the first time from metabolomics analysis performed in the clonal cell line BRIN-BD11 in the presence of exendin-4.

4)   E-TGN and E-MAM$_2$ upregulated the expression of the GLP-1 receptor gene and downregulated the inflammatory-linked transcript for NFkB. As this action was more pronounced compared to that of exendin-4 alone, further

investigations in possible modulation of inflammatory responses in the presence of E-TGN and E-MAM$_2$ were carried out.

5)   E-TGN and E-MAM$_2$ did not alter the phenotype of our antigen-presenting cell model, while dampening the release of inflammatory mediators when these cells are activated.

8.1 FUTURE STUDIES

The studies presented here provide the foundation for further investigation into the properties of E-TGN and E-MAM$_2$. With regards to insulin secretion, the logical next step to be taken in order to assess the suitability of these peptides for *in vivo* begins with *in vitro* plasma degradation studies. Through this experiment, possible degradation fragments could be assayed for insulinotropic actions and their stability over time could guide future structure optimization. This approach has already been proven successful for d-Ala^2-GIP (Gault et al., 2008) and xenin-related peptides (Craig et al., 2018). Pharmacokinetics parameters could then be considered for the hybrid peptides E-TGN and E-MAM$_2$, possibly followed by *in vivo* studies in pre-clinical models, glucose and insulin sensitivity would help assess their potential as anti-diabetic agents.

Another important aspect to consider is the binding site for these peptides. In fact, based on their localisation and density, future clinical implications can be considered in light of the multiple actions the peptides could have on organs and tissues. With regards to the target organs for diabetic complications, further *in vitro* studies monitoring the actions of E-TGN and E-MAM$_2$ in the liver, adipose tissue and muscle, including the cardiac muscle, represents an extension of the actions we have only partially uncovered in the cellular models used in this study.

In terms of metabolomics analysis, measuring the rate of glucose consumption could support the hypothesis of an increased generation of ATP as an anti-diabetic action following exendin-4 treatment. To take this study further, a principal component analysis (PCA), by which mathematical sample clustering can be used to discriminate differences across treatments could highlight further details we might have not been captured by comparing labelling percentages only. Further experiments using ^{13}C-NMR to trace glucose could help complete the informative, yet limited overview we obtained on glucose fate in the extracellular space. Once this is established, extending this to the hybrid peptides E-TGN and E-MAM$_2$ to

assess how their modulation of glucose metabolism compares to that of exendin-4 should be considered.

Gene expression studies using advanced technologies such as microarray and performed on isolated islets would provide a more comprehensive picture of the transcriptome, and integration with measurement of protein levels could shed light on the translation of mRNAs into functional proteins under the established conditions.

Expanding on the BM-DCs activation experiments, T-cell activation could be monitored by phenotypic characterisation, and their cytokine release profile could be investigated to assess their polarisation in the presence of the peptides for an eventual role in conferring tolerogenic properties to dendritic cells. This would allow for a broader application of the peptides for immunomodulatory studies that could contribute to successful beta-cell transplantation relevant to type 1 diabetes in particular.

The findings presented in this study, together with the possibility to elaborate on such different aspects of the novel hybrid peptides E-TGN and E-MAM$_2$ provide an original contribution to the field of peptide drug discovery as a tool for targeting complex diseases such as T2D.

9. REFERENCES

Aaboe, K., Knop, F.K., Vilsboll, T., Vølund, A., Simonsen, U., Deacon, C.F., Madsbad, S., Holst, J.J., Krarup, T. (2009) KATP channel closure ameliorates the impaired insulinotropic effect of glucose-dependent insulinotropic polypeptide in patients with type 2 diabetes. *J. Clin. Endocrinol. Metab.* 94, 603–608. https://doi.org/10.1210/jc.2008-1731

Abdel-Wahab, Y.H.A., Patterson, S., Flatt, P.R., Conlon, J.M. (2010) Brevinin-2-related Peptide and its [D4K] analogue stimulate insulin release in vitro and improve glucose tolerance in mice fed a high fat diet. *Horm. Metab. Res.* 42, 652–656. https://doi.org/10.1055/s-0030-1254126

Abdel-Wahab, Y.H.A., Power, G.J., Flatt, P.R., Woodhams, D.C., Rollins-Smith, L.A., Conlon, J.M. (2008) A peptide of the phylloseptin family from the skin of the frog Hylomantis lemur (Phyllomedusinae) with potent in vitro and in vivo insulin-releasing activity. *Peptides* 29, 2136–2143. https://doi.org/10.1016/j.peptides.2008.09.006

Abrantes, A.M., Tavares, L.C., Pires, S., Casalta-lopes, J., Mendes, C., Simões, M., Grazina, M.M., Carvalho, R.A., Botelho, M.F. (2014) Metabolic Effects of Hypoxia in Colorectal Cancer by 13C NMR Isotopomer Analysis. https://doi.org/10.1155/2014/759791.

Adeva-Andany, M., López-Ojén, M., Funcasta-Calderón, R., Ameneiros-Rodríguez, E., Donapetry-García, C., Vila-Altesor, M., Rodríguez-Seijas, J. (2014) Comprehensive review on lactate metabolism in human health. *Mitochondrion* 17, 76–100. https://doi.org/10.1016/j.mito.2014.05.007

Advani, A., Bugyei-Twum, A., Connelly, K.A. (2013) Cardiovascular Effects of Incretins in Diabetes. *Can. J. Diabetes* 37, 309–314. https://doi.org/10.1016/j.jcjd.2013.06.010

Ahrén, B. (2005) Exenatide: A novel treatment of Type 2 diabetes. *Therapy* 2, 207–222. https://doi.org/10.1586/14750708.2.2.207

Alamshah, A., Spreckley, E., Norton, M., Kinsey-Jones, J.S., Amin, A., Ramgulam, A., Cao, Y., Johnson, R., Saleh, K., Akalestou, E., Malik, Z., Gonzalez-Abuin, N., Jomard, A., Amarsi, R., Moolla, A., Sargent, P.R., Gray, G.W., Bloom, S.R., Murphy, K.G. (2017) L-phenylalanine modulates gut hormone release and glucose tolerance, and suppresses food intake through the calcium-sensing receptor in rodents. *Int. J. Obes.* 41, 1693–1701. https://doi.org/10.1038/ijo.2017.164

Alcazar, O., Tiedge, M., Lenzen, S. (2000) Importance of lactate dehydrogenase for the regulation of glycolytic flux and insulin secretion in insulin-producing cells. Biochem. J. 352, 373–380. https://doi.org/10.1042/0264-6021:3520373

Alexis, N.E., Lay, J.C., Almond, M., Bromberg, P.A., Patel, D.D., Peden, D.B., (2005) Acute LPS inhalation in healthy volunteers induces dendritic cell

maturation in vivo. *J. Allergy Clin. Immunol.,* 115, 345–350. https://doi.org/10.1016/j.jaci.2004.11.040

AL-Zuaidy, M.H., Mumtaz, M.W., Hamid, A.A., Ismail, A., Mohamed, S., Razis, A.F.A., (2017) Biochemical characterization and 1H NMR based metabolomics revealed Melicope lunu-ankenda leaf extract a potent anti-diabetic agent in rats. BMC Complement. *Altern. Med*. 17, 1–17. https://doi.org/10.1186/s12906-017-1849-2

Andersson, T., Berggren, P.O., Gylfe, E. (1981) Effects of glucose on the calcium content of intact βcells and cellular organelles. *Ups. J. Med. Sci.* 86, 165–170. https://doi.org/10.3109/03009738109179224

Andrali, S.S., Smapley, M.L., Vanderford, N.L., Özcan, S. (2008) Glucose regulation of insulin gene expression in pancreatic β-cells. *Biochem. J.*, 415, 1–10. https://doi.org/10.1042/BJ20081029

Andreasen, A.S., Kelly, M., Berg, R.M.G., Møller, K., Pedersen, B.K. (2011) Type 2 diabetes is associated with altered NF-κB DNA binding activity, JNK phosphorylation, and AMPK phosphorylation in skeletal muscle after LPS. *PLoS One*, 6. https://doi.org/10.1371/journal.pone.0023999

Andrikopoulos, S., Fam, B.C., Holdsworth, A., Visinoni, S., Ruan, Z., Stathopoulos, M., Thorburn, A.W., Joannides, C.N., Cancilla, M., Balmer, L., Proietto, J., Morahan, G. (2016) Identification of ABCC8 as a contributory gene to impaired early-phase insulin secretion in NZO mice. *J. Endocrinol.*, 228, 61–73. https://doi.org/10.1530/JOE-15-0290

Asalla, S., Girada, S.B., Kuna, R.S., Chowdhury, D., Kandagatla, B., Oruganti, S., Bhadra, U., Bhadra, M.P., Kalivendi, S.V., Rao, S.P., Row, A., Ibrahim, A., Ghosh, P.P., Mitra, P. (2016) Restoring mitochondrial function: A small molecule-mediated approach to enhance glucose stimulated insulin secretion in cholesterol accumulated pancreatic beta cells. *Sci. Rep.* 6, 1–17. https://doi.org/10.1038/srep27513

Ashcroft, F.M. (2005). ATP-sensitive potassium channelopathies : focus on insulin secretion. *J Clin Invest.,* 115, 2047–2058. https://doi.org/10.1172/JCI25495.in

Attoub, S., Mechkarska, M., Sonnevend, A., Radosavljevic, G., Jovanovic, I., Lukic, M.L., Conlon, J.M., (2013) Esculentin-2CHa: A host-defense peptide with differential cytotoxicity against bacteria, erythrocytes and tumor cells. *Peptides* 39, 95–102. https://doi.org/10.1016/j.peptides.2012.11.004

Babenko, A.Y., Savitskaya, D.A., Kononova, Y.A., Trofimova, A.Y., Simanenkova, A. V., Vasilyeva, E.Y., Shlyakhto, E. V. (2019) Predictors of effectiveness of glucagon-like peptide-1 receptor agonist therapy in patients with type 2 diabetes and obesity. *J. Diabetes Res.* 2019. https://doi.org/10.1155/2019/1365162

Bain, J.R., Stevens, R.D., Wenner, B.R., Ilkayeva, O., Muoio, D.M., Newgard, C.B. (2009) *Moving From Information to Knowledge* 58. https://doi.org/10.2337/db09-0580

Banchereau, J., Steinman, R.M. (1998) Dendritic cells and the control of immunity. *Nature* 392, 245–252. https://doi:10.1038/32588

Banerjee, S.S., Aher, N., Patil, R., Khandare, J. (2012) Poly(ethylene glycol)-Prodrug Conjugates: Concept, Design, and Applications. *J. Drug Deliv.* 2012, 1–17. https://doi.org/10.1155/2012/103973

Behrends, V., Giskeødegård, G.F., Bravo-Santano, N., Letek, M., Keun, H.C. (2019) Acetaminophen cytotoxicity in HepG2 cells is associated with a decoupling of glycolysis from the TCA cycle, loss of NADPH production, and suppression of anabolism. *Arch. Toxicol.* 93, 341–353. https://doi.org/10.1007/s00204-018-2371-0

Behrends, V., Tredwell, G.D., Bundy, J.G. (2011) A software complement to AMDIS for processing GC-MS metabolomic data. *Anal. Biochem.* 415, 206–208. https://doi.org/10.1016/j.ab.2011.04.009

Bertola, A., Ciucci, T., Rousseau, D., Bourlier, V., Duffaut, C., Bonnafous, S., Blin-wakkach, C., Anty, R., Iannelli, A., Gugenheim, J., Tran, A., Bouloumié, A., Gual, P., Wakkach, A (2012) Identification of Adipose Tissue Dendritic Cells Correlated With Obesity-Associated Insulin-Resistance and Inducing Th17 Responses in Mice and Patients. *Diabetes.,* 61, 2238-47. https://doi.org/10.2337/db11-1274

Best, C.H., Scott D.A. (1923) The Preparation of Insulin. *J. Biol. Chem.* 57, 709-723.

Bhat, V.K., Kerr, B.D., Flatt, P.R., Gault, V.A. (2013) A novel GIP-oxyntomodulin hybrid peptide acting through GIP , glucagon and GLP-1 receptors exhibits weight reducing and anti-diabetic properties. *Biochem. Pharmacol.*, 85, 1655–1662. https://doi.org/10.1016/j.bcp.2013.03.009

Bloom, S.R., Edwards, A. V. (1975) The release of pancreatic glucagon and inhibition of insulin in response to stimulation of the sympathetic innervation. *J. Physiol.* 253, 157–173. https://doi.org/10.1113/jphysiol.1975.sp011185

Boland, B.B., Rhodes, C.J., Grimsby, J.S. (2017) The dynamic plasticity of insulin production in β-cells. *Mol. Metab*. 6, 958–973. https://doi.org/10.1016/j.molmet.2017.04.010

Boussageon R., Supper I., Bejan-Angoulvant T., Kellou N., Cucherat M., Boissel J., Kassai B., Moreau A., Gueyffier F., Cornu C. (2012) Reappraisal of Metformin Efficacy in the Treatment of Type 2 Diabetes: A Meta-Analysis of Randomised Controlled Trials. *PLoS Med.,*9:e1001204. https://doi.org/10.1371/journal.pmed.1001204

Brennan, Lorraine, Shine, A., Hewage, C., Malthouse, J.P.G., Brindle, K.M., Mcclenaghan, N., Flatt, P.R., Newsholme, P. (2002) A Nuclear Magnetic Resonance – Based Demonstration of Substantial Oxidative L -Alanine Metabolism and L -Alanine – Enhanced Glucose Metabolism in a Clonal Pancreatic beta-cell line. Diabetes 51, 1714–1721.

Brownlee, M. (2001) Biology of Diabetic Complications. *Nature* 414, 813–820.

Buescher J.M., Antoniewicz M.R., Boros L.G., Burgess S.C., Brunengraber H., Clish C.B., DeBerardinis R.J., Feron O., Frezza C., Ghesquiere B., Gottlieb E., Hiller K., Jones R.G., Kamphorst J.J., Kibbey R.G., Kimmelman A.C., Locasale J.W., Lunt S.Y., Maddocks O.D., Malloy C., Metallo C.M., Meuillet E.J., Munger J., Nöh K., Rabinowitz J.D., Ralser M., Sauer U., Stephanopoulos G., St-Pierre J., Tennant D.A., Wittmann C., Vander Heiden M.G., Vazquez A., Vousden K., Young J.D., Zamboni N., Fendt S.M. (2015) A roadmap for interpreting (13)C metabolite labeling patterns from cells. *Curr Opin Biotechnol.*,34, 189-201. https://doi:10.1016/j.copbio.2015.02.003.

Buteau, J., Roduit, R., Susini, S., Prentki, M. (1999) Glucagon-like peptide-1 promotes DNA synthesis, activates phosphatidylinositol 3-kinase and increases transcription factor pancreatic and duodenal homeobox gene 1 (PDX-1) DNA binding activity in beta (INS-1)- cells. *Diabetologia* 42, 856–864. https://doi.org/10.1007/s001250051238

Calderon, B., Carrero, J. A., Unanue, E. R. (2014). The central role of antigen presentation in islets of Langerhans in autoimmune diabetes. *Curr Opin Immunol*, *26*, 32–40. doi:10.1016/j.coi.2013.10.011

Calderon, B., Suri, A., Miller, M.J., Unanue, E.R. (2008) Dendritic cells in islets of Langerhans constitutively present β cell-derived peptides bound to their class II MHC molecules. *Proc. Natl. Acad. Sci. U. S. A.* 105, 6121–6126. https://doi.org/10.1073/pnas.0801973105

Cani P.D., Amar J., Iglesias M.A., Poggi M., Knauf C., Bastelica D., Neyrinck A.M., Fava F., Tuohy K.M., Chabo C., Waget A., Delmée E., Cousin B., Sulpice T., Chamontin B., Ferrières J., Tanti J.F., Gibson G.R., Casteilla L., Delzenne N.M., Alessi M.C., Burcelin R. (2007) Metabolic endotoxemia initiates obesity and insulin resistance. *Diabetes,* 56, 1761-72. https://doi.org/10.2337/db06-1491

Carlessi, R., Chen, Y., Rowlands, J., Cruzat, V.F., Keane, K.N., Egan, L., Mamotte, C., Stokes, R., Gunton, J.E., Bittencourt, P.I.H. De, Newsholme, P. (2017) GLP-1 receptor signalling promotes β-cell glucose metabolism via mTOR-dependent HIF-1α activation. *Sci. Rep.* 7, 1–13. https://doi.org/10.1038/s41598-017-02838-2

Carlessi, R., Lemos, N.E., Dias, A.L., Oliveira, F.S., Brondani, L.A., Canani, L.H., Bauer, A.C., Leitão, C.B., Crispim, D. (2015) Exendin-4 protects rat islets against loss of viability and function induced by brain death. *Mol. Cell. Endocrinol.* 412, 239–250. https://doi.org/10.1016/j.mce.2015.05.009

Carvalho, D.S., de Almeida, A.A., Borges, A.F., Campos, V. (2018) Treatments for diabetes mellitus type II: New perspectives regarding the possible role of calcium and cAMP interaction. *Eur. J. Pharmacol.* 830, 9–16. https://doi.org/10.1016/j.ejphar.2018.04.002

Cen, J., Sargsyan, E., Bergsten, P. (2016) Fatty acids stimulate insulin secretion from human pancreatic islets at fasting glucose concentrations via mitochondria-dependent and -independent mechanisms. *Nutr. Metab.* 13, 1–9. https://doi.org/10.1186/s12986-016-0119-5

Chakrabarti, S.K., James, J.C., Mirmira, R.G. (2002) Quantitative assessment of gene targeting in vitro and in vivo by the pancreatic transcription factor, Pdx1. Importance of chromatin structure in directing promoter binding. *J. Biol. Chem.* 277, 13286–13293. https://doi.org/10.1074/jbc.M111857200

Chang Xia C., Rao X, and Jixin Zhong J. (2017) Role of T Lymphocytes in Type 2 Diabetes and Diabetes-Associated Inflammation. *J Diabetes Res*, 2017:6. https://doi.org/10.1155/2017/6494795

Chang-Chen, K.J., Mullur, R., Bernal-Mizrachi, E. (2008) B-Cell Failure As a Complication of Diabetes. *Rev. Endocr. Metab. Disord.* 9, 329–343. https://doi.org/10.1007/s11154-008-9101-5

Chatterjee, S., Khunti, K., Davies, M.J. (2017) Type 2 diabetes. *Lancet* 389, 2239–2251. https://doi.org/10.1016/S0140-6736(17)30058-2

Chen, Y., Tian, J., Tian, X., Tang, X., Rui, K., Tong, J., Lu, L., Xu, H., Wang, S., (2014) Adipose tissue dendritic cells enhances inflammation by prompting the generation of Th17 cells. *PLoS One* 9, 1–8. https://doi.org/10.1371/journal.pone.0092450

Cheng, X., Ji, Z., Tsalkova, T., Mei, F. (2008) Epac and PKA: A tale of two intracellular cAMP receptors. *Acta Biochim. Biophys. Sin. (Shanghai).* 40, 651–662. https://doi.org/10.1111/j.1745-7270.2008.00438.

Chepurny O.G., Holz G.G. (2002) Over-expression of the glucagon-like peptide-1 receptor on INS-1 cells confers autocrine stimulation of insulin gene promoter activity: a strategy for production of pancreatic beta-cell lines for use in transplantation. *Cell Tissue Res.*, 307(2),191-201. https://doi: 10.1007/s00441-001-0494-7.

Collin, M., Bigley, V. (2018) Human dendritic cell subsets: an update. *Immunology* 154, 3–20. https://doi.org/10.1111/imm.12888

Conlon, J.M., Al-Ghaferi, N., Ahmed, E., Meetani, M.A., Leprince, J., Nielsen, P.F. (2010) Orthologs of magainin, PGLa, procaerulein-derived, and proxenopsin-derived peptides from skin secretions of the octoploid frog Xenopus amieti (Pipidae). *Peptides* 31, 989–994. https://doi.org/10.1016/j.peptides.2010.03.002

Conlon, J.M., Mechkarska, M., Abdel-Wahab, Y.H., Flatt, P.R. (2018) Peptides from frog skin with potential for development into agents for Type 2 diabetes therapy. *Peptides* 100, 275–281. https://doi.org/10.1016/j.peptides.2017.09.001

Conlon, J.M., Musale, V., Attoub, S., Mangoni, L. (2017) Cytotoxic peptides with insulin-releasing activities from skin secretions of the Italian stream frog Rana italica (Ranidae). *J Pept Sci*, 23(10):769-776. https://doi.org/10.1002/psc.3025

Corinti, S., Albanesi, C., la Sala, A., Pastore, S., Girolomoni, G. (2001) Regulatory Activity of Autocrine IL-10 on Dendritic Cell Functions. *J. Immunol.*, 166, 4312–4318. https://doi.org/10.4049/jimmunol.166.7.

Corkey B.E., Deeney J.T., Yaney G.C., Tornheim K., Prentki M. (2000) The role of long-chain fatty acyl-CoA esters in β-cell signal transduction. *J Nutr,* 130:299S–304S.

Craig, S.L., Gault, V.A., Irwin, N. (2018) Emerging therapeutic potential for xenin and related peptides in obesity and diabetes. *Diabetes. Metab. Res. Rev.* 34, 1–5. https://doi.org/10.1002/dmrr.3006

Cunningham G.A., McClenaghan N.H., Flatt P.R., Newsholme P. (2005) L-Alanine induces changes in metabolic and signal transduction gene expression in a clonal rat pancreatic beta-cell line and protects from pro-inflammatory cytokine-induced apoptosis. *Clin Sci (Lond)*, 109(5):447-55. https://doi.org/10.1042/CS20050149

Das, U.N., Rao, A.A. (2007) Gene expression profile in obesity and type 2 diabetes mellitus. *Lipids Health Dis.* 6, 1–19. https://doi.org/10.1186/1476-511X-6-35

De Heer, J., Holst, J.J. (2007) Sulfonylurea compounds uncouple the glucose dependence of the insulinotropic effect of glucagon-like peptide 1. *Diabetes* 56, 438–443. https://doi.org/10.2337/db06-0738

Del Coco, L., Vergara, D., De Matteis, S., Mensà, E., Sabbatinelli, J., Prattichizzo, F., Bonfigli, A.R., Storci, G., Bravaccini, S., Pirini, F., Ragusa, A., Casadei-Gardini, A., Bonafè, M., Maffia, M., Fanizzi, F.P., Olivieri, F., Giudetti, A.M. (2019) NMR-Based Metabolomic Approach Tracks Potential Serum Biomarkers of Disease Progression in Patients with Type 2 Diabetes Mellitus. *J. Clin. Med.* 8, 720. https://doi.org/10.3390/jcm8050720

Diakogiannaki, E., Dhayal, S., Childs, C.E., Calder, P.C., Welters, H.J., Morgan, N.G. (2007) Mechanisms involved in the cytotoxic and cytoprotective actions of saturated versus monounsaturated long-chain fatty acids in pancreatic β-cells. *J. Endocrinol.* 194, 283–291. https://doi.org/10.1677/JOE-07-0082

D'Ignazio, L., Rocha, S. (2016). Hypoxia Induced NF-κB. *Cells*, *5*(1), 10. https://doi:10.3390/cells5010010

Dixon, G., Nolan, J., Clenaghan, N.H.M.C., Flatt, P.R. (2004) Arachidonic acid , palmitic acid and glucose are important for the modulation of clonal pancreatic β -cell insulin secretion , growth and functional integrity. https://doi.org/10.1042/CS20030261

Donath, M.Y., Meier, D.T., Böni-Schnetzler, M. (2019) Inflammation in the Pathophysiology and Therapy of Cardiometabolic Disease. *Endocr. Rev.* 40, 1080–1091. https://doi.org/10.1210/er.2019-00002

Donath, M.Y., Shoelson, S.E. (2011) Type 2 diabetes as an inflammatory disease. *Nat. Rev. Immunol.* 11, 98–107. https://doi.org/10.1038/nri2925

Doyle, I.R.E.E., Wang, X., Zhou, J.I.E., Egan, J.M. (2001) Glucagon-Like Peptide-1 Causes Pancreatic Duodenal Homeobox-1 Protein Translocation from the Cytoplasm to the Nucleus of Pancreatic β-Cells by a Cyclic Adenosine Monophosphate / Protein Kinase A-Dependent Mechanism 142, 1820–1827.

Drucker D.J. (2006) The biology of incretin hormones. *Cell Metab.*, 3(3):153-65.

Drucker D.J. (2018) Mechanisms of Action and Therapeutic Application of Glucagon-like Peptide-1. *Cell Metab.*, 27(4):740-756. https://doi: 10.1016/j.cmet.2018.03.001.

Drucker, D.J., Philippe, J., Mojsov, S., Chick, W.L., Habener, J.F. (1987) Glucagon-like peptide I stimulates insulin gene expression and increases cyclic AMP levels in a rat islet cell line. *Proc. Natl. Acad. Sci. U. S. A.* 84, 3434–3438. https://doi.org/10.1073/pnas.84.10.3434

Dzhura, I., Chepurny, O.G., Kelley, G.G., Leech, C.A., Roe, M.W., Dzhura, E., Afshari, P., Malik, S., Rindler, M.J., Xu, X., Lu, Y., Smrcka, A. V., Holz, G.G. (2010) Epac2-dependent mobilization of intracellular Ca2+ by glucagon-like peptide-1 receptor agonist exendin-4 is disrupted in β-cells of phospholipase C-ε knockout mice. *J. Physiol.* 588, 4871–4889. https://doi.org/10.1113/jphysiol.2010.198424

Eguchi, K., Nagai, R. (2017) Islet inflammation in type 2 diabetes and physiology Find the latest version : Islet inflammation in type 2 diabetes and physiology. *J. Clin. Invest.* 127, 14–23. https://doi.org/10.1172/JCI88877.

Ehses, J.A., Perren, A., Eppler, E., Ribaux, P., Pospisilik, J.A., Maor-Cahn, R., Gueripel, X., Ellingsgaard, H., Schneider, M.K.J., Biollaz, G., Fontana, A., Reinecke, M., Homo-Delarche, F., Donath, M.Y. (2007) Increased number of islet-associated macrophages in type 2 diabetes. *Diabetes* 56, 2356–2370. https://doi.org/10.2337/db06-1650

Eldor, R., Yeffet, A., Baum, K., Doviner, V., Amar, D., Ben-Neriah, Y., Christofori, G., Peled, A., Carel, J.C., Boitard, C., Klein, T., Serup, P., Eizirik, D.L., Melloul, D. (2006) Conditional and specific NF-κB blockade protects pancreatic beta cells from diabetogenic agents. *Proc. Natl. Acad. Sci. U. S. A.* 103, 5072–5077. https://doi.org/10.1073/pnas.0508166103

Eng, J., Kleinman, W.A., Singh, L., Singh, G., Raufman, J.P. (1992) Isolation and characterization of exendin-4, an exendin-3 analogue, from Heloderma suspectum venom. Further evidence for an exendin receptor on dispersed acini from guinea pig pancreas. *J. Biol. Chem.* 267, 7402–7405.

Erspamer, V., Melchiorri, P. (1980) Active polypeptides: from amphibian skin to gastrointestinal tract and brain of mammals. *Trends Pharmacol. Sci.* 1, 391–395. https://doi.org/10.1016/0165-6147(80)90060-7

Feurle, G.E., Hamscher, G., Kusiek, R., Meyer, H.E., Metzger, J.W. (1992) Identification of xenin, a xenopsin-related peptide, in the human gastric mucosa and its effect on exocrine pancreatic secretion. *J. Biol. Chem.* 267, 22305–22309.

Finan, B., Ma, T., Ottaway, N., Müller, T.D., Habegger, K.M., Heppner, K.M., Kirchner, H., Holland, J., Hembree, J., Raver, C., Lockie, S.H., Smiley, D.L., Gelfanov, V., Yang, B., Hofmann, S., Bruemmer, D., Drucker, D.J., Pfluger, P.T., Perez-Tilve, D., Gidda, J., Vignati, L., Zhang, L., Hauptman, J.B., Lau, M., Brecheisen, M., Uhles, S., Riboulet, W., Hainaut, E., Sebokova, E., Conde-

Knape, K., Konkar, A., DiMarchi, R.D., Tschöp, M.H. (2013) Unimolecular dual incretins maximize metabolic benefits in rodents, monkeys, and humans. *Sci. Transl. Med.*, 5. https://doi.org/10.1126/scitranslmed.3007218

Flanagan, S.E., Clauin, S., Bellanné-Chantelot, C., De Lonlay, P., Harries, L.W., Gloyn, A.L., Ellard, S. (2009) Update of mutations in the genes encoding the pancreatic beta-cell KATP channel subunits Kir6.2 (KCNJ11) and sulfonylurea receptor 1 (ABCC8) in diabetes mellitus and hyperinsulinism. *Hum. Mutat.* 30, 170–180. https://doi.org/10.1002/humu.20838

Fourmy, D. (2017) Hybrid peptides in the landscape of drug discovery. *Peptides* 90, A1–A2. https://doi.org/10.1016/j.peptides.2017.01.010

Fu, Z., Gilbert, E. R., & Liu, D. (2013) Regulation of insulin synthesis and secretion and pancreatic Beta-cell dysfunction in diabetes. *Curr Diabetes Rev*, *9*(1), 25–53.

Furman, B.L. (2012) The development of Byetta (exenatide) from the venom of the Gila monster as an anti-diabetic agent. *Toxicon* 59, 464–471. https://doi.org/10.1016/j.toxicon.2010.12.016

Fusco, J., Xiao, X., Prasadan, K., Sheng, Q., Chen, C., Ming, Y.C., Gittes, G. (2017) GLP-1/Exendin-4 induces β-cell proliferation via the epidermal growth factor receptor. *Sci. Rep.* 7, 1–6. https://doi.org/10.1038/s41598-017-09898-4

Gault, V.A., Kerr, B.D., Irwin, N., Flatt, P.R. (2008) C-terminal mini-PEGylation of glucose-dependent insulinotropic polypeptide exhibits metabolic stability and improved glucose homeostasis in dietary-induced diabetes. *Biochem. Pharmacol.* 75, 2325–2333. https://doi.org/10.1016/j.bcp.2008.03.011

Gault, V.A., Martin, C.M.A., Flatt, P.R., Parthsarathy, V., Irwin, N. (2015) Xenin-25[Lys13PAL]: a novel long-acting acylated analogue of xenin-25 with promising antidiabetic potential. *Acta Diabetol.* 52, 461–471. https://doi.org/10.1007/s00592-014-0681-0

Gault, V.A., Porter, D.W., Irwin, N., Flatt, P.R. (2011) Comparison of sub-chronic metabolic effects of stable forms of naturally occurring GIP(1-30) and GIP(1-42) in high-fat fed mice. *J. Endocrinol.* 208, 265–271. https://doi.org/10.1530/JOE-10-0419

Gembal, M., Gilon, P., Henquin, J.C. (1992) Evidence that glucose can control insulin release independently from its action on ATP-sensitive K+ channels in mouse B cells. *J. Clin. Invest.* 89, 1288–1295. https://doi.org/10.1172/JCI115714

Ghasemi, A., Jeddi, S. (2017) Anti-obesity and anti-diabetic effects of nitrate and nitrite. *Nitric Oxide - Biol. Chem.*, 70, 9–24. https://doi.org/10.1016/j.niox.2017.08.003

Ghasemi, A., Zahediasl, S. (2013) Potential therapeutic effects of nitrate/nitrite and type 2 diabetes mellitus. *Int J Endocrinol Metab.*, 11, 63–64.

Gilon, P., Henquin, J.C. (1992) Influence of membrane potential changes on cytoplasmic Ca2+ concentration in an electrically excitable cell, the insulin-secreting pancreatic B-cell. J. *Biol. Chem.* 267, 20713–20720.

Gloyn, A.L., Pearson, E.R., Antcliff, J.F., Proks, P., Bruining, G.J., Slingerland, A.S., Howard, N., Srinivasan, S., Silva, J.M.C.L., Molnes, J., Edghill, E.L., Frayling, T.M., Temple, I.K., Mackay, D., Shield, J.P.H., Sumnik, Z., van Rhijn, A., Wales, J.K.H., Clark, P., Gorman, S., Aisenberg, J., Ellard, S., Njølstad, P.R., Ashcroft, F.M., Hattersley, A.T. (2004) Activating Mutations in the Gene Encoding the ATP-Sensitive Potassium-Channel Subunit Kir6.2 and Permanent Neonatal Diabetes. *N. Engl. J. Med.* 350, 1838–1849. https://doi.org/10.1056/nejmoa032922

Gonzalez, L.L., Garrie, K., Turner, M.D. (2018) Type 2 diabetes – An autoinflammatory disease driven by metabolic stress. *Biochim. Biophys. Acta - Mol. Basis Dis.*, 1864, 3805–3823. https://doi.org/10.1016/j.bbadis.2018.08.034

Gowda, G. A., Zhang, S., Gu, H., Asiago, V., Shanaiah, N., & Raftery, D. (2008) Metabolomics-based methods for early disease diagnostics. *Exp Rev Mol Diagn*, *8*(5), 617–633. doi:10.1586/14737159.8.5.617

Gray, L.R., Tompkins, S.C., Taylor, E.B. (2014) Regulation of pyruvate metabolism and human disease. *Cell. Mol. Life Sci.* 71, 2577–2604. https://doi.org/10.1007/s00018-013-1539-2

Grumbach, I.M., Chen, W., Mertens, S.A., Harrison, D.G. (2005) A negative feedback mechanism involving nitric oxide and nuclear factor kappa-B modulates endothelial nitric oxide synthase transcription. *J. Mol. Cell. Cardiol.*, 39, 595–603. https://doi.org/10.1016/j.yjmcc.2005.06.012

Guo, X.R., Wang, X.L., Li, M.C., Yuan, Y.H., Chen, Y., Zou, D.D., Bian, L.J., Li, D.S. (2015) PDX-1 mRNA-induced reprogramming of mouse pancreas-derived mesenchymal stem cells into insulin-producing cells in vitro. *Clin. Exp. Med.* 15, 501–509. https://doi.org/10.1007/s10238-014-0319-0

Hadadian, S., Shamassebi, D. N., Mirzahoseini, H., Shokrgozar, M. A., Bouzari, S., Sepahi, M. (2015) Stability and biological activity evaluations of PEGylated human basic fibroblast growth factor. *Adv Biomed Res*, *4*, 176. doi:10.4103/2277-9175.164001

Hagemann, D., Holst, J.J., Gethmann, A., Banasch, M., Schmidt, W.E., Meier, J.J. (2007) Glucagon-like peptide 1 (GLP-1) suppresses ghrelin levels in humans via increased insulin secretion. *Regul. Pept.* 143, 64–68. https://doi.org/10.1016/j.regpep.2007.03.002

Hamid, M., McCluskey, J.T., McClenaghan, N.H., Flatt, P.R. (2002) Comparison of the secretory properties of four insulin-secreting cell lines. *Endocr. Res.* 28, 35–47. https://doi.org/10.1081/ERC-120004536

Han, Y.E., Chun, J.N., Kwon, M.J., Ji, Y.S., Jeong, M.H., Kim, H.H., Park, S.H., Rah, J.C., Kang, J.S., Lee, S.H., Ho, W.K. (2018) Endocytosis of K ATP

Channels Drives Glucose-Stimulated Excitation of Pancreatic β Cells. *Cell Rep.* 22, 471–481. https://doi.org/10.1016/j.celrep.2017.12.049

Hansen, K. B., Vilsbøll, T., & Knop, F. K. (2010) Incretin mimetics: a novel therapeutic option for patients with type 2 diabetes – a review. *Diabetes Metab Syndr Obes.,* 3: 155–163.

Hao, T., Hongtao, Z., Li, S., Tian, H. (2017) Glucagon-like peptide 1 receptor agonist ameliorates the insulin resistance function of islet β cells via the activation of PDX-1/JAK signaling transduction in C57/BL6 mice with high-fat diet-induced diabetes. *Int. J. Mol. Med.* 39, 1029–1036. https://doi.org/10.3892/ijmm.2017.2910

Harris, J.M., Chess, R.B. (2003) Effect of pegylation on pharmaceuticals 2, *Nat Rev Drug Discov.*, 214–221. https://doi.org/10.1038/nrd1033

Hasib, A., Ng, M.T., Gault, V.A., Khan, D., Parthsarathy, V., Flatt, P.R., Irwin, N. (2017) An enzymatically stable GIP/xenin hybrid peptide restores GIP sensitivity, enhances beta cell function and improves glucose homeostasis in high-fat-fed mice. *Diabetologia* 60, 541–552. https://doi.org/10.1007/s00125-016-4186-y

Henninot A., Collins J.C., Nuss J.M. (2018) The Current State of Peptide Drug Discovery: Back to the Future? *J. Med. Chem.,* 61, 4, 1382-1414. https://doi.org/10.1021/acs.jmedchem.7b00318

Hinke S.A., Gelling R.W., Pederson R.A., Manhart S., Nian C., Demuth H.U., McIntosh C.H. (2002) Dipeptidyl peptidase IV-resistant [D-Ala(2)]glucose-dependent insulinotropic polypeptide (GIP) improves glucose tolerance in normal and obese diabetic rats. *Diabetes*, 51(3):652-61. https://doi.org/10.2337/diabetes.51.3.652

Hisatomi M., Hidaka H., Niki I. (1996) Ca2+/calmodulin and cyclic 3,5' adenosine monophosphate control movement of secretory granules through protein phosphorylation/dephosphorylation in the pancreatic beta-cell. *Endocrinology*, 137 (11), 4644–4649. https://doi.org/10.1210/endo.137.11.8895328

Hodgkin, M.N., Hills, C.E., Squires, P.E. (2008) The calcium-sensing receptor and insulin secretion: a role outside systemic control 15 years on. *J. Endocrinol.* 199, 1–4. https://doi.org/10.1677/joe-08-0261

Hodson D.J., Tarasov A.I., Gimeno Brias S., Mitchell R.K., Johnston N.R., Haghollahi S., Cane M.C., Bugliani M., Marchetti P., Bosco D., Johnson P.R., Hughes S.J., Rutter G.A. (2014) Incretin-modulated beta cell energetics in intact islets of Langerhans. *Mol Endocrinol.*, 28(6):860-71. https://doi:10.1210/me.2014-1038.

Hohnholt, M.C., Blumrich, E.M., Waagepetersen, H.S., Dringen, R. (2017) The antidiabetic drug metformin decreases mitochondrial respiration and tricarboxylic acid cycle activity in cultured primary rat astrocytes. *J. Neurosci. Res.* 95, 2307–2320. https://doi.org/10.1002/jnr.24050

Hornigold, D.C., Roth, E., Howard, V., Will, S., Oldham, S., Coghlan, M.P., Blouet, C., Trevaskis, J.L. (2018) A GLP-1:CCK fusion peptide harnesses the synergistic effects on metabolism of CCK-1 and GLP-1 receptor agonism in mice. *Appetite* 127, 334–340. https://doi.org/10.1016/j.appet.2018.05.131

Hotamisligil, G.S., Shargill, N.S., Spiegelman, B.M. (1993) Adipose expression of tumor necrosis factor-α: Direct role in obesity-linked insulin resistance. *Science* (80-.). 259, 87–91. https://doi.org/10.1126/science.7678183

Hu, F.B. (2011) Globalization of diabetes: The role of diet, lifestyle, and genes. *Diabetes Care* 34, 1249–1257. https://doi.org/10.2337/dc11-0442

Huang, M., Joseph, J.W. (2012) Metabolomic analysis of pancreatic β-cell insulin release in response to glucose *Islets,* 4(3):210-22. https://doi: 10.4161/isl.20141.

Huang, X.T., Li, C., Peng, X.P., Guo, J., Yue, S.J., Liu, W., Zhao, F.Y., Han, J.Z., Huang, Y.H., Yang-Li, Cheng, Q.M., Zhou, Z.G., Chen, C., Feng, D.D., Luo, Z.Q. (2017) An excessive increase in glutamate contributes to glucose-toxicity in β-cells via activation of pancreatic NMDA receptors in rodent diabetes. *Sci. Rep.* 7, 1–14. https://doi.org/10.1038/srep44120

Hui, S., Ghergurovich, J.M., Morscher, R.J., Jang, C., Teng, X., Lu, W., Esparza, L.A., Reya, T., Zhan, L., Yanxiang Guo, J., White, E., Rabinowitz, J.D. (2017) Glucose feeds the TCA cycle via circulating lactate. *Nature* 551, 115–118. https://doi.org/10.1038/nature24057

Ichinose, K., Maeshima, Y., Yamamoto, Y., Kinomura, M., Hirokoshi, K., Kitayama, H., Takazawa, Y., Sugiyama, H., Yamasaki, Y., Agata, N., Makino, H. (2006) 2-(8-Hydroxy-6-methoxy-1-oxo-1H-2-benzopyran-3-yl) propionic acid, an inhibitor of angiogenesis, ameliorates renal alterations in obese type 2 diabetic mice. Diabetes 55, 1232–1242. https://doi.org/10.2337/db05-1367

Inaba, K., Inaba, M., Romani, N., Aya, H., Deguchi, M., Ikehara, S., Muramatsu, S., Steinman, R.M. (1992) Generation of large numbers of dendritic cells from mouse bone marrow cultures supplemented with granulocyte/macrophage colony-stimulating factor. *J. Exp. Med.*, 176, 1693–1702. https://doi.org/10.1084/jem.176.6.1693

Irwin, N., Flatt, P.R. (2009) Evidence for beneficial effects of compromised gastric inhibitory polypeptide action in obesity-related diabetes and possible therapeutic implications. *Diabetologia* 52, 1724–1731. https://doi.org/10.1007/s00125-009-1422-8

Irwin, N., Flatt, P.R. (2013) Enteroendocrine hormone mimetics for the treatment of obesity and diabetes. *Curr. Opin. Pharmacol.* 13, 989–995. https://doi.org/10.1016/j.coph.2013.09.009

Irwin, N., Flatt, P.R. (2015) New perspectives on exploitation of incretin peptides for the treatment of diabetes and related disorders GLP-1. *World J Diabetes*, 6, 1285–1295. https://doi.org/10.4239/wjd.v6.i15.1285

Irwin, N., Frizelle, P., O'Harte, F.P.M., Flatt, P.R. (2013) (pGlu-Gln)-CCK-8[mPEG]: A novel, long-acting, mini-PEGylated cholecystokinin (CCK) agonist that improves metabolic status in dietary-induced diabetes. *Biochim. Biophys. Acta - Gen. Subj.* 1830, 4009–4016. https://doi.org/10.1016/j.bbagen.2013.04.004

Irwin, N., Pathak, V., Flatt, P.R. (2015) A novel CCK-8/GLP-1 hybrid peptide exhibiting prominent insulinotropic, glucose-lowering, and satiety actions with significant therapeutic potential in high-fat-fed mice. *Diabetes* 64, 2996–3009. https://doi.org/10.2337/db15-0220

Itoh, Y., Kawamata, Y., Harada, M., Kobayashi, M., Fujii, R., Fukusumi, S., Ogi, K., Hosoya, M., Tanaka, Y., Uejima, H., Tanaka, H., Maruyama, M., Satoh, R., Okubo, S., Kizawa, H., Komatsu, H., Matsumura, F., Noguchi, Y., Shinohara, T., Hinuma, S., Fujisawa, Y., Fujino, M. (2003) Free fatty acids regulate insulin secretion from pancreatic β cells through GPR40. *Nature* 422, 173–176. https://doi.org/10.1038/nature01478

Iwaya, C., Nomiyama, T., Komatsu, S., Kawanami, T., Tsutsumi, Y., Hamaguchi, Y., Horikawa, T., Yoshinaga, Y., Yamashita, S., Tanaka, T., Terawaki, Y., Tanabe, M., Nabeshima, K., Iwasaki, A., Yanase, T. (2017) Exendin-4, a Glucagonlike Peptide-1 Receptor Agonist, Attenuates Breast Cancer Growth by Inhibiting NF- k B Activation. *Endocrinology,* 158, 4218–4232. https://doi.org/10.1210/en.2017-00461

Iype, T., Francis, J., Garmey, J.C., Schisler, J.C., Nesher, R., Weir, G.C., Becker, T.C., Newgard, C.B., Griffen, S.C., Mirmira, R.G. (2005) Mechanism of insulin gene regulation by the pancreatic transcription factor Pdx-1: Application of pre-mRNA analysis and chromatin immunoprecipitation to assess formation of functional transcriptional complexes. *J. Biol. Chem.* 280, 16798–16807. https://doi.org/10.1074/jbc.M414381200

Janjuha, S., Singh, S.P., Tsakmaki, A., Neda Mousavy Gharavy, S., Murawala, P., Konantz, J., Birke, S., Hodson, D.J., Rutter, G.A., Bewick, G.A., Ninov, N. (2018) Age-related islet inflammation marks the proliferative decline of pancreatic beta-cells in zebrafish. *Elife* 7, 1–24. https://doi.org/10.7554/eLife.32965

Jitrapakdee, S., Vidal-Puig, A., Wallace, J.C. (2006) Anaplerotic roles of pyruvate carboxylase in mammalian tissues. *Cell. Mol. Life Sci.* 63, 843–854. https://doi.org/10.1007/s00018-005-5410-y

Jo, S.H., Chen, J., Xu, G., Grayson, T.B., Thielen, L.A., Shalev, A. (2018) miR-204 controls glucagon-like peptide 1 receptor expression and agonist function. *Diabetes* 67, 256–264. https://doi.org/10.2337/db17-0506

Jones, B., Bloom, S.R., Buenaventura, T., Tomas, A., Rutter, G.A. (2018) Control of insulin secretion by GLP-1. *Peptides* 100, 75–84. https://doi.org/10.1016/j.peptides.2017.12.013

Jones, P.M., Kitsou-Mylona, I., Gray, E., Squires, P.E., Persaud, S.J. (2007) Expression and function of the extracellular calcium-sensing receptor in

pancreatic β-cells. *Arch. Physiol. Biochem.* 113, 98–103. https://doi.org/10.1080/13813450701531185

Jonkers, F.C., Guiot, Y., Rahier, J., Henquin, J.C. (2001) Tolbutamide stimulation of pancreatic β-cells involves both cell recruitment and increase in the individual Ca2+ response. *Br. J. Pharmacol.* 133, 575–585. https://doi.org/10.1038/sj.bjp.0704108

Kahn S.E., Cooper M.E., Del Prato S. (2014) Pathophysiology and treatment of Type 2 Diabetes: Perspectives on the past, present and future. *Lancet.*,383(9922):1068-1083. https://doi.org/10.1201/9781420038798.sec2

Kalwat, M.A., Cobb, M.H. (2017) Mechanisms of the amplifying pathway of insulin secretion in the β cell. *Pharmacol. Ther.* 179, 17–30. https://doi.org/10.1016/j.pharmthera.2017.05.003

Kang, G., Chepurny, O.G., Rindler, M.J., Collis, L., Chepurny, Z., Li, W.H., Harbeck, M., Roe, M.W., Holz, G.G. (2005) A cAMP and Ca2+ coincidence detector in support of Ca2+-induced Ca2+ release in mouse pancreatic β cells. *J. Physiol.*, 566, 173–188. https://doi.org/10.1113/jphysiol.2005.087510

Kanno, T., Rorsman, P., Göpel, S.O. (2002) Glucose-dependent regulation of rhythmic action potential firing in pancreatic β-cells by KATP-channel modulation. *J. Physiol.* 545, 501–507. https://doi.org/10.1113/jphysiol.2002.031344

Kastin, A.J., Akerstrom, V. (2003) Entry of exendin-4 into brain is rapid but may be limited at high doses. *Int. J. Obes.* 27, 313–318. https://doi.org/10.1038/sj.ijo.0802206

Keane, D.C., Takahashi, H.K., Dhayal, S., Morgan, N.G., Curi, R., Newsholme, P. (2011) Arachidonic acid actions on functional integrity and attenuation of the negative effects of palmitic acid in a clonal pancreatic β-cell line. *Clin. Sci.* 120, 195–206. https://doi.org/10.1042/CS20100282

Khondkaryan, L., Margaryan, S., Poghosyan, D., Manukyan, G. (2018) Impaired Inflammatory Response to LPS in Type 2 Diabetes Mellitus. *Int J Inflam.*, 14, 2157434..https://doi.org/10.1155/2018/2157434

Kiely, A., McClenaghan, N.H., Flatt, P.R., Newsholme, P. (2007) Pro-inflammatory cytokines increase glucose, alanine and triacylglycerol utilization but inhibit insulin secretion in a clonal pancreatic β-cell line. *J. Endocrinol.* 195, 113–123. https://doi.org/10.1677/JOE-07-0306

Kim, W., & Egan, J. M. (2008) The Role of Incretins in Glucose Homeostasis and Diabetes Treatment. *Pharmaco Rev,* 60(4), 470–512.

Kiss, A., Juhász, L., Seprényi, G., Kupai, K., Kaszaki, J., Végh, Á. (2010) The role of nitric oxide, superoxide and peroxynitrite in the anti-arrhythmic effects of preconditioning and peroxynitrite infusion in anaesthetized dogs. *Br. J. Pharmacol.* 160, 1263–1272. https://doi.org/10.1111/j.1476-5381.2010.00774.x

Klein, M.S., Shearer, J. (2016) Metabolomics and Type 2 Diabetes: Translating Basic Research into Clinical Application. *J. Diabetes Res.* 2016. https://doi.org/10.1155/2016/3898502

Kolb H., Mandrup-Poulsen T. (2010) The global diabetes epidemic as a consequence of lifestyle-induced low-grade inflammation. *Diabetologia,* 53(1):10-20. https://doi: 10.1007/s00125-009-1573-7.

Kolterman, O.G., Buse, J.B., Fineman, M.S., Gaines, E., Heintz, S., Bicsak, T.A., Taylor, K., Kim, D., Aisporna, M., Wang, Y., Baron, A.D. (2003) Synthetic exendin-4 (exenatide) significantly reduces postprandial and fasting plasma glucose in subjects with type 2 diabetes. *J. Clin. Endocrinol. Metab.* 88, 3082–3089. https://doi.org/10.1210/jc.2002-021545

Konstantopoulos, N., Foletta, V.C., Segal, D.H., Shields, K.A., Sanigorski, A., Windmill, K., Swinton, C., Connor, T., Wanyonyi, S., Dyer, T.D., Fahey, R.P., Watt, R.A., Curran, J.E., Molero, J.C., Krippner, G., Collier, G.R., James, D.E., Blangero, J., Jowett, J.B., Walder, K.R. (2011) A gene expression signature for insulin resistance. *Physiol. Genomics* 43, 110–120. https://doi.org/10.1152/physiolgenomics.00115.2010

Korner, J., Cline, G.W., Slifstein, M., Barba, P., Rayat, G.R., Febres, G., Leibel, R.L., Maffei, A., Harris, P.E. (2019) A role for foregut tyrosine metabolism in glucose tolerance. *Mol. Metab.* 23, 37–50. https://doi.org/10.1016/j.molmet.2019.02.008

Koska J., Saremi A., Bahn G., Yamashita S., Reaven P.D., Veterans Affairs Diabetes Trial Investigators (2013) The effect of intensive glucose lowering on lipoprotein particle profiles and inflammatory markers in the Veterans Affairs Diabetes Trial (VADT). *Diabetes Care*, 36:2408-2414. https://doi.org/10.2337/dc12-2082

Koska, J., Ortega, E., Bunt, J.C., Gasser, A., Impson, J., Hanson, R.L., Forbes, J., De Courten, B., Krakoff, J. (2009) The effect of salsalate on insulin action and glucose tolerance in obese non-diabetic patients: Results of a randomised double-blind placebo-controlled study. *Diabetologia* 52, 385–393. https://doi.org/10.1007/s00125-008-1239-x

Koubaa, M., Mghaieth, S., Thomasset, B., Roscher, A. (2012) Gas chromatography-mass spectrometry analysis of 13C labeling in sugars for metabolic flux analysis. *Anal. Biochem.* 425, 183–188. https://doi.org/10.1016/j.ab.2012.03.020

Kubo, F., Miyatsuka, T., Sasaki, S., Takahara, M., Yamamoto, Y., Shimo, N., Watada, H., Kaneto, H., Gannon, M., Matsuoka, T.A., Shimomura, I. (2016) Sustained expression of GLP-1 receptor differentially modulates β-cell functions in diabetic and nondiabetic mice. *Biochem. Biophys. Res. Commun.* 471, 68–74. https://doi.org/10.1016/j.bbrc.2016.01.177

Lamanna C, Monami M., Marchionni N., Mannucci E. (2011) Effect of metformin on cardiovascular events and mortality: a meta-analysis of randomized clinical

trials. *Diabetes Obes Metab.,* 13:221-228.
http://doi.wiley.com/10.1111/j.1463-1326.2010.01349.x

Lamont, B.J., Drucker, D.J. (2008) Differential Antidiabetic Efficacy of Incretin
Agonists 57. https://doi.org/10.2337/db07-1202.AUC

Larsen, C. M., Faulenbach, M., Vaag, A., Ehses, J. A., Donath, M. Y., & Mandrup-
Poulsen, T. (2009) Sustained effects of interleukin-1 receptor antagonist
treatment in type 2 diabetes. *Diabetes care*, *32*(9), 1663–1668.
doi:10.2337/dc09-0533

Lawrence T. (2009) The nuclear factor NF-kappaB pathway in inflammation. *Cold
Spring Harbor perspectives in biology,* 1(6), a001651.
doi:10.1101/cshperspect.a001651.

Le Lay, J., Stein, R. (2006) Involvement of PDX-1 in activation of human insulin
gene transcription. *J. Endocrinol.,* 188, 287–294.
https://doi.org/10.1677/joe.1.06510

Lee, Y.S., Jun, H.S. (2016) Anti-Inflammatory Effects of GLP-1-Based Therapies
beyond Glucose Control. *Mediators Inflamm.,* 2016, 26–32.
https://doi.org/10.1155/2016/3094642

Leibiger, B., Moede, T., Uhles, S., Berggren, P.O., Leibiger, I.B. (2002) Short-term
regulation of insulin gene transcription. Biochem. Soc. Trans. 30, 312–317.
https://doi.org/10.1042/bst0300312

Lernmark, Å. (1974) The preparation of, and studies on, free cell suspensions from
mouse pancreatic islets. *Diabetologia* 10, 431–438.
https://doi.org/10.1007/BF01221634

Li, Y., Cao, X., Li, L.X., Brubaker, P.L., Edlund, H., Drucker, D.J. (2005) β-Cell
Pdx1 expression is essential for the glucoregulatory, proliferative, and
cytoprotective actions of glucagon-like peptide-1. *Diabetes* 54, 482–491.
https://doi.org/10.2337/diabetes.54.2.482

Lu, H., Yao, K., Huang, D., Sun, A., Zou, Y., Qian, J., Ge, J. (2013) High glucose
induces upregulation of scavenger receptors and promotes maturation of
dendritic cells. *Cardiovasc. Diabetol.*, 12, 1. https://doi.org/10.1186/1475-
2840-12-80

Lynch, H., Sempowski, G.D. (2013) LDH assay. *Methods Mol Biol* 979, 1–12.
https://doi.org/10.1007/978-1-62703-290-2

MacDonald, P.E., Joseph, J.W., Rorsman, P. (2005) Glucose-sensing mechanisms in
pancreatic β-cells. *Philos. Trans. R. Soc. B Biol. Sci.* 360, 2211–2225.
https://doi.org/10.1098/rstb.2005.1762

MacDonald, P.E., Rorsman, P. (2006) Oscillations, intercellular coupling, and
insulin secretion in pancreatic β cells. *PLoS Biol.* 4, 167–171.
https://doi.org/10.1371/journal.pbio.0040049

Maedler, K., Halban, P.A., Donath, M.Y., Maedler, K., Sergeev, P., Ris, F.,
Oberholzer, J., Joller-jemelka, H.I., Spinas, G.A., Kaiser, N., Halban, P.A.,

Donath, M.Y. (2002) Glucose-induced beta cell production of IL-1beta contributes to glucotoxicity in human pancreatic islets. *J Clin Invest*, 110(6), 851–860. https://doi:10.1172/JCI15318

Malone, J.I., Cuthbertson, D.D., Malone, M.A., Schocken, D.D. (2006) Diabetic Rats. *Cardiovasc. Diabetol.* 6, 2–7. https://doi.org/10.1186/1475-2840-5-2

Malozowski, S., Sahlroot, J.T. (2007) Interleukin-1-receptor antagonist in type 2 diabetes mellitus. *N. Engl. J. Med.* 357, 302–303. https://doi.org/10.1056/NEJMc071324

Mangoni, M.L. (2011) Host-defense peptides: From biology to therapeutic strategies. *Cell. Mol. Life Sci.* 68, 2157–2159. https://doi.org/10.1007/s00018-011-0709-3

Marenah, L., Flatt, P.R., Orr, D.F., McClean, S., Shaw, C., Abdel-Wahab, Y.H.A. (2004) Skin secretion of the toad Bombina variegata contains multiple insulin-releasing peptides including bombesin and entirely novel insulinotropic structures. *Biol. Chem.* 385, 315–321. https://doi.org/10.1515/BC.2004.027

Marenah, L., Flatt, P.R., Orr, D.F., Shaw, C., Abdel-Wahab, Y.H.A. (2006) Skin secretions of Rana saharica frogs reveal antimicrobial peptides esculentins-1 and -1B and brevinins-1E and -2EC with novel insulin releasing activity. *J. Endocrinol.* 188, 1–9. https://doi.org/10.1677/joe.1.06293

Marso S.P., Bain S.C., Consoli A., Eliaschewitz F.G., Jódar E., Leiter L.A., Lingvay I., Rosenstock J., Seufert J., Warren M.L., Woo V., Hansen O., Holst A.G., Pettersson J., Vilsbøll T. (2016) Semaglutide and Cardiovascular Outcomes in Patients with Type 2 Diabetes. *New Engl J Med.*, 375:1834-1144. https://doi:10.1056/NEJMoa1607141.

Martin, C.M.A., Gault, V.A., McClean, S., Flatt, P.R., Irwin, N. (2012) Degradation, insulin secretion, glucose-lowering and GIP additive actions of a palmitate-derivatised analogue of xenin-25. *Biochem. Pharmacol.* 84, 312–319. https://doi.org/10.1016/j.bcp.2012.04.015

Martin, C.M.A., Irwin, N., Flatt, P.R., Gault, V.A. (2013) A novel acylated form of (d-Ala2)GIP with improved antidiabetic potential, lacking effect on body fat stores. *Biochim. Biophys. Acta - Gen. Subj.* 1830, 3407–3413. https://doi.org/10.1016/j.bbagen.2013.03.011

Martínez, D., Vermeulen, M., Euw, E. Von, Maggíni, J., Ceballos, A., Trevani, A., Nahmod, K., Salamone, G., Barrio, M., Amigorena, S., Geffner, J., Euw, E. Von, Sabatte, J., Maggı, J., Ceballos, A., Nahmod, K., Salamone, G., Barrio, M., Giordano, M., Amigorena, S., Geffner, J. (2007) Extracellular Acidosis Triggers the Maturation of Human Dendritic Cells and the Production of IL-12. *J Immunol.,* 179, 1950-9. https://doi.org/10.4049/jimmunol.179.3.1950

Matsuzaki, K. (1998) Magainins as paradigm for the mode of action of pore forming polypeptides. *Biochim. Biophys. Acta - Rev. Biomembr.* 1376, 391–400. https://doi.org/10.1016/S0304-4157(98)00014-8

Mbongue, J.C., Nieves, H.A., Torrez, T.W., Langridge, W.H.R. (2017) The role of dendritic cell maturation in the induction of insulin-dependent diabetes mellitus. *Front. Immunol.* 8, 1–9. https://doi.org/10.3389/fimmu.2017.00327

McClenaghan N.H., Barnett C.R., Ah-Sing E., Abdel-Wahab Y.H., O'Harte F.P., Yoon T.W., Swanston-Flatt S.K., Flatt P.R. (1996a) Characterization of a novel glucose-responsive insulin-secreting cell line, BRIN-BD11, produced by electrofusion. *Diabetes.*, 45(8):1132-40.

McClenaghan, N.H. (2007) Physiological regulation of the pancreatic β-cell: Functional insights for understanding and therapy of diabetes. *Exp. Physiol.* 92, 481–496. https://doi.org/10.1113/expphysiol.2006.034835

McClenaghan, N.H., Barnett, C.R., Flatt, P.R. (1998) Na+ cotransport by metabolizable and nonmetabolizable amino acids stimulates a glucose-regulated insulin-secretory response. *Biochem. Biophys. Res. Commun.* 249, 299–303. https://doi.org/10.1006/bbrc.1998.9136

McClenaghan, N.H., Barnett, C.R., O'Harte, F.P.M., Flatt, P.R. (1996b) Mechanisms of amino acid-induced insulin secretion from the glucose-responsive BRIN-BD11 pancreatic B-cell line. *J. Endocrinol.* 151, 349–357. https://doi.org/10.1677/joe.0.1510349

McClenaghan, N.H., Flatt, P.R. (1999) Engineering cultured insulin-secreting pancreatic B-cell lines. *J. Mol. Med.* 77, 235–243. https://doi.org/10.1007/s001090050344

Mechkarska, M., Kolodziejek, J., Musale, V., Coquet, L., Leprince, J., Jouenne, T., Nowotny, N., Conlon, J.M. (2019) Peptidomic analysis of the host-defense peptides in skin secretions of Rana graeca provides insight into phylogenetic relationships among Eurasian Rana species. *Comp. Biochem. Physiol. - Part D Genomics Proteomics* 29, 228–234. https://doi.org/10.1016/j.cbd.2018.12.006

Meier, J.J., Nauck, M.A. (2010) Is the diminished incretin effect in type 2 diabetes just an epi-phenomenon of impaired β-cell function? *Diabetes* 59, 1117–1125. https://doi.org/10.2337/db09-1899

Melloul D., Marshak S., Cerasi E. (2002) Regulation of insulin gene transcription. *Diabetologia,* 45(3):309-26.

Meloni, A.R., Deyoung, M.B., Lowe, C., Parkes, D.G. (2013) GLP-1 receptor activated insulin secretion from pancreatic β-cells: Mechanism and glucose dependence. *Diabetes, Obes. Metab.* 15, 15–27. https://doi.org/10.1111/j.1463-1326.2012.01663.x

Moore, S.W.M., Bhat, V.K., Flatt, P.R., Gault, V.A., McClean, S. (2015) Isolation and characterisation of insulin-releasing compounds from Crotalus adamanteus, Crotalus vegrandis and Bitis nasicornis venom. *Toxicon* 101, 48–54. https://doi.org/10.1016/j.toxicon.2015.05.002

Mora-Ortiz, M., Nuñez Ramos, P., Oregioni, A., Claus, S.P. (2019) NMR metabolomics identifies over 60 biomarkers associated with Type II Diabetes

impairment in db/db mice. *Metabolomics* 15, 1–16.
https://doi.org/10.1007/s11306-019-1548-8

Morey, M., O'Gaora, P., Pandit, A., Hélary, C. (2019) Hyperglycemia acts in
synergy with hypoxia to maintain the pro-inflammatory phenotype of
macrophages. *PLoS One* 14, 1–17.
https://doi.org/10.1371/journal.pone.0220577

Movassat J., Beattie G.M., Lopez A.D., Hayek A. (2002) Exendin 4 up-regulates
expression of PDX 1 and hastens differentiation and maturation of human fetal
pancreatic cells. *J Clin Endocrinol Metab.*, 87(10):4775-81.

Nanjan, M.J., Mohammed, M., Prashantha Kumar, B.R., Chandrasekar, M.J.N.
(2018) Thiazolidinediones as antidiabetic agents: A critical review. *Bioorg.
Chem.* 77, 548–567. https://doi.org/10.1016/j.bioorg.2018.02.009

Nauck, M.A., Heimesaat, M.M., Orskov, C., Holst, J.J., Ebert, R., Creutzfeldt, W.
(1993) Preserved incretin activity of glucagon-like peptide 1 [7-36 amide] but
not of synthetic human gastric inhibitory polypeptide in patients with type- 2
diabetes mellitus. *J. Clin. Invest.* 91, 301–307.
https://doi.org/10.1172/JCI116186

Neels, J.G. (2009) Obese Insulin Resistant Animals 8, 301–309.
https://doi.org/10.1016/j.cmet.2008.08.015.Ablation

Newsholme, P., Krause, M. (2012) Nutritional Regulation of Insulin Secretion:
Implications for Diabetes. *Clin. Biochem. Rev.* 33, 35–47.

Nikolajczyk, B., Jagannathan-Bogdan, M., Shin, H., Gyurko R. (2011) State of the
union between metabolism and the immune system in type 2 diabetes. *Genes
Immun* 12, 239–250. https://doi.org/10.1038/gene.2011.14

Nolan, C.J., Leahy, J.L., Delghingaro-Augusto, V., Moibi, J., Soni, K., Peyot, M.L.,
Fortier, M., Guay, C., Lamontagne, J., Barbeau, A., Przybytkowski, E., Joly,
E., Masiello, P., Wang, S., Mitchell, G.A., Prentki, M. (2006) Beta cell
compensation for insulin resistance in Zucker fatty rats: Increased lipolysis and
fatty acid signalling. *Diabetologia* 49, 2120–2130.
https://doi.org/10.1007/s00125-006-0305-5

Nunemaker C.S. (2016) Considerations for Defining Cytokine Dose, Duration, and
Milieu That Are Appropriate for Modeling Chronic Low-Grade Inflammation
in Type 2 Diabetes. *J Diabetes Res.*, 2016:2846570.

Nyenwe, E. A., Jerkins, T. W., Umpierrez, G. E., & Kitabchi, A. E. (2011)
Management of type 2 diabetes: evolving strategies for the treatment of
patients with type 2 diabetes. *Metabolism*, 60(1): 1–23.

O'Harte, F., Gault, V., Parker, J., Harriott, P., Mooney, M., Bailey, C., Flatt, P.
(2002) Improved stability, insulin-releasing activity and antidiabetic potential
of two novel N-terminal analogues of gastric inhibitory polypeptide: N-acetyl-
GIP and pGlu-GIP. *Diabetologia* 45, 1281–1291.
https://doi.org/10.1007/s00125-002-0894-6

Ojo, O., Srinivasan, D., Owolabi, B., Flatt, P., Abdel-Wahab, Y. (2015a). Magainin-Related Peptides Stimulate Insulin-Release and Improve Glucose Tolerance in High Fat Fed Mice. *Protein Pept. Lett.* 22, 256–263. https://doi.org/10.2174/0929866521666141229105757

Ojo, O.O., Abdel-Wahab, Y.H.A., Flatt, P.R., Mechkarska, M., Conlon, J.M. (2011) Tigerinin-1R: A potent, non-toxic insulin-releasing peptide isolated from the skin of the Asian frog, Hoplobatrachus rugulosus. *Diabetes, Obes. Metab.* 13, 1114–1122. https://doi.org/10.1111/j.1463-1326.2011.01470.x

Ojo, O.O., Conlon, J.M., Flatt, P.R., Abdel-Wahab, Y.H.A. (2013) Frog skin peptides (tigerinin-1R, magainin-AM1, -AM2, CPF-AM1, and PGla-AM1) stimulate secretion of glucagon-like peptide 1 (GLP-1) by GLUTag cells. *Biochem. Biophys. Res. Commun.* 431, 14–18. https://doi.org/10.1016/j.bbrc.2012.12.116

Ojo, O.O., Srinivasan, D.K., Owolabi, B.O., Conlon, J.M., Flatt, P.R., Abdel-Wahab, Y.H.A., (2015b). Magainin-AM2 improves glucose homeostasis and beta cell function in high-fat fed mice. *Biochim. Biophys. Acta - Gen. Subj.* 1850, 80–87. https://doi.org/10.1016/j.bbagen.2014.10.011

Ojo, O.O., Srinivasan, D.K., Owolabi, B.O., Flatt, P.R., Abdel-Wahab, Y.H.A., (2015c) Beneficial effects of tigerinin-1R on glucose homeostasis and beta cell function in mice with diet-induced obesity-diabetes. Biochimie 109, 18–26. https://doi.org/10.1016/j.biochi.2014.11.018

Ojo, O.O., Srinivasan, D.K., Owolabi, B.O., Vasu, S., Conlon, J.M., Flatt, P.R., Abdel-Wahab, Y.H.A. (2015d) Esculentin-2cha-related peptides modulate islet cell function and improve glucose tolerance in mice with diet-induced obesity and insulin resistance. *PLoS One* 10, 1–17. https://doi.org/10.1371/journal.pone.0141549

Okamoto, M., Ohara-Imaizumi, M., Kubota, N., Hashimoto, S., Eto, K., Kanno, T., Kubota, T., Wakui, M., Nagai, R., Noda, M., Nagamatsu, S., Kadowaki, T. (2008) Adiponectin induces insulin secretion in vitro and in vivo at a low glucose concentration. *Diabetologia* 51, 827–835. https://doi.org/10.1007/s00125-008-0944-9

O'Neill C.M., Lu C., Corbin K.L., Sharma P.R., Dula S.B, Carter J.D, Ramadan J.W., Xin W., Lee J.K., Nunemaker C.S (2013) Circulating Levels of IL-1B+IL-6 Cause ER Stress and Dysfunction in Islets From Prediabetic Male Mice. *Endocrinology*, 154(9): 3077–3088. https://doi: 10.1210/en.2012-2138.

Ottosson-Laakso, E., Krus, U., Storm, P., Prasad, R.B., Oskolkov, N., Ahlqvist, E., Fadista, J., Hansson, O., Groop, L., Vikman, P. (2017) Glucose-induced changes in gene expression in human pancreatic islets: Causes or consequences of chronic hyperglycemia. *Diabetes* 66, 3013–3028. https://doi.org/10.2337/db17-0311

Owolabi, B.O., Musale, V., Ojo, O.O., Moffett, R.C., McGahon, M.K., Curtis, T.M., Conlon, J.M., Flatt, P.R., Abdel-Wahab, Y.H.A. (2017) Actions of PGLa-AM1 and its [A14K] and [A20K] analogues and their therapeutic potential as anti-

diabetic agents. *Biochimie* 138, 1–12.
https://doi.org/10.1016/j.biochi.2017.04.004

Pan, C.Q., Buxton, J.M., Yung, S.L., Tom, I., Yang, L., Chen, H., MacDougall, M., Bell, A., Claus, T.H., Clairmont, K.B., Whelan, J.P. (2006) Design of a long acting peptide functioning as both a glucagon-like peptide-1 receptor agonist and a glucagon receptor antagonist. *J. Biol. Chem.* 281, 12506–12515. https://doi.org/10.1074/jbc.M600127200

Pantic, J.M., Jovanovic, I.P., Radosavljevic, G.D., Arsenijevic, N.N., Conlon, J.M., Lukic, M.L. (2017) The potential of frog skin-derived peptides for development into therapeutically-valuable immunomodulatory agents. *Molecules* 22. https://doi.org/10.3390/molecules22122071

Pantic, J.M., Mechkarska, M., Lukic, M.L., Conlon, J.M. (2014) Effects of tigerinin peptides on cytokine production by mouse peritoneal macrophages and spleen cells and by human peripheral blood mononuclear cells. *Biochimie* 101, 83–92. https://doi.org/10.1016/j.biochi.2013.12.022

Parenti, A., Pala, L., Paccosi, S., Rotella, C.M. (2017) Potential Role for Dendritic Cells in Endothelial Dysfunction, Diabetes and Cardiovascular Disease. *Curr. Pharm. Des*,. 23, 1435–1444. https://doi.org/10.2174/1381612823666170124125826

Parkes, D.G., Pittner, R., Jodka, C., Smith, P., Young, A. (2001) Insulinotropic actions of exendin-4 and glucagon-like peptide-1 in vivo and in vitro. *Metabolism.* 50, 583–589. https://doi.org/10.1053/meta.2001.22519

Patsouris D., Li P.P., Thapar D., Chapman J., Olefsky J.M., Neels J.G. (2008) Ablation of CD11c-positive cells normalizes insulin sensitivity in obese insulin resistant animals. *Cell Metab*. 2008 Oct;8(4):301-9. https://doi:10.1016/j.cmet.2008.08.015.

Pennington, M.W., Czerwinski, A., Norton, R.S. (2018) Peptide therapeutics from venom: Current status and potential. *Bioorganic Med. Chem.* 26, 2738–2758. https://doi.org/10.1016/j.bmc.2017.09.029

Perez-Alcantara, M., Honoré, C., Wesolowska-Andersen, A., Gloyn, A.L., McCarthy, M.I., Hansson, M., Beer, N.L., van de Bunt, M. (2018) Patterns of differential gene expression in a cellular model of human islet development, and relationship to type 2 diabetes predisposition. *Diabetologia* 61, 1614–1622. https://doi.org/10.1007/s00125-018-4612-4

Pollack, R.M., Donath, M.Y., LeRoith, D., Leibowitz, G. (2016) Anti-inflammatory agents in the treatment of diabetes and its vascular complications. *Diabetes Care* 39, S244–S252. https://doi.org/10.2337/dcS15-3015

Premilovac, Di., Gasperini, R.J., Sawyer, S., West, A., Keske, M.A., Taylor, B. V., Foa, L. (2017) A New Method for Targeted and Sustained Induction of Type 2 Diabetes in Rodents. *Sci. Rep.* 7, 1–10. https://doi.org/10.1038/s41598-017-14114-4

Pukala, T. L., Bertozzi, T., Donnellan, S. C., Bowie, J. H., Surinya-Johnson, K. H., Liu, Y., Jackway, R. J., Doyle, J. R., Llewellyn, L. E. and Tyler, M. J. (2006) Host-defence peptide profiles of the skin secretions of interspecific hybrid tree frogs and their parents, female Litoria splendida and male Litoria caerulea. *FEBS Journal*, 273: 3511–3519. https://doi.org/10.1111/j.1742-4658.2006.05358.x

Rácz, G.Z., Kittel, Á., Riccardi, D., Case, R.M., Elliott, A.C., Varga, G. (2002) Extracellular calcium sensing receptor in human pancreatic cells. *Gut* 51, 705–711. https://doi.org/10.1136/gut.51.5.705

Rasschaert J., Flatt P.R., Barnett C.R., McClenaghan N.H., Malaisse W.J. (1996) D-glucose metabolism in BRIN-BD11 islet cells. *Biochem Mol Med.,* 57(2):97-105.

Reinbothe, T.M., Alkayyali, S., Ahlqvist, E., Tuomi, T., Isomaa, B., Lyssenko, V., Renström, E. (2013) The human L-type calcium channel Cav1.3 regulates insulin release and polymorphisms in CACNA1D associate with type 2 diabetes. *Diabetologia* 56, 340–349. https://doi.org/10.1007/s00125-012-2758-z

Robinson, E., Cassidy, R.S., Tate, M., Zhao, Y., Lockhart, S., Calderwood, D., Church, R., McGahon, M.K., Brazil, D.P., McDermott, B.J., Green, B.D., Grieve, D.J. (2015) Exendin-4 protects against post-myocardial infarction remodelling via specific actions on inflammation and the extracellular matrix. *Basic Res. Cardiol.* 110. https://doi.org/10.1007/s00395-015-0476-7

Roney K. (2013) Bone marrow-derived dendritic cells. *Methods Mol Biol.*, 1031:71-6. https://doi: 10.1007/978-1-62703-481-4_9.

Rosario, W., Singh, I., Wautlet, A., Patterson, C., Flak, J., Becker, T.C., Ali, A., Tamarina, N., Philipson, L.H., Enquist, L.W., Myers, M.G., Rhodes, C.J. (2016) The brain-to-pancreatic islet neuronal map reveals differential glucose regulation from distinct hypothalamic regions. *Diabetes* 65, 2711–2723. https://doi.org/10.2337/db15-0629

Rowlands, J., Cruzat, V., Carlessi, R., Newsholme, P. (2018) Peptides Insulin and IGF-1 receptor autocrine loops are not required for Exendin-4 induced changes to pancreatic β -cell bioenergetic parameters and metabolism in BRIN-BD11 cells. *Peptides*, 100, 140–149. https://doi.org/10.1016/j.peptides.2017.11.015

Sai, K.P., Jagannadham, M.V., Vairamani, M., Raju, N.P., Devi, A.S., Nagaraj, R., Sitaram, N. (2001) Tigerinins: Novel Antimicrobial Peptides from the Indian Frog Rana tigerina. *J. Biol. Chem.* 276, 2701–2707. https://doi.org/10.1074/jbc.M006615200

Sas, K.M., Karnovsky, A., Michailidis, G., Pennathur, S. (2015) Metabolomics and diabetes: Analytical and computational approaches. *Diabetes* 64, 718–732. https://doi.org/10.2337/db14-0509

Sato, Y., Inoue, M., Yoshizawa, T., Yamagata, K. (2014) Moderate hypoxia induces β-cell dysfunction with HIF-1-independent gene expression changes. *PLoS One* 9, 1–20. https://doi.org/10.1371/journal.pone.0114868

Schulla, V., Renstro, E., Feil, R., Feil, S., Franklin, I., Gjinovci, A., Jing, X., Laux, D., Lundquist, I., Magnuson, M.A., Obermu, S., Olofsson, C.S., Salehi, A., Wendt, A., Klugbauer, N., Wollheim, C.B., Rorsman, P., Hofmann, F. (2003) Impaired insulin secretion and glucose tolerance in b cell-selective Ca V 1 . 2 Ca 2 + channel null mice. *EMBO J.*, 22,15. 3844–3854. https://doi: 10.1093/emboj/cdg389.

Seino, S., Miki, T. (2003) Physiological and pathophysiological roles of ATP-sensitive K+ channels. *Prog. Biophys. Mol. Biol.* 81, 133–176. https://doi.org/10.1016/S0079-6107(02)00053-6

Seino, S., Shibasaki, T. (2005) PKA-Dependent and PKA-Independent Pathways for cAMP-Regulated Exocytosis. *Physiol. Rev.* 85, 1303–1342. https://doi.org/10.1152/physrev.00001.2005

Seino, Y., Fukushima, M., Yabe, D. (2010) GIP and GLP-1, the two incretin hormones: Similarities and differences. *J. Diabetes Investig.* 1, 8–23. https://doi.org/10.1111/j.2040-1124.2010.00022.x

Shanik, M.H., Xu, Y., Skrha, J., Dankner, R., Zick, Y., Roth, J. (2008) Insulin resistance and hyperinsulinemia: is hyperinsulinemia the cart or the horse? *Diabetes Care* 31 Suppl 2. https://doi.org/10.2337/dc08-s264

Shibasaki, T., Takahashi, H., Miki, T., Sunaga, Y., Matsumura, K., Yamanaka, M., Zhang, C., Tamamoto, A., Satoh, T., Miyazaki, J.I., Seino, S. (2007) Essential role of Epac2/Rap1 signaling in regulation of insulin granule dynamics by cAMP. *Proc. Natl. Acad. Sci. U. S. A.* 104, 19333–19338. https://doi.org/10.1073/pnas.0707054104

Sicree, B.R., Shaw, J., Zimmet, P. (2011) The Global Burden: Diabetes and Impaired Glucose Tolerance. *Diabetes Atlas* 1–105. https://doi.org/10.1097/01.hjr.0000368191.86614.5a

Siegel, E.G., Wollheim, C.B., Kikuchi, M., Renold, A.E., Sharp, G.W. (1980) Dependency of cyclic AMP-induced insulin release on intra- and extracellular calcium in rat islets of Langerhans. *J. Clin. Invest.* 65, 233–241. https://doi.org/10.1172/JCI109665

Sikimic, J., McMillen, T.S., Bleile, C., Dastvan, F., Quast, U., Krippeit-Drews, P., Drews, G., Bryan, J. (2019) ATP binding without hydrolysis switches sulfonylurea receptor 1 (SUR1) to outward-facing conformations that activate K ATP channels. *J. Biol. Chem.* 294, 3707–3719. https://doi.org/10.1074/jbc.RA118.005236

Simonsen, L., Holst, J.J., Deacon, C.F. (2006) Exendin-4, but not glucagon-like peptide-1, is cleared exclusively by glomerular filtration in anaesthetised pigs. *Diabetologia* 49, 706–712. https://doi.org/10.1007/s00125-005-0128-9

Sithara, S., Crowley, T.M., Walder, K., Aston-Mourney, K. (2017) Gene expression signature: A powerful approach for drug discovery in diabetes. *J. Endocrinol.* 232, R131–R139. https://doi.org/10.1530/JOE-16-0515

Skarbaliene, J., Rigbolt, K.T., Fosgerau, K., Billestrup, N. (2017) In-vitro and in-vivo studies supporting the therapeutic potential of ZP3022 in diabetes. *Eur. J. Pharmacol.* 815, 181–189. https://doi.org/10.1016/j.ejphar.2017.09.026

Skelin, M., Rupnik, M. (2011) cAMP increases the sensitivity of exocytosis to Ca2+ primarily through protein kinase A in mouse pancreatic beta cells. *Cell Calcium* 49, 89–99. https://doi.org/10.1016/j.ceca.2010.12.005

Smyth, L.A., Ratnasothy, K., Moreau, A., Alcock, S., Sagoo, P. (2013) Tolerogenic donor-derived dendritic cells risk sensitisation in vivo due to processing and presentation by recipient antigen- presenting cells. *J Immunol,* 190, 4848–4860. https://doi.org/10.4049/jimmunol.1200870.

Solomon, T.P.J., Knudsen, S.H., Karstoft, K., Winding, K., Holst, J.J., Pedersen, B.K. (2012) Examining the effects of hyperglycemia on pancreatic endocrine function in humans: Evidence for in vivo glucotoxicity. *J. Clin. Endocrinol. Metab.* 97, 4682–4691. https://doi.org/10.1210/jc.2012-2097

Spranger J., Kroke A., Möhlig M., Hoffmann K., Bergmann M.M., Ristow M., Boeing H., Pfeiffer A.F. (2003) Inflammatory cytokines and the risk to develop type 2 diabetes: results of the prospective population-based European Prospective Investigation into Cancer and Nutrition (EPIC)-Potsdam Study. *Diabetes*, 52(3):812-7. https://doi.org/10.2337/diabetes.52.3.812.

Srinivasan, D., Ojo, O.O., Abdel-Wahab, Y.H.A., Flatt, P.R., Guilhaudis, L., Conlon, J.M., (2014) Insulin-releasing and cytotoxic properties of the frog skin peptide, tigerinin-1R: A structure-activity study. *Peptides* 55, 23–31. https://doi.org/10.1016/j.peptides.2014.02.002

Srinivasan, D.K., Ojo, O.O., Owolabi, B.O., Conlon, J.M., Flatt, P.R., Abdel-Wahab, Y.H.A. (2016) [I10W]tigerinin-1R enhances both insulin sensitivity and pancreatic beta cell function and decreases adiposity and plasma triglycerides in high-fat mice. *Acta Diabetol.* 53, 303–315. https://doi.org/10.1007/s00592-015-0783-3

Stefanovic-Racic, M., Yang, X., Turner, M.S., Mantell, B.S., Stolz, D.B., Sumpter, T.L., Sipula, I.J., Dedousis, N., Scott, D.K., Morel, P.A., Thomson, A.W., O'Doherty, R.M. (2012) Dendritic cells promote macrophage infiltration and comprise a substantial proportion of obesity-associated increases in CD11c + cells in adipose tissue and liver. *Diabetes* 61, 2330–2339. https://doi.org/10.2337/db11-1523

Straub, S.G., Sharp, G.W.G. (2004) Hypothesis: One rate-limiting step controls the magnitude of both phases of glucose-stimulated insulin secretion. *Am. J. Physiol. - Cell Physiol.* 287, 565–571. https://doi.org/10.1152/ajpcell.00079.2004

Stumvoll M., Goldstein B.J., Van Haeften T.W. (2005) Type 2 diabetes: principles of pathogenesis and therapy. *Lancet*, 365: 1333–46.

Sul, H.S., Latasa, M.-J., Moon, Y., Kim, K.-H. (2000) Symposium: The Role of Long Chain Fatty Acyl-CoAs as Signaling Molecules in Cellular Metabolism Regulation of the Fatty Acid Synthase Promoter by Insulin 1,2. *J. Nutr* 130, 315–320.

Sundara RS., Longhi, M.P. (2016) Dendritic cells and adipose tissue. *Immunology*, 149, 353–361. https://doi.org/10.1111/imm.12653

Surendar, J., Mohan, V., Pavankumar, N., Babu, S., Aravindhan, V. (2012) Increased Levels of Serum Granulocyte-Macrophage Colony-Stimulating Factor Is Associated with Activated Peripheral Dendritic Cells in Type 2 Diabetes Subjects. *Diabetes Technol Ther.*, 14, 344-9. https://doi.org/10.1089/dia.2011.0182

Syme R., Glück S. (2001) Generation of dendritic cells: role of cytokines and potential clinical applications. *Transfus Apher Sci.*, 24:117-24.

Taneera, J., Storm, P., Groop, L. (2014) Downregulation of type II diabetes mellitus and maturity onset diabetes of young pathways in human pancreatic islets from hyperglycemic donors. *J. Diabetes Res.*, 2014. https://doi.org/10.1155/2014/237535

Tang, C., Ahmed, K., Gille, A., Lu, S., Gröne, H.J., Tunaru, S., Offermanns, S. (2015) Loss of FFA2 and FFA3 increases insulin secretion and improves glucose tolerance in type 2 diabetes. *Nat. Med.* 21, 173–177. https://doi.org/10.1038/nm.3779

Tapadia, M., Carlessi, R., Johnson, S., Utikar, R., Newsholme, P. (2019) Lupin seed hydrolysate promotes G-protein-coupled receptor, intracellular Ca2+ and enhanced glycolytic metabolism-mediated insulin secretion from BRIN-BD11 pancreatic beta cells. *Mol. Cell. Endocrinol.* 480, 83–96. https://doi.org/10.1016/j.mce.2018.10.015

Tarasov A., Dusonchet J., Ashcroft F. (2004) Metabolic regulation of the pancreatic beta-cell ATP-sensitive K+ channel: a pas de deux. Diabetes, 53 (Suppl 3): S113-22. https://doi.org/10.2337/diabetes.53.suppl_3.S113

Tengholm, A. (2012) Cyclic AMP dynamics in the pancreatic β-cell. *Ups. J. Med. Sci.* 117, 355–369. https://doi.org/10.3109/03009734.2012.724732

Teramoto, S., Miyamoto, N., Yatomi, K., Tanaka, Y., Oishi, H., Arai, H., Hattori, N., Urabe, T. (2011) Exendin-4, a glucagon-like peptide-1 receptor agonist, provides neuroprotection in mice transient focal cerebral ischemia. *J. Cereb. Blood Flow Metab.* 31, 1696–1705. https://doi.org/10.1038/jcbfm.2011.51

Tian, G., Sagetorp, J., Xu, Y., Shuai, H., Degerman, E., Tengholm, A. (2012) Role of phosphodiesterases in the shaping of sub-plasma-membrane cAMP oscillations and pulsatile insulin secretion. *J. Cell Sci.* 125, 5084–5095. https://doi.org/10.1242/jcs.107201

Torimoto, K., Okada, Y., Mori, H., Otsuka, T., Kawaguchi, M., Matsuda, M., Kuno F., Sugai K., Sonoda S., Hajime M., Tanaka K., Arao T., Tanaka, Y. (2015). Effects of exenatide on postprandial vascular endothelial dysfunction in type 2

diabetes mellitus. *Cardiovasc Diabetol*, 14: 25. https://doi: 10.1186/s12933-015-0188-1.

Tzoulaki, I., Ebbels, T.M.D., Valdes, A., Elliott, P., Ioannidis, J.P.A. (2014) Design and analysis of metabolomics studies in epidemiologic research: A primer on-omic technologies. *Am. J. Epidemiol.* 180, 129–139. https://doi.org/10.1093/aje/kwu143

Van 't Veer, L.J. Van, Dai, H., Vijver, M.J. Van De, Kooy, K. Van Der, Marton, M.J., Witteveen, A.T., Schreiber, G.J., Kerkhoven, R.M., Roberts, C., Bernards, A., Friend, S.H., Linsley, P.S. (2002) Gene expression profiling predicts clinical outcome of breast cancer. *Nature,* 415(6871):530-6. https://doi:10.1038/415530a

Vasu, S., McClenaghan, N.H., McCluskey, J.T., Flatt, P.R. (2014) Mechanisms of toxicity by proinflammatory cytokines in a novel human pancreatic beta cell line, 1.1B4. Biochim. Biophys. Acta - Gen. Subj. 1840, 136–145. https://doi.org/10.1016/j.bbagen.2013.08.022

Vasu, S., McGahon, M.K., Charlotte Moffett, R., Curtis, T.M., Michael Conlon, J., Abdel-Wahab, Y.H.A., Flatt, P.R. (2017) Esculentin-2CHa(1-30) and its analogues: Stability and mechanisms of insulinotropic action. *J. Endocrinol.* 232, 423–435. https://doi.org/10.1530/JOE-16-0453

Velmurugan, K., Balamurugan, A.N., Loganathan, G., Ahmad, A., Hering, B.J., Pugazhenthi, S. (2012) Antiapoptotic actions of exendin-4 against hypoxia and cytokines are augmented by CREB. *Endocrinology* 153, 1116–1128. https://doi.org/10.1210/en.2011-1895

Vetere, A., Choudhary, A., Burns, S.M., Wagner, B.K. (2014) Targeting the pancreatic β-cell to treat diabetes. *Nat. Rev. Drug Discov.* 13, 278–289. https://doi.org/10.1038/nrd4231

Wallace, M., Whelan, H., Brennan, L. (2013) Metabolomic analysis of pancreatic beta cells following exposure to high glucose. *Biochim. Biophys. Acta - Gen. Subj.* 1830, 2583–2590. https://doi.org/10.1016/j.bbagen.2012.10.025

Wang T.J., Martin G. Larson, Ramachandran S. Vasan, Susan Cheng, Eugene P. Rhee, Elizabeth McCabe, Gregory D. Lewis, Caroline S. Fox, Paul F. Jacques, Céline Fernandez, Christopher J. O'Donnell, Stephen A. Carr, Vamsi K. Mootha, Jose C. Florez, Amand, C.B., Clish, and R.E.G. (2011) Metabolite profiles and diabetes. *Nat. Med.* 17, 448–453. https://doi.org/10.1038/nm.2307.Metabolite

Wang, C., Yang, C., Chen, Y. chen, Ma, L., Huang, K. (2019). Rational Design of Hybrid Peptides: A Novel Drug Design Approach. *Curr. Med. Sci*. 39, 349–355. https://doi.org/10.1007/s11596-019-2042-2

Wang, W., Li, J., Wu, K., Azhati, B., Rexiati, M. (2016) Culture and identification of mouse bone marrow-derived dendritic cells and their capability to induce T lymphocyte proliferation. Med. Sci. Monit. 22, 244–250. https://doi.org/10.12659/MSM.896951

Wellen, K. E., Hotamisligil, G. S. (2005) Inflammation, stress, and diabetes. *J Clin Invest*, *115*(5), 1111–1119. https://doi:10.1172/JCI25102

Welters, H.J., Tadayyon, M., Scarpello, J.H.B., Smith, S.A., Morgan, N.G. (2004) Mono-unsaturated fatty acids protect against β-cell apoptosis induced by saturated fatty acids, serum withdrawal or cytokine exposure. *FEBS Lett.* 560, 103–108. https://doi.org/10.1016/S0014-5793(04)00079-1

Widenmaier, S.B., Kim, S.J., Yang, G.K., De Los Reyes, T., Nian, C., Asadi, A., Seino, Y., Kieffer, T.J., Kwok, Y.N., McIntosh, C.H.S. (2010) A GIP receptor agonist exhibits β-cell anti-apoptotic actions in rat models of diabetes resulting in improved β-cell function and glycemic control. *PLoS One 5*. https://doi.org/10.1371/journal.pone.0009590

Williams, N.L., Morris, J.L., Rush, C., Govan, B.L., Ketheesan, N. (2011) Impact of streptozotocin-induced diabetes on functional responses of dendritic cells and macrophages towards Burkholderia pseudomallei. *FEMS Immunol. Med. Microbiol.,* 61, 218–227. https://doi.org/10.1111/j.1574-695X.2010.00767.x

Wolak, M., Staszewska, T., Juszczak, M., Gałdyszyńska, M., Bojanowska, E. (2019) Anti-inflammatory and pro-healing impacts of exendin-4 treatment in Zucker diabetic rats: Effects on skin wound fibroblasts. *Eur. J. Pharmacol.* 842, 262–269. https://doi.org/10.1016/j.ejphar.2018.10.053

Wu, N., Yang, M., Gaur, U., Xu, H., Yao, Y., Li, D. (2016) Alpha-ketoglutarate: Physiological functions and applications. *Biomol. Ther.* 24, 1–8. https://doi.org/10.4062/biomolther.2015.078

Wu, Y., Ding, Y., Tanaka, Y., Zhang, W. (2014) Risk factors contributing to type 2 diabetes and recent advances in the treatment and prevention. *Int. J. Med. Sci.* 11, 1185–1200. https://doi.org/10.7150/ijms.10001

Xu, G., Chen, J., Jing, G., Shalev, A. (2013) Thioredoxin-interacting protein regulates insulin transcription through microRNA-204. *Nat. Med.* 19, 1141–1146. https://doi.org/10.1038/nm.3287

Xu, G., Kaneto, H., Laybutt, D.R., Duvivier-kali, V.F., Trivedi, N., Suzuma, K., King, G.L., Weir, G.C., Bonner-weir, S. (2007) Downregulation of GLP-1 and GIP Receptor Expression by Hyperglycemia. Diabetes 56, 1551–1558. https://doi.org/10.2337/db06-1033.Ad-GFP

Yajima, H., Komatsu, M., Sato, Y., Yamada, S., Yamauchi, K., Sharp, G.W.G., Aizawa, T., Hashizume, K. (2001) Norepinephrine inhibits glucose-stimulated, Ca2+-independent insulin release independently from its action on adenylyl cyclase. *Endocr. J.* 48, 647–654. https://doi.org/10.1507/endocrj.48.647

Yang, S.N., Berggren, P.O. (2006) The role of voltage-gated calcium channels in pancreatic β-cell physiology and pathophysiology. *Endocr. Rev.* 27, 621–676. https://doi.org/10.1210/er.2005-0888

Yao, K., Lu, H., Huang, R., Zhang, S., Hong, X., Shi, H., Sun, A., Qian, J., Zou, Y., Ge, J., (2011) Changes of dendritic cells and fractalkine in type 2 diabetic

patients with unstable angina pectoris: A preliminary report. *Cardiovasc. Diabetol.* 10, 50. https://doi.org/10.1186/1475-2840-10-50

Ying, W., Fu, W., Lee, Y.S., Olefsky, J.M. (2019) The role of macrophages in obesity-associated islet inflammation and β-cell abnormalities. *Nat. Rev. Endocrinol.* https://doi.org/10.1038/s41574-019-0286-3

Yokoi, N., Gheni, G., Takahashi, H., Seino, S. (2016) β-Cell glutamate signaling: Its role in incretin-induced insulin secretion. *J. Diabetes Investig.* 7, 38–43. https://doi.org/10.1111/jdi.12468

Yusta, B., Baggio, L.L., Estall, J.L., Koehler, J.A., Holland, D.P., Li, H., Pipeleers, D., Ling, Z., Drucker, D.J. (2006) GLP-1 receptor activation improves β cell function and survival following induction of endoplasmic reticulum stress. *Cell Metab.* 4, 391–406. https://doi.org/10.1016/j.cmet.2006.10.001

Zeng, M., Che, Z., Liang, Y., Wang, B., Chen, X., Li, H., Deng, J., Zhou, Z. (2009) GC-MS based plasma metabolic profiling of type 2 diabetes mellitus. *Chromatographia* 69, 941–948. https://doi.org/10.1365/s10337-009-1040-0

Zhang, H., Sturchler, E., Zhu, J., Nieto, A., Cistrone, P.A., Xie, J., He, L., Yea, K., Jones, T., Turn, R., Di Stefano, P.S., Griffin, P.R., Dawson, P.E., McDonald, P.H., Lerner, R.A. (2015) Autocrine selection of a GLP-1R G-protein biased agonist with potent antidiabetic effects. *Nat. Commun.* 6, 1–13. https://doi.org/10.1038/ncomms9918

Zhang, M., Houamed, K., Kupershmidt, S., Roden, D., Satin, L.S. (2005) Pharmacological Properties and Functional Role of K slow Current in Mouse Pancreatic β-Cells . *J. Gen. Physiol.* 126, 353–363. https://doi.org/10.1085/jgp.200509312

Zhong, J., Rao, X., Deiuliis, J., Braunstein, Z., Narula, V., Hazey, J., Mikami, D., Needleman, B., Satoskar, A.R., Rajagopalan, S. (2013) A potential role for dendritic cell/macrophage-expressing DPP4 in obesity-induced visceral inflammation. Diabetes 62, 149–157. https://doi.org/10.2337/db12-0230

Zhu Y., Liu Q., Zhou Z., Ikeda Y. (2017) PDX1, Neurogenin-3, and MAFA: critical transcription regulators for beta cell development and regeneration. *Stem Cell Res Ther.*, 8(1):240. https://doi:10.1186/s13287-017-0694-z.